UNIVERSITÀ DEGLI STUDI DI MILANO

PhD School of Technological Innovation for Agricultural, Food and Environmental sciences cycle XXV

Department of Agricultural and Environmental Sciences
Production, Landscape, Agro-energy (*DISAA*)

Measurements and Mathematical Modelling of Water Fluxes in an Agro-Ecosystem of Maize

(AGR/08)

PhD candidate**: FATMA WASSAR**
(**R08774**)

Supervisor: Prof. Claudio Gandolfi
PhD coordinator: Prof. Roberto Pretolani

Academic Year 2011-2012

Dedication

To the two pillars of my life:

my mother Aicha and my father Mohamed

To

my sisters Samira and Najla

and

my brothers Habib and Ramzi

To you……………………………………I dedicate this thesis

With all my love

Fatma

Acknowledgments

One of the joys of completion is to look over the journey past and remember all the persons, friends and family who have helped and supported me along this long but fulfilling road.

Completing my PhD degree is probably the most challenging activity of my life. The best and worst moments of my doctoral journey have been shared with many people. It would not have been possible to write this doctoral thesis without the help and support of the kind people around me, to only some of whom it is possible to give particular mention here.

Foremost, I would like to express my sincere gratitude to my supervisor **Prof. Claudio Gandolfi** for the continuous support of my PhD study and research, for his patience, motivation, enthusiasm, and immense knowledge. His guidance helped me in all the time of research and writing of this thesis. His ability to select and to approach compelling research problems, his high scientific standards, and his hard work set an example. I admire his ability to balance research interests and personal pursuits. Above all, he made me feel a friend, which I appreciate from my heart. I could not have imagined having a better supervisor and mentor for my PhD study.

My thanks also go out to the support I received from the collaborative work I undertook with the ACCA project. I am, especially grateful to **Dr. Arianna Facchi** for her help and collaboration in data collection, and for many inspiring discussions during my PhD work.

In addition, I have been very privileged to get, to know and to collaborate with many other great people who became friends over the three years. I learned a lot from you about life, research, how to tackle new problems and how to develop techniques to solve them. **Dr. Olfa Gharsallah** has been a pleasure to work with. She helped me in numerous ways during various stages of my PhD and became a dear sister.

The good advice, support of **Dr. Enrico Chiaradia** and **Dr. Michele Rienzner** have been invaluable on both an academic and a personal level. They have been providing precious feedbacks and assistances to my research and dissertation writing. And for which I am extremely grateful. I also thank them for always pushing me to think deep about why we are doing the work and to set clear goals. Without their support and encouragement, this dissertation would not have existed.

A special thanks to **Daniele Ferrari**, his technical excellence and tremendous grasp of experimental issues had a great impact on me.

It has been a great privilege to spend three years in the ***Department of Agricultural Engineering (hydraulic section) at University of Milan,*** and its members will always remain dear to me. In particular I would like to thank **Antonia Moreno Carrera** "a nice and sweet lady, the heart of the department that is full of life and joy", **Bianca Ortuani, Chiara Vergani** "a nice friend with whom I enjoyed sharing chat", **Chiara Bassanelli, Prof Gian Battista Bischetti, Dr Paula Morando and Sandra Cesari de Maria** for their help, friendship and moral support.

I would like also to thank both **Dr. Ettore Bernardoni** and **Dr. Marco Carozzi** for their help during the laboratory work.

Furthermore, **Ahmed Hussien** have always been a constant source of encouragement during my postgraduate studies. I admire his persistent and meticulous attitude. He was always available to cheer me up and he was always accessible and willing to help. Apparently, he is an angel from God shedding light on secular issues from a spiritual angle. He had been a role model for me to follow unconsciously and has always been one of my best counselors. Thanks Ahmed for being such a caring and wonderful friend since we met 5 years ago and for accepting to become one of my best friends. I will always pray for God to keep our friendship forever.

My deepest gratitude goes to my family for their unflagging love and support throughout my life.They instilled within me a love of creative pursuits. This dissertation is simply impossible without them. I am indebted to my father, **Mohamed Wassar**, for his care and love. As a typical father, he worked to support the family and spare no effort to provide the best possible environment for me to grow up and attend school. He had never complained in spite of all the hardships in his life. I cannot ask for more from my mother, **Aicha Idoudi**, as she is simply perfect. I have no suitable word that can fully describe her everlasting love to me. I remember many sleepless nights with her accompanying me when I was young and each time I have an exam . I remember her constant support when I encountered difficulties and I remember, most of all, her continuous "Doaa". Mother, I love you. To my sisters, **Samira** and **Najla** and my brothers **Hbib** and **Ramzi,** in testimony of my love and my knowledge for the encouragement and the sustain that you didn't stop bringing to me during all my life. You really let me feel proud of you. To my uncle **Dr. Mohamed Wassar**, who is always my ideal person looking for his encourage, and support. To my lovely **grand-parents** who are representing for me love, respect, traditions and culture.

I have been fortunate to come across many funny and good friends, without whom life would be bleak. I would like to express my deeply appreciation for all the happy moments shared with the precious friends in “Arcagna”. These joyful place has filled my life with cheerful days, and was source of support and encourage. I will always admire the common values between friends from different parts of the world, and I will keep them in my memory long after I leave the place. Special thanks go to **Nader El Badry** for his ever-present support and for making me laugh as often and as loudly as he has. He was always a real big brother. **Souhir Sghayer** was a nice friend and roommate, with whom I enjoyed talking about everything. **Moez Maghrebi**, I thank for his beautiful singing and the nice atmosphere he created in our dormitory. I would also like to thank **Elahe Tavakol** for her support and encouragement throughout. **Rim Ghabriche,** despite the short period of our knowledge has become a close and a dear friend. **Mohamed, Wahid, Batista, Gabriele, Bouabid, Emanulae, Khaled, Roudayna,** I thank for parties, dinners and plays we enjoy together.

I would like to thank **Imen Jmai, Imed Cherigui, Yammouni**, **Angelo Belverato, Ramroum, Malek, Wided, Saoussen, Dalila, Lamy, Ahmed T**… for their love and encouragement. And, thank you for your support when I have needed it the most. Thank you with all my heart

Summary

During the agricultural seasons 2010 and 2011, monitoring work was carried out in maize field in the experimental farm “A. Menozzi” (Landriano-Pavia) of the University of Milan. Measurements of water balance components on field scale (soil humidity, evapotranspiration, soil water potential, groundwater table depth etc.) were used to build enriched database to be utilized in this study.

Water retention characteristics are crucial input parameters in modeling of water flow and solute transport. Several field methods, laboratory methods and theoretical models for such determinations exist, each having their own limitations and advantages (Stephens, 1994). Comparisons between estimated, field and laboratory results is vital to test their validity under different conditions. This study attempts to evaluate and compare those methods. The soil water retention characteristics were determined in two representative sites (PMI-1 and PMI-5) located in Landriano field, in Lombardy region, northern Italy. In the laboratory, values of both volumetric water content *(θ)* and soil water matric potential *(h)* were measured using the tensiometric box and pressure plate apparatus. In field soil water content was measured with SENTEK probes, and matric potential with tensiometers. The retention curve characteristics were determined by common and recent PTFs that use soil properties such as particle-size distribution (sand, silt, and clay content), organic matter or organic carbon content, and dry bulk density. Field methods are more representative than laboratory and estimation methods for determining water retention characteristics (Marion et al., 1996). Therefore, field retention curves were compared against retention curves obtained from laboratory measurements and PTFs estimations using root mean square error (RMSE) and bias. The laboratory measurements showed the highest ranking for the validation indices. The second best technique was the PTF Rosetta (Schaap et al. 2001). The lowest prediction accuracy was observed for the Rawls and Brakensiek (1985) PTF which is in contradiction with previous finding (Calzolari et al., 2001), showing that this function is well representing the retention characteristics of the area. We conclude that the Rosetta PTF developed by Schaap et al (2001) appears to be well suited to predict the soil moisture retention curve from easily available soil properties.

Modeling water dynamics in the Soil-Plant-Atmosphere (SPA) continuum is an important aspect of crop water management and water transfer through the unsaturated zone is a key hydrological process connecting atmosphere, surface water and groundwater. Many simulation models of water dynamics in the SPA and/or soil crop system have already been developed. Therefore, the use of simplified agro-hydrological models may represent a useful and simple tool to simulate water fluxes

in the SPA. A physically based approach model SWAP (Van Dam et al., 1997) and a conceptual model IDRAGRA (Gandolfi et al., 2011) were selected to evaluate their performance in simulating water balance components such as soil water content (SWC) in the root zone and actual evapotranspiration (ETact). IDRAGRA is a novel model that has been developed recently in the Engineering Department of the University of Milan, and was compared to a more standardized widely used model (SWAP). Data on various agronomic aspects required for IDRAGRA and SWAP were collected during 2011 growing season of spring-summer maize in two representative sites of the field (PMI-1 and PMI-5).

PTF-Rosetta soil hydraulic parameters were fed to the two models intending to compare them with cost-effect, affordable work, and less sophisticated methodology to identify the soil characteristics.. SWAP showed a good performance in estimating ETact and SWC in the root zone in the two sites. Similarly, IDRAGRA showed good fitting with measured data.

Then the two tested models were run to assess capillary rise contribution to satisfy maize water requirement and groundwater recharge. When considering the daily variation of the groundwater table, groundwater contribution is able to meet from 47 to 60% for IDRAGRA and from 40 to 65% for SWAP of total maize water requirement.

Finally, groundwater table depths were fixed virtually at 0.8m, 1m, 1.5m, 2m and 3m. It was found that the capillary rise from groundwater decreases with the increase of the groundwater table depth. A higher contribution is observed when the water table is higher or equal to 1 m. When the water table depth reached 2m the capillary was still contributing to maize water requirement for both models

The deep percolation estimated by SWAP was much higher than the one estimated by IDRAGRA. Accordingly, the net recharge to the water table was considerable with SWAP simulations. While for IDRAGRA model the deep percolation was always lower than the capillary rise which lead to a negligible net recharge

Taking all together, a simpler model like IDRAGRA can provide comparable performances to a more complex model, like SWAP, and could therefore be a good tool for estimating water balance components for practical applications, especially for irrigation management.

List of Figures

List o f Tables

List of Abbreviations

SPAC: Soil Plant Atmosphere Continuum

SWC: Soil Water Content

FDR: Frequency Domain Reflectometry

TDR: Time Domain Reflectometry

SWP: Soil Water Potential

SWRC: Soil Water Retention Curve

SWAP: Soil Water Atmosphere Plant

IDRAGRA: Idraulica Agraria

VGM: Van Genuchten-Mualem

ETpot: potential evapotranspiration

ETact: actual evapotranspiration

Tpot: potential transpiration

Tact: actual Transpiration

Epot: potential Evaporation

Eact: actual Evaporation

LAI: Leaf Area Index

%CC: Percentage of Canopy Cover

PTF: Pedo-Transfert-Function

PTF-R: Rosetta Pedo-Transfert-Function

PTF-RB: Rawls and Brakensiek Pedo-Transfert-Function

K_c: crop coefficient

K_{cb}: basal crop coefficient

TAW: Total Available Water

RAW: Ready Available Water

K_s: stress coefficient

Table of Contents

1 INTRODUCTION

Water is destined to be critical resource of our Century, since the demand for fresh water will continue to increase while the supply dwindles. The first impacts are already seen in areas such as the Mediterranean and Central Asia, where water resources are exhausted by overuse, pollution and drought. In the future years, a sharp increase in water withdrawals is foreseen to meet the needs of urban, agricultural, industrial, and environmental sectors. Given that the biggest water problem worldwide is scarcity (Jury and Vaux, 2005), there is significant uncertainty about what the level of water supply will be for future generations.

Water resources management is one of the most pressing environmental issues, especially because of the competition between industry, agriculture, municipal and energy utilization of water resources. At the global level, 80%–90% of all the water is consumed in agriculture. Unfortunately, water use efficiency in agriculture is poor with more than 50% water losses, making it possible to save enormous water quantities in the agricultural sector, when compared with other sectors (Hamdi et al., 2003). Moreover, in many regions of the world, plant growth and crop yields are limited by water deficits. More frequent and intense droughts waves and areas of land characterized as very dry, have increased in recent decades (Dai et al., 2004).

Water resources are consumed extensively not only in dry but also in sub-humid environments. Irrigation water use per unit of surface area is largest in arid regions with high cropping intensity while inter-annual variations of irrigation water use are largest in humid regions (Siebert and Döll., 2007).

Currently, irrigated agriculture is caught between two perceptions that are contradictory; some perceive that agriculture is highly inefficient by growing water-guzzling crops (Postel et al., 1996), while others emphasise that irrigation is essential for the production of sufficient food in the future, given the anticipated increases in food demand due to world population growth and changes in diets (Dyson., 1999).

Water balances are important to follow water dynamics in agricultural and natural ecosystems. They indicate, in space and time, conditions under which plants grow and develop, and are useful in the interpretation of plant behavior during periods that differ from the ordinary local climatic conditions, such as periods of water excess or deficit. These aspects are important for crop management and the understanding of the behavior of water in an agro-ecosystems.

Precise knowledge of all components of water balance is essential to optimize water use in irrigated agriculture. However, water balance components are difficult to measure in required time intervals because their measuring is time consuming and costly. Hence methods that can estimate water balance components based on the combined use of available measurement data and an appropriate model are required.

Water transfer through the unsaturated zone is a key hydrological process connecting atmosphere, surface water and groundwater (Gandolfi et al., 2006).

The unsaturated zone is inextricably involved in many aspects of hydrology: infiltration, evaporation, groundwater recharge, soil moisture storage and soil erosion. It also contributes to the spatial and temporal distributions of plant communities under naturally occurring rainfed conditions and serves as a modifying influence on the production of cultivated crop species. Thus the vadose zone represents the conduit through which liquid and gaseous constituents are attenuated and transformed as they are exchanged in both directions between the soil surface and the water table.

During the last years, the impetus to understand and manage the unsaturated zone stems from its recognition as a key factor in the improvement and protection of the quality of groundwater supplies.

In recent studies, the unsaturated zone has been the consistent focus of attention of many scientific discipline and sector of society regarding its conservation, use, or management (Nielson et al., 1986; Van Dam et al., 2003; Simunek., 2005; Gandolfi et al., 2006).

Effective management of resources can only be achieved if decisions are based on solid information. Thus, in few countries, it is possible to base demand management strategies on accurate data. In times of economic difficulty, data collection and research are often the first activities to be cut. Better models are required to make predictions, particularly since our climate is likely to change substantially over the next 50 years.

Modeling the soil water fluxes in the unsaturated zone of the soil has become an important tool for evaluation of different agro-hydrological situations. Soil water fluxes models have been developed because the soil moisture regime is affected by a multitude of simultaneous factors such as soil texture and structure, precipitation and evaporation or transpiration, soil cover by plants, root distributions in the soil, irrigation and drainage, planting date, tillage, grazing, etc. Since so many factors may affect the soil moisture regime, it is often impossible to assess the influence of any one factor without computer model. Only by using computer models, simultaneous effects of many factors on the soil moisture regime can be studied.

Many models of varying degree of complexity and dimensionality have been developed during the past several decades to quantify the basic physical and chemical processes affecting water flow and pollutant transport in the unsaturated zone. Computer models based on analytical and numerical solutions of the flow and solute transport equations are now increasingly being used for a wide range of applications in research and management of natural subsurface systems.

Modeling approaches range from relatively simple analytical and semi-analytical models to more complex numerical codes that permit consideration of a large number of simultaneous nonlinear processes.

Whereas analytical and semi-analytical solutions are still more popular for most relatively simple applications. The ever-increasing power of personal computers and the development of more accurate and numerically stable solution techniques have given rise to the much wider use of numerical models in recent decades. The wide use of numerical models has also been significantly enhanced by their availability in both public and commercial domains, and by the development of sophisticated graphics-based interfaces that tremendously simplify their use.

In order to provide successful decision support, it is essential that the model is performing accurately and reliably, which provide a good representation of reality so that the model can be used to predict an observable phenomenon with enough accuracy and precision (Comegna and Vitale., 1996).

Field data collection in a specific sites is crucial to understand processes and to provide essential elements for models calibration and validation, and also allow to compare different approaches and to choose the most suitable for the context of agro-ecosystems in Lombardy soils.

1.1 Structure and Objectives of the thesis

The **first objective** of the thesis is the creation of a **data-base collection** in an agro-ecosystem of maize in Lombardy region through the implementation of intensive field monitoring activities carried out in 2010-2011. The monitoring has involved the measurement of multiple parameters related to the soil, the vegetation and the atmosphere, and was conducted in an integrated manner at different spatial scales (see *chapter 4*).

A **second objective** is the evaluation of the general applicability and the prediction accuracy of some of the most commonly developed Pedo-Transfert Functions, PTFs on estimating soil retention parameters Then to compare the estimated soil retention characteristics to those measured in the field and laboratory (see *chapter 5*).

A **third objective** of this study is to **evaluate the performance** of two **hydrological models** (**SWAP and IDRAGRA**) in simulating soil water balance parameters such as soil **water content** and **actual evapotranspiration** (see *chapter 6*).

The models were selected on the basis of several criteria: SWAP allow a very detailed calculation of soil water movement; the second criteria was the method of calculation of evapotranspiration for which the two models differ. Finally, the study focused on those models because IDRAGRA is a novel model that has been developed recently in the Department of agricultural engineering of the University of Milan (recently the name has been changed to DISAA, www.disaa.unimi.it). It was intended to compare it to a more standardize widely used model (SWAP).

The quantification of **capillary contributions** from **shallow water tables** towards **crop water uptake** is considered to be a very **important management aspects**, to ensure conservation of water and soil resources. This rate, in addition to the **recharge rate**, are known to be the **most difficult and uncertain components** for estimation of **groundwater budget**. For that reason, **the <u>fourth objective</u>** of the thesis is to **provide or estimate in realistic way**, on the basis of the **analysis** and **processing of collected data**, the **relative contribution** of **capillary rise** to satisfy the water requirement of maize and the **groundwater recharge** through the application of tested mathematical models: SWAP and IDRAGRA (see *chapter 6*, *part 6.8*).

The above objectives will be addressed through following chapters

Chapter 2 presents a literature review and focuses on hydraulic fluxes in the unsaturated zone and hydrological models and describes in detail the two models selected for the study.

Chapter 3 presents a literature review for groundwater recharge and capillary rise contribution to satisfy crop water requirement.

Chapter 4 will discuss about the study area, monitoring activities carried out and the main parameters collected during the two agricultural seasons 2010 and 2011.

Chapter 5 compares different techniques to measure and estimate soil retention curve characteristics which are considered to be an important input data for both models involved in this study.

Chapter 6, which is the main stay of the thesis, describes in detail the comparison between the two models SWAP and IDRAGRA in simulating water balance components. Then it will focuses on the use of the two tested models to assess capillary rise contribution to satisfy maize water requirements and groundwater recharge.

Chapter 7 contains general conclusions of the work.

2 Unsaturated zone: hydraulic fluxes and hydrological models (SWAP and IDRAGRA)

2.1 Introduction

The unsaturated zone, sometimes called the vadoze zone, is the zone between the ground surface and the water table. The term unsaturated zone is somewhat of a misnomer because the capillary fringe above the groundwater rain-saturated top are portions that are saturated (Delleur., 1998). For this reason some authors (e.g., Bouwer., 1978) prefer the term vadoze zone. The unsaturated zone is the hydrological connection between the surface water components of the hydrological cycle and the groundwater components.

The unsaturated zone plays a crucial role and is inextricably involved in many aspects of hydrology: infiltration, evaporation, groundwater recharge, soil moisture storage, and soil erosion. It also contributes to the spatial and temporal distributions of plant communities under naturally occurring rainfed conditions and serves as a modifying influence on the production of cultivated crop species. Thus the vadoze zone represents the conduit through which liquid and gaseous constituents are attenuated and transformed as they are exchanged in both directions between the soil surface and the water table (Nielsen et al., 1986).

During the past decade, the impetus to understand and manage the unsaturated zone stems from its recognition as a key factor in the improvement and protection of the quality of groundwater supplies.

Descriptions of the unsaturated zone and solute movement through is fundamental for the study of the hydrological cycle and have been given by many authors (Nielsen et al., 1986; Santini and D'Urso., 1999; Romano and Santini., 2002).

2.2 Water fluxes in the unsaturated zone in a field scale

The state of water in the soil is described in terms of the amount of water and the energy associated with the forces which hold the water in the soil. The amount of water is defined by water content and the energy state of water which is water potential. Plant growth, soil temperature, chemical transport, and groundwater recharge are all dependent on the state of water in the soil. While there is a unique relationship between water content and water potential for a particular soil, these physical properties describe the state of water in soil in distinctly different manners. It is important to understand the distinction when choosing a soil water measuring instrument.

2.2.1 The Soil-Plant-Atmosphere Continuum

The movement of water from the soil, into the roots, through the xylem and from the leaf into the atmosphere, occurs because of a series of water potential gradients. The system that involves the soil, the plant's roots, the xylem, the leaf and the atmosphere, is called the Soil-Plant-Atmosphere Continuum (SPAC), which is a pathway for the movement of water from the soil into the atmosphere. Water flows from soil to roots, through xylem, mesophyll and wall cells, and it evaporates through the substomatal cavities. From the substomatal cavities it diffuses out of the stomata, through the leaf and the canopy into the atmosphere. The value of the water potential is higher (less negative) in the soil and decreases along the transpiration pathway. The water potential values in the different elements of the system (saturated and unsaturated soil, plant's roots, plant's xylem, plant's leaves, atmosphere) are determining a series of water potential gradients that are the driving forces for water movement. Under a given gradient, the magnitude of the flux depends on the value of the resistance terms along the pathway. According to Campbell., (1985), within the plant the xylem resistance is negligible compared to other resistances. The major resistance are the endodermis, where water enters the root steele and in the leaf in the bundle sheath. Usually, in the plant the potential drops occur for 60% to 70% in the endodermis and 30% to 40% in the leaf.

To understand the driving forces that determine the movement of water through the SPAC, it is useful to describe the relationship between water potential and relative humidity at a liquid-air interface with the Kelvin equation:

$$\psi = \frac{RT}{M_w} ln h_r \qquad (2.1)$$

where ψ is the water potential (J kg^{-1}) in the air, R is the gas constant (8.3143 J mol−1 K^{-1}), T is the temperature (K), M_w is the molecular weight of water (0.018 kg mol^{-1}), and h_r is the relative humidity (expressed as a fraction from 0 to 1). Equation 2.1 can be inverted:

$$h_r = exp\frac{M_w \psi}{RT} \qquad (2.2)$$

to obtain the relative humidity from water potential.

For instance, according to Equation 2.1, the atmosphere at 0.6 of relative humidity, at 20°C, has a water potential of 69,133 J kg^{-1}. For a loamy soil, at 20°C and at field capacity (which is the soil water content after water in the largest pores has drained away and the rate of downward movement has become small), the water potential is about −33 J kg^{-1}, and according to Equation 2.2 the corresponding relative humidity (hr) at the liquid-air interface is 0.9997. This large difference in water potential between the soil and the atmosphere is the driving force for water movement from the soil into the atmosphere.

When water is uptake from the soil into the roots, it moves into the xylem and into the leaves and it undergoes a series of changes that reduce the water potential, but the changes are not as dramatic as they are between the soil (or the plant) and the atmosphere. The soil water potential SWP usually ranges from values close to zero (when the soil is at or close to saturation) to values of −1,000 to −2,000 J kg^{-1} and lower when the soil is very dry. The leaf water potential usually ranges from −100 J kg^{-1} for a well watered plant to −2,000 J kg^{-1} for a water stressed plant.

These values of water potential show that, in the SPAC, the large water potential gradient occurs between the leaf and the atmosphere (when the atmosphere relative humidity decreases), and it is precisely this gradient that determines plant transpiration and it supports the water cycle as known. Moreover, the change of phase between liquid and vapor occurring between the leaf and the leaf boundary layer requires a relatively high amount of energy (the latent heat of vaporization), which determine a plant's decrease of temperature and it is a key phenomena for the plant's thermal regulation. The transpiration process (regulated by the plant through the stomata) has therefore also a key role in the plant's thermal regulation (Campbell and Norman., 1998).

Knowledge of soil and plant water potential is hence of utmost importance for soil water availability itself (Bittelli., 2010). Indeed, the concept of soil water content (or soil wetness) is not sufficient and sometime misleading, to describe the availability of soil water for plants, because it is otherwise the energy state of water that determines the flow of water in the soil-plant-atmosphere continuum. However, the relationship between soil water content and water potential is an important property that is described in the following paragraph (2.2.2).

2.2.2 Soil water content (SWC)

The quantity of water in soil is expressed in two different units, as the volumetric water content θ_v and the gravimetric water content θ_g. The volumetric water content is the volume of liquid water per volume of soil, and the gravimetric water content is the mass of water per mass of dry soil.

The mass of water per volume of soil is obtained by multiplying θ_v by ρ_w, the density of water. This is also equal to the product of θ_g and ρ_b, the dry soil bulk density. Thus $\rho_w \theta_v = \rho_b \theta_g$

$$\theta_v = \frac{\rho_b \theta_g}{\rho_w} \qquad (2.3)$$

Measurement of soil water content

The gravimetric water content θ_g of a sample of moist soil is measured by weighting the moist soil sample, drying it to remove the water, and reweighing it. The customary method of drying is to place the sample in an oven at 105°C for 24 h.

The volumetric water content can be estimated from θ_g with Eq.(2.3) if the bulk density ρ_b is known. In order to measure ρ_b, an undisturbed sample of soil must be taken and its volume estimated. A soil core could be taken by pushing a cylinder into the soil, which encloses a sample in the known volume of the coring tube. However, it is extremely difficult to take such samples without compacting the soil and thus changing its density.

There is a different ways to measure the volumetric water content without disturbing the soil sample for example; gamma ray attenuation, neutron attenuation, time domain reflectometry (TDR)(Jury *et al.,* 1991), Frequency Domain Reflectometry, FDR (see Figure 2.1).

Gamma ray attenuation method uses a radioactive source to emit a beam of gamma rays into a soil sample. The attenuation or absorption of the beam is recorded by a gamma ray detector after the beam has passed through a known length of soil. This value is used to determine the total density of the soil sample. Then, if the density of solids and any other liquids present in the sample are known, the total density can be used to determine the volumetric water content. Field samples must retain their original structure and density for accurate measurement.

Neutron probes are another way to measure soil moisture content. A probe inserted in the ground emits low-level radiation in the form of neutrons. These collide with the hydrogen atoms contained in water, which is detected by the probe. The more water content in the soil, the more neutrons are scattered back at the device. Neutron probes are very accurate measurement devices when used properly but are expensive compared to most other measurement methods and generally have to be registered with the federal government due to radioactive elements used to emit the neutrons. TDR is an electromagnetic method in which the applied signal is guided along a transmission line through a soil sample. TDR systems measure the water content of the soil by measuring how long it takes the pulse to come back. Examples of this sensor include the Campbell CR616 and the IMKO Trime. TDR soil moisture measurement devices require a device to generate the electronic pulse and need to be carefully calibrated in order to precisely measure the amount of time it takes for the pulse to propagate down the line and back again. They are also sensitive to the salt content of soil and relatively expensive compared to some measurement methods.

Frequency Domain Reflectometry (FDR) sensor sends an electromagnetic wave along its probes and measure the frequency of the reflected wave, which varies with water content.

During the two years of our experiment, the FDR probes were selected to measure soil water content for different reasons: FDR probes are inexpensive for multiple site measurements, it has a low power consumption, so batteries can work for long time; there is no need for an expensive cable tester; the probes can be buried for a long time, because they are designed to withstand harsh environmental conditions; and continuous monitoring of soil moisture at several locations is easily automated using datalogger. Examples of sensors in this category include the AquaSPY C-probe, and the Sentek EnviroSCAN Probe which was used in our experiment to measure the volumetric soil water content.

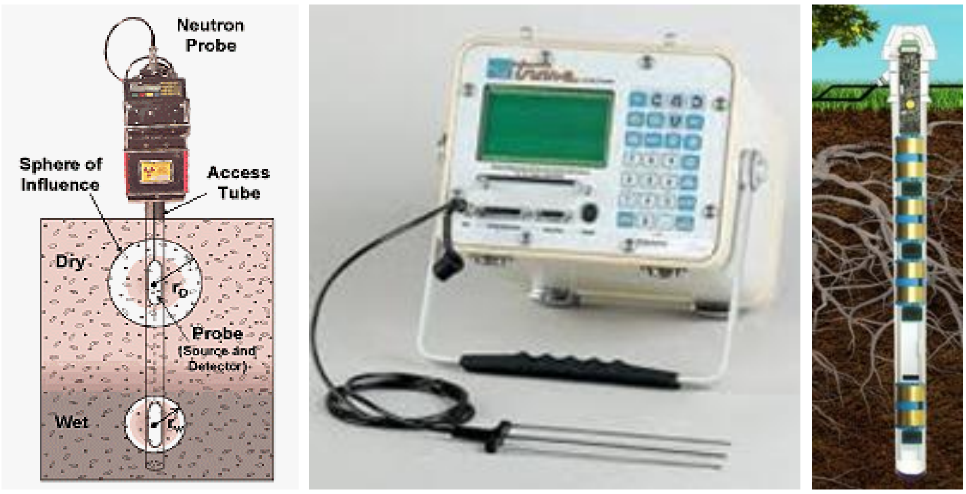

Figure 2.1. Neutron probes to measure soil moisture content (left), TDR (center) and Sentek EnviroSCAN Probe (right)

2.2.3 Soil water potential (SWP)

The movement of water occurs within the soil profile, between the soil and plant roots, and between the soil and the atmosphere. As in all natural systems, movement of a material is dependent on energy gradients. Soil water potential is an expression of the energy state of water in soil and must be known as numerous forces. If no adhesive forces were present, the water molecules would move through the soil at the same velocity as in free air minus delays from collisions with the solid matter. Soil water potential accounts for adhesive and cohesive forces and describes the energy status of soil water.

The components of water potential are the following:

✓ Gravitational Potential ψ_z (Z is Head Units), it is the energy per unit volume of water required to move an infinitesimal amount of pure, free water from the reference elevation z_0 to the soil water elevation z_{soil}. It has the value $\Psi_z = \rho_w g(Z_{soil} - Z_0)$ (2.4)

✓ Solute Potential ψ_s (s in Head Units), it is the change in energy per unit volume of water when solutes identical in composition to the soil solution at the point of interest in the soil are added to pure, free water at the elevation of the soil.

✓ Matric Potential ψ_m (h in Head Units), it is the energy per unit volume of water required to transfer an infinitesimal quantity of water from a reference pool of soil water at the elevation of the soil to the point of interest in the soil at reference air pressure.

✓ Air Pressure Potential ψ_a (a in Head Units), it is defined as the change in potential energy per unit volume of water when the soil air pressure is changed from the pressure P_0 of the reference state to the pressure P_{soil} of the soil.

✓ Hydrostatic Pressure Potential ψ_p (p in Head Units), it is defined as the water pressure exerted by overlaying unsupported (saturated) water on the point of interest in the soil. By definition, it is equal to the water pressure exerted by the height of water between the point of interest z_{soil} and the water table (saturated- unsaturated soil interface Z_{wt}; $\Psi_p = \rho_p g(Z_{wt} - Zsoil$ (2.5)

Since the SWP represents an energy, it should be expressed as a unit of energy per unit mass (J kg^{-1}) or per unit volume of water (Jm^{-3}). The former is preferable because it does not require to include in the computation the changes of water volume with temperature. However, SWP is often expressed in related units such as energy per unit weight, which is equivalent of head of water. The energy is equivalent to the pressure exerted by a liquid column of a given height. For instance, a column of water of 10 meters correspond to a pressure of 1 bar.

Another common unit which is the pressure (Pa or bar), derived from the first methods developed to measure the soil water potential such as the tensiometers and the pressure plate apparatus. This unit is based on the definition of energy per unit volume. Since pressure in a fluid can be seen to be a measure of energy per unit volume, energy is given by the product of pressure by volume (E=P*V). Usually the SWP is expressed as a negative number because it represents the energy required to transfer the soil water to the reference state described above. The term "suction" and "tension" are definitions developed to avoid using the negative sign and to represent SWP as a positive numbers.

The SWP can range over several orders of magnitude, from a few Joules per kilogram when the soil is close to saturation to minus thousand of Joules per kilogram when soil is very dry.

For agricultural applications usually the range of interest is between 0 and approximately -1,500 J kg^{-1}, the latter being defined as the soil water potential at the permanent wilting point of many cultivate crops.

Soil water potential measurements: different instruments

The general principle for SWP measurement is *hydraulic equilibrium* between the water held in the soil and the measuring device. Equilibrium can be reached for the liquid phase or for the vapor phase. Tensiometers (one of the most common devices and the instrument used in our experiment) are based on the equilibrium between liquid water in soil and liquid water in a porous cup. The small pores of the porous cup allows the establishment of an *hydraulic continuum* between the tensiometer water reservoir and the soil. The pressure changes determined by the differences between pressure inside the tensiometers and the soil are then detected by a pressure sensor.

Other instruments, such as heat dissipation sensors or dielectric sensors are also based on the equilibration of a ceramic cup with the surrounding soil. In this case, however, a property of the ceramic (*i.e.,* thermal conductivity, dielectric permittivity) that depends on the ceramic water content is measured. Since there is a relationship between the ceramic water content and the ceramic water potential (the ceramic's water retention curve) it is possible, through calibration curves, to obtain the soil water potential of the ceramic's pore water. Under the assumption of *hydraulic equilibrium*, the water potential of the ceramic cup should be equal to the one of the surrounding soil.

Other instruments, such as thermocouple psychrometry or dew point potential meters are based on the equilibrium of the vapor phase. The water potential in the air phase is related to relative humidity. Therefore, the measurement of relative humidity and temperature of air in equilibrium with soil allows for obtaining the water potential. Thermocouple psychrometry is based on temperature difference between a dry bulb and wet-bulb temperature. When the relative humidity of the vapor phase is low, the vapor pressure deficit will be high, the evaporation rate will be high and therefore the temperature depression will be higher. In the dew point methods, the saturation vapor pressure is first measured by a thermometer, the temperature of a close-chamber is decreased until dew forms on a chilled mirror. The dew-point temperature can be then used to obtain the relative humidity.

The method that have been used to measure the soil water potential in the field will be explained in detail in the following paragraph:

<u>Tensiometers</u>

They are porous ceramic cups, connected to a pressure sensor (manometer or pressure transducer) through a water-filled tube. The water-filled tube is placed into contact to the soil through a rigid porous membrane. The membrane allows water movement through the device, but not air movement. The cup is placed into the soil and the pores in the ceramic cup reach equilibrium with the soil water matric potential of the surrounding soil. When the matric potential of the soil is lower (more negative) than in the tensiometer, a water potential gradient is established and water from the tensiometer is attracted by the surrounding porous media, creating a suction that is detected by the pressure sensor. The pressure is read by the pressure sensor, which indicates the value of the soil matric potential. There are a variety of tensiometers classified based on their design and on the measuring device used to sense the pressure changes. A common classification is between mechanical and electronic tensiometers. In the first ones the change in pressure is detected by a mechanical pressure gauges, while in the second ones (tensiometers used in our experiment) the change in pressure is detected by an electronic pressure transducers. Usually, a membrane is deformed by a pressure change and a pressure transducer is connected to the membrane. The use of electric pressure transducers allow to obtain more precise reading and to collect the data through a data-logger, therefore allowing multiplexing and automation. Figure 2.2 shows two tensiometers: (a) a traditional tensiometer with a manual manometer, (b) a tensiometer equipped with a pressure transducer connected to a data logger. Recently, advanced transducers are installed directly into the porous ceramic cup (Sisson et al., 2002). Another advancement proposed by a manufacturer (UMS, Munich, Germany) is to use a self-refilling tensiometers. The range of tensiometers is restricted by the air entry pressure of the porous membrane, which can be derived by the well-known Young-Laplace equation that relates the water potential to the pore radius. The pore size of the ceramic material may change, although common ceramics used for tensiometers have maximum pore radius in the range of a few microns (2–3 µm). According to the manufacturer (T5-X. User Manual 2009) the most recent tensiometers can measure water potential from 0 to 200 J kg^{-1}. Other tensiometers that could reach further water potential were described by Tamari et al., (1993). The increase in the tensiometer range can be achieved by employing a series of manufacturing techniques. For instance, the surfaces of the ceramic should be strongly hydrophilic, the air entry value should be low-enough, and not air bubbles or cavities should be present in the device. These features are dependent on the manufacturing techniques and the choice of the materials used to build the device.

A common limitation for the use of tensiometers is the formation of air bubbles (cavitation) in the water-reservoir (*i.e.*, the water-filled tube). This phenomena occurs when the water potential decreases and the liquid water pressure inside the tube approaches its vapor pressure (at the temperature of the tensiometer), determining spontaneous evaporation and formation of air bubbles. Indeed, the lower limit of the range described above is determined by the issue of formation of air bubbles. This problem usually require refilling of the tensiometer. Tensiometers may have a lag in SWP reading in respect the soil condition because of the hydraulic resistance of the cup or limited contact between the cup and the soil. This problem is particularly pronounced in swelling soils where swelling and shrinking may create air gaps between the cup and the surrounding soil, increasing the resistance to water flow and creating a lack of continuum between the liquid phase in soil and in the ceramic cup. In general, the reading depends on the sensitivity of the device and the resistance of the ceramic cup to water flow. Modern tensiometers, equipped with small water reservoirs and precise electronic pressure transducers have partially addressed this issue and in condition of good contact between the sensor and the soil, the response time can be in the range of a few seconds. However, since the resistance to flow changes both with the resistance of the ceramic cup and the resistance of the surrounding soil, in increasingly drier conditions the response time can become much longer due to increasing resistances to water flow. Tensiometer reading may change depending on the size of the ceramic cup, providing different SWP measurements. According to Hendrickx *et al.*, (1994) an increase in tensiometer cup size reduced the variability of SWP measurements. Specifically, they suggested that the typical cup size of 42.3 cm^2 will determine a relatively large SWP measurement variability, therefore larger cup sizes should be used for field monitoring. In general, tensiometers have the following advantages: direct measurement, easy to use, generally inexpensive, continuous reading using pressure transducers and dataloggers, low skills requirement and not affected by salinity. The disadvantages are: limited range of SWP, may take long equilibration time and cavitations (air bubbles form in the water tube) preventing the reading at low water potentials.

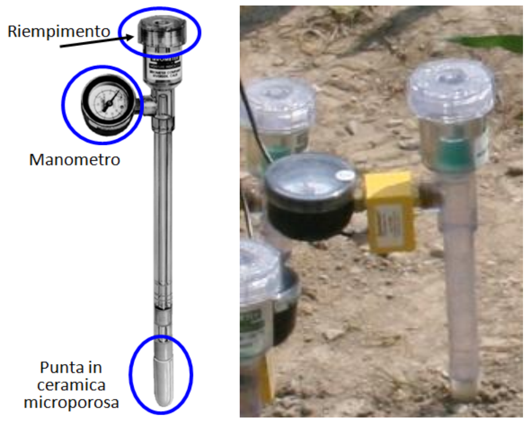

Figure 2.2. tensiometers: (a) a traditional tensiometer with a manual manometer, (b) a tensiometer equipped with a pressure transducer connected to a data logger.

2.2.4 Soil retention curve

When a soil is completely saturated (i.e., the pore space is entirely filled with water), at equilibrium with free water, and at the same height, the potential is zero, because the gravitational, the matric and the hydrostatic pressure are zero. If the pressure is changed (for instance by increasing the

elevation in respect to the free water, or allowing an external pressure) a negative potential is determined in the soil sample and the pores start to desaturate (water leaves the soil sample).
The largest pores are the one that desaturates first and, at increasingly lower water potential values corresponding water potential is called air entry potential, since it is the value corresponding to the initial entering of air into the saturated soil.
As the pores desaturate, the total soil water content of the soil sample decreases. The relationship between the water potential and the corresponding values of soil water content is called the Soil Water Retention Curve (SWRC) Figure 2.3 shows an example of three SWRC for soils having different textural composition. The Salkum sample (silty clay loam) is the soil with the largest water holding capacity, followed by the Walla Walla (silt loam) and the L-soil (sand) samples, showing that the shape of the SWRC depends primarily on texture. Usually, the largest the clay content the greater the water holding capacity. While the largest the sand content the smaller the water holding capacity, because sandy soils are mostly characterized by large pores that quickly desaturate, leaving a small amount of water at lower water potentials. The depth of the soil profile has also an important role in determining the soil water holding capacity.

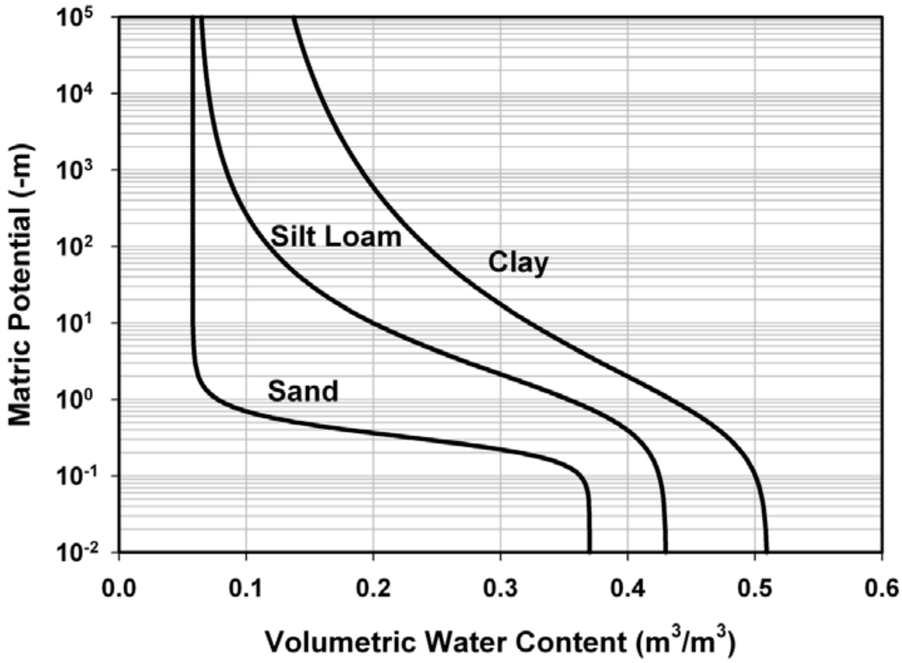

Figure 2.3 Typical soil water characteristic curves for soils of different texture (Dolph et al., 1992).

The SWRC, together with the hydraulic conductivity curve (relating the soil water potential and the unsaturated hydraulic conductivity) are the most important soil hydraulic properties. They affect the soil water budget, since it affects the ability of the plant’s roots to uptake water from the soil, the amount of water percolating into the groundwater, the microbial decomposition and therefore phenomena such as soil fertility, salinization and aridity.

Many methods are available to determine the SWRC, including pressure plates apparatus, thermocouple psychrometry, heat dissipation sensors, and dew point potential meters. Among these methods, pressure plate apparatus was used in our laboratory experiments to determine SWRC. The retention curve were also constructed from water potential and soil water content field data.

2.2.5 Unsaturated conductivity curve

The hydraulic conductivity of a soil is a measure of the soil's ability to transmit water when submitted to a hydraulic gradient. Hydraulic conductivity is defined by Darcy's law, which, for one-dimensional vertical flow, can be written as follows:

$$U = -K\frac{dh}{dz} \qquad (2.6)$$

Where *U* is Darcy's velocity (or the apparent average velocity of the soil fluid through a geometric cross-sectional area within the soil), *h* is the hydraulic head, and *z* is the vertical distance in the soil. The coefficient of proportionality, *K*, in Equation 2.6 is called the hydraulic conductivity.

The hydraulic conductivity *K* represents the ability of a soil to conduct water and is considered to be a constant under the saturated conditions. Under unsaturated conditions, the hydraulic conductivity is a function of *h*. the rate at which water is being conducted through the soil is product of the hydraulic conductivity and the hydraulic head gradient *dh/dz* (driving force). The negative sign indicates that the flow of water takes place in the direct conditions of decreasing *h*.

The term coefficient of permeability is also sometimes used as a synonym for hydraulic conductivity. On the basis of equation 2.6, the hydraulic conductivity is defined as the ratio of Darcy's velocity to the applied hydraulic gradient. The dimension of *K* is the same as that for velocity, that is length per unit of time[LT^{-1}].

Hydraulic conductivity is one of the hydraulic properties of the soil; the other involves the soil's fluid retention characteristics. These properties determine the behavior of the soil fluid within the soil system under specified conditions. More specifically, the hydraulic conductivity determines the ability of the soil fluid to flow through the soil matrix system under a specified hydraulic gradient. The soil fluid retention characteristics determine the ability of the soil system to retain the soil fluid under a specified pressure condition.

The hydraulic conductivity depends on the soil grain size, the structure of the soil matrix, the type of soil fluid and the relative amount of soil fluid (saturation) present in the soil matrix. The important properties relevant to the solid matrix of the soil include pore size distribution, pore shape, tortuosity, specific surface, and porosity. In relation to the soil fluid, the important properties include fluid density and fluid viscosity (μ), For a subsurface system saturated with the soil fluid, the hydraulic conductivity, *K* can be expressed as follows (Bear 1972):

$$K = \frac{k\rho g}{\mu} \qquad (2.7)$$

Where *k*, the intrinsic permeability of the soil, depends only on properties of the solid matrix, and *g* is called the fluidity of the liquid, represents the properties of the percolating fluid. The hydraulic conductivity(*K*) is expressed in terms of length per unit of time [LT^{-1}], the intrinsic permeability, *k*, is expressed in L^2 and the fluidity in $L^{-1}T^{-1}$.

2.3 SWAP model

2.3.1 Introduction

SWAP is a one-dimensional transient model to simulate water flow in a heterogeneous soil-root system (Figure 2.4), which can be under the influence of groundwater (Feddes et al., 1978; Belmans et al., 1983). The model is including solute transport, heat flow and crop growth in the atmosphere-plant soil environment (Van Dam et al., 1997). SWAP includes hysteresis according to Kool and Parker., (1987), the possibility for simulating preferential flow, and adsorption and decomposition processes of nutrients and pesticides as described by Boesten and Van Der Linden., (1991).

SWAP calculates the soil water flow with the Richards equation based on Darcy's law. In order to solve this equation, the soil hydraulic functions for each layer should be known. The soil hydraulic functions, which relates the soil water content, pressure head and unsaturated hydraulic conductivity, are described by the Van Genuchten-Mualem (VGM) parameters (Van Genuchten., 1987; Mualem., 1976). The root water uptake is described semi empirically by a sink term ,which is a function of the maximum root water uptake, the soil water pressure head and the salt concentration (Feddes et al., 1978; Homaee., 1999). The maximum root water uptake at a particular depth is proportional to the root length, which is prescribed as a function of the relative rooting depth (Feddes et al., 1988; Prasad., 1988). At the bottom of the system, boundary conditions can be described with various options, e.g. water table depth, flux to/from semi-confined aquifer, flux to/

from open surface drain, an exponential relationship between bottom flux and water table, or zero flux, free drainage and free outflow (Van Dam et al., 1997).

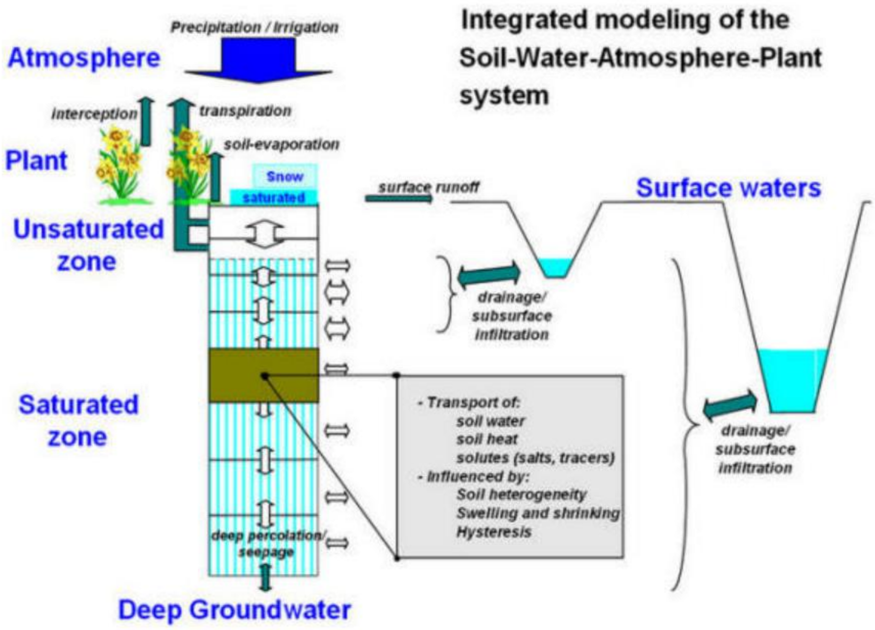

Figure 2.4 Schematic representation of process incorporated in SWAP (Adapted from http://www.alterra-research.nl)

2.3.2 Soil water flow

As introduced before SWAP is based of Richard equation which is a combination of Darcy' law and continuity equation.

Darcy's equation is given as :

$$q = K(h)\frac{\partial(h+z)}{\partial z} \quad (2.8)$$

Continuity equation for soil water is:

$$\frac{\partial\theta}{\partial t} = -\frac{\partial q}{\partial z} - S(h) \quad (2.9)$$

Where q is the soil water flux density (positive upward) (cm d^{-1}), h is the soil water pressure head (cm), z is the vertical co-ordinate (cm) taken as positive upward, θ is the volumetric water content (cm^3 cm^{-3}), t is the time (d) and S is the water extraction rate by plant roots (cm^3 cm^{-3} d^{-1}). Combination of equation (2.8) and (2.9) gives Richard equation which reads as:

$$C(h)\frac{\partial h}{\partial t} = \frac{\partial}{\partial z}\left[K(h)\left(\frac{\partial h}{\partial z}+1\right)\right] - S(h) \qquad (2.10)$$

where C is the water capacity $(\partial\theta/\partial h)$ (cm^{-1}). Richard equation is solved through an implicit finite difference scheme as described by Van Dam and Feddes., (2000). The equation has a clear physical basis at a scale where soil can be considered as a continuum of soil, air and water. SWAP solves equation (2.10) numerically for both the saturated and unsaturated zone, subject to specified initial and boundary conditions and with known relations between soil water content (θ), soil water pressure head (h) and unsaturated hydraulic conductivity (K).

These relationships, which are generally called soil hydraulic functions are described by Van Genuchten., (1980) and Muallem., (1976) or by tabular values. The analytical soil water retention, $\theta(h)$ function proposed by Van Genuchten reads:

$$\theta = \theta_{res} + \frac{\theta_{sat}-\theta_{res}}{(1+|\alpha h|^{n})^{m}} \qquad (2.11)$$

Where θ_{sat} (cm^3 cm^{-3}) is the saturated water content, θ_{res} (cm^3 cm^{-3}) is the residual water content in the dry range and α (cm^{-1}), n (-) and m (-) are the empirical shape factors and h is soil water pressure head . m is given as :

$$m = 1 - \frac{1}{n} \qquad (2.12)$$

Using the above $\theta(h)$relation and applying the theory on the unsaturated hydraulic conductivity by Muallem., (1976), the following $K(\theta)$ function results in equation:

$$K = K_{sat}\, S_e^{\lambda}\left[1-\left(1-S_e^{\frac{1}{m}}\right)^{m}\right]^{2} \qquad (2.13)$$

Where K_{sat} (cm d^{-1}) is the saturated hydraulic conductivity, exponent λ is the tortuosity factor, which can be fixed at 0.5 (Romano and Santin., 1999, D'urso., 2001) and S_e is the relative saturation defined as:

$$S_e = \frac{\theta - \theta_{sat}}{\theta_{sat} - \theta_{res}} \qquad (2.14)$$

In the vertical direction, the model considers the existence of heterogeneity in the form of horizons or layers within the soil profile. These layers are subdivided in space intervals called soil compartments. Halfway in each soil compartment a node is identified for which the hydraulic properties are calculated.

The Muallem-Van Genuchten soil parameters can be also obtained from pedotransfer functions given in SWAP model as an alternate option. The function is developed by Wosten et al., (1998) and is based on "Hypress" database for European soils. Pedotransfer functions predict the hydraulic characteristics for a specific soil with easily obtainable texture, organic matter content and bulk density.

The extraction of potential water from soil by plants equals to its potential transpiration. The plant cell pumps water from roots to stomata cavity in which vaporization takes place. The potential root water extraction rate at certain depth may be determined by root length density and the atmospheric conditions. The availability of soil moisture to plant roots depend upon the potential at which these water is bound to soil matrix. If the soil water potential is greater than the plant water potential in absolute term (because the potential in unsaturated zone is negative), crops comes under water stress.

The potential water extraction per day as a function of depth is given as:

$$S_{pot}(z) = \frac{l_{root}(z)}{\int_{-D_{root}}^{0} l_{root}(z)dz} T_{pot} \qquad (2.15)$$

where S_{pot} (z) is the potential water extraction rate, D_{root} is the root zone depth (cm), T_{pot} is the potential transpiration, l_{root} (z) is the root length density (cm^3 cm^{-3}). Soil water pressure head heterogeneity over the root zone does not play an important role in water uptake. The roots appear to take up water from the relatively wetter parts of the root zone to compensate for the water deficit in the drier parts (Homaee et al., 2002).

SWAP can handle every distribution of root length density. In practice however, precise data on root length density distribution is not available. In the present study, a uniform root length density distribution is assumed, which leads to a simplified form of equation (2.15) (Feddes et al., 1978):

$$S_{pot}(z) = \frac{T_{pot}}{D_{root}} \qquad (2.16)$$

Stress due to dry or wet conditions and high salinity concentration may reduce S_{pot} (z).

Water stress in SWAP is described by the function proposed by Feddes et al. (1978):

$$S_a(z) = \alpha_{rw} S_{pot}(z) \tag{2.17}$$

where α_{rw} is a dimentional reduction coefficient for root water uptake . the values of α_{rw} varies between 0 and 1 (Figure 2.5).

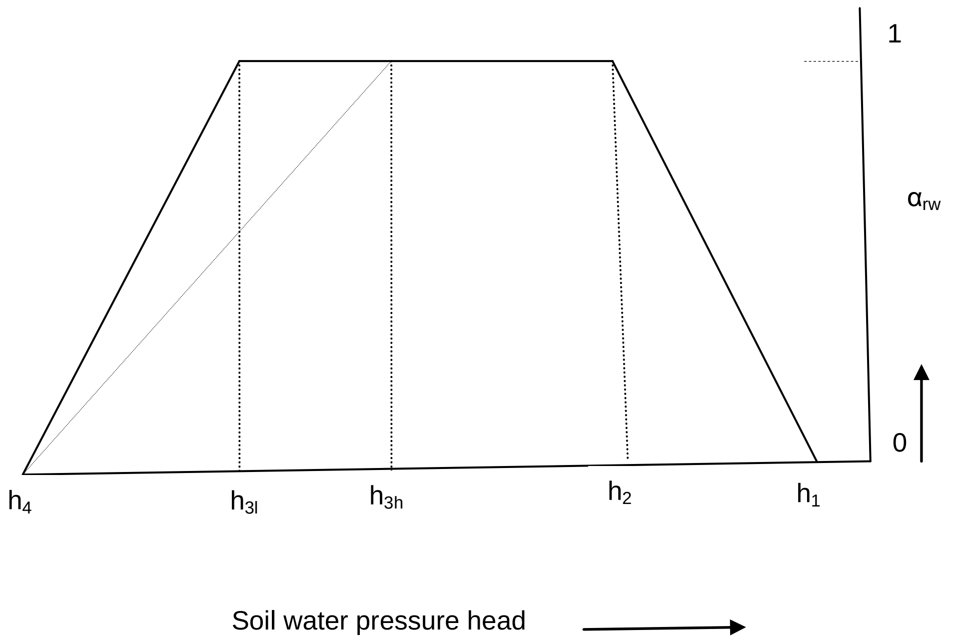

Figure 2.5. Dimensional sink term variable, α_{rw} as a function of soil pressure head h and potential transpiration rate, T_{pot} (Feddes et al., 1978)

when α_{rw} is equal to 1, water extraction by plant is at its potential capacity.

h_1= the pressure head is at near saturation below above, no water uptake takes place due to oxygen deficiency.

h_2= pressure head at which water extraction is optimal for plant.

h_{3h}= pressure head at which stomata start to close due to water limitation and/or presence of salts; evaporative demand of atmosphere is very high.

h_{3l}= pressure head at which stomata start to close due to water limitation and/or presence of salts; evaporative demand of atmosphere is very low.

h_4= pressure head below which plant cannot extract water (wilting point) critical pressure head values from sink term function for different crops can be obtained from Taylor and Ashcrof., (1972), Wesseling et al., (1991) given in SWAP manual. Sink term describe water uptake response of crop to different water pressure heads in the soil matrix.

Reduction of water uptake due to salt stress needs input of crop salt threshold value (EC value above which salt stress occurs) and the decline of root water uptake above this threshold level, according to the Mass and Hoffman., (1977) concept.. In the present only water stress is considered.

Integrating $S_a(z)$ over the entire root zone yields actual transpiration rate, T_{act} (cm d^{-1}) as

$$T_{act} = \int_{-D_{root}}^{0} S_a(z)dt \quad (2.18)$$

2.3.3 Simple crop cycle

This option is useful when crop growth doesn't need to be simulated or when crop growth input data are insufficient. The simple crop growth model represents as green canopy that intercepts precipitation, transpires and shades the ground leaf area index or soil cover fraction, crop height and rooting depth as a function of development stage are specified. The simple model doesn't calculate crop potential or actual yield. Crop development can be either modeled linearly (fixed length of the crop cycle) or can be controlled by the temperature sum (variable length of the crop cycle). Fixed crop cycle is used.

2.3.4 Irrigation

Irrigation in SWAP can be prescribed at fixed time or scheduled according to a number of criteria depending upon the economical and physical constraints of the irrigated area. The scheduling criteria define the time and depth of irrigation application. Fixed irrigation can be specified the whole year round but scheduled irrigation can be active only during cropping period.

Five timing criteria can be selected to generate the irrigation schedule. These includes (1) allowable daily stress, (2) allowable depletion of readily available water in the root zone, (3) allowable depletion of totally available water in the root zone, (4) allowable depletion amount of water in the root zone and (5) critical pressure head or water content at certain depth. Each of the options gives the opportunity to define the timing criteria as a function of crop development stages.

Two application depth criteria can be selected in SWAP. Back to field capacity ensures that the soil water content in the root zone is brought back to field capacity. The option is useful in case of sprinkler and micro-irrigation system, which allow a variation of irrigation application depth.

Another option is to specify fixed amount of water. This option is suited for gravity systems, which allows little variation in irrigation application depth.

2.3.5 Boundary conditions

The wide range of upper and lower boundary conditions being offered in SWAP is one of the key advantages of the model.

Top boundary condition:

The upper boundary of the soil profile was described on daily basis by ET_{pot}, rainfall and irrigation.

Reference evapotranspiration

The reference evapotranspiration used in SWAP is directly calculated with the Penman-Monteith equation using daily climatic meteorological data. Reference evapotranspiration ET_0 (cm d^{-1}) can be also used as input when necessary weather data are not available. The meteorological data were collected from weather station for the regional agency for environmental protection installed near the study area. The data includes daily values of maximum and minimum air temperature, wind speed, rainfall, solar radiation and relative humidity. The maximum and minimum temperature and the relative humidity were used to calculate the actual vapor pressure (kPa) as input in the SWAP model.

The reference evapotranspiration rate ET_0 (cm d^{-1}) from a canopy covering soil surface can be estimated using well known Penman-Monteith:

$$ET_0 = \frac{8640s(R_n - G) + C_p\rho_a(e_s - e_a)/r_{ah}}{(s + \gamma(1 + r_c/r_{ah}))\lambda} \qquad (2.19)$$

Where,

- R_n is net radiation flux (Wm^{-2})
- G is soil heat flux (Wm^{-2})
- C_p is heat capacity of air ($Jkg^{-1}K^{-1}$)
- ρ_a is air density (kgm^{-3})
- (e_s-e_a) is vapor pressure deficits (kPa)
- r_c is crop resistance (sm^{-1})
- r_{ah} is aerodynamic resistance for heat transport (sm^{-1})
- λ is latent heat of vaporization of water (Jkg^{-1})

- γ is psychrometric constant (kPa)

General formula for interception of precipitation by canopy (Von Hoyningen-Hune (1983); Braden (1985) given in SWAP is:

$$P_i = aLAI\left[1 - \frac{1}{1 + \frac{bP_{gross}}{aLAI}}\right] \qquad (2.20)$$

Where P_{i} is the intercepted precipitation (cm), P_{gross} is gross precipitation (cm), a is an empirical parameter which is equal to 0.28 for most of the crops and b is the soil cover fraction.

A drawback is that at shallow groundwater tables (which is our case) the simulated phreatic surface fluctuations are very sensitive to the soil hydraulic functions and the top boundary condition. If the top and bottom boundary condition not properly match, or the soil hydraulic functions deviate from reality, strong fluctuations of water fluxes across the lower boundary may result.

<u>Potential soil evaporation and plant transpiration</u>

The potential evaporation under a standing crop is derived from Penman-Monteith equation (2.19) by neglecting aerodynamic term. The aerodynamic term will be small because wind velocity near soil surface is relatively very small which makes aerodynamic resistance very large. Thus the only source of soil evaporation is radiation that reach soil surface. E_p is related to leaf area index, *LAI* (Belmans et al., 1983):

$$E_p = E_{po}e^{-cLAI} \qquad (2.21)$$

where E_{po} is the potential evaporation rate of a wet bare soil, *Ep* is the soil evaporation rate, c is the extinction coefficient of global solar radiation (-) assumed as 0.45. it is assumed as the product of extinction coefficient for diffuse and direct light.

Incorporating soil cover fraction (SC), the potential evaporation reads:

$$E_p = (1 - SC)ET_{po} \qquad (2.22)$$

Where ET_{po} is the evapotranspiration of dry canopy.

The potential transpiration rate, T_{pot} equals potential evapotranspiration rate ET_{po} of dry canopy, corrected for time needed to evaporate intercepted water by canopy, and minus soil evaporation:

$$T_{pot} = \left[1 - \frac{P_i}{ET_{pw}}\right] ET_{po} - E_p \qquad (2.23)$$

where ET_{pw} is the potential evapotranspiration rate of wet crop calculated using eq 2.19 assuming r_c=0

Actual soil evaporation

When the soil is wet, E_{act} is determined by the atmospheric demand and equals E_{pot}. In the case of dry soil, the soil hydraulic conductivity decreases, which reduces evaporation to E_a and is controlled by the maximum possible soil water flux E_{max} in the top few centimeters of soil. Soil hydraulic properties should be known for top few centimeters of soil, which are difficult to measure and variable in time due to rain, cultivation and crack formation (Van Dam et al, 1997).

In the present study, in SWAP it will be determined the actual evaporation rate by taking the minimum value of the potential evaporation rate from meteorological data, the maximum soil water flux according to Darcy, and the maximum evaporation rates according to the empirical functions.

Bottom boundary conditions

The bottom boundary condition can be specified as pressure head (Dirichlet condition), flux (Neumann condition) or a combination of two (Cauchy condition). With lower boundary specified, the connection between upper boundary condition, unsaturated soil column and the saturated zone is established. Once this relation is in place, surface water management influencing ground water depth like crop transpiration and irrigation application can be simulated options available in SWAP for bottom boundary conditions include, groundwater level as a function of time, flux to/from semi confined aquifer, flux to /from open surface drain, an upward flux as a function of groundwater or zero flux, free drainage and free outflow.

In our case, the daily measured groundwater table depth was used to describe the bottom boundary of the soil profile. In this case a field-average groundwater level is given as a function of time. SWAP will linearly interpolate between the days at which the groundwater levels are specified. The main advantage of this boundary condition is the easy recording of the phreatic surface in case of a present groundwater tables.

2.3.6 Soil hydraulic properties

For model applications, the soil profile was divided into five layers. The first layers is from 0-17cm, the second from 17-37cm, the third from 37-57cm, the fourth from 57-80cm and the fifth from 80-400cm. The relations between field measured soil water pressure head, field measured soil moisture content and unsaturated hydraulic conductivity were specified for each soil layer defined in the soil profile description. The Mualem-Van Genuchten (Van Genuchten., 1980) equations as incorporated in SWAP were used to determine the relationship between soil water content and hydraulic conductivity as a function of the pressure head. This relationship is defined on the basis of residual and saturated water content and parameters α, n and l, which determine the shape of the curve. The unsaturated hydraulic conductivity (K_{sat}) was estimated in a first step from the average between the values obtained using the ROSETTA Pedo-Transfer Functions (PTF) (Schaap et al., 2001) and the Rawls and Brakensiek., (1989) (see chapter 5), both widely adopted in the literature. Then automatic calibration was carried out using the algorithm of optimization SCEM-UN (Shuffled Complex Evolution Metropolis, Vrugt et al., 2003) in order to obtain the appropriate values of K_{sat} for the four layers.

2.4 IDRAGRA model

2.4.1 Introduction

IDRAGRA is a distributed-parameter, conceptual model, which allows the simulation of the distribution of irrigation water and the computation of the soil-water balance on a daily basis (Vassena et al., 2012). The model includes three main modules devoted to specific tasks: water sources, conveyance and distribution, soil-water balance (Gandolfi et al., 2010).

2.4.2 Soil hydraulic balance

The water-balance module (Galelli et al., 2010) accounts for the spatial variability of soils and crops and of meteorological and irrigation inputs, by subdividing the basin with a regular squared mesh in a usual application of the model: soil and crop characteristics, meteorological inputs, and irrigation supply are homogeneous in each cell of the mesh but may vary from cell to cell. Each cell identifies a soil volume which extends from the soil surface to the lower limit of the root zone. The representation of hydrological processes is one-dimensional (1D). The soil volume of each cell is subdivided into two layers: the top one (evaporative layer) represents the upper few centimeters of the soil, while the bottom one (transpirative layer) represents the root zone and has a time-varying depth Z_r. The two layers are modeled as two non-linear reservoirs in cascade. The water percolating out of the bottom layer constitutes the recharge to the groundwater system. The dynamics of the water content in the evaporative (top/first) layer of the cell is governed by the following balance equation:

$$\frac{dU_1}{dt} = P - I + Q_r - E_r - Q_1 + Q_i \qquad (2.24)$$

where: *dU1* [L] is the variation of water content of the layer per unit surface area of the cell during a time interval *dt*; *P* is the rainfall rate; *I* is the canopy interception; Q_r is the net runoff from the cell; E_r is the evaporation rate; Q_1 is the outflow to the second layer; Q_i is the irrigation supply. The dimensions of the terms in the right-hand-side of Eq. (2.24) are [L T^{-1}].

A similar equation holds for the dynamics of the water content U_2 [L] in the transpirative (bottom/second) layer:

$$\frac{dU_2}{dt} = Q_1 - T_r - Q_2 \qquad (2.25)$$

where T_r [L T–1] is the transpiration rate and Q_2 [L T–1] is the outflow from the root zone to the deeper subsoil.

Equations (2.24) and (2.25) are solved with an implicit finite difference scheme, with an hourly numerical integration time step.

For the comparison with SWAP model , IDRAGRA was applied to a single cell suitably parameterized (so it was not applied in a distributed way)

The following paragraphs describe the procedures for calculating the terms of evaporation (E), transpiration (T), the fluxes, Q_u, Q_g, Q_s and Q_e and the canopy interception I.

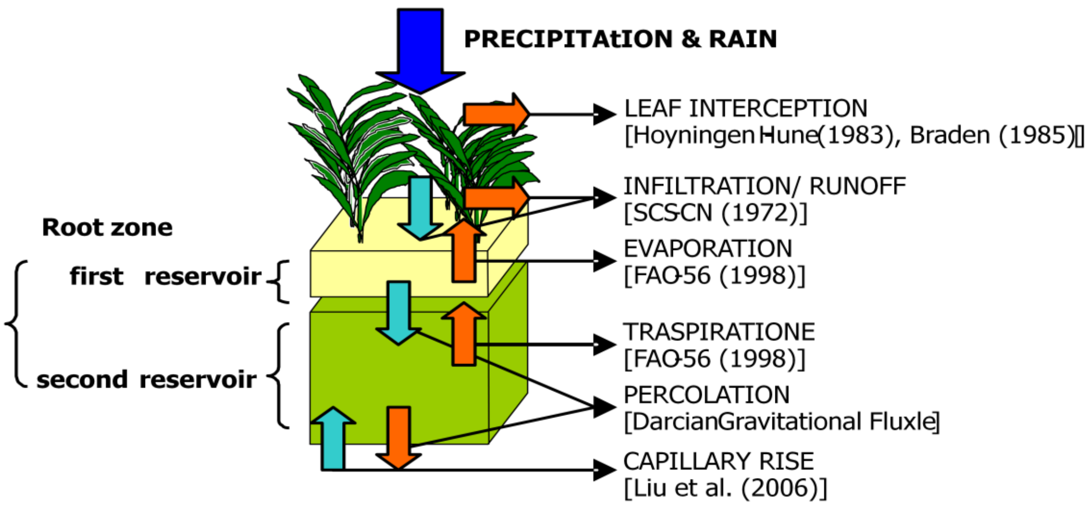

Figure 2.6 Schematic representation of process incorporated in IDRAGRA

2.4.3 Reference evapotranspiration

Evaporation and transpiration rates are estimated using the dual crop coefficient method proposed by Allen *et al*., (1998). According to this method; first, calculates the reference evapotranspiration using the Penman-Monteith equation:

$$ET_0 = \frac{0.408\Delta(R_n - G) + \gamma \frac{900}{T + 273} u_2(e_s - e_a)}{\Delta + \gamma(1 + 0.34u_2)} \qquad (2.26)$$

where :

ET_0 reference evapotranspiration (mm day^{-1}),

Rn: net radiation at the crop surface (MJ m-2 day^{-1}),

G: soil heat flux density (MJ m-2 day^{-1}),

T: air temperature at 2 m height (°C),

u_2: wind speed at 2 m height (m s^{-1}),

es: saturation vapour pressure (kPa),

ea: actual vapour pressure (kPa),

es-ea: saturation vapour pressure deficit (kPa),

Δ: slope vapour pressure curve (kPa °C^{-1}),

T: psychrometric constant (kPa °C^{-1}).

2.4.4 Actual transpiration

The transpiration rate T is obtained by multiplying ET_0 by a basal crop coefficient K_{cb} that takes into account the transpiration of the crop under optimum conditions, and by a coefficient K_s, which varies from 0 to 1 and is considered to quantify the effect of soil water stress on crop evapotranspiration (ET_c) :

$$T = K_s K_{cb} ET_0 \qquad (2.27)$$

The values of K_{cb} vary from one crop to another and for each crop it depends on the phenological stages. The curves which describe the daily trend of K_{cb} are characterized by four phases: Initial period (planting or green-up until about 10% ground cover; Crop Development period; from 10% ground cover until about 70% ground cover and higher (the maximum of the cover); *Mid Season period*; from 70% ground cover to the beginning of the late season period (the onset of senescence); and *Late Season period* (beginning of senescence or mid grain or fruit fill until harvest, crop death, frost-kill, or full senescence). An example of the curve is illustrated in Figure 4.7 the .K_{cb} values for different crops and different phenological stages are reported from various sources in the literature (Allen et al., 1998). These values ($K_{cb(tab)}$) are relative to a sub-humid climate (minimum relative humidity RH_{min}= 45%) and medium wind speed conditions (u_2 =2 m/s, 2 m above vegetation). To adjust K_{cb} for other conditions, the following equation is adopted:

$$K_{cb} = K_{cb(tab)} + [0.04(u_2 - 2) - 0.004(RH_{min} - 45)]\left(\frac{h}{3}\right)^{0.3} \qquad (2.28)$$

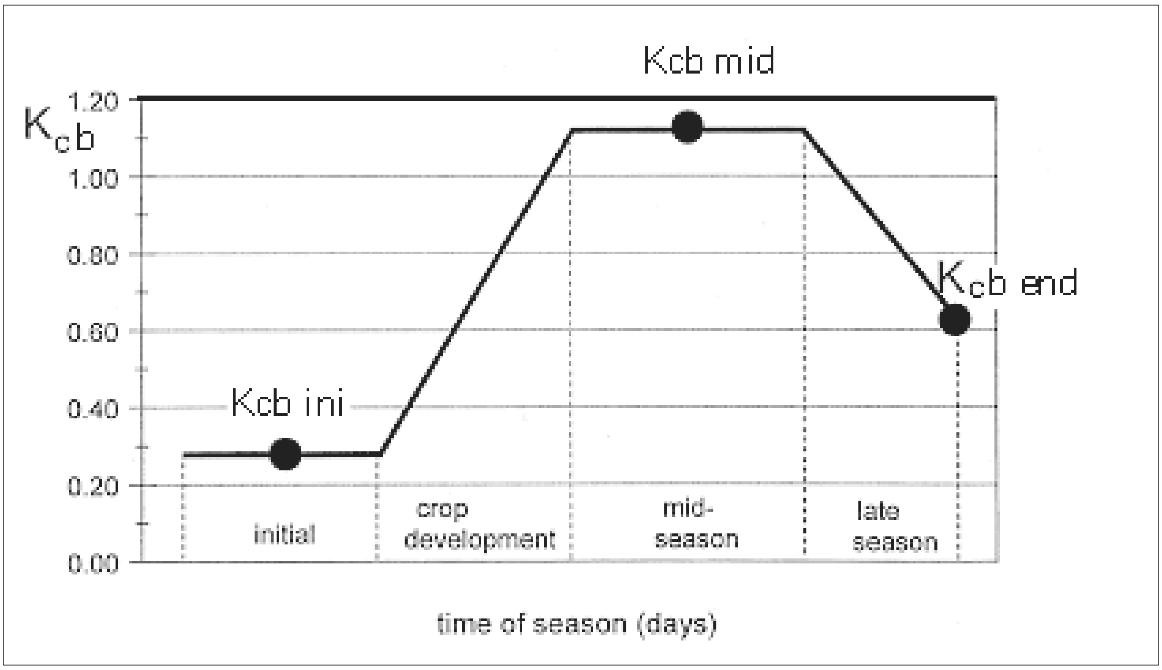

Figure 2.7 Constructed basal crop coefficient (kcb) curve (Allen et al., 1998)

The coefficient K_s varies from 0 to 1 and is used to represent the effect of limiting the transpiration due to low humidity conditions in the soil. The calculation of K_s is related to the following parameters in relation with the root zone: the Total Available Water for the crop TAW (mm) and the Ready Available Water RAW (mm) estimated as following:

$$TAW = 1000(\theta_{FC} - \theta_{WP})Z_r \qquad (2.29)$$

$$RAW = pTWA \qquad 0 < p < 1 \qquad (2.30)$$

where:

θ_{FC} the soil water content in the root zone at field capacity

θ_{WP} the soil water content in the root zone at wilting point

Z_r root depth (m) and p is a coefficient which varies from 0 to 1.

The values of the coefficient p are tabulated (Allen et al., 1998) for different crops and evapotranspiration under standard conditions (absence of stress) equal to 5 (mm / d). The value of p is adjusted according to the values of evapotranspiration under different conditions with the following formula:

$$p = p_{tab} + 0.04(5 - ET_c) \qquad (2.31)$$

The trend of K_s in relation with soil humidity Θ is illustrated in Figure 2.8 and calculated as following:

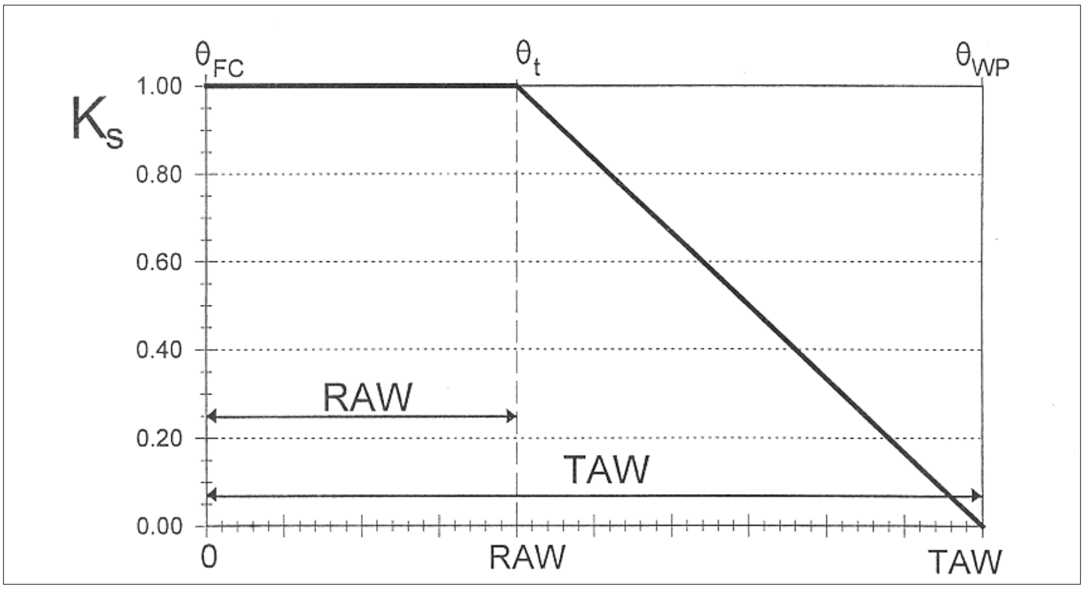

Figure 2.8 Trend of the water stress coefficient (Allen et al., 1998)

$$K_s = \begin{cases} 1 & if 0 \leq D_2 < RAW \\ \dfrac{TAW - D_2}{TAW - RAW} = \dfrac{TAW - D_2}{(1-p)TAW} & if RAW \leq D_2 < RAW \end{cases} \quad (2.32)$$

Where D2: water deficit, volume of water necessary to bring the average water content, θ, in the transpirative zone to the field capacity:

$$D_2 = 1000(\theta_{fc} - \theta)Z_r \quad (2.33)$$

2.4.5 Actual evaporation

The evaporation rate E is calculated by multiplying the evaporative coefficient Ke (determined as a function of soil moisture conditions), and reference evapotranspiration ET_0:

$$E = K_e ET_0 \quad (2.34)$$

The calculation of the coefficient K_e is done following the methodology of Allen et al, (1998):

$$K_e = min(K_r(k_{cmax} - K_{cb}), f_{ew}K_{cmax}) \quad (2.35)$$

where: K_{cb} is the basal crop coefficient; K_{cmax} is the maximum value of the sum K_{cb} + K_e which normally follows the rain or irrigation; K_r is the evaporation reduction coefficient (this coefficient varies with the amount of water available in the upper soil layer from where water is transferred to the evaporating soil surface layer. Kr is 1 if the soil is sufficiently wet (after rain or irrigation) and the soil evaporation is not hampered by water depletion. Kr decreases when the soil water depletion increases and is zero when the upper layer of the soil becomes air dry (AquaCrop manual., (2011); f_{ew} is the fraction of soil that is not covered by vegetation and wet, from which come the majority of evaporation. The calculation consists of :

✓ Determination of K_{cmax}:

$$K_{cmax} = max\left(\left\{1.2 + [0.04(u_2 - 2) - 0.004(RH_{min} - 45)]\left(\frac{h}{3}\right)^{0.3}\right\}, K_{cb} + 0.05\right) \quad (2.36)$$

where RH_{min} and u_2 are the minimum value of relative humidity (%) and the wind speed (ms^{-1}) measured at 2 m above the ground; h is the plant height (m).

✓ defining the coefficient Kr, according to a methodology which provides a threshold of soil moisture below which the available water is no longer able to fully support the evaporation. Then TEW (Total Evaporable Water, mm), and REW (Readily Evaporable Water, mm) are defined, which is a function of the characteristics of the soil (values tabulated as a function of texture) and represents the maximum volume of water that can evaporate without restrictions. TEW can be calculated as follows:

$$TEW = 1000(\theta_{fc,1} - 0.5\theta_{wp,1})Z_e \quad (2.37)$$

Where Z_e is the depth of the evaporative zone (m), θ_{fc} is the soil water content at field capacity and θ_{wp} is the water content at wilting point. The trend of K_r in relation to the value of the deficit D_1 (or the water content θ_1) is illustrated in Figure 2.9 and calculated as follows:

$$K_r = \begin{cases} 1 & \text{if } 0 \le D_2 < REW \\ \dfrac{TEW - D_1}{TEW - REW} = \dfrac{TEW - D_1}{(1 - P)TEW} & \text{if } REW \le D_1 < TEW \end{cases} \quad (2.38)$$

✓ define the coefficient f_{ew}, starting from the minimum between the value ($1-f_c$), which measures the average degree of land not covered by vegetation and the coefficient f_w which gives the average value of the fraction of wet soil during the rain or the irrigation.

$$f_{ew} = min(1 - f_c, f_w) \quad (2.39)$$

The coefficient f_w depends on the method of irrigation adopted (for surface irrigation it is always equal to 1) and is always equal to 1 during the rain. The coefficient f_c depends not only on the type of vegetation but also on the crop phenological stage. In the absence of direct measurements, it can be calculated using the expression:

$$f_c = \left(\frac{K_{cb} - K_{cmin}}{K_{cmax} - K_{cmin}}\right)^{(1+0.5h)} \quad (2.40)$$

Where: K_{cb} is the basal crop coefficient; K_{cmin} is the minimum value of $K_{cb} + K_e$ for dry bare soil (K_{cmin} can be assume between 0.15 and 0.20); K_{cmax} is the maximum value of $K_{cb} + K_e$ and h is the average plant height (m).

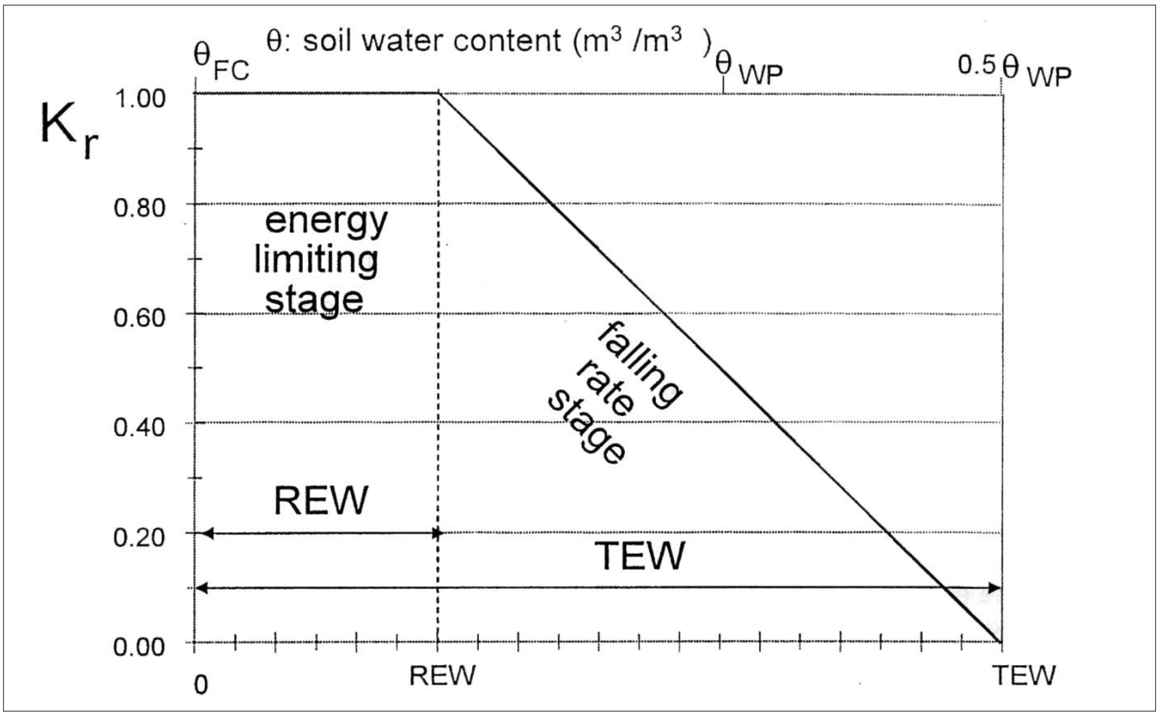

Figure 2.9 The reduction coefficient Kr (Allen et al., 1998)

2.4.6 Surface Runoff

The precipitation, after a partial interception by the vegetation, reaches the ground. This water supply can penetrate the soil (infiltration) or flows over the land (runoff). The study of these two processes, highly interdependent, is one of the classic topics on hydrology and is documented by many publications. More rigorous approaches are quite complex and even difficult to use in operational practice. Numerous methods are also available, based on a simplified interpretation of the processes, easier to use (see, for example, CIGR., 1999). Among these, certainly one of the most popular and well documented is the Curve Number method of the Soil Conservation Service of the United States (USDA-SCS., 1972). The runoff curve number (also called a curve number or simply CN) is an empirical parameter used in hydrology for predicting direct runoff or infiltration from rainfall excess. The runoff curve number is based on the area's hydrologic soil group, land use, treatment and hydrologic condition. The runoff equation is:

$$Q_u = \frac{(P - I_a)^2}{P - I_a - S} \qquad (2.41)$$

Where Q is runoff [L]; P is rainfall , S is the potential maximum soil moisture retention after runoff begins, Ia is the initial abstraction, or the amount of water before runoff, such as infiltration, or rainfall interception by vegetation; and it is generally assumed that Ia= 0.2S where:

$$S = 25.4\left(\frac{1000}{CN} - 10\right) \qquad (2.42)$$

So Q_u becomes:

$$Q_u = \frac{\left[P - 5.08\left(\frac{1000}{CN} - 10\right)\right]^2}{\left[P + 20.32\left(\frac{1000}{CN} - 10\right)\right]} \qquad (2.43)$$

The parameter CN depends on land use, soil hydraulic characteristics, land slope and humidity conditions.

The values of the reference CN (CN_{II}^{tab}), for a slopes of 5%, and average humidity conditions between field capacity and wilting point (Antecedent Moisture condition II), are tabulated in USDA-SCS., (1972), as a function of four factors that characterize the local conditions of the soil: usage, practices and hydrological classifications and conditions. With regard to the classification, the soils are classified by SCS, into four hydrological groups - A, B, C, and D - according to the infiltration capacity and the intensity of transmission that characterizes them. The value CN_{II}^{tab}, is adjusted for slopes different from 5%:

$$CN_{II}^{slo} = CN_{II}^{tab} + \frac{CN_{II}^{tab}\{1 - exp[0.00673(100 - CN_{II}^{tab})]\}}{3}\,[1 - 2exp(-13.86i)] \qquad (2.44)$$

An additional correction can be made in order to take into account different phenological stages

$$CN_{II} = \begin{cases} \left(CN_{II}^{slo}\right)_{bare\ soil} & (1) \\ 2CN_{II}^{slo} - \left(CN_{II}^{slo}\right)_{bare\ soil} & (2) \\ CN_{II}^{slo} & (3) \\ \left(CN_{II}^{slo}\right)_{bare\ soil} & (4) \end{cases} \qquad (2.45)$$

where

(1): the period before sowing

(2): the period between sowing and harvesting

(3): the period of the maximum development and just before harvesting

(4): the period after harvesting

Finally, a last correction is setup to take into account the relative soil humidity (SWAT website). The considered humidity value is the sum of relative humidity on the two layers: $\theta = \theta_1 + \theta_2$. For the corresponding soil moisture conditions Θ_{wp} and Θ_{fc}, (Antecedent Moisture Conditions I and III, respectively) the value of the CN is modified as following:

$$CN_I = CN_{II} - \frac{20(100 - CN_{II})}{100 - CN_{II} + exp[2.533 - 0.636(100 - CN_{II})]} \qquad (2.46)$$

$$CN_{III} = CN_{II} exp[0.00673(100 - CN_{II})] \qquad (2.47)$$

For intermediate moisture conditions, the CN value is obtained by linearly interpolating its extremes:

$$\text{CN} = \begin{cases} \frac{CN_{II} - CN_I}{\Theta_{fc,wp} - \Theta_{wp}}(\Theta - \Theta_{wp}) + CN_I & if\ \Theta_{wp} \le \Theta < \Theta_{fc,wp} \\ \frac{CN_{III} - CN_{II}}{\Theta_{fc} - \Theta_{fc,wp}}(\Theta - \Theta_{fc,wp}) + CN_{I\,I} & if\ \Theta_{fc,wp} \le \Theta < \Theta_{fc} \\ \frac{CN_{IV} - CN_{III}}{\Theta_{sat} - \Theta_{fc}}(\Theta - \Theta_{fc}) + CN_{III} & if\ \Theta_{fc} \le \Theta < \Theta_{sat} \\ CN_{IV} & if\ \Theta \ge \Theta_{sat} \end{cases} \qquad (2.48)$$

where the threshold values for CN_{IV} and $\Theta_{fc,\,wp}$ are:

$$CN_{IV} = 95 \qquad \Theta_{fc,wp} = \Theta_{wp} + \frac{2}{3}(\Theta_{fc} - \Theta_{wp}) \qquad (2.49)$$

2.4.7 Canopy Interception

In IDRAGRA, the canopy interception is calculated as for SWAP model using the general formula proposed by Von Hoyningen-Hüne., (1983) and Braden., (1985)

$$I = a\ LAI\left(1 - \frac{1}{1 + \frac{bp}{a\ LAI}}\right) \qquad (2.50)$$

Where:

I: intercepted precipitation (cm d^{-1})

p: gross precipitation (cm d^{-1})

LAI: leaf area index (-).LAI value depends on crop development

a: empirical coefficient (cm d^{-1})

b: soil cover fraction (= LAI/3)

the two parameters in the latter equation, LAI and b, are strongly correlated, and generally we assume that b = LAI/3.

Regarding a, it is almost constant for the most common crops and it can be assumed to be a=0.25cm.

The method of Von Hoyningen-Hüne and Braden is based on daily precipitation values, so
daily rainfall must be specified in the meteorological input file.

Once the interception is calculated, it is possible to determine the value of efficient precipitation P_{eff} as a difference between gross rainfall and interception: $P_{eff} = P-I$

2.4.8 Infiltration

There are two events contribute in the generation of runoff and infiltration phenomina, rain and irrigation intervention, if sprinkler methods are used. The values of runoff Q_u and infiltration Q_i are expressed by the following equations:

$$Q_u = Q_u^{rain} + Q_u^{irr} \qquad (2.51)$$

$$Q_i = Q_i^{rain} + Q_i^{irr} \qquad (2.52)$$

Where Q_u^{rain} and Q_u^{irr} are the runoff related to rain and irrigation events respectively. Similarly Q_i^{rain} and Q_i^{irr} are the infiltration due to rain and irrigation.

Depending on the event, the latter equations are calculated as following:

Rain event: in this case, the value of Q_u^{rain} is calculated as following:

$$Q_u = \frac{(P - I_a)^2}{P - I_a - S} \qquad (2.53)$$

Then a comparison is made between the values of I_a ; initial loss of the CN model, and I; loss due to the crop interception estimated with Von Hoyningen-Hüne., (1983) and Braden., (1985) methods. In order to consider the maximum value of efficient precipitation , losses are minimized as following:

$$P_{eff} = \begin{cases} P - I & if\ I \leq I_a \\ P - I_a & if\ I > I_a \end{cases} \qquad (2.54)$$

Where P is the gross precipitation.

With the adjusted value of efficient precipitation calculated by the difference between the quantities of infiltrated water in the soil:

$$Q_i^{rain} = P_{eff} - Q_u^{rain} \qquad (2.55)$$

Irrigation event: in this case the irrigation supply is not processed by the CN model but it is assumed that there is no water lost by runoff:

$$Q_u^{irr} = 0 \qquad (2.56)$$

$$Q_i^{irr} = P_{eff} = P - I \qquad (2.57)$$

2.4.9 Percolation

The percolation in IDRAGRA is understood as both, outgoing water from evaporative to transpiration layer and the water coming out of this layer to the groundwater. The percolation is influenced by the presence of shallow water table, which can reduce the water flux or even contribute to a water supply in the root zone.

As in the case of the runoff and infiltration, the description of the percolation process requires mathematical formulations rather complex at least in the applications to entire irrigation districts, while these formulae may not be as representative when applied to larger scales. Accordingly, it is common to use simplified approaches, while within the limits of validity of the hypothesis on which they are based, are much easier to use. In the case of the water balance equation (eq 2.24 and 2.25), and for the use of a daily time step, it is justified to choose a simple approach, based on the assumption that the percolation occurs at a constant rate, equal to the hydraulic conductivity for specific soil moisture conditions. At each daily time step, the flows of percolation Q_e and Q_s [mm] are expressed by the following relations:

$$Q_e = 3600(K_1(\theta_1)\Delta t)10 \qquad (2.58)$$

$$Q_s = 3600(K_2(\theta_2)\Delta t)10 \qquad (2.59)$$

Where K_1 and K_2 (cm / h) are, respectively, the hydraulic conductivity of evaporative and transpiration layers; the hydraulic conductivity depends on the soil moisture content and is expressed following Brooks & Corey (1964):

$$K_1(\theta_1) = K_{sat,1}\left(\frac{\theta_1 - \theta_{r,1}}{\theta_{sat,1} - \theta_{r,1}}\right)^n \qquad (2.60)$$

$$K_2(\theta_2) = K_{sat,2}\left(\frac{\theta_2 - \theta_{r,2}}{\theta_{sat,2} - \theta_{r,2}}\right)^n \qquad (2.61)$$

where $K_{sat,1}$ and $K_{sat,2}$ are the conductivity at saturation of the two layers, $\theta_{sat,\,1}$ and $\theta_{sat,1}$, $\theta_{r,1}$ and $\theta_{r,2}$ are respectively the moisture contents at saturation and residues, and n is geometrical factor. The percolation model expressed by equations (2.58) and (2.59) was adjusted in order to take into account the major flows in transit through the basin during an irrigation event, due to the spatial variability of the actual contributions in the field. For a soil model formed of “p” of basins, the percolation flow of the j^{th} basin is expressed as following:

$$Q_j = 3600\big(K_j(\theta_j)\Delta t\big)10 \qquad for\ j = 1 \ldots p \qquad (2.62)$$

In the proposed model of two basins, the percolation flows Q_1 and Q_2 are respectively Q_e and Q_s. The modification of the model reproduces a trend of percolation in time, with an exponential decrease and therefore, the latter equation is corrected to be:

$$Q_j^* = a\left(K_{sat,j} method\ of\ irrigation\right)e^{-g}\ \ Q_j \qquad per j = 1 \dots p \qquad (2.63)$$

Where g is the number of days elapsed since the last irrigation, a is a parameter that depends on the methodology of irrigation and in the simulation it is assumed to be inversely proportional to K_{sat}:

$$a = \begin{cases} a^{sup} & if\ K_{sat,j} \le K_{sat,j}^{inf} \\ \dfrac{a^{sup} - a^{inf}}{K_{sat,j}^{inf} - K_{sat,j}^{sup}}\left(K_{sat,j} - K_{sat,j}^{sup}\right) + a^{inf} & if\ K_{sat,j}^{inf} < K_{sat,j} < K_{sat,j}^{sup} \\ a^{inf} & if\ K_{sat,j} \le K_{sat,j}^{sup} \end{cases} \qquad (2.64)$$

Where:

$k_{sat,j}^{inf}$ value assumed by 10 percent of the $K_{sat,j}$ value of j^{th} reservoir

$k_{sat,j}^{sup}$ value assumed by 90 percent of the $K_{sat,j}$ value of j^{th} reservoir

a^{inf} minimum value that the parameter a can assume in the range of values attributed to the irrigation method adopted:

$$a^{inf} = \begin{cases} 5\ for\ surface\ irrigation \\ 10\ for\ sprinkler\ iriigation \end{cases}$$

a^{sup} maximum value that the parameter a can assume in the range of values attributed to the irrigation method adopted:

$$a^{sup} = \begin{cases} 15\ for\ surface\ irrigation \\ 30\ for\ sprinkler\ irrigation \end{cases}$$

For surface irrigation a varies in 5÷15 while in 10÷30 for sprinkler irrigation

2.4.10 Cappilary rise

The process of capillary rise is produced as a result of the particular gradient of matric potential, that are determined in the presence of a shallow water table. Capillary rise is strongly influenced by the soil water content and the evapotraspiration rate, as well as by the soil properties.

Several authors (Doorenbos and Pruitt., 1977, Malik et al., 1989, Li and Dong., 1998; Said., 1999; Martin and Gilley., 1993; Danuso et al., 1995; Deproost and Raes., 2003) have proposed an empirical relationships that estimates the capillary rise , which are incorporated in reservoir models for the description of the dynamics of soil water content in the soil. In IDRAGRA it has been selected the relation proposed recently by Liu et al., (2006).

According to the adopted approach, the capillary rise flow is estimated at 1 m depth from the ground (assuming the roots at a constant depth of 1m). The maximum G_{max} capillary rise depends only on the depth of the water table: with decreasing the depth, capillary rise increases. If the water table is particularly very shallow, with a depth less than a critical value D_{wc} (critical groundwater depth), the process tends to become stable to a maximum value assumed to be equal to the potential transpiration T_c.

The actual value of capillary rise G_c is calculated based on water content of the root zone. The capillary rise equals to zero when the water content exceeds a threshold W_c (critical soil water storage), expressed as a function of soil characteristics and water table depth. When the hydrological processes reduce the water content, capillary rise increases to its maximum value G_{max}. The capillary rise does not depend on water content when it gets below a certain threshold W_s (steady soil water storage), which is a function of soil characteristics and water table depth. If the water content is between the two thresholds, the flow of capillary rise varies linearly between zero and Gmax. This is expressed by the relation:

$$G_c = \begin{cases} G_{max}(D_w, ET_c) & if\ W < W_s(D_w) \\ G_{max}(D_w, ET_c)\left[\dfrac{W_c(D_w) - W}{W_c(D_w) - W_s(D_w)}\right] & if\ W_s(D_w) < W < W_c(D_w) \\ 0 & if\ W > W_c(D_w) \end{cases} \quad (2.65)$$

where G_c is capillary rise (mm/d), W is the water content in a soil thickness of 1m (mm), ET_c is the potential evapotranspiration (mm/d), and D_w is the water table depth (m), G_{max} is the maximum value of capillary rise (mm/d), and is function only of water depth and evapotranspiration.

The two critical threshold of water content in the root zone, W_c and W_s are defined by the following relations:

$$W_c = a_1 D_w^{b_1} \quad (2.66)$$

$$W_s = a_2 D_w^{b_2} \quad (2.67)$$

b_1 and b_2 are empirical parameters that depend on the type of soil, a_1 is a parameter that is suggested to put equal to W_{fc} (mm) for a thickness of 1m), a_2 is given by the relation:

$$a_2 = 1.1\,\frac{W_{fc} - W_{wp}}{2} \quad (2.68)$$

where W_{wp} (mm) is water content at wilting point.

The critical depth of groundwater, D_{wc}, is calculated using the following relations:

$$D_{WC} = \begin{cases} a_3 ET_c + b_3 & if\ ET_c \le 4mmd^{-1} \\ 1.4 & if\ ET_c > 4mmd^{-1} \end{cases} \quad (2.69)$$

where a_3 and b_3 are empirical parameters that depend on the type of soil.

Finally, the value G_{max} is calculated according to the following relations:

$$G_{max} = \begin{cases} ET_c & if\ D_W \leq D_{WC} \\ a_4 D_w^{b_4} & if\ D_W \leq D_{WC} \end{cases} \quad (2.70)$$

where a_4 and b_4 are again empirical parameters that depend on soil type.

Because the soil water balance model takes into account the time variation of the root depth and considers the flow of capillary rise in the transpiration layer, the relation (eq 2.65) has been modified as follows:

$$G_c = \begin{cases} G_{max}(Dr_w, ET_c) & if\ \theta_2 < \ \theta_{s,2}(Dr_w) \\ G_{max}(Dr_w, ET_c)\left[\dfrac{\theta_{c,2}(Dr_w) - \theta_2}{\theta_{c,2}(Dr_w) - \theta_{s,2}(Dr_w)}\right] & if\ \theta_{s,2}(Dr_w) < \theta_2 < \theta_{c,2}(Dr_w) \\ 0 & if\ \theta_2 > \ \theta_{c,2}(Dr_w) \end{cases} \quad (2.71)$$

Where D_{rw} (m) is a variable which takes into account the greater influence of the water table during the growth of roots, defined by the following relation:

$$Dr_w = 1 + Dz_w \quad (2.72)$$

Where D_{zw} (m) is the distance between the water table and the roots, D_{zw} is less than the effective water table depth, so as to have (for the same depth of the water) a greater capillary rise.

θ_2, $\theta_{c,2}$, $\theta_{s,2}$ are respectively the average values of water content (-) of the transpiration layer and the two water contents of upper and lower threshold of the same layer. θ_2 is expressed by the relation:

$$\theta_2 = \frac{W_2}{1000(Z_r - Z_e)} \quad (2.73)$$

Where W_2 is the water content (mm) of the transpiration layer at the thickness of Z_r - Z_e (m), Z_r is the root depth and Z_e is the thickness of the evaporative layer respectively; relations are valid for $\theta_{c,2}$ and $\theta_{s,2}$. Similarly, because of the variability of the root depth, the relation (of D_{wc}) that defines the critical value of water table depth D_{wc} (m), below which the maximum value of capillary rise is assumed to be equal to the potential transpiration T_c, and has been modified according to the following relationship:

$$D_{WC} = \begin{cases} a_3 ET_c + b_3 & if\ ET_c \leq 4mmd^{-1} \\ Z_r + 0.4 & if\ ET_c > 4mmd^{-1} \end{cases} \quad (2.74)$$

3 Ground Water Recharge And Capillary Rise Contribution To Supply Plant Water Requirement

3.1 Introduction

World population today is about 6.5 billion and it is estimated that it will increase up to 9.1 billion by the year 2050 (UN, 2004). Irrigation supplies approximately 40% of the world foodstuffs on less than 18% of the arable land and has a significant future role in meeting the projected world food demand (Ayars et al., 2006). It is estimated that irrigation consumes more than 80% of the fresh water with an appreciable contribution coming from groundwater resources. This makes it the greatest user of water, very far from its other competitors, mainly urban, industrial and environmental use. It is more than certain that competition among agricultural, urban, industrial and environmental needs will be even more intense in the near future. Any effort towards improving irrigation efficiency is worthwhile because it can lead to saving large quantities of good quality water .

Most of the 750-800 billion m^3yr^{-1} of global groundwater withdrawals are used for agriculture (Shah et al., 2000). During the last 10 to 20 years, there has been a significant increase in the utilization of groundwater resources for agricultural irrigation, because of their widespread distribution and low development cost (Clarke et al., 1996). This has not been restricted to semi-arid regions, but also occurred in more humid areas, in order to provide a greater intensity as well as more reliable supplies for existing cultivated areas. Groundwater can be obtained either by extraction from aquifers or by means of capillary rise.

The humid climate is characterized by a surplus of precipitation over soil evaporation and plant transpiration, and no distinct monsoon. Precipitation becomes the primary source of recharge, whereas seepage from watercourses, other surface bodies, terrain depressions, fractures, and diversion from denser soil or paved areas contribute indirectly with a trivial volume (Lerner *et al.*, 1990). Once infiltrated and reduced by evapotranspiration, the rest of the moisture percolates down through the vadose zone to the water table, which, when it is shallow, allows for some to be driven back by a capillary rise in response to the evapotranspiration demand.

The rates of recharge and discharge (by direct evaporation and crop root uptake through capillary rise) are known to be the most difficult and uncertain components to estimate in groundwater budget, and they often vary spatially and temporally, (Xu et al., 2012; Hendrickx and Walker, 1997; Sophocleous., 2005).

This issue has dragged increasing attentions during the last decades and reputedly attends were carried out to find the best way for more realistic estimation of those rates.

3.2 Groundwater Recharge

3.2.1 Introduction

Groundwater recharge can be defined as the amount of water added to the groundwater reservoir in excess of soil moisture deficits and evapotranspiration by direct percolation through the vadose zone. It is the resultant of variable weather conditions, root uptake, processes of soil water flow, and vadose zone properties (Gehrels., 1999).

There are various sources of recharge to a groundwater system. Direct (precipitation and irrigation) recharge in which water is added to the groundwater reservoir in excess to soil moisture deficits and evapotranspiration. Indirect recharge is that type where water percolates to water table through the beds of surface watercourses. The current study deals with direct recharge.

Quantitative understanding of the process of groundwater recharge is fundamental to the sustainable management of groundwater resources (Scanlon et al., 2002).

3.2.2 Factors that affect groundwater recharge

Groundwater recharge can be affected by many parameters and complex processes which themselves are influenced by many factors. Precipitation is affected by climatic factors such as wind and temperature, resulting in complex and dynamic distributions while the intensity and spatial distribution of precipitation influences the amount of the recharge.

Large scale vegetation determines the amount of net rainfall, infiltration rate, deep drainage and the available storage capacity of the groundwater system. Any change in vegetation, say from forest to grassland can have a large effect on recharge. The nature of land cover has a big influence on recharge and hence groundwater recharge modeling should not assume that vegetation is a constant factor. For example, the removal of the indigenous vegetation in large parts of south eastern Australia more than 100 years ago caused a significant increase in groundwater recharge (Scanlon et al., 2006).

Vegetation influences recharge through interception and transpiration. The amount of stored water that can be removed by vegetation depends mainly on the rooting depth (Jyrkama and Sykes., 2007). It will be known that the degree of water saturation of the root zone determines the distribution of hydraulic conductivity and as a result the percolation to the groundwater table. It also influences the water uptake by roots and thus the actual evapotranspiration (Berendrecht., 2004).

Thus the process of groundwater recharge is not only influenced by the spatial and temporal variability in the major climate variables, but also dependent on the spatial distribution of land-surface properties and the depth and hydraulic properties of the underlying soils.

3.2.3 Groundwater recharge estimation techniques

A number of methodologies are used to estimate recharge. According to many authors (Jimenez-Martinez et al., 2009; Bethune et al., 2008; Moon et al., 2004) these can be classified as:

- direct or indirect;
- physical, chemical, or isotopic;
- methods based on the analysis of inflow, outflow, or aquifer response;
- methods based on the unsaturated or saturated zones; and
- methods based on numerical modeling of groundwater flow, soil-water flow, both soil and groundwater flows, or modeling of the hydrologic balance at plot, field, or watershed scales.

Additional classifications also exist. Within each methodology, a number of estimation techniques are available. Here we combine these methodologies into two groups: *physical methods* and *tracer methods*.

Physical Methods

Physical methods rely on direct measurements of hydrological parameters, or on estimates of soil and/or aquifer physical parameters. Physical methods are frequently used to estimate precipitation recharge because they are quick, inexpensive, or straightforward. Nevertheless, with prudent appreciation of their limitations, physical methods can be a helpful tool for evaluating precipitation recharge.

Indirect Physical Methods

Indirect physical methods for estimating groundwater recharge consist of:

- empirical methods,
- water balance methods based on estimates of soil physical properties, and
- numerical modeling methods.

Methods relying on estimates of soil physical parameters generally fall into the following classes:

- soil-water balance,
- zero-flux plane method,
- estimation of water fluxes beneath the root zone using unsaturated hydraulic conductivity and the gradient in soil-water potential, and

• estimation of water fluxes in the saturated zone based on Darcy's law and flow-net analysis.

Additional methods also exist that may not fit well into one of these classes, such as gravity surveys for measuring changes in aquifer storage resulting from recharge events. Increased accuracy in measuring temporal variations in the Earth's gravity field has recently allowed the use of gravity observations to deduce subsurface water mass changes resulting from precipitation and consequent recharge events.

Water Balances: This group of methods estimates recharge as the *residual* of all other fluxes. The principle is that other fluxes can be measured or estimated more easily than recharge. Examples of water balance methods include:

- *Soil-moisture budgets*: The basis of recharge estimation using a soil moisture balance technique is that a soil becomes free draining when the moisture content of the soil reaches a limiting value called the field capacity; excess water then drains through the soil to become recharge. To determine when the soil reaches this critical condition it is necessary to simulate soil moisture conditions on a daily basis throughout the year. This involves the representation of the relevant properties of the soil and the capacity of crops to collect moisture from the soil and to transpire water to the atmosphere. If no crops are growing or if there is only partial crop cover, bare soil evaporation must be considered. Bare soil evaporation is important both in semi-arid locations to represent soil moisture conditions at the end of the dry season and in temperate climates where recharge occurs in winter when evaporation is usually the major loss from soil. The input to the soil moisture balance is infiltration which is equals the daily precipitation minus interception or runoff.
- *River-channel water balances:* upstream and downstream flows are differenced to calculate recharge or–more accurately–*transmission losses*. (A related stream hydrograph analysis technique based on baseflow-separation techniques is founded on steady-state water-balance calculations, whereby the estimate of discharge based on baseflow-separation or baseflow-recession analysis of the stream hydrograph, must equal recharge. This technique is considered too empirical and approximate to give reliable quantitative estimates.)
- *Water-table rises:* the volume stored beneath a rising water table is equated to recharge, after allowing for other inflows and outflows such as pumping wells and aquifer through flow.

The simplicity of the latter method made it a popular one. However, calculating the volume of water stored between lowest and highest water table positions over a study period interval involves reliable estimates of the aquifer's *specific yield* values, which may be difficult to obtain.

The advantages of water-balance methods are that they use readily available data (rainfall, runoff, water levels), are easy to apply, and account for all water entering a system. The major disadvantage is that recharge is the residual or remainder of all other hydrologic components in the water balance equation, and constitutes only a small difference between large-number components, such as precipitation and evapotranspiration. Other disadvantages include the difficulty of estimating other fluxes in the water balance equation. For example, evapotranspiration cannot be measured easily, yet it is often the largest outward flux. Physical properties like specific yield are central to some water-balance methods, such as those based on water-table rises, but are not easily defined or measured.

Zero-Flux Plane Method: The zero-flux plane (ZFP) method relies on locating a plane of zero hydraulic gradient in the soil profile. Recharge during a time interval is obtained by summation of the changes in water content below this plane. Unfortunately, the method breaks down in periods of high infiltration when the hydraulic gradient becomes positive downward throughout the profile. This is when recharge fluxes are likely to be highest. Use of this technique can give good estimates of recharge for periods during the year when the ZFP exists.

Estimation of Unsaturated Water Fluxes: Several studies have reported use of unsaturated zone hydraulic conductivity $K(\theta)$ or $K(\psi)$, and water retention data, (ψ, θ), to solve either Darcy's law or Richards' equation in the unsaturated zone, and to estimate soil-water flux for periods of months to years. If the water flux is calculated at such a depth in the profile that no further extraction by roots occurs, then the flux will be equal to groundwater recharge

$$R = K(\theta)\Delta H_T$$

where ΔH_T is the total head gradient. For most soil systems, $H_T = H_g + H_m$, where H_g is the gravity head and H_m is the *matric suction* head.

Both $K(\theta)$ and $K(\psi)$ relationships are difficult and time consuming to determine, in the field or in the laboratory, with difficulty and uncertainty increasing with soil dryness. Slight differences in measured water content translate into large differences in unsaturated hydraulic conductivity. As a result the annual recharge flux could vary significantly, depending on how the mean hydraulic conductivity is computed.

Estimation of Saturated Water Fluxes: An equivalent method for recharge estimation, based on saturated flow governed by Darcy's law, is simpler, especially when assuming steady state conditions and employing flow-net analysis. The only measurements needed are values of hydraulic head and hydraulic conductivity to construct a quantitative *flow net*. This consists of a set of intersecting lines of equal hydraulic head values (known as equipotential lines) and flow lines representing two-dimensional steady flow through a porous medium. Two-dimensional, vertical flow nets constructed along the general groundwater flow direction from water table and hydraulic head field measurements provide an approximate but straightforward way of identifying areas of recharge and discharge, and thus of estimating recharge.

Numerical Models for Estimating Recharge: Different types of models are available for estimating groundwater recharge:

- numerical models that solve one-, two-, or three-dimensional forms of the water flow or Richards equation,
- parametric hydrologic models that use a numerical or analytical relationship between infiltration or precipitation and recharge,
- groundwater flow models, and
- combined or integrated watershed and groundwater models.

Numerical modeling methods take transient flows and storage changes into account and can include spatial variability of physical properties, of which hydraulic conductivity is one of the most important. However, data requirements and computing load are both high. Such models are used to estimate model parameters based on known values of hydraulic head. Such an approach is known as a solution of an inverse problem. This is in contrast to the forward or direct problem, where model parameters are considered known and hydraulic head is computed.

Should one possess the analytical expressions for hydraulic head and transmissivity in the groundwater flow equation, determination of recharge would be a trivial exercise of calculus in computing the derivatives of the groundwater flow equation. However, hydraulic heads are always measured with a degree of inaccuracy. Differentiating such noisy data leads to large errors in recharge estimation.

Integrated watershed and groundwater models allow a complete analysis of the land-based hydrologic cycle, thus providing the means for evaluating the impacts of land use, irrigation development, and climate change on both surface water and groundwater resources. Such models allow predictions of the impact of management changes on total water supplies, including recharge. The seasonal variation of water table levels and recharge can be more accurately predicted by the soil-moisture accounting system employed in the integrated model than by using only a groundwater model. This increased flexibility, however, comes at the expense of increased complexity and the expertise needed to use integrated watershed modeling effectively. Although integrated models require extensive data, such integrated modeling constrains the adjustment of model parameters during calibration because overall water budgets must be observed. Whereas traditional methods used to calibrate groundwater models may include adjustments to recharge rates, in an integrated model recharge is completely constrained by the overall water budget for the surface-water system. In addition, stream–aquifer interactions, including stream-derived recharge, are constrained by the generated amount of surface runoff to streams. This, in turn, impacts on the stream stage and thus the driving forces for stream–aquifer interaction.

The principal advantages of the numerical methods are that they attempt to represent the actual physical processes of interest, and that they allow predictions of future recharge regimes resulting from different land uses and climatic changes. These advantages are often countered by the need to make simplifying assumptions in order to reduce the computational effort. For example, numerical models of the soil zone usually assume a single-porosity medium with no spatial variation in properties. In practice many soils may have dual porosity, with preferred pathways during high saturation: in other words, at times of recharge.

The correct timescale for such models depends on the rate of fluctuation of heads, varying from seconds for rainfall into soil to seasonal or longer spans for seepage between aquifers. Effectively addressing the multiple temporal (as well as spatial) scales involved in recharge estimation constitutes a major problem in modeling recharge processes. In addition to such obstacles and uncertainties, large data requirements often make application of numerical models difficult.

Direct Physical Methods

In contrast to the numerous indirect physical methods, there is only one *direct* method for estimating diffuse recharge. This involves the construction of a lysimeter. Lysimeters comprise enclosed blocks of disturbed or undisturbed soil, with or without vegetation, that are hydrologically isolated from the surrounding soil in order to assess or control various elements of the water balance. There is also only one direct method for estimating indirect recharge associated with surface water bodies in direct hydraulic connection with an underlying aquifer. This involves the use of seepage meters inserted in the streambed or lakebed that can provide direct point measurements of localized recharge.

Lysimeters are expensive and permanent instruments. They are typically filled with disturbed soils, which generally have water content profiles that differ to some degree from those found in surrounding soils. Drainage can occur only when a water table develops at the base of the lysimeter, unless solution samplers (such as ceramic cup extractors) and a vacuum system are installed at the base. This last factor, however, is unlikely to be a problem if the lysimeter is relatively deep and the vegetation is shallow-rooted. While lysimeters have been useful in quantifying drainage at waste sites under arid conditions, they have limited ability to document the spatial variability produced by natural and human-induced changes in surface and subsurface flow pathways. Construction cost and logistics limit size and depth to generally no more than a few square meters and a 3 m depth, although lysimeters as deep as 18 m have been constructed. Because lysimeters are effective for the study of recharge mechanisms, and yield the high-quality data needed in computer model calibration for simulating the water balance, some specialists recommend that more lysimeter-recharge studies be undertaken worldwide in a variety of climatic and soil conditions. However, the initial construction costs and the long-term monitoring requirements represent a serious extended commitment.

Seepage meters were originally developed to measure canal seepage losses. They involve a seepage bell or cylinder that is pushed into the canal-bed sediment, the infiltration rate being measured by constant or falling head techniques. Their advantages include being:

- lightweight and easily transportable,
- relatively cheap,
- simple to operate,
- rapidly measurable, and
- producing observations that are directly convertible into a seepage value.

Difficulties are encountered in gravelly or stony sediments, or in sandy sediments, which may be washed from around the seepage cylinder by eddy currents and sediment disturbance, or because of an ineffective seal around the inserted seepage cylinder. The number of measurements per unit of area needed to arrive at a reasonable average depends on the degree of heterogeneity in the seepage loss at the specific site. In conclusion, the seepage meter gives a rapid and direct measurement at low cost, but the figures obtained are only point measurements.

Tracers for Recharge Estimation

The natural tracers most commonly used in recharge studies are ^{3}H, ^{14}C, ^{36}Cl, ^{15}N, ^{18}O, ^{2}H, ^{13}C, and Cl. Of these, the first three are radioactive, with half-lives of 12.3, 5700, and 301 000 years, respectively. Their current concentrations in the hydrologic cycle have been affected greatly by nuclear testing. Both tritium, ^{3}H and chlorine-36, ^{36}Cl from atmospheric testing have been used for soil-water tracing and recharge studies. These techniques only provide point or field scale information. A significant disadvantage of tracer techniques is that they do not directly measure recharge and therefore, lead to inaccurate estimates (Lerner *et al.*, 1990).

3.2.4 Accuracy of Recharge Estimates

Because recharge is not easy to measure directly, estimates of its value are prone to large errors. Four common types of error are discussed below. The most serious and common type of error arises when the recharge process is not fully understood, or when too many simplifying assumptions are made. Another common error relates to temporal and spatial variability. Most recharge processes are non-linear in relation to time. For example, a low-intensity rainfall might cause no recharge because of a high rate of evapotranspiration, whereas the same amount over a shorter time period might be sufficient to saturate the soil and cause recharge. Thus, errors will arise if temporal variations are ignored: for example by using monthly, annual, or long-term average data. Recharge is also non-linear with respect to spatial variations of inputs and physical properties of soils and aquifers.

Measurement error is also a significant issue, and is connected with the equipment used to make measurements. This kind of error is generally not overlooked. The last type of error is calculation errors which can be avoided by care and checking, especially of units.

3.2.5 Historical Review of Ground Water Recharge

Previous studies have been done to estimate groundwater recharge in different climate with different methods.

In the Aroca catchment of Uganda, Taylor et al., (1996) found that groundwater recharge, predicted by the soil moisture balance techniques, has been confirmed by flow modeling studies and was 200 mm year $^{-1}$.

The simulations done by Jimenez-Martinez et al., (2009) in Spain using a root zone modeling approach in which irrigation, evapotranspiration, and soil moisture dynamics for specific crops and irrigation regimes were simulated with the HYDRUS-1D software package indicated that water use by the crops was below potential levels despite regular irrigation. The fraction of applied water (irrigation plus precipitation) going to recharge ranged from 22% for a summer melon crop to 68% for a fall lettuce crop. In total, they estimated that irrigation of annual fruits and vegetables produces 26 hm^3 y^{-1} of groundwater recharge to the top unconfined aquifer.

Ji et al., (2007), found that the model simulation on components of water balance using observed field data indicated that large quantities- about 43% of irrigation water (amounting to 840mm)- were consumed by deep percolation, only small (less than 41%) proportions of irrigation water used by plants for transpiration.

Recharge calculated by Bekesi et al., (1999) in Manawatu region of New Zeland for a 28-year period and 300 simulations done for each station were found adequate to estimate mean annual recharge to within 10 mm.

Bethune et al., (2008) conducted a lysimeter experiment in southeastern Australia to quantify deep percolation (DP) response under irrigated pasture to soil type, water table depth, and pending time during surface irrigation. A simple conceptual model was developed and tested to describe DP response. The proposed conceptual model provided an effective representation of DP for most of the soils investigated by representing only the dominant processes contributing to DP. For most of the soils, steady-state percolation was the dominant process contributing to DP.

Ochoa et al., (2011) found that water balance calculations at the valley scale showed that 33% of the total water distributed in this agricultural valley contribute to potential aquifer recharge. Similar to reports by Willis et al., (1997) and Jaber et al., (2006), the more water applied, the more deep percolation was observed.

A distributed parameter ecohydrological model was applied by Zhang et al., (1999) in southeast Australia for estimating groundwater recharge which was 5% of the annual rainfall. This low value was due to the low amount of precipitations during the study period.

A modified water-table fluctuation technique was developed by Moon et al., (2004) to estimate a groundwater recharge ratio (calculated as the ratio of water-level rise to the cumulative rainfall amount) from the water level-monitoring data and corresponding precipitation records. The recharge ratio during the rainy season was calculated as the ratio of water-level rise to the cumulative rainfall amount. Using this technique, groundwater recharge ratios were calculated for each of the different types of well and then averaged for each river basin based on the proportion of hydrograph types. The average recharge ratios of the Han and Keum River basins were 10.0 and 8.3%, respectively, while those of the Nakdong basin and the Youngsan and Seomjin River basin were 6.1 and 6.6%, respectively.

Lu et al., (2009) used the Hydrus-1D model and calculations showed that recharge on average is about 175 mm/year in the piedmont plain to the west of Hebei plain, and 133 mm/year in both the central alluvial and lacustrine plains and the coastal plain to the east. Temporal and spatial variations in the recharge processes were significant in response to rainfall and irrigation. Groundwater recharge from irrigation in the Hebei plain accounted for about 27% to 49% of the total precipitation plus irrigation.

Anuraga et al., (2006) found that the average recharge for all simulation units in south of India was 156 mm/year, which represented 17% of the average rainfall.

Keese et al., (2005) found that the highest simulated long-term (30 year) mean annual recharge (51–709 mm/yr) in non vegetated sandy profiles represents 23 to 60% (from arid to humid climate) of mean annual precipitation. The most realistic long-term (30 year) recharge estimates based on vegetated, texturally variable soils range from 0.2 to 118 mm/yr, representing 0.1 to 10% (arid–humid) of long-term mean annual precipitation.

Mileham et al., (2007) calibrated a soil-moisture balance model (SMBM) in the humid tropics of equatorial Uganda and estimated that the mean annual recharge was 104 mm/year.

Results found by Ochoa et al., (2007) showed that for an alfalfa-grass field with sandy loam soil, deep percolation from flood irrigation is a significant source of shallow groundwater recharge. They attributed the rapid response of shallow groundwater to deep percolation to a relatively shallow water table, to a highly permeable sandy loam soil, and to an aging alfalfa field likely promoting development of macropores. With a much deeper water table, less permeable soil, or frequently tilled field, we might expect to see a muted response to the same irrigation applications.

Sibanda et al., (2009) assumed for the recharge area covering the middle and eastern part of Nyamandhlovu, aerial recharge rates in the range of 15–20 mm/year representing 2.7–3.6% of the long-term average annual rainfall of 555 mm/year. Larsen et al. (2002) predicted for adjoining areas in the Mid Zambezi basin recharge rates on the order of 20–25 mm/year, Obakeng., (2007) found for its similar region in northeast Botswana a recharge rate of 15 mm/year, and Beekman et al., (1996) adopted recharge values for Botswana in the range of 10–25 mm/year.

Sun and Cornish.,(2005) used SWAT model to estimate shallow groundwater recharge in the headwaters of the Liverpool Plains. They found that the estimated annual average recharge for the past 44 years is 5.3 mm/yr. Figure 5 also shows a trend of dry and wet cycles in recharge throughout the modelling period. Over the last two decades (1980s and 1990s), the estimated recharge rate was approximately 6 mm/yr (1980s) and 8 mm/yr (1990s), respectively, while the two decades before these showed a recharge of approximately 3 mm/yr.

Wang et al., (2012) defined the deep percolation in their study in Shanxi province, China as the water passes flowing downwards below 0–120 cm soil column and calculated it based on a water balance equation, finding that the deep percolation takes up a large proportion, up to 46.7% and 31.4% respectively from flood irrigation for summer corn and sprinkler irrigation for winter wheat

3.3 Capillary Rise Contribution to Supply Plant Water Requirement

3.3.1 Introduction

Shallow water tables are a common feature of many irrigation areas due to high recharge rates and, frequently, reduced drainage rates. Proper utilization of shallow water tables can contribute significantly, through capillary rise in the root zone. Capillary rise may be considered as an important contribution to agro-productivity (Beltrao et al., 1996; Wallender et al.,1979). Under dry climate, water table contribution to crop evapotranspiration may reduce or even completely eliminate irrigation requirements without compromising crop yields (Pratharpar and Qureshi., 1998; Nosetto et al., 2009). When utilized improperly, however, shallow water tables can result in severe crop and soil losses due to salinization of the upper part of the root zone.

The quantification of capillary contributions from shallow water tables towards crop water requirements is therefore considered to be a very important management tool, to ensure conservation of water and soil resources. Ground water has been studied extensively as a supplemental source of irrigation water (Rhoades et al., 1989; Ayars et al., 1993, 2006). The use of shallow ground water table by crops depends on several factors such as depth of the water table, hydraulic properties of the soil, stage of the crop growth, ground water quality, etc. Quantification of the water taken by the roots from the shallow water table is of great significance and has been a topic of extensive research in the last few decades.

3.3.2 Factors affecting capillary rise contribution to plant water requirement

Studies of crop water use from shallow ground water generally report the water depth below the soil surface, but the important statistic is the distance between the ground water surface or the nearly saturated zone and the bottom of the root zone. The flux to the root zone will be determined by the unsaturated soil hydraulic conductivity, which is determined by the soil type, and the soil matric potential gradient established in the soil profile as a result of both crop water use and evaporation from the soil surface.

The root system is the least quantified aspect of the system and it is one of the most important components since it is the conduit between the vegetative portion of the plant and the soil water. Neither root development in relation to the crop growth stage, nor maximum rooting depth is reported in studies on crop water use from shallow ground water. Crop water use from ground water will not be significant until the root zone develops into the proximity of the water table and there is an adequate gradient to induce flow to the root system. It is obvious that the quicker the root system develops to its maximum depth, the longer will be the opportunity for crop use and the larger will be the contribution from the ground water. The soil type will determine the required position of the root zone relative to the water table to allow significant crop use.

Any plant may extract water from shallow ground water. Plant characteristics that affect the potential contribution of ground water to the crop water requirement include salt tolerance, length of growing season, and rooting characteristics. The crop growing season will impact the total crop water use in several ways. A perennial crop will have a well developed root zone in the second and subsequent years of production and thus the root zone will be well positioned to use water during the entire growing season. Annual crops grow a root system each year and have limited time available to use shallow ground water. Total use is determined by the time it takes to develop a large demand and to have the root zone close enough to the ground water to get significant transport to the root zone. The longer the growing season, the longer is the potential use from shallow ground water. If the crop has short growing period (90 days) there is limited opportunity for crop use compared to a crop with a growing period of 200 days. Particularly when the last period in the growth cycle will be the time that the maximum demand will occur.

For crops to effectively use shallow ground water, the water table will have to be maintained at a pre-determined depth. The drainage laterals also need to be installed perpendicular to the surface grade of the field to insure that water table control is possible on the entire field (Ayars., 1996). The ideal water table control scenario would be to have the water table close to the bottom of the crop root zone early in the season and have it recede as the root zone develops. This should maintain a relatively constant distance between the bottom of the root zone and the saturated zone. This conceptually would permit the maximum use of water by the crop from the shallow ground water. The distance will depend on the soil type, close with sand and progressively larger for the finer textured soil, and the irrigation system and its management. Systems with poor uniformity and potential for large amounts of deep percolation would require greater distance between the root zone and water table. The source of the water creating the shallow ground water will also determine the effectiveness of any management system developed to utilize ground water. If shallow ground water results primarily from deep percolation loss due to poor irrigation practices, improvements in irrigation efficiency will reduce the water being contributed to shallow ground water and will reduce the potential usefulness. If the shallow ground water is being sustained by lateral regional flow from inefficient irrigation, channel leakage, and rainfall, then there is a potential for sustained water use from shallow ground water.

Irrigation system management has a direct impact on the potential for crop water use. This includes the depth of application, the uniformity of application, and the frequency of application. Surface irrigation methods, such as flood, furrow, and basin, generally apply large volumes of water in short periods of time and may have a low application frequency. Unless these systems are well designed, installed, and managed there may be poor distribution uniformity with excessive deep percolation losses resulting in water logging, loss of production, poor crop health, and excess additions to shallow ground water in some areas and under irrigation in others. In fields with controlled drainage there is the potential for redistribution of the groundwater through the subsurface drainage system that will contribute to the ground water in the under irrigated areas. As a result, the under-irrigated areas may have more crop water use from shallow ground water than the over-irrigated portions of the field. However, on the whole there will be less crop water use than if the crop was uniformly irrigated.

3.3.3 Methods for capillary rise estimation

Water balance approach

Much of the research related to crop water use from shallow ground water has been done under field conditions (Kruse et al., 1985, 1993; Follett et al., 1974; Benz et al., 1978, 1981) and the water table contribution to the crop water requirement was calculated as a closure term in the water balance equation. The limitations to this approach are the accurate characterization of the crop evapotranspiration (ET_c), the variability of the soil characteristics, and the depth to the water table. The water balance calculation also required an estimate of the change in stored soil water. With the advent of new technologies, (TDR, capacitance probes) for soil water measurements there are options for improving this component of the equation. When possible, field studies will probably provide the most realistic data for crop water use from shallow ground water but finding sites that are suitable for this type of research is a problem. An ideal site is one that has a water table that doesn't fluctuate or that can be controlled, that has soil that is not to saline, and is large enough to be representative of the area.

Direct measurement using lysimeters

Lysimeters, weighing and drainage, have also been used to study crop water use from shallow ground water (Yang et al., 2011; Kahlown et al., 2005; Soppe and Ayars., 2003; Bethune and Batey., 2002; Slavich et al., 2002; Rogers., 2001; Hutmacher et al., 1996; Kruse et al., 1993; Prathapar and Meyer., 1992). Lysimeter studies have the advantage of good control on most of the variables in the water balance equation. The water table is generally controlled at a fixed depth during the experiment which eliminates one variable in the interpretation of the results. The water fluxes to the soil mass and from the soil mass can be accurately measured. With a weighing lysimeter, the evapotranspiration (ET) can be measured accurately while soil water measurements are required for a drainage lysimeter. In either case, the effect of soil variability on the result is minimized. However, lysimeters are expensive to build and maintain and are often not representative of the field conditions for the crop.

Deterministic soil water flux models

Deterministic soil water flux models are either such as those using the Richards equation, e.g., the models SWACROP (Kabat et al., 1992), WAVE (Vanclooster et al., 1994) and SWAP (Ahmad et al., 2002), or adopting transient state analytical approaches as models MUST (De Laat., 1995) and TSAM (Jorenush and Sepaskhah., 2003). However, these deterministic approaches require a more complete description of the soil hydraulic properties than the conceptual models, which often limit their use due to current lack of such soil data and to difficulties inherent to operationally obtain them.

3.3.4 Historical review of capillary rise contribution to crop water requirement

Previous studies has widened our knowledge in quantifying capillary rise contribution to plant water requirement.

Wallender et al., (1979) determined that groundwater contribution represented 59-70% of total season evapotranspiration (ET) in furrow irrigated cotton crop Ayars and Schoneman., (1986) found that capillary rise from a water table of 1.7–2.1m deep contributed up to 37% of evapotranspiration (ET) of a cotton crop.

Prathapar and Qureshi., (1998) observed that under shallow water table conditions irrigation can be reduced by up to 80% without affecting crop yield and increasing soil salinization. Soppe and Ayars., (2003) by using weighing lysimeters maintained a water table at 1.5m depth, found that ground water contributed up to 40% of daily water used by sunflower crop. On a seasonal basis, 25% of the total crop water use originated from the ground water. They proved that the largest contribution occurred at the end of the growing season when roots were fully developed. They found also that the applied irrigation in the presence of a water table was 46% less than irrigation applied to the crop without a water table.

The results of studies done by Kahlown et al., (2005) showed that the contribution of groundwater in meeting the crop water requirements varied with the water-table depth. With the water table at 0.5 m depth, wheat met its entire water requirement from the groundwater and sunflower absorbed more than 80% of its required water from groundwater. However maize and sorghum were found to be water logging sensitive crops whose yield were reduced with higher water table. They found also that maximum sugarcane yield was obtained with the water table at or below 2 m depth. They concluded that the water-table depth of 1.5–2 m was optimum for all the crops studied.

Raes et Deproost., (2003) found that the capillary rise from the groundwater to the surface of a bare soil as simulated by UPFLOW model was significant in medium-textured soil types (loam and silt). In coarse-textured soils (sand) and especially fine-textured soils (silty clay), the upward water movement was found important when the groundwater was less than 1m below the soil surface. It was found by Babajimopoulos et al., (2007) that under the specific field conditions groundwater contribution to the root zone was about 3.6 mm/day. This amount to about 18% of the transpired water for the period 1 July to 11 September 2004. Therefore, groundwater is a very significant source of water to cover crop demands. The contribution of groundwater increases as root length increases. This directs them to conclude that cultivation practice should lead to more frequent irrigation events with small amounts of water during the period when root length is small. The interval between irrigation events can be increased when roots have been fully developed taking advantage of the presence of the groundwater.

Grismer and Gates ., (1988) reported that under arid conditions, water table can supply as 60-70% of crop's water requirement. Dardanelli et al., (2002) reported that when present, the water table contribution varied among locations between 15 and 25% of the alfa alfa water use, and was not related to the groundwater depth. It was found that the decrease in water table depth reduced the contribution to corn by 22% compared that of sorghum; while increasing of the irrigation interval of the sorghum increased the fraction of water that obtained from the ground water (Ayar et al., 1999 and Sepaskhah et al., 2003). Moreover, contribution of ground water from 1.6 to 2.4 m depth to winter wheat water use grown into sandy soil in a weighing lysimeter was found to be 16.6% of its total evapotranspiration (Yang et al., 2000). Gutowski et al., (2002) found that during relatively dry periods, up to 33% of monthly evapotranspiration was derived from groundwater-supported evapotranspiration. Simulation results of York et al., (2002) indicated that from 5% (wet year) to 20% (dry year) of the evapotranspiration was drawn from groundwater in a catchment in northeastern Kansas.

Zeineldin and Aldakheel., (2010) found that shallow water table can contribute by 26% to the water requirement of palm trees. Portela et al., (2009) reported that groundwater supplied an important amount of water to crops with corn obtaining approximately half of its water needs. Under rain-fed condition, Liu and Luo., (2011) found that groundwater contribution was able to meet more than 65% of the potential evapotranspiration of winter wheat when water table was at or above 150 cm depth. However, they concluded that it could meet the entire water requirement at or above 110 cm water table depth.

By using proper irrigation management, cotton (Hutmacher et al., 1996) and alfalfa (Ayars et al., 2009) have been shown to take-up between 20 and 50% of their water requirement from shallow groundwater in column experiments. Furkusta et al., (2009) found that shallow water table contributed by 55% up to 82% to actual evapotranspiration of cotton. Jaber et al., (2006) reported that in Florida the groundwater is contributing only around 9% of ET.

Hurst et al., (2004), found that sugarcane can uptake a large proportion of their water requirement from shallow water tables. Sugarcane will not require surface irrigation when fresh water tables are within 1m of the soil surface. Then deeper water tables (1>m) may also be capable of meeting the water requirements of mature sugarcane. Water table as deep as 2m are still likely to have a positive impact on the sugarcane water balance and where irrigation is required, the amount will be dependent on local rooting characteristics such as rooting depth and density.

Water tables can contribute high proportions, and sometimes all of the evapotranspiration requirements for sugarcane crops with no detriment to yields. For a sugarcane crop in Columbia, Cenicana., (1984, as cited in Torres and Hanks, 1989) found that yields were not improved by irrigation when a water table was maintained between 1.2 and 1.5 m. In India, a water table at 1m provided 65% of sugarcane evapotranspiration in a sandy loam soil (Hunsigi and Srivastava., 1977). In another Indian study (Gupta and Yadav., 1993) groundwater contributions were 91, 86 and 55% of sugarcane potential evapotranspiration for water tables at 0.2, 0.4 and 0.6m in a sandy loam soil during summer, respectively. Sugarcane yield was, however, significantly lower at the 0.2m water table depth, possibly because of water logging.

Shallow water table may have negative effects on crops as well. If water table is too shallow, crop yield could decrease due to water logging and root anoxia (Nosetto et al., 2009). For example, in South and South-East Asia, excess moisture caused by shallow water table is the second most important production constraint for maize crop (Rathore et al., 1996). Improper irrigation would deteriorate the water logging condition (Bandyopadhyay and Mallick., 2003). When water table is very shallow, soil water logging limited the root growth of winter wheat due to the reduced oxygen concentration of the soil (Brisson et al., 2002). In general, water table contribution decreases with the increase of water table depth or irrigation quantity, or the reduction of irrigation spacing (Ayar et al., 2006). When water table is very shallow, irrigation may be eliminated to maximize water table contribution and avoid water logging problem.

Moreover, it is possible to control the water table depth by managing irrigation and drainage system to maximize the water use efficiency (WUE) (Gowing et al., 2009).

Ahmad et al., (2002) reported that sustainability of irrigation with groundwater is obtained if a reduction in irrigation with groundwater by 36% is obtained. An annual recharge of 38.9 cm is estimated in rice–wheat systems, and a reduction of 62% in groundwater extraction is required to reach sustainability of groundwater use at field scale.

Xu et al., (2012) integrated a Soil–Water–Atmosphere–Plant (SWAP) package into a groundwater flow model (MODFLOW) in such a way that the SWAP package calculates vertical flux for MODFLOW, while MODFLOW provides averaged water table depth to determine the bottom boundary condition for SWAP zones. Their result showed that groundwater recharge was closely related to the irrigation and rainfall, while large groundwater capillary rise was contributed to crop water use during the crop growing period from June to middle August.

4 Description of the Field Activities

4.1 Introduction

For the study of water fluxes and water balance at field scale, there was an intensive monitoring activities to measure the main variables and collect necessary data for the implementation of the two models SWAP and IDRAGRA. These monitoring activities were carried out in cooperation with the personnel of the departments who are involved in a wider project, funded by Regione Lombardia (AC-CA project), which encompasses also monitoring the carbon dioxide fluxes.

Long season *Zea Mays* variety (class 600-700) was seeded in the field. In particular, after manure application and soil operations (a traditional tillage) maize was sown with inter-row and row distances of about 70 and 20 cm. Emergence was always within 7-10 days. In Landriano, maize is always grown to produce forage for livestock. In 2010 and 2011 maize was seeded in April and harvested at the dough stage It was irrigated only once in 2010, while no irrigation events were applied in 2011.

The monitoring activities were conducted in the experimental farm “Campo dei Sassi Menozzi” of the agricultural faculty located in “Landriano” in Pavia province.

Several campaigns were carried out to monitor crop biometric parameters (leaf area index, crop height, rooting depth) and soil properties. Standard meteorological variables (rainfall, radiation, temperature, humidity, wind speed, wind direction) were measured on a hourly time step over a grass coverage by the two standard stations of the regional meteorological network (ARPA) closest to the experimental sites. In particular, in the case of Landriano the ARPA station is placed in the same farm, at about 200 m distance from the experimental field.

4.2 Description of the study area

Data described in detail in the following parts of the chapter were collected during the cropping seasons 2010 and 2011 in a maize field of 10 ha located in Northern Italy (Figure 4.1). The experimental field is located in Landriano, Pavia (45°19’ N, 9°15’ E, 88 m a.s.l.). Instruments for detailed monitoring of water fluxes were installed in the field on 2010. A micrometeorological eddy covariance (EC) station was located approximately in the centre of the field.

The soil in Landriano is deep (1.5-2.0 m) with a sandy loam texture.

The climate is humid subtropical following the Koppen classification and humid continental following the Stralher classification. In the cropping season (April-September) the average temperature is around 19°C, while rainfall is 250-300 mm. The field is irrigated by surface irrigation. When maize is grown, one or maximum two irrigations are normally conducted. The limited number of irrigation is due to the presence of a shallow water table (80-120 cm below the topographic surface) contributing significantly to the satisfaction of the crop water needs.

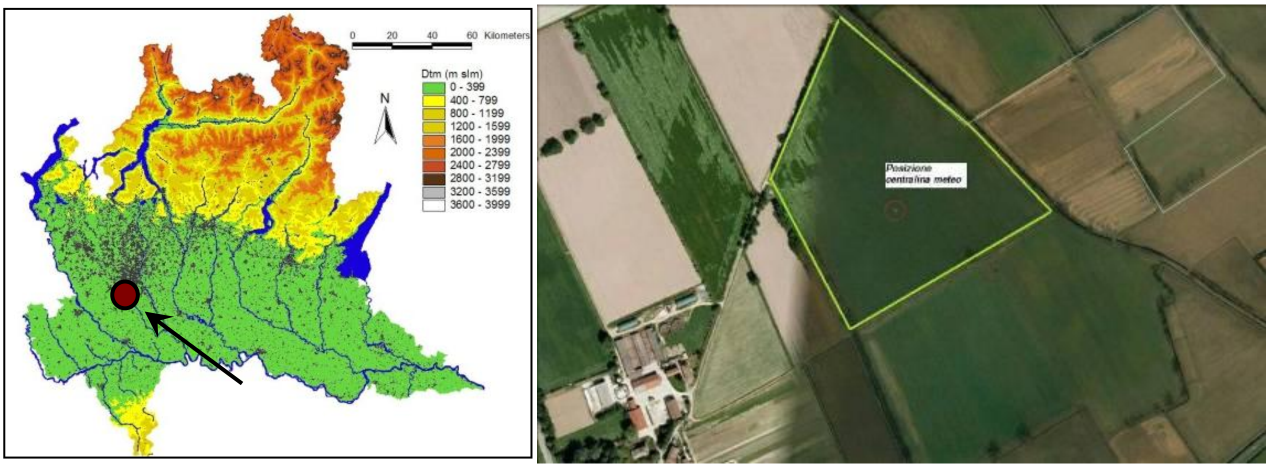

Figure 4.1Landriano field location

Concerning the methodology for collecting and analyzing data, the project includes two different, but complementary, methods; First, the net flow of H_2O that was monitored by the Eddy covariance technique, which is used for direct measurement of surface layer fluxes of water and Carbone between the surface and the turbulent atmosphere in reference to the area included in the footprint of the stations (about 1-3 ha, depending on wind speed and direction, plant height and level of measurement). Second, they were measured in the field for more detailed scale, the different components of water cycle through periodic campaigns of measurements.

The monitoring was conducted in 6 representative sites placed in different pedological conditions (including the station Eddy-covariance, 1C, 2C, 3C, 4C, 5C, 6C, 7C) (see Figure 4.3). In each site was installed instruments for water status monitoring (see Figure 4.2):

- ✓ 4 tensiometers installed at 4 different depths to measure soil water potential
- ✓ Probes of humidity installed also at 4 different depths to measure soil water content based on the principle of FDR measurements.
- ✓ And a piezometer completed with a pressure transducer (STS) to measure GW table depth.

Figure 4.2 Different instruments installed in each site for soil water status monitoring

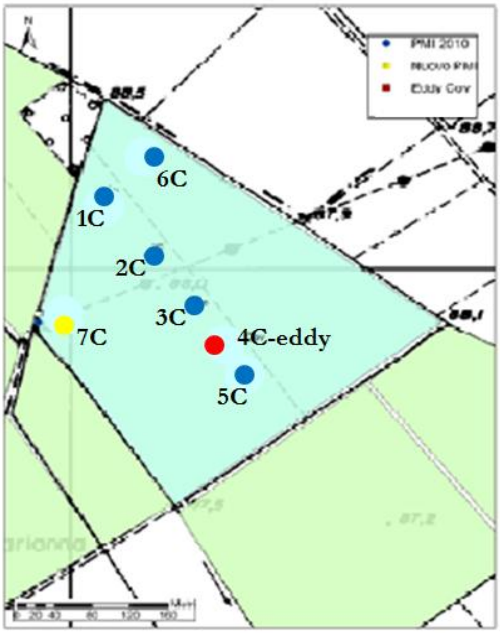

Figure 4.3 Location of the six sites of monitoring

4.3 Monitoring of Soil Water Status

4.3.1 Soil Water Content

Direct measurements (laboratory) of volumetric soil water content, were made twice for soil samples collected at different depth during de-installation of Sentek humidity probes (October 2010 and march 2011), and were used to calibrate the same probes according to the procedure indicated by Sentek technologies (2001).

Sentek probes (Figure 2.1, right) acquired a frequency value which is then processed through a calibration curve to a volumetric water content value.

The default parameters of this curve are assigned by Sentek. These parameters can be modified by the user to make response in term of water content closest to that measured in the laboratory for a specific soil. What is revealed by performing this analysis with data collected from the field “Sassi” is that the calibration curve suggested by Sentek is sufficiently accurate for this type of soil.

It is therefore preserved for Sentek probes the default parameterization, shown at left in Figure 4.4. To the right in the same figure, are shown the values of water content using the default calibration curve depending on the water content measured in the laboratory.

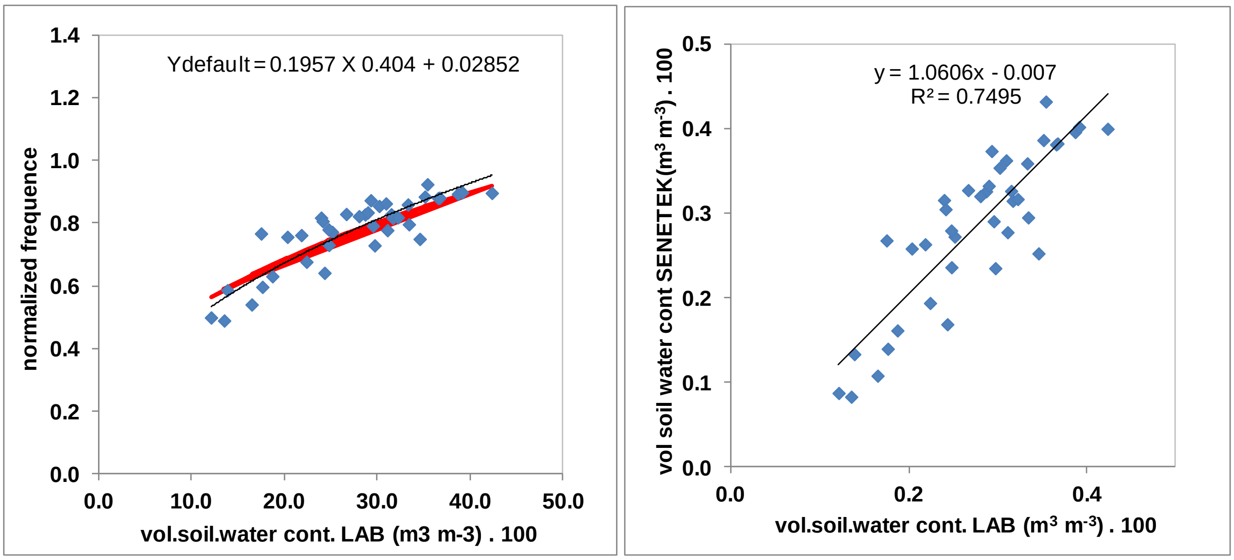

Figure 4.4 Normalized frequencies measured by Sentek versus volumetric water contents determined in the laboratory, in red is default curve of Sentek, in black the experimental curve (left), volumetric water content measured by Sentek with the default calibration curve versus volumetric water content determined in the laboratory (right)

Campbell CS616 TDR probes Figure 2.1 installed at the Eddy meteo station (PMI-4) gives soil water content in microseconds. To transform them into volumetric soil water content, Campbell gives the following calibration equation:

$$\theta_v = c_0 + c_1 * period + c_2 * period^2$$

Where θ_v is the volumetric soil water content (m^3/m^3); period is the time of occurring the signal (μsec); c_0,c_1,c_2 are the Campbell default parameter. Values for the calibrated parameters are presented in the following Table 4.1 (Baroni., 2007):

Table 4.1. Calibrated parameters for the CS616 probes in the Sassi field (Baroni., 2007)

Depth (cm)	c_o	c_1	c_2
5-50	-0.0663	-0.0124	0.0009
70	-0.0663	-0.032	0.0013
100	-0.0663	-0.0024	0.0004

Figure 4.5 reveals the values of volumetric water content (%) measured at different depths in the PMI-1, 2, 3, 4, 5 and 6 from setting up date (May 2010) until the de-installation of the Sentek probes (March 2011). In particular, except for the PMI-4, sensors were placed at a depth of 7 cm, 27 cm, 47 cm, 67 cm. In the PMI-4, Campbell TDR probes were installed at depths of 5 cm, 20 cm, 35 cm, 50 cm, 70 cm, 100 cm. PMI-2 and 3 probes had some problems after harvesting and were subsequently restored. For almost all the probes, there was a loss of data due to overwriting during the first week of September 2010. The lack of data after 3rd August 2010 in the PMI-4 was due to the malfunction of the CR5000 datalogger. Data at 100 cm depth were available after that date, because it is connected to the CR23X datalogger. In the PMI-3 , the sensor placed at 67cm depth was not working properly during 2010. It may be noted also that in all sites, the probes placed at a depth greater than 60-70cm are usually close to saturation. By moving towards the surface, SWC varied according to evapotranspiration and percolation occurred in the upper part of the profile.

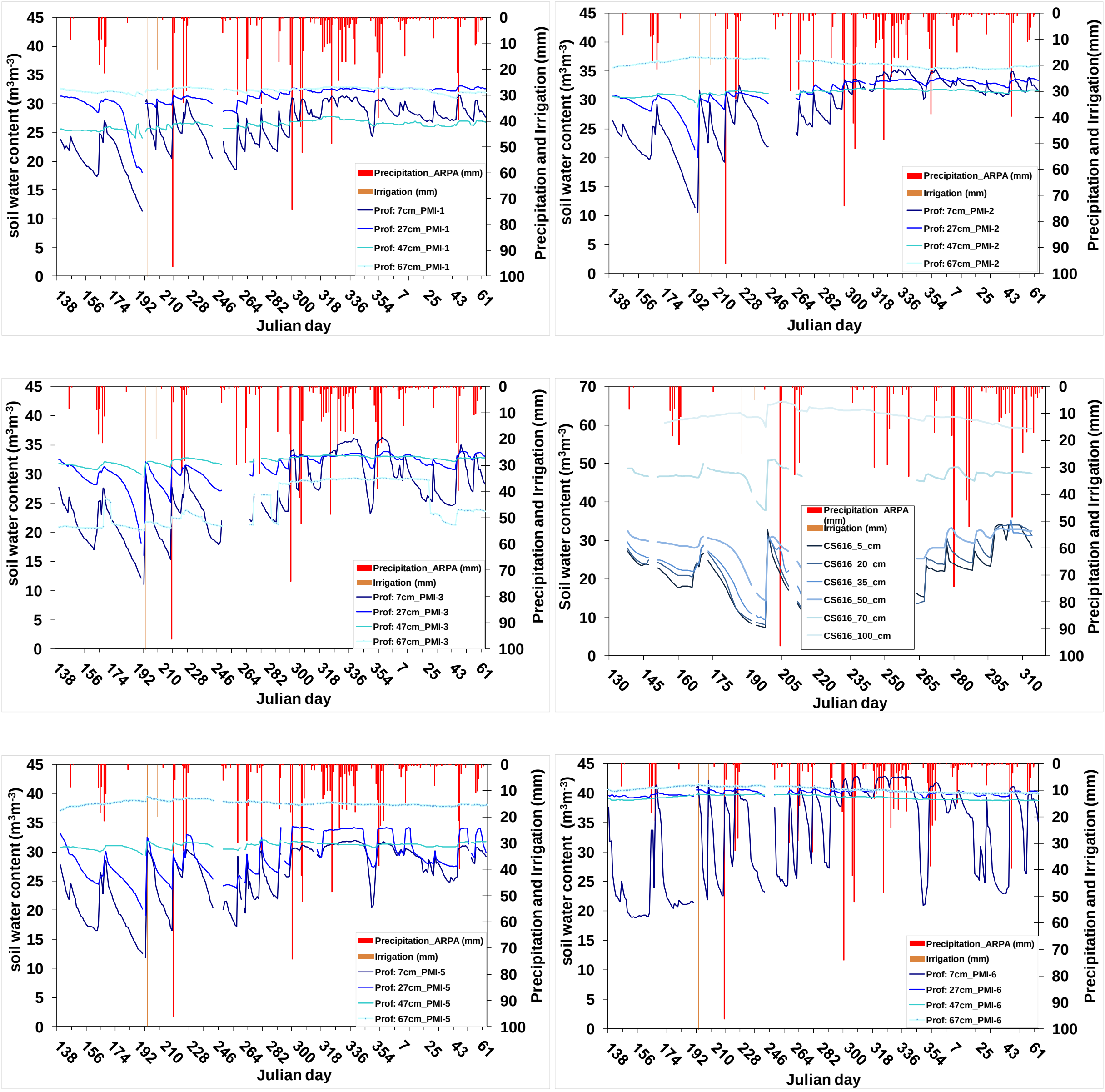

Figure 4.5 Soil water content (m^3m^{-3}) at different soil depth for all PMI from the beginning of the season 2010 until march 2011.

A different behavior is noted for the TDR probe installed at 70 cm depth in the micrometeorological station (PMI-4). This difference is probably related to the difference in topography of this site (Eddy station was placed inside a sort of hump).

Figure 4.5 presents how PMI-1 and 2 were influenced by the two irrigations conducted during July. This was because the irrigation of the north-west sector started the night before 18 of July and water broke embankments and reached the latter sites. While water did not reach the PMI-3, 4 and 5. The hydrological behavior of PMI-6 differed from the other sites. The probes placed below 27 cm seemed always under saturation. On the other hand, the water content at the surface varied widely in between saturation and unsaturation conditions (between 20 and 40m^3m^{-3}).

Figure 4.6 shows the trends of water content measured by sensors on the five Sentek probes at the depths 7 cm and 67 cm respectively. It is noticed that probes aligned along the transect have a similar behavior with a small difference related to the soil texture (percentage of clay increases going from PMI-1 to PMI-5). In the deepest layers, the soil water content was high, almost saturated conditions. The SME-6 is characterized with a high percentage of loam which confirm the elevated water content in this site.

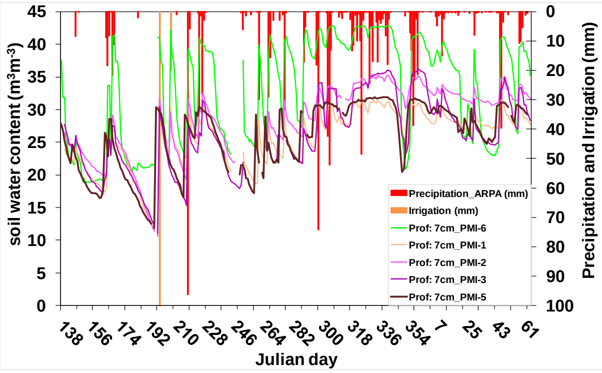

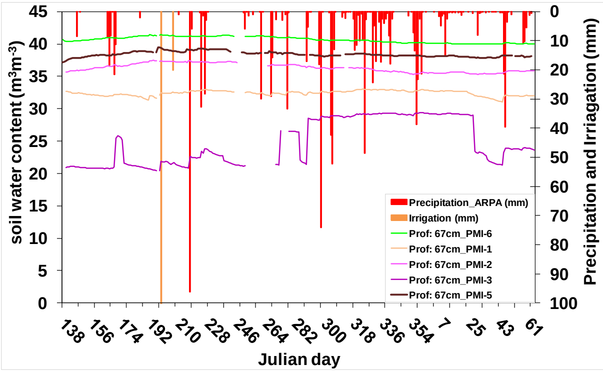

Figure 4.6 Soil water content (m3m-3) at the depth 7 and 67 cm for the sites PMI-1, PMI-2, PMI-3, PMI-5 and PMI-6 from the beginning of the season until march 2011

In Figure 4.7 are reported the values of water content (m^3/m^3) measured at different depth in the PMI-1, 2, 3, 4, 5, 7 from April 2011 up to October 2011.

Comparing the trend of the curves of soil water content at various depths measured at Eddy Station with measurements at other sites, we noted that trends are similar. In the site PMI-7 which was a control site (irrigated during the agricultural season 2011 on 24 May and 21 July), the SWC was the highest among all. This difference is more evident for the first two depths (7cm, 27cm) where humidity was always higher than 20%. Except PMI-7, soil water content during the agricultural season 2011, was lower than that registered during the season 2010.

In both sites 2C and 5C, we lost data for a few days due to malfunction of the batteries which were required to replace them every time we download data.

In the site 3C, the same problem of the last year was also encountered during this year: the probe of SENTEK at 67cm was not working properly which was clear in the curve and the low values of SWC.

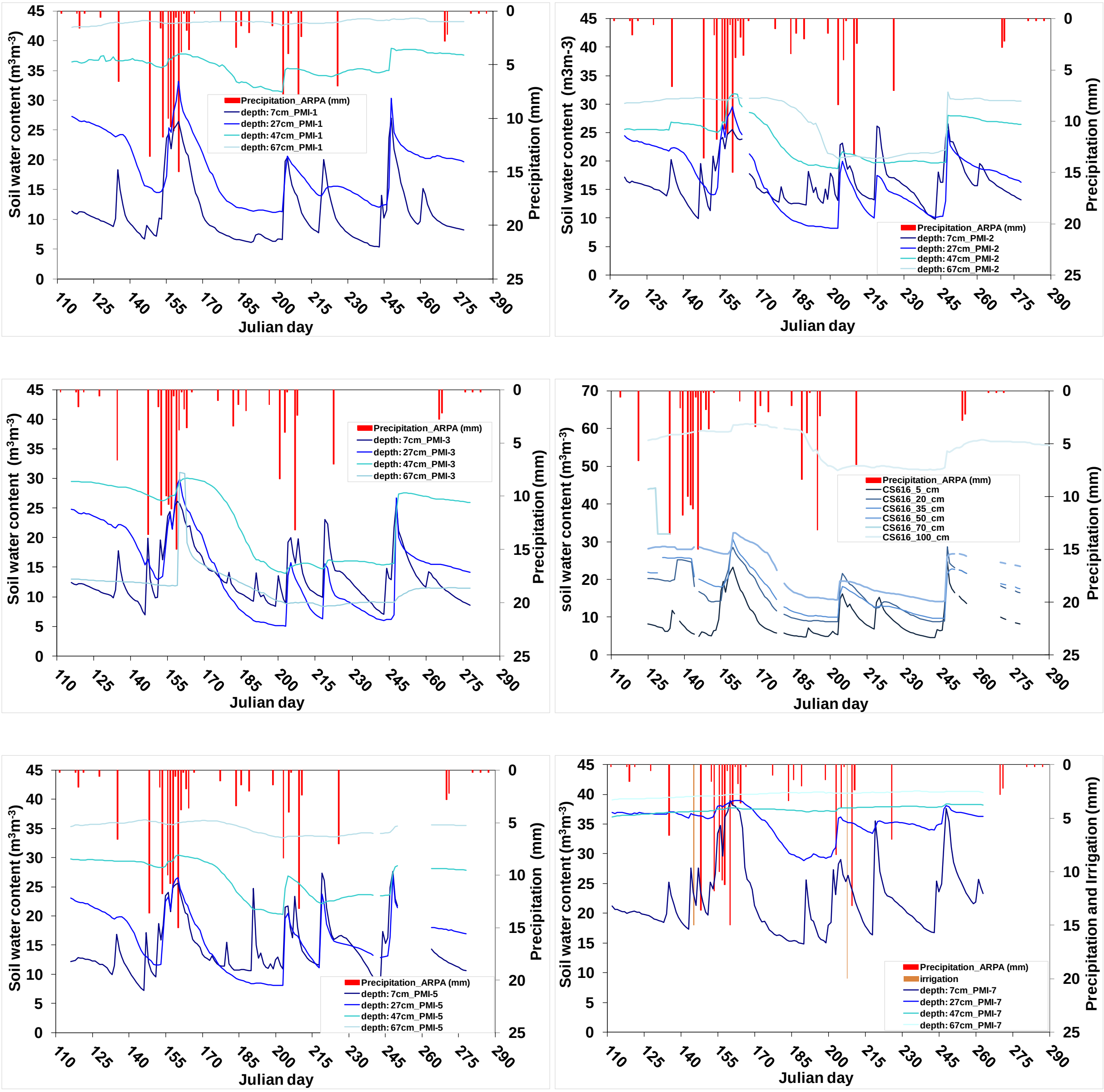

Figure 4.7 Soil water content (m3m-3) at different soil depth for all PMI during the 2011 season

In all sites, except the control site 7C, we noticed a stress period during summer season (July-August), and it was more obvious during campaigning measurements, when plants were visually showing drought stress symptoms (dryness, yellowing and leaf roll).

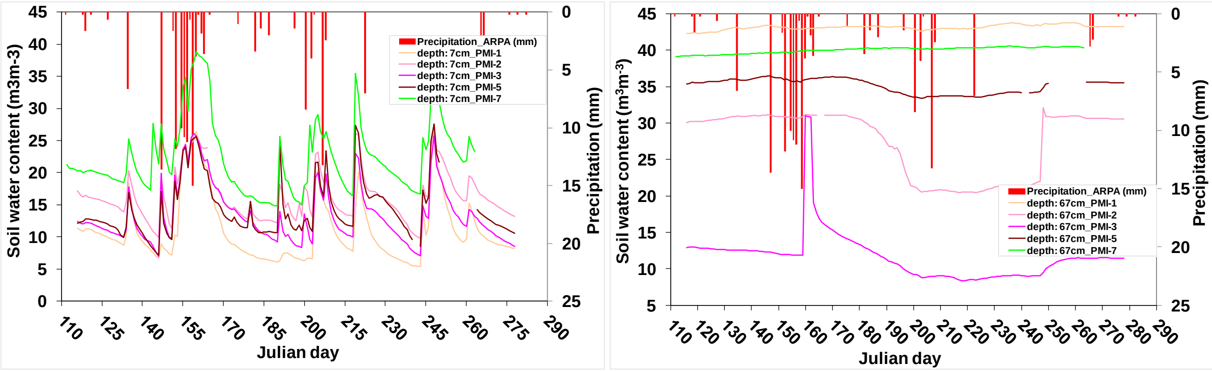

Figure 4.8 Soil water content (m3m-3) at the depth 7 and 67 cm for the sites PMI-1, PMI-2, PMI-3, PMI-5 and PMI-6 during the 2011 season

The trends of superficial probes exhibited low values of soil water content, specially comparing them to values registered during the season 2010. Excluding PMI-7, SWC was always around 10-15m^3/m^3 except days after precipitation events (Figure 4.8). For both seasons (2010 and 2011), PMI-1 was always presenting the highest SWC at 67cm depth. This can be attributed to the location of this site which was near the canal. These results were also proved by the shallow groundwater level in the same site for both seasons.

In addition to the daily monitoring of SWC presented in the previous figures, it was interesting to focus our analysis on a semi- hourly scale in order to demonstrate daily oscillation in the upper part of the profile.

Figure 4.9 is presenting an example of the progress of SWC between 6 and 10 June 2010. The other graph presents air humidity and air temperature for the same period.

Peaks for SWC were registered every day around 14:00-15:00 (solar hour). A first interpretation is that the cycle of daily "wetting" of soil surface is due to condensation phenomena of the air humidity that occurred in the early hours of the morning. This hypothesis was supported by the conditions of maximum humidity presented in the field during the pre-dawn measurements (always wet leaves). The latter situation was always faced even during hot and dry days of July. The delay of the peak may be due to the depth of measured soil humidity (7 cm). However, further studies are needed to demonstrate this hypothesis and see how much this moisture can eventually contribute to plant-water requirement.

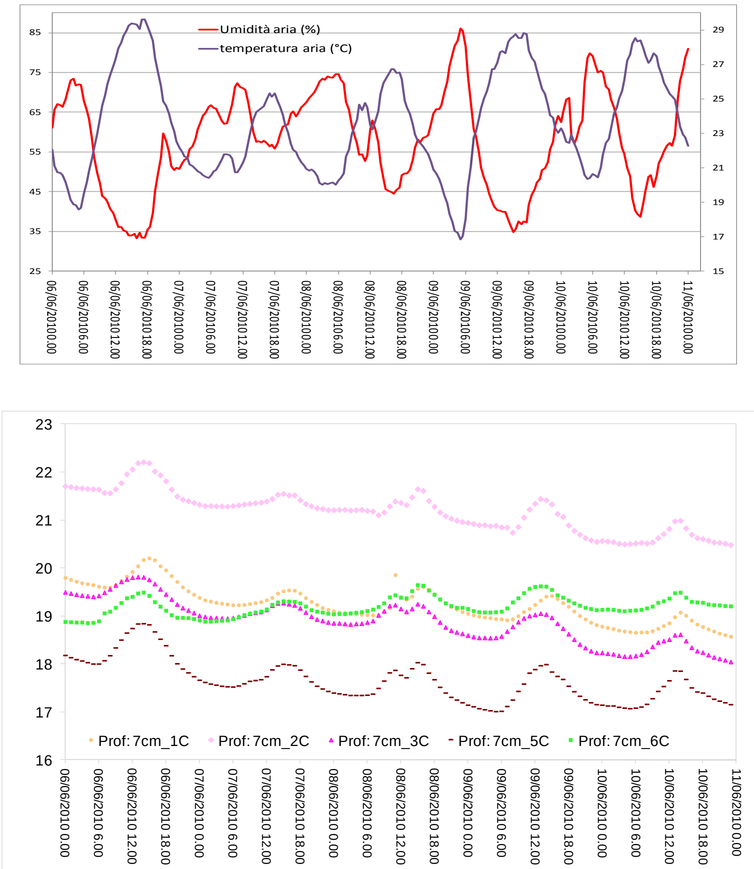

Figure 4.9 volumetric soil water content at 7 cm (%) measured with Sentek probe during the period of 6-10 June 2010; U(%) e T(°C) of the air for the same period

4.3.2 Groundwater level

Figure 4.10, presents the values of groundwater level measured during the agricultural season in the PMI-1, 2, 3, 4, 5, 6 from May 2010 up to March 2011 and in PMI-1, 2, 3, 4, 5, 7 from April 2011 until October 2011.

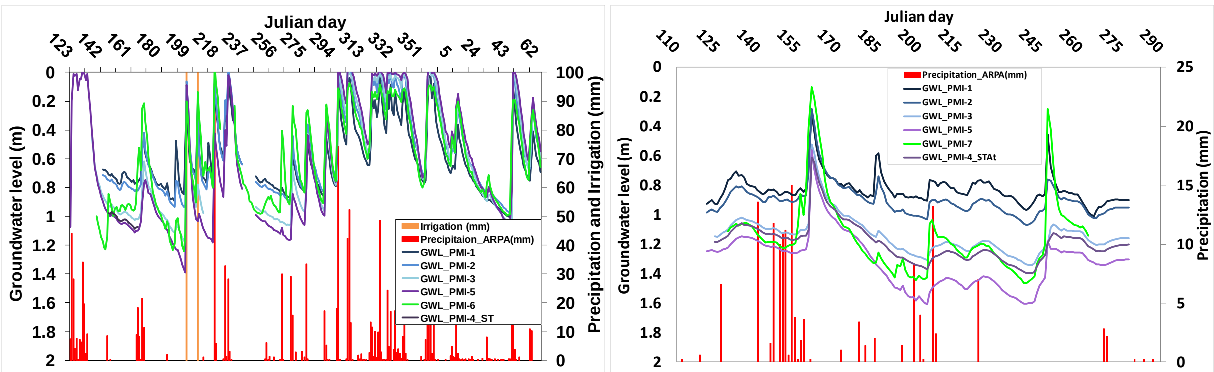

Figure 4.10 Groundwater level (m) for all PMI from May 2010 until march 2011 (left) and from April 2011 until October 2011 (right)

STS transducer in the PMI-5 was installed before the precipitations of May 2010. It measured a groundwater depth equal to zero (saturated soil) for the period between the beginning of the installation till half of May 2010. The other STS transducers were installed after 20 May 2010.

The Figure 4.10 maintains the same trend of ground water level measured in all sites PMI, with values increasing as far as we go from canal. This increase is mainly due to the structure of experimental field which is characterized by slope going from north-east to south-west, causing decrease in ground water level, going from 1C to 5C.

Groundwater level in the PMI-6 represented a particular behavior. Surface water table was very close to ground surface after intense precipitation or irrigation event. Later it decreased quickly and came back to normal level. This behavior is not confirmed by the probes of humidity placed at 27 and 47 cm depth which were always near saturation. Probably this difference is related to the loamy texture specially characterizing this site, or to its topography which allowed water stagnation in the surface.

The STS transducer installed in the micrometeorological station worked just for some days. The values registered were between collected values in the PMI-3 and PMI-5 located respectively upstream and downstream of the PMI-4. During the winter, we noticed a great agreement between the trends of groundwater level in all sites comparing to those of the agricultural season. In March all instrumentation were de-installed in order to allow works in the field and then are reinstalled in April 2011 for the new agricultural season. We noticed again a deviation between trends with a decrease of groundwater levels going far from the canal.

The ground water level in the control site PMI-7 showed the same behavior as in site PMI-5. This similarity is majorly attributed to the similarity in soil texture. It is worth to highlight the peaks in the curve of PMI-7 were assumed to be due to irrigation applied on 24 May and 21 July 2011, and due to the precipitation received at the beginning of September 2011. But, these two irrigations were applied with a small amount (15, 20mm), and were not enough to support the shallow ground water level in this site or to justify the high water content registered by the sensors placed at 47 and 67 cm. This water content can be justified by the high percentage of loam which characterized the deepest layers in this site.

4.3.3 Soil water potential

For both seasons, we installed in each site 4 tensiometers near the humidity probes at depth close to that used for probes (10, 30, 50, 70 cm). The tensiometers in sites PMI-1and 4 were connected to data logger. The data logger connected to the tensiometers in PMI-1 was a small one close to them, while that one connected to tensiometers in PMI-4 was a CR23X data logger available in Eddy-station.

Figure 4.11 and **Errore. L'origine riferimento non è stata trovata.** demonstrates the automatically collected matric potentials data in the previous two sites in relation with precipitation and ground water level for the agricultural seasons 2010 and 2011, respectively. We noticed that in PMI-1 the soil water potential became positive after precipitation. This attributed to the high surface level of the water table exceeding the porous cap of the tensiometer. Therefore, the reported measurements are actually hydrostatic pressure measurement rather than matric potential. While for PMI-4 (2010), the positive data were mainly collected from the tensiometer at depth 70 cm during the season 2010, where the porous cap was always under the water table level. During 2011 season, the latter tensiometer was not working properly because always were giving positive values that were not supported by any evidence. In the same figure, it is also shown the refill of tensiometer. It was required to refill the tensiometers repeatedly, particularly during summer period.

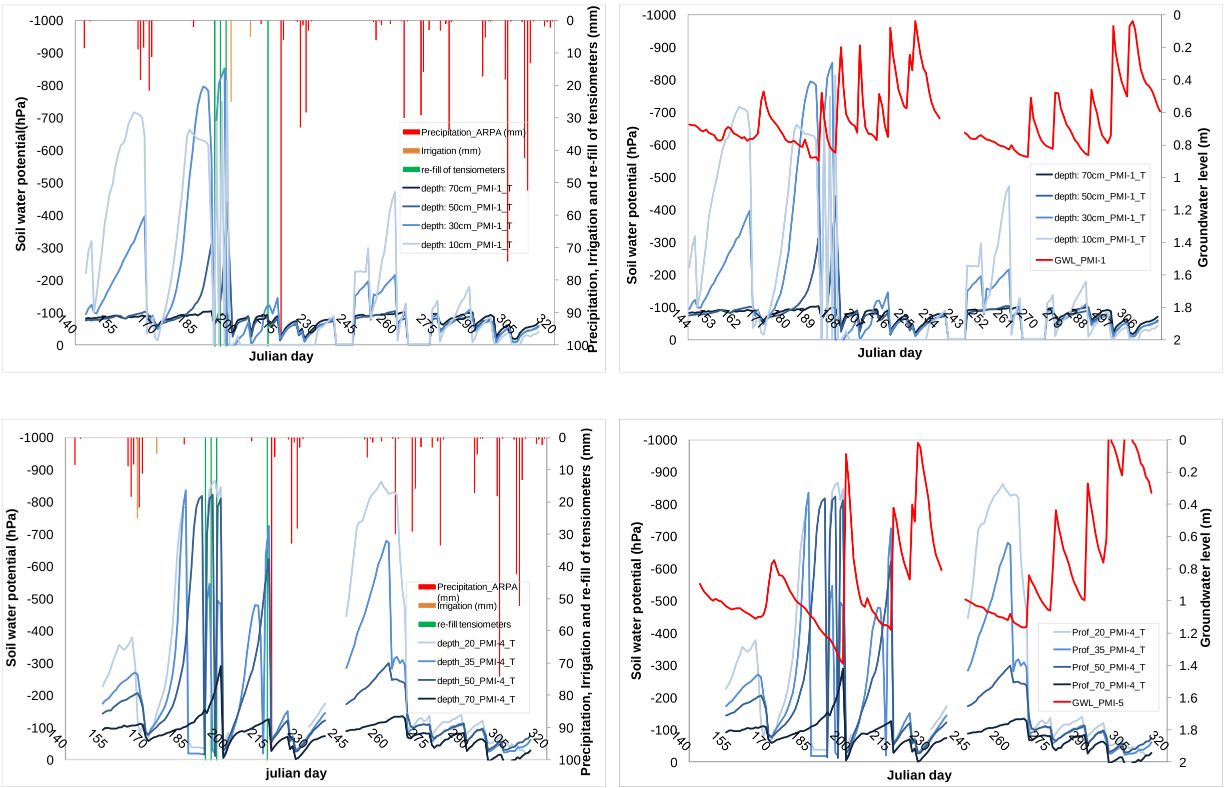

Figure 4.11 Matric Potential (hPa) for the sites PMI-1 (7cm, 27 cm, 47 cm, 67 cm) and PMI-4 (20 cm, 35 cm, 50 cm e 70 cm). In addition Precipitation, Irrigation and re-fill of tensiometers (left) and Groundwater level (right) during the 2010 season.

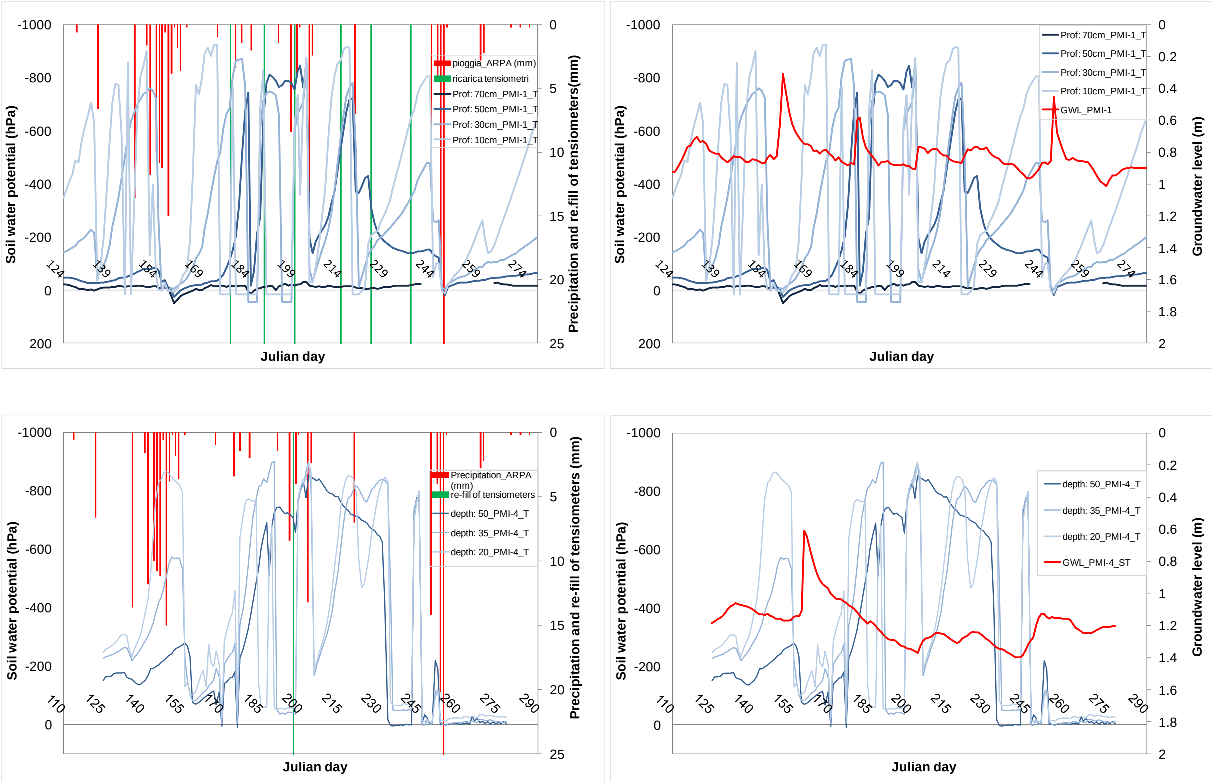

Figure 4.12 Matric Potential (hPa) for the sites PMI-1 (7cm, 27 cm, 47 cm, 67 cm) and PMI-4 (20 cm, 35 cm, 50 cm e 70 cm). In addition Precipitation, Irrigation and re-fill of tensiometers (left) and Groundwater level (right) during the 2011 season.

The Figure 4.13 and Figure 4.14 are presenting the famous relation between soil water content and soil water potential: soil retention curve.

The water retention curve, together with the hydraulic conductivity curve (relating the soil water potential and the unsaturated hydraulic conductivity) are the most important soil hydraulic properties. They affect the soil water budget, since they affect the ability of the plant's roots to uptake water from the soil and the amount of water percolating into the groundwater. The field values of SWC and SWP presented in the figures were used to determine the field retention curve for four depth in which probes were installed.

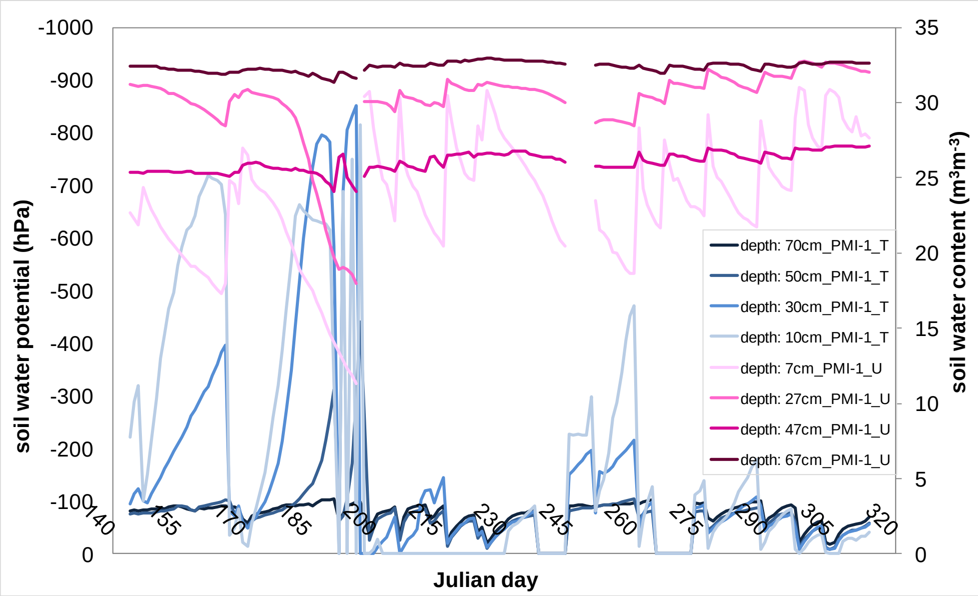

Figure 4.13 Site PMI-1: Matric potentials (hPa) and soil water content (m3m-3) at the forth depth of instruments installation (7cm, 27 cm, 47 cm, 67 cm) for the 2010 season.

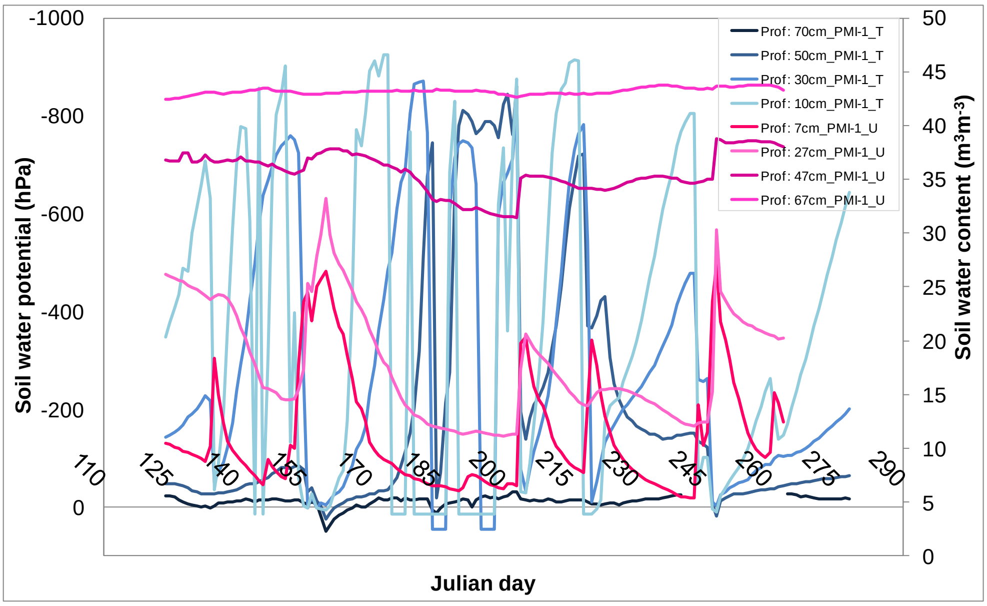

Figure 4.14 Site PMI-1: Matric potentials (hPa) and soil water content (m3m-3) at the forth depth of instruments installation (7cm, 27 cm, 47 cm, 67 cm) for the 2011 season.

show the matric potential manually collected at pre-dawn (5-7 solar hour) and mid-day (11-13 solar hour) during measurement campaigns and in the 6 experimental sites for the agricultural seasons 2010 and 2011 respectively. We can conclude from the figures that as deep as we go, the potential is less negative, because the porous caps are under water table level.

Generally, the potentials measured at pre-dawn were lower than those measured at the mid-day. During the 24 campaigns, the potentials were also measured between hours 17:00-19:00 and 21:00-23:00 (solar time) and the results demonstrated that potentials measured during the hours 17:00-19:00 were lower than those measured at the mid-day. While measurements during hours 21:00-23:00 were always lower than those at pre-dawn.

For the agricultural season 2010 and for all sites, the more negative potentials were recorded on 13 July and those closest to zero on 22 of July (respectively upstream and downstream irrigation event on 18 July, we have to remember as well that PMI-1, 2 and 6 were also affected by the second irrigation on 24 July).

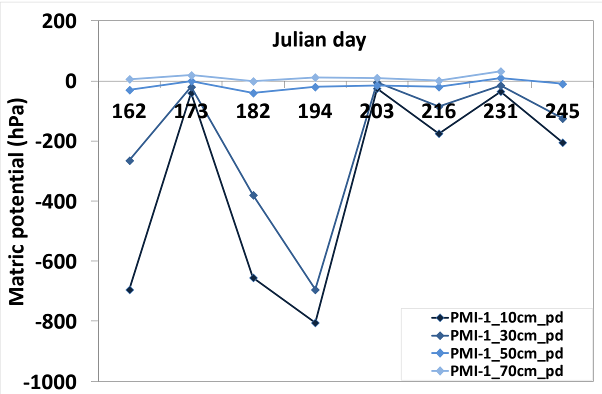

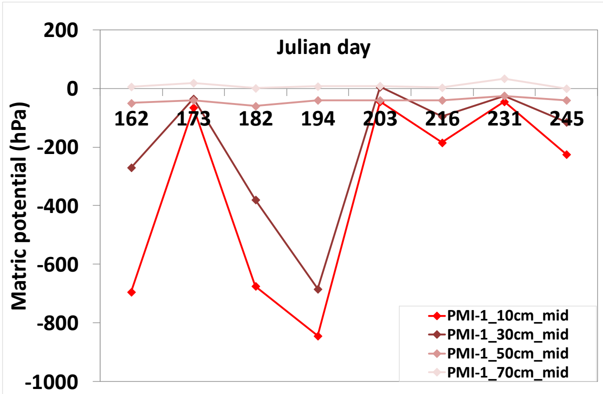

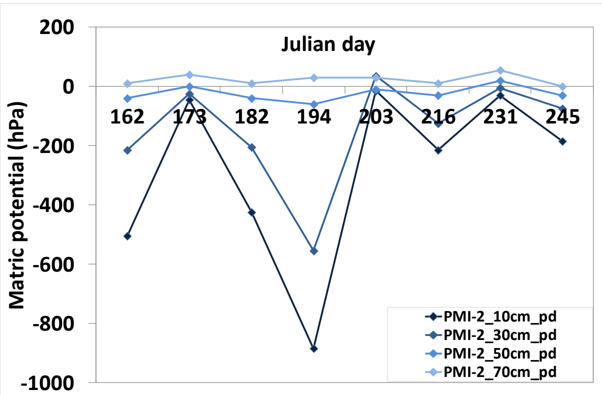

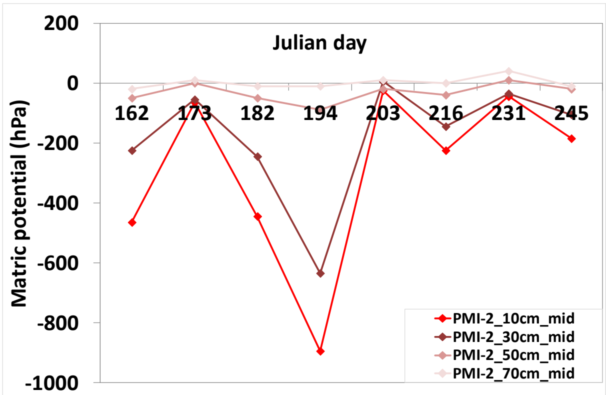

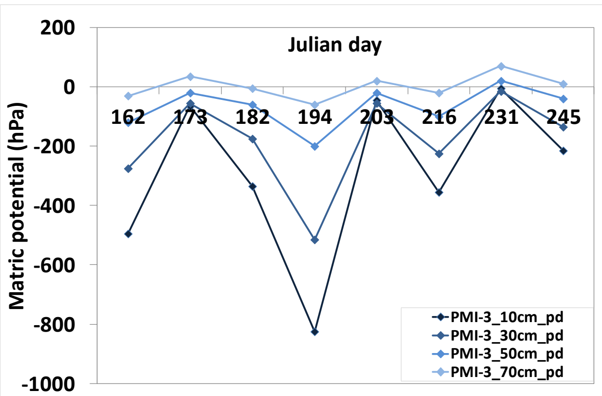

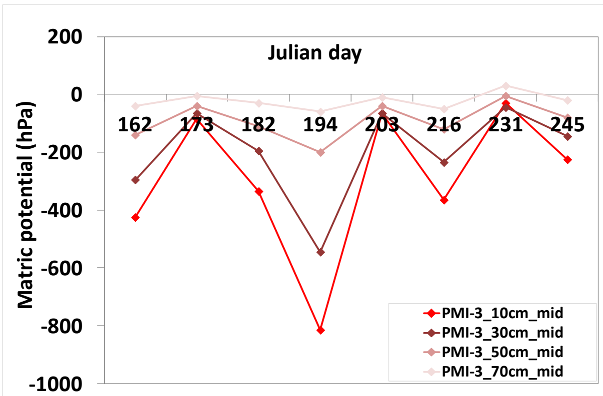

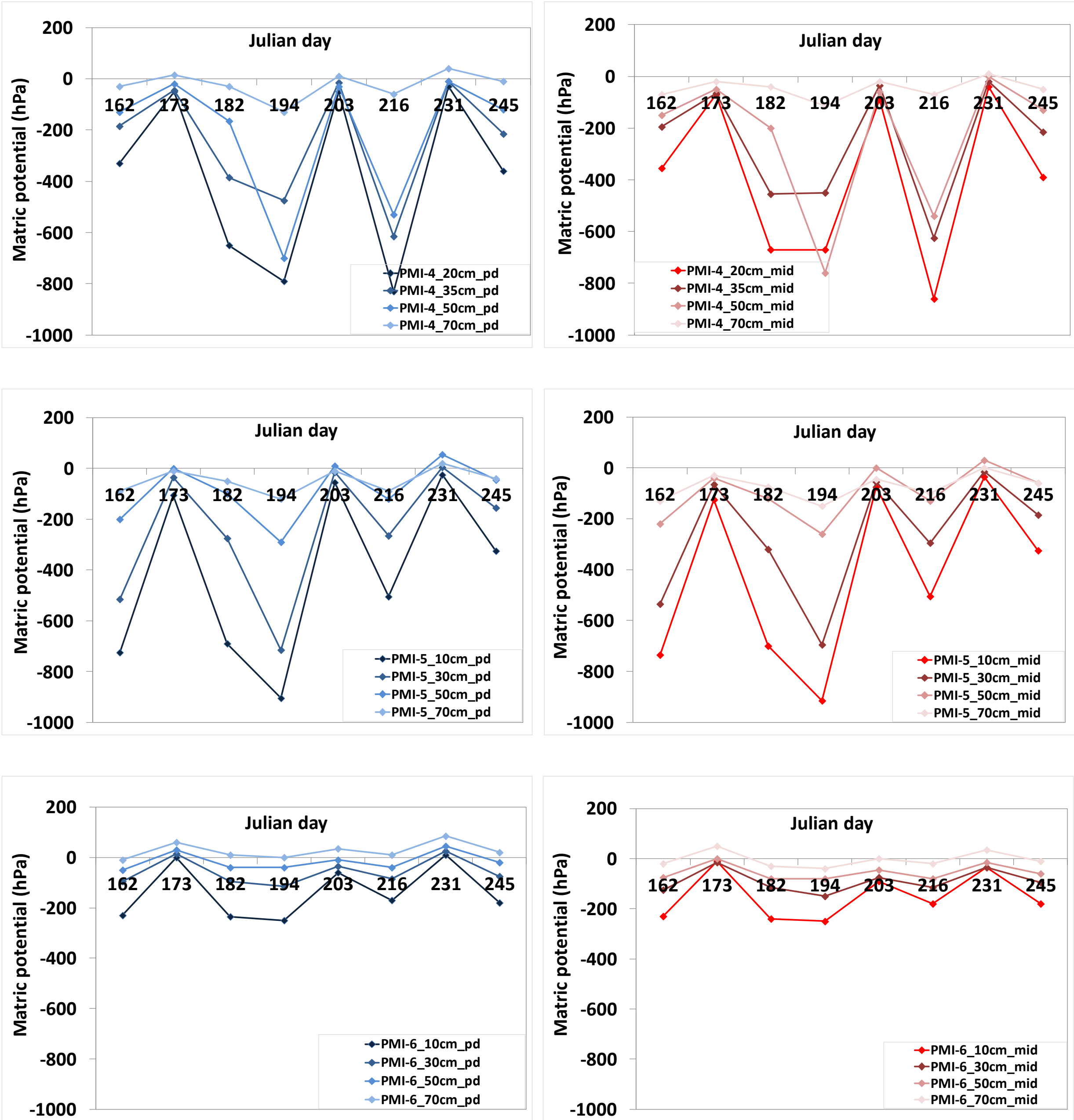

Figure 4.15 manual reading of soil water potential at predawn and midday for the six PMI during the 2010 season .

For the agricultural season 2011, positive potentials were more or less reached during the first two campaigns (June) when a big amount of precipitation occurred. On the other hand, negative values were particularly on summer period, specially July. The same conclusion was confirmed by the automatically collected measurements previously discussed.

During whole season, the only tensiometers that kept relatively low matric potentials (>-400hPa) were placed at depths of 30, 50 and 70cm in the PMI-1 and at 70cm in the PMI-2, due to the presence of shallow groundwater table.

At the end of the season, we noticed, particularly in sites PMI-1, 2 and 7, the potentials were close to zero, almost for all depths. It was also noticed the increase of ground water level during the same period.

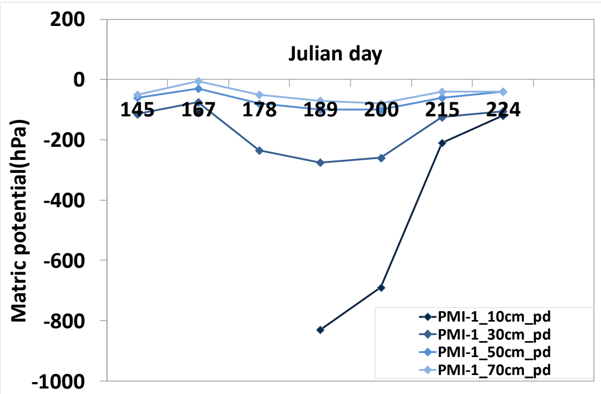

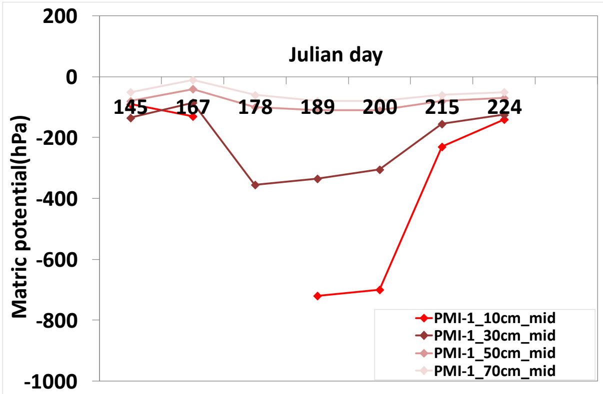

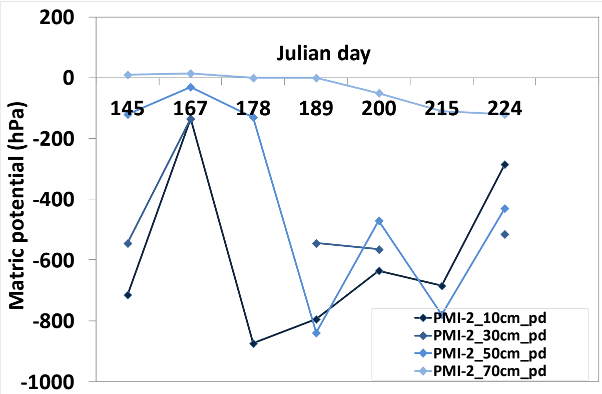

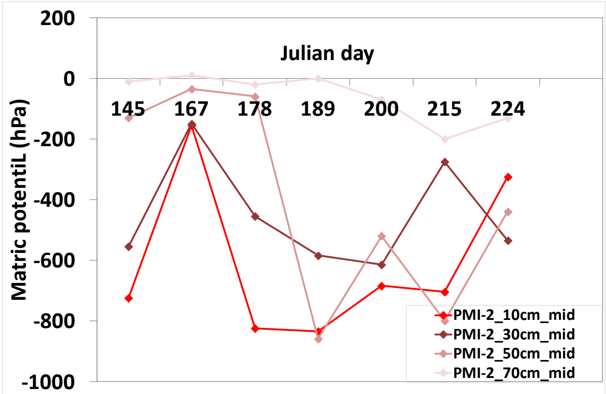

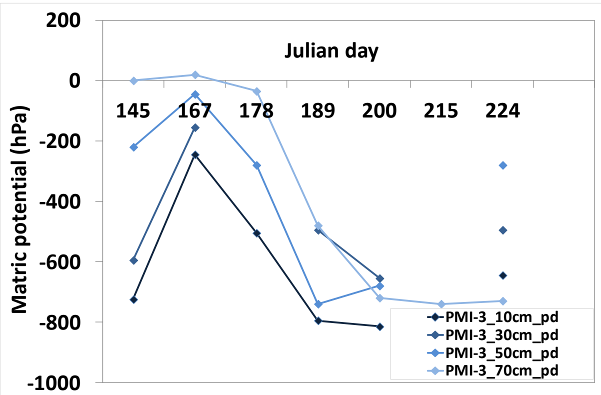

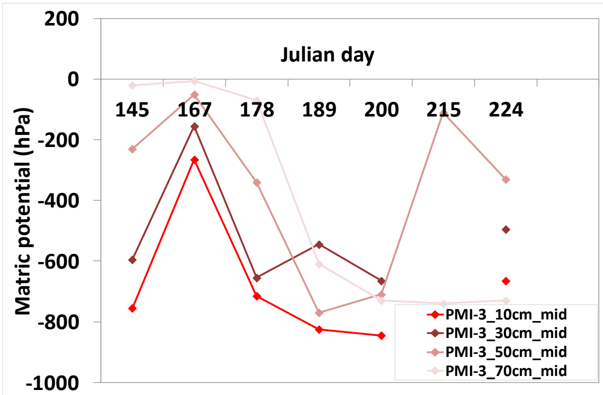

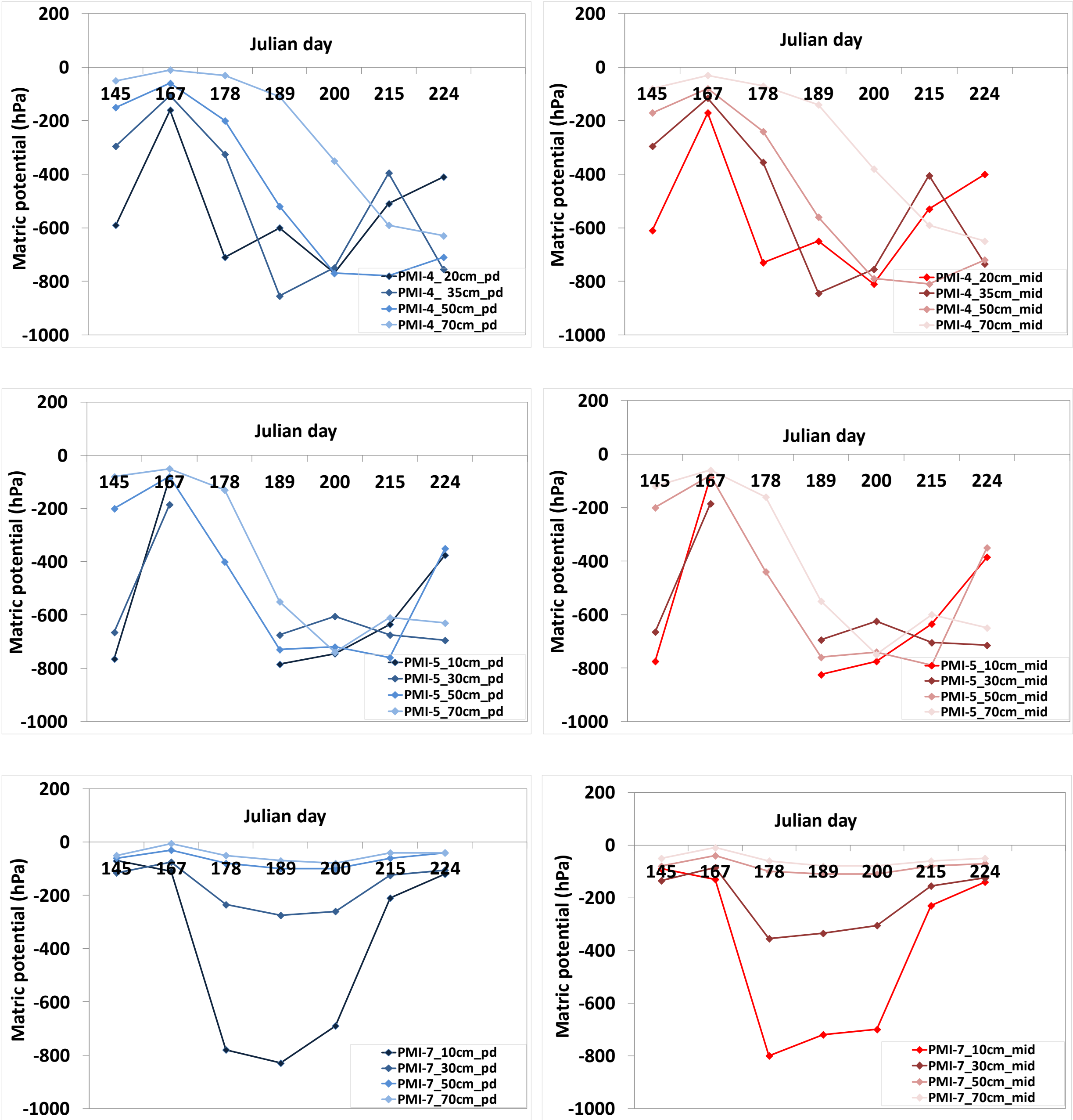

Figure 4.16 Manual reading of soil water potential at predawn and midday for the six PMI during the 2011 season .

4.4 Monitoring of actual evapotranspiration: Eddy covariance technique

Data used to calculate actual evapotranspiration were collected during 2010 and 2011 in a micrometeorological station located in our experimental fields of maize in Landriano in province of Pavia (45° 2' Nord, 9° 1' East).

The micrometeorological eddy covariance (EC) station (Figure 4.17) was located approximately in the centre of the field. The stations were equipped with a 4-components radiometer (Kipp & Zonen CNR-1), an infrared gas analyzer (LI-COR 7500) and a 3D sonic anemometer (Young RM-

81000V). Soil heat flux plates (Hukseflux HFP01) and soil thermocouples (ELSI) allowed to close the surface energy balance. Five soil moisture sensors (Campbell Sci., CS616) and tensiometers (Irrometer) were installed in a profile close to the eddy station at depths of 5, 20, 35, 50, 70 cm at the Landriano site.

Piezometers with pressure transducer devices (STS) completed the equipment in the station. The micrometeorological data were acquired at 20 Hz and then averaged on a half-hourly basis.

Figure 4.17 Eddy covariance station of Landriano

4.5 Campaigns of measurments

Below are presented the results of the experimental campaigns conducted during various phenological stages for the agricultural seasons 2010 and 2011.

4.5.1 Plant biometric parameters

Figure 4.18 and Figure 4.19 present plant biometric parameters monitored during the agricultural seasons 2010 and 2011. In particular the left figure presents trends of measured leaf area index with ceptometer (LAI) and percentage of canopy cover (%CC) derived from digital photo camera.

While, the right figure presents plan height (h) and stem diameter measured with the meter and “calibro”, respectively.

Figure 4.18 demonstrates how during the 2010 season, plants of maize were not showing the same phonological stages. This was supported by a difference of reaching the maximum LAI (during flowering stage) which was anticipated in PMI-1 in respect to the other PMI. Plant height and stem diameter were also different between PMI. In particular, a good development was noticed in PMI-1,2 and 3. Plant development in PMI-5 was more continuous and was in delay in PMI-4. This delay was mainly related to the bad germination rate which obliged us to transplant manually.

On PMI-6, plants faced some difficulties which could be attributed to water stagnation characterizing this site.

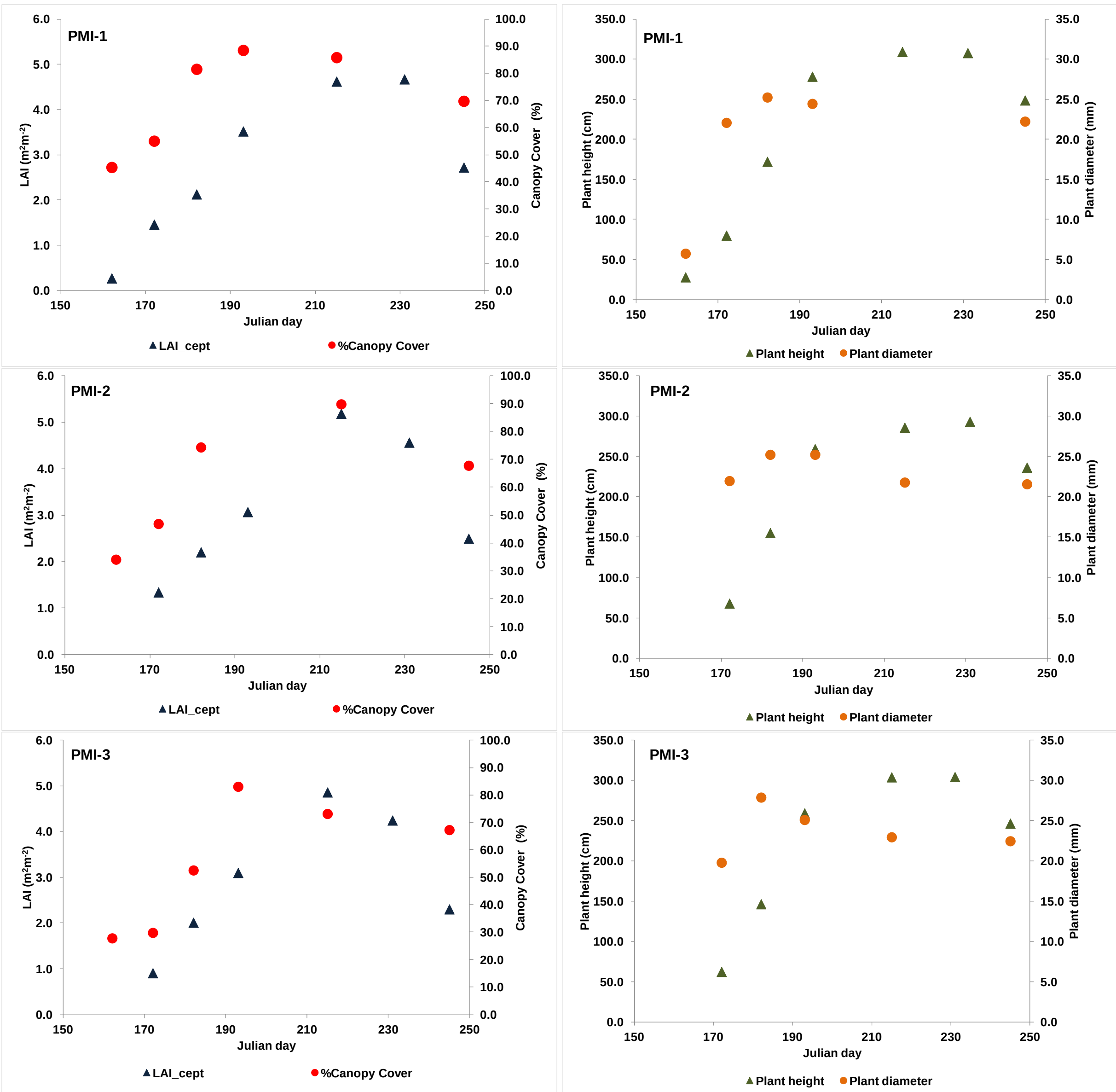

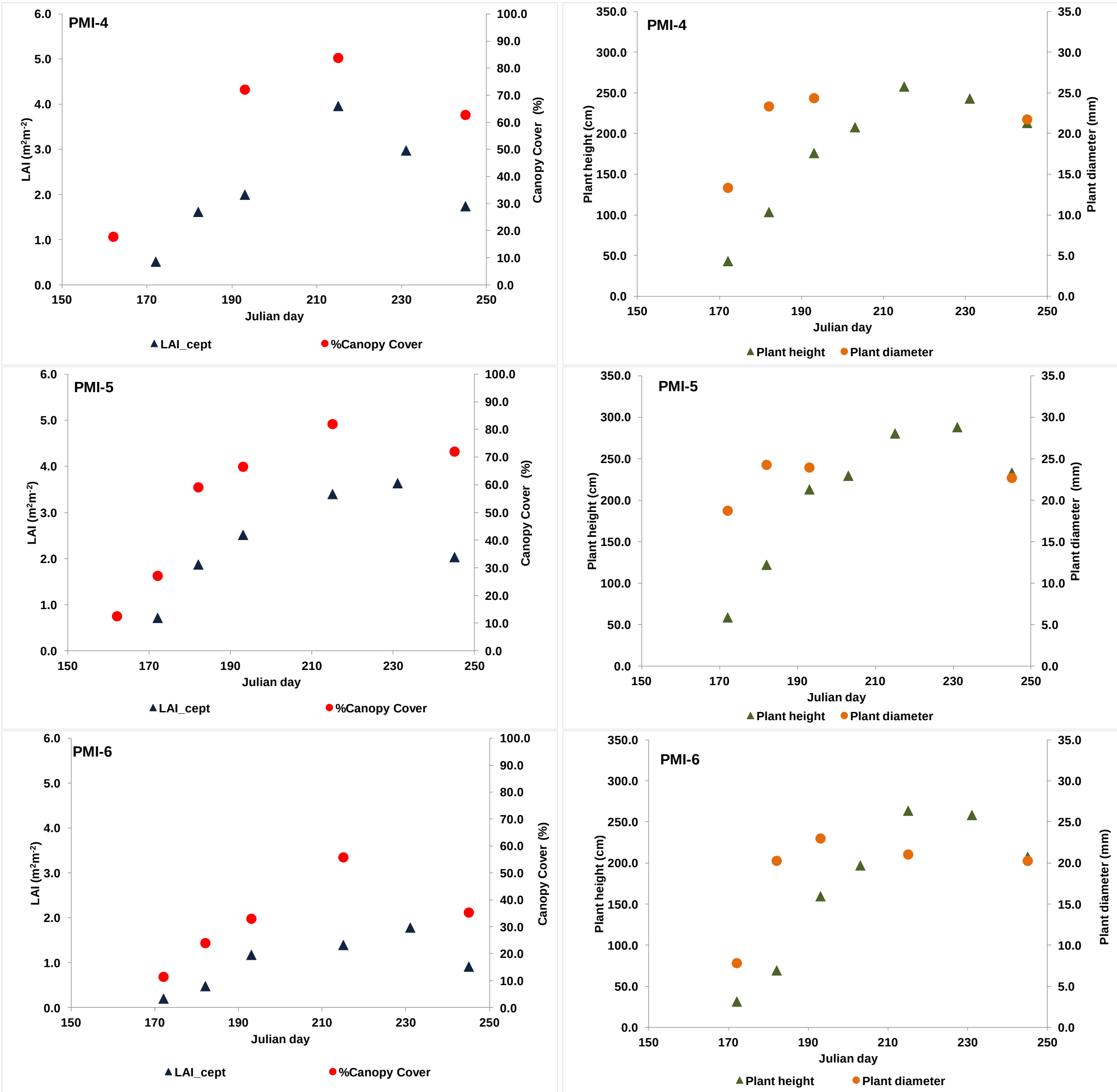

Figure 4.18 Trends of Leaf Area Index (LAI) and canopy cover (left) plant height and plant diameter (right) during the 2010 season for all PMI

In the absence of irrigation in 2011 season, PMI-3 and 5 showed greater LAI, %CC and plant height than those achieved during 2010 season. This was probably related to difficulties faced by plants after a huge amount of precipitation received at the beginning of the season 2010.

Starting from end of June, plants in PMI-1 and 2 illustrated some stress symptoms and this was also evident with LAI results. PMI-4 and PMI-7 presented an intermediate behavior in between other sites.

It can be noticed for all PMI and for both agricultural seasons that the maximum stem diameter was achieved 20- 30 days before reaching LAI and %CC peaks with a maximum value equals 27mm.

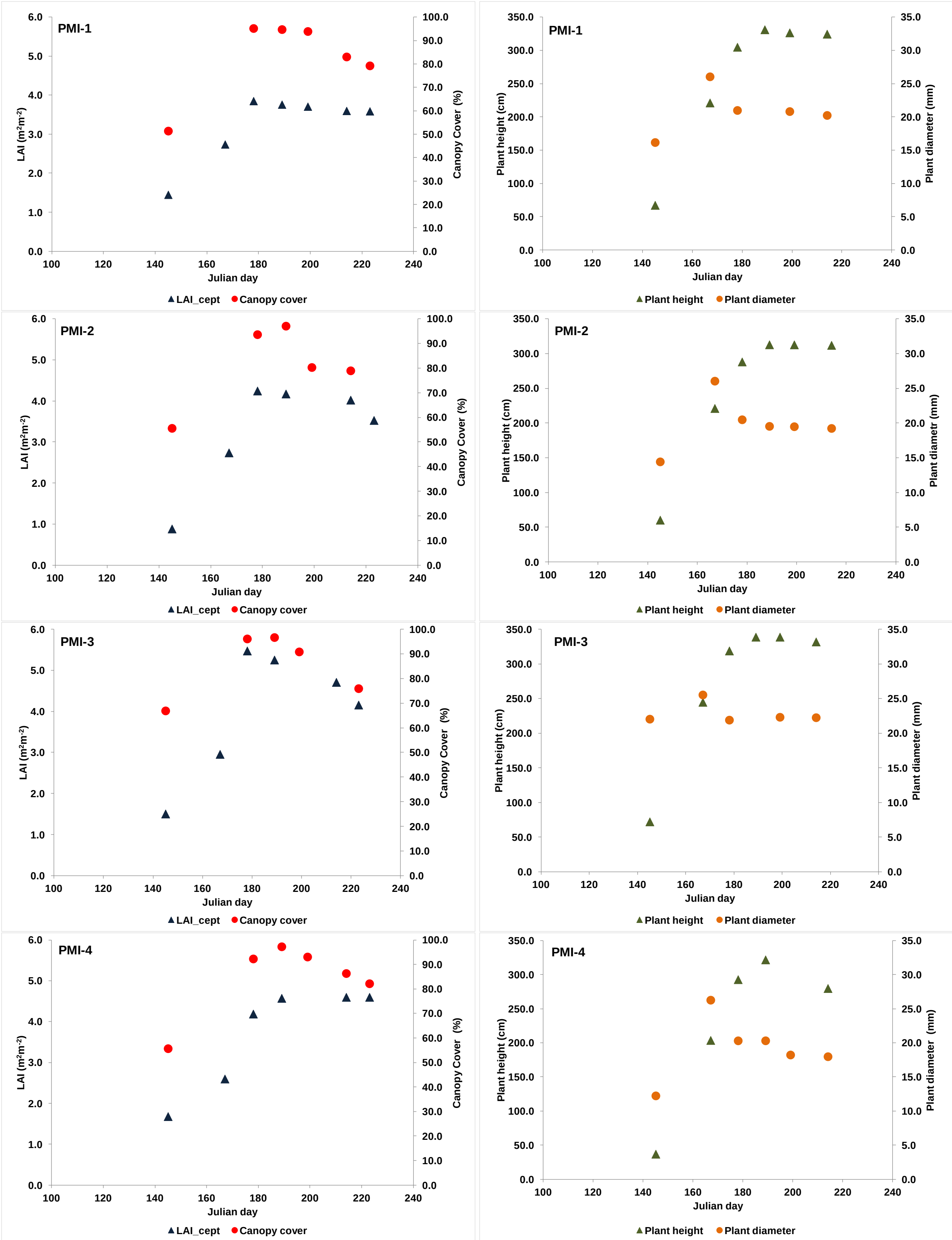
PMI-1
LAI (m²m⁻²)
Canopy Cover (%)
Julian day
▲LAI_cept ●Canopy cover
PMI-1
Plant height (cm)
Plant diameter (mm)
Julian day
▲Plant height ●Plant diameter
PMI-2
LAI (m²m⁻²)
Canopy Cover (%)
Julian day
▲LAI_cept ●Canopy cover
PMI-2
Plant height (cm)
Plant diametr (mm)
Julian day
▲Plant height ●Plant diameter
PMI-3
LAI (m²m⁻²)
Canopy Cover (%)
Julian day
▲LAI_cept ●Canopy cover
PMI-3
Plant height (cm)
Plant diameter (mm)
Julian day
▲Plant height ●Plant diameter
PMI-4
LAI (m²m⁻²)
Canopy Cover (%)
Julian day
▲LAI_cept ●Canopy cover
PMI-4
Plant height (cm)
Plant diameter (mm)
Julian day
▲Plant height ●Plant diameter

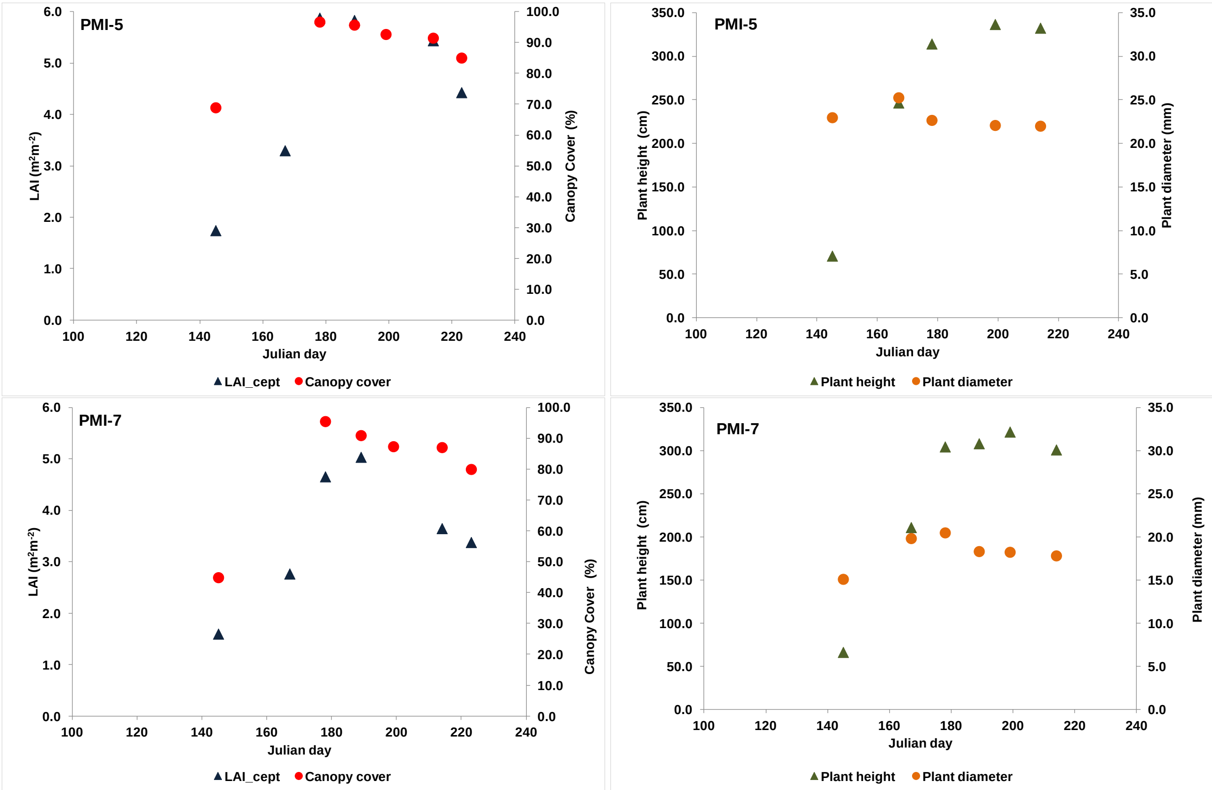

Figure 4.19 Trends of Leaf Area Index (LAI) and canopy cover (left) plant height and plant diameter (right) during the 2011 season for all PMI

During the monitoring campaigns 2010, two indirect methods were used to measure LAI (ceptometer and digital camera with an objective fish eye). It was also directly measured LAI with a destructive method.

Figure 4.20 presents a correlation between values of LAI obtained from destructive method and those obtained from the indirect measures; (a) LAI with ceptometer; (b) “effective” LAI with digital camera; and (c) “real” LAI with digital camera.

The “real” LAI in comparison with “effective” LAI is taking in consideration the real spatial distribution of leaves. Values acquired from measurements with ceptometer tended to underestimate those measured by destructive method, but the correlation is well supported (slope = 0.85 and R^2= 0.77).“Effective” LAI measured with digital camera underestimated more the destructive values (slope = 0.73; R^2= 0.56). Considering “real” LAI, the correlation was proved (slope= 0.73; R^2= 0.84). However the regression line presented an interception which was not negligible (1.591). Obtained results confirm the previous study done by Facchi et al., 2010 in the same field.

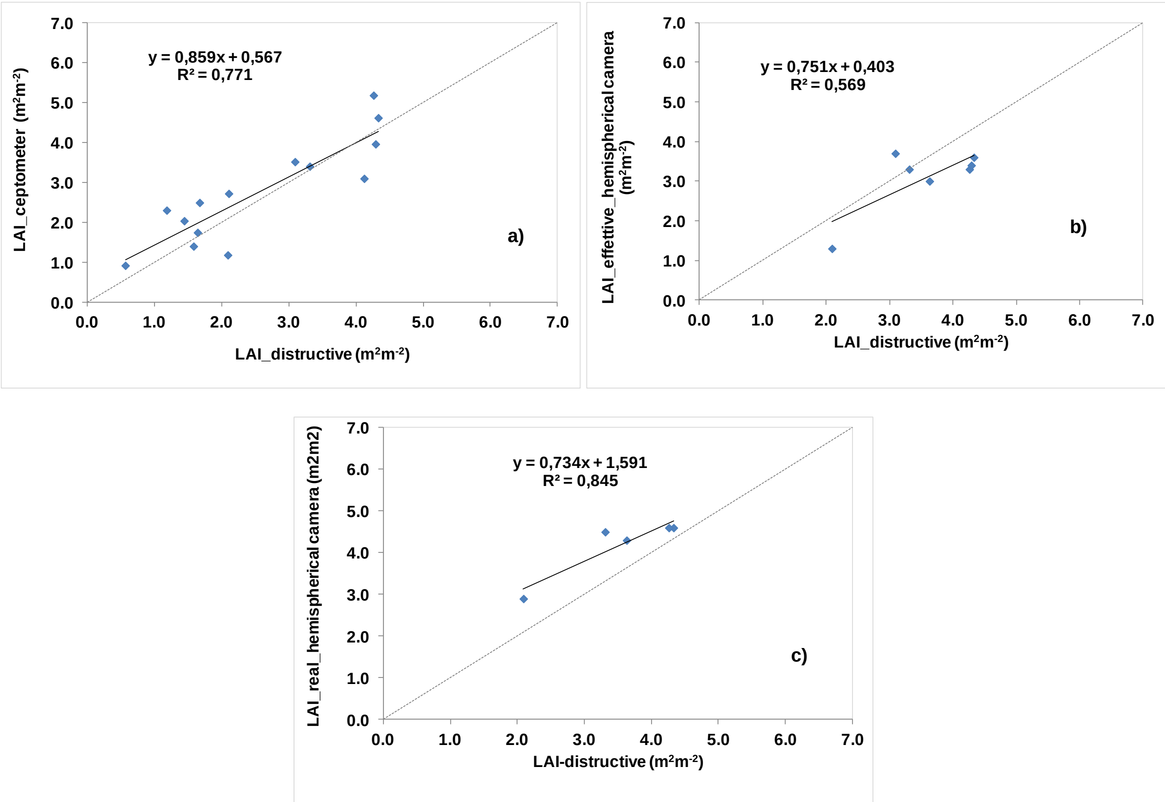

Figure 4.20 Correlation between measured LAI with the destructive method e: (a) LAI with ceptometer; (b) LAI "effettive" with a photographic camera with obiective fish-eye; (c) LAI "real" with a photographic camera with obiective fish-eye

Plant rooting depth was measured once in 2010 in 3 PMI (1,3 and 5). The obtained values were around 45cm. This value is very low compared to reported values in the literature for Maize (around 1m, Allen *et al*., 1998). The low value could be justified with the shallow water table during the same season.

For the agricultural season 2011, rooting depth was measured in the same latter sites during three different times (25 May, 21 June and 1 September). The corresponding values were 25, 60 and 65-90cm respectively. These high values can be explained by absence of irrigation and low water table levels in compare with 2010 season. Plants developed roots in order to extract water.

4.6 Soil hydraulic characteristics

4.6.1 Soil texture and organic matter content

Soil texture analysis were done for all PMI (1, 2, 3, 4, 5, 6 and 7) in the four depth used for instruments installation using the hydrometer of Andreansen method. For PMI-6, soil texture analysis were previously done on 2006.

Figure 4.21 presents the percentage of sand, loam, clay and skeleton for the four depth (7, 27, 47 and 67cm). the percentage of gravels was not done for PMI-4. Values reported in figures were the average of the three replications done.

Results demonstrated a variability in soil texture for all the field in particularly in the upper layers.

PMI-6 presented a high percentage of loam comparing to other PMI. PMI-1 and 2 were characterized with a high percentage of gravels specially in the deepest layers and a sandy texture. PMI-5 has more loam and clay content. PMI-3 and 4 had an intermediate behavior. PMI-7 which was the control irrigated site for 2011 had a similar texture to PMI-4 but a lower percentage of clay in the deepest layers.

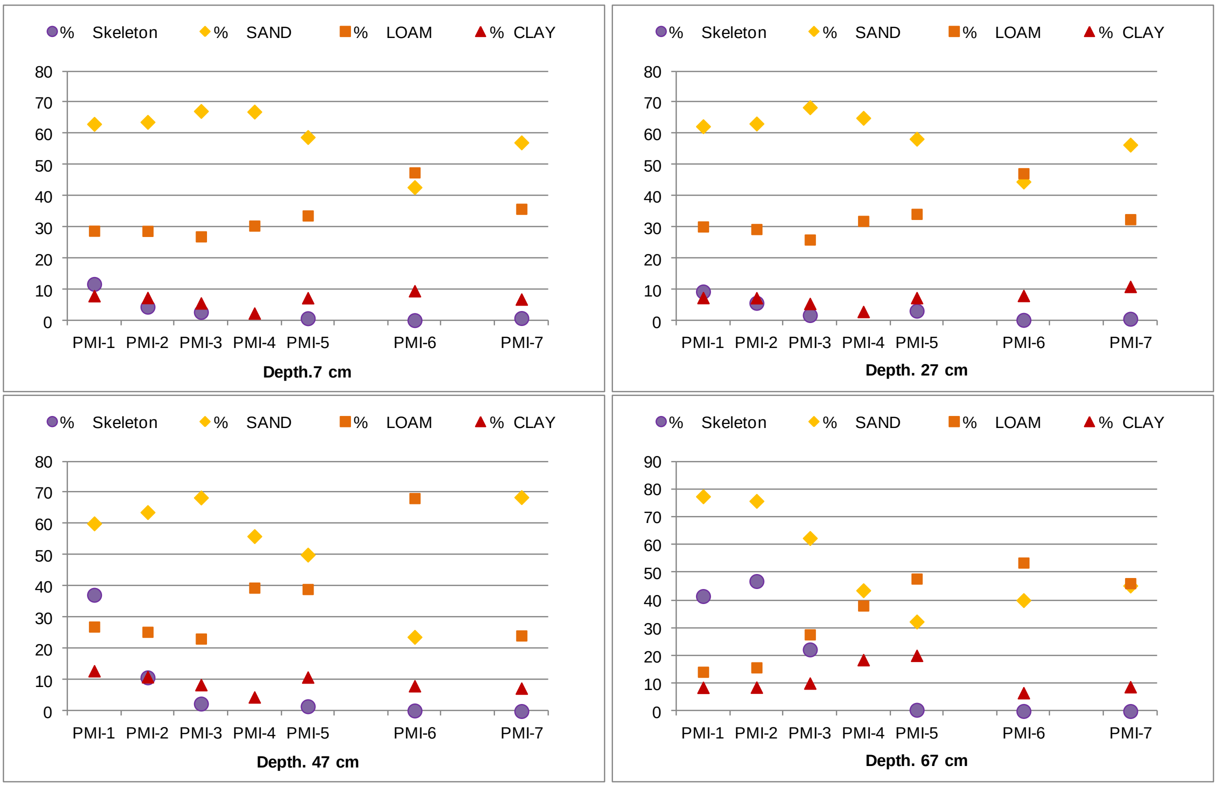

Figure 4.21 Percentages of skeleton e, Sand, Loam and Clay for all PMI at the four depth of the instruments installation

Percentage of organic matter content for the first 40cm of the soil are presented in the Table 4.2

It can be noticed that all PMI except PMI-6 have similar organic matter content. While PMI-6 presents a very low content.

Table 4.2 Organic matter determined from 0-40 cm on March 2010

sites	PMI-1	PMI-2	PMI-3	PMI-4	PMI-5	PMI-6
O.M (% in weight)	2.12	2.03	1.94	1.93	1.89	1.13

4.6.2 Bulk density

During the two experimental years, it was done for the whole agricultural season undisturbed soil sampling in order to determine bulk density ($kg.m^{-3}$) in laboratory.

Figure 4.22 illustrated trends of average and standard deviation of bulk density in all PMI at different four soil depth (7, 27, 47, 67cm).

For PMI-4 and 7, statistic calculations were done for 2 and 3 samples respectively. While for other PMI, it was done for 6 to 9 samples.

Bulk density for the two first layers (agricultural horizon) in all PMI varied between 1.2 and 1.4 $kg.m^{-3}$. Differences were more evident between PMI at 27cm depth than those measured at 7cm depth. Measured bulk density is in a good accordance with values reported in the literature (1.5-1.6 $kg.m^{-3}$ for sandy soils and 1.3-1.4 $kg.m^{-3}$ for medium textured soils). It was also reported that latter values can decrease by 15-25% after field works and this is true in particularly for the upper layers.

Figures demonstrate that bulk density was varying with depth for all PMI. For some PMI, bulk density higher for the upper layers and this could be justified by soil compaction due to field works. While the opposite is true for the deepest layers where roots caused some aeration.

Bulk density analysis confirmed soil characteristics variation in a field scale. It demonstrated also the existence of their time variation after field works and water supply (precipitations and irrigation).

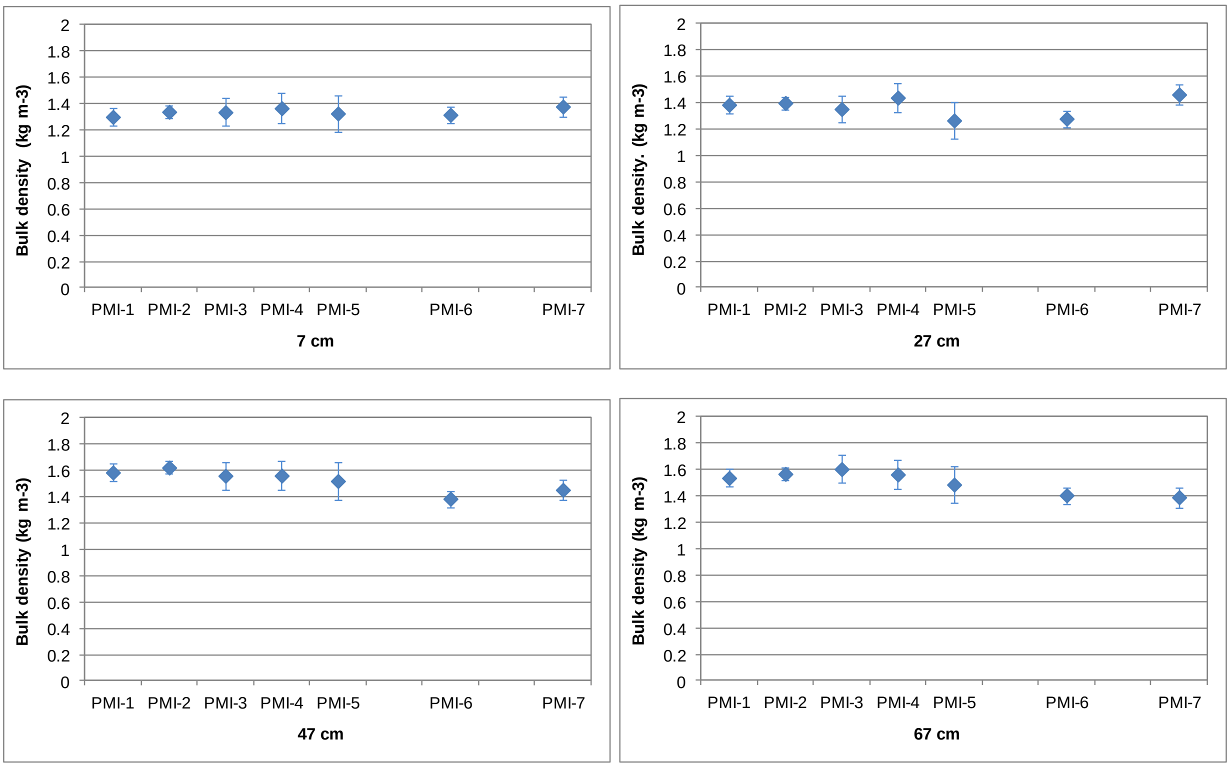

Figure 4.22 Mean and standard deviation of the bulk density (kg m-3) measured for all PMI at four depths

4.6.3 Field Soil Retention Curve

In order to determine the soil retention curve, analysis were done for samples taken in PMI-1 and PMI-5 which were the most representative sites for the whole field.

Technique of Richard apparatus and tensiometric box were used. Analysis were done using two replications for each depth (7, 27, 47, 67cm). In order to draw the retention curve, soil water content was determined for 10 different pressures (0.01bar, 0.05bar, 0.1bar, 0.33bar, 0.5bar, 1bar, 3bar, 5bar, 7bar and 15bar). In particularly for a pressure of 0.01bar and 0.05bar, analysis were done using the tensiometric box. While from 0.1bar up to 15 bar Richard apparatus was used.

For high pressures (5, 7 and 15 bar), analysis were done with disturbed samples. In the literature it was proved that at high pressure, the corresponding soil water content is independent of the soil structure. (Bastiaanssen et al., 1996).

The soil retention curve measured with different techniques will be discussed in detail in the following chapter (5).

5 Comparison of The Predicted and Measured Soil Retention Curve

5.1 Introduction

The soil water retention curve describes the relationship between series of the water contents of a soil (θ) from very wet to very dry and the matric suction (h) at which the water is held at each θ value. It is a physical soil property which describes the soil porous system. It depends basically on soil structure, texture, organic matter content, and bulk density. It will therefore vary both vertically (diagnostic horizons/layers in the profile) and horizontally in any field. Stratified sampling according to diagnostic horizons or specific layers is a prerequisite to determine the overall hydrological behavior of a soil profile (ISO., 2009). Because of that, the hydrological behavior of soils to agriculture, forestry, hydrology, engineering and pollution research concerning the soil water retention characteristics of soil is important.

Information on soil water retention is needed for example: (i) to determine plant available-water in the soil. i.e. the portion of water that can be readily absorbed by plant roots (van Rensburg., 1988); (ii) to evaluate soils for irrigation purposes; (iii) to estimate the soils pore size distribution (Kutilek., 2004); (iv) to check changes in the structure of a soil, e.g. caused by tillage, mixing of soil layers (Kutilek, 2004); (v) to predict other soil physical properties, e.g. hydraulic conductivity (Mualem, 1976; van Genuchten, 1980); (vi) to provide inputs in most water balance and hydrological models (Bennie et al., 1994). Consequently, owing to their relative importance in many disciplines, information about water retention characteristics can be useful for farmers and governments as a planning tool for development and investment strategies.

These properties are difficult to measure and therefore require the use of both direct and indirect methods to adequately describe them with improved accuracy. Several field methods, laboratory methods and theoretical models for such determinations exist, each having their own limitations and advantages (Stephens., 1994).

In situ methods are considered to be more representative than laboratory methods for determining water retention characteristics (Marion et al.,1996). This is mainly because of the larger volume of soil involved and the preservation of soil structure during the experiment. The former procedure also avoids changes in pore size distribution and continuity which may be caused during the collection and transportation of undisturbed samples. Such changes may substantially influence the measured θ-h relationship, particularly near the wet end ($h < 10$ kPa) where most water flow occurs (Kutilek., 2004). Reliable results can, however, be obtained if samples are carefully collected and

handled. The routine use of field methods is often restricted by cost and time considerations, including the cost of instrumentation, especially when large areas have to be characterized for their hydraulic properties. Nevertheless, the θ-h relationships are frequently determined in the laboratory. As large numbers of representative, carefully collected samples from different locations can be dealt with simultaneously in the laboratory, this method is considered a valuable alternative to in situ measurements (Marion et al.,1993). But due to difficulties and labor costs when measuring soil water retention curve (SWRC) in the laboratory as well, it has become necessary to develop methods to describe the function utilizing readily available data, such as soil particle-size distribution or soil texture, organic matter content, and dry bulk density.
Many empirical models for SWRC have been developed (Brooks and Corey., 1964; Van Genuchten., 1980; Russo., 1988; Leij et al., 1997). These models are referred to as Pedotransfer functions, PTFs (Bouma., 1989). In these models, parameters were usually estimated by fitting the functions with measured data, and the PTFs were used empirically to describe the relationship between the parameters and basic soil data (Wosten and Van Genuchten., 1988; Vereecken et al., 1989; Scheinost et al., 1997; Schaap et al., 1998; Minasny et al., 1999; Elsenbeer., 2001; Wosten et al., 2001).

The aim of our study was, therefore, to evaluate (i) the general applicability and (ii) the prediction accuracy of some of the most commonly cited and some recently developed PTFs that use soil properties such as particle-size distribution (sand, silt, and clay content), organic matter or organic C content, and dry bulk density to predict the soil retention curve. Then to compare the estimated soil retention characteristics to those measured in the field and laboratory

5.2 Objectives of the study

In light of the above discussion, it still requires extensive comparisons between estimated, field and laboratory results to determine their validity for a range of different soils. However this study attempts to make a contribution specifically in this connection.
Therefore, the main objective of the study is to characterize and compare field, laboratory and estimated soil hydraulic properties of an experimental field in north of Italy and then to use those data to run the two hydrological models SWAP and IDRAGRA.

5.3 Literature review

Field, laboratory and theoretical methods for estimating the hydraulic properties have been reviewed by many authors. Hence, the main focus of this chapter is essentially to give a short review of the theoretical background of relevant soil hydraulic properties and processes.

5.3.1 Soil hydraulic properties

Water movement within the soil profile is an important component of agricultural and environmental studies and the understanding of it will help to solve problems related to irrigation, subsurface drainage contributions to groundwater, growth of saline seeps, and water disposal. Adequate and effective management of soil and water therefore often necessitates characterization of water retention and hydraulic conductivity functions of the area concerned. These functions collectively are referred to as soil hydraulic properties (Klute and Dirksen., 1986).

5.3.2 The Purpose of Hydraulic Measurements

Methods to determine hydraulic properties differ with respect to their accuracy, measurement range, difficulty of implementation, and demand for time and capital. Before selecting a specific measurement method, the purpose of the measurements must be manifest. Purposes may be classified into three groups.

(i) Soil hydraulic properties are often needed for a hydraulic classification of soils, in a similar manner as the particle size distribution is used for a textural classification. Knowledge of basic hydraulic properties, such as field capacity or plant available water content, is useful for a variety of purposes, where soil moisture storage, soil wetness (affecting oxygen supply for plant roots and redox state of soil), surface runoff, susceptibility to soil erosion, and other large-scale properties of soils are of interest. Indirect methods are often appropriate for this group (Schaap., 2005).

(ii) Today's prevalent demand for hydraulic properties is their use in numerical simulation of water transport by Richards' equation. Estimation of water recharge through the vadose zone for water balance calculations are a classic application, but more important is now their use for agricultural, ecological, and environmental purposes, such as irrigation control, fertilizer management, and contaminant fate modeling. The focus of subsurface models of water and solute transport has increasingly been shifted toward environmental research, with the primary concern on the subsurface fate and transport of various substances, such as nutrients, pesticides, pathogens, pharmaceuticals, viruses, bacteria, colloids, and toxic trace elements (Simunek., 2005). The crucial bottleneck for the successful application of these models is their parameter estimation requirements.

(iii) Finally, accurate measurement of soil hydraulic properties is required for a further improvement in the basic understanding of soil hydraulic processes, that is, in order to test and improve the process knowledge we have. Examples are the understanding and assessment of non equilibrium phenomena in water flow, further progress in describing hysteresis in soil water flow, and the question up to which scale the Richards equation process model provides an appropriate effective process representation for unsaturated water transport (Durner and Flûhler., 2005).

Whereas the demand on accuracy, resolution, precision, and reliability of the measurements is moderate for the first group, it is higher for the second and third (Chimungu., 2009). For the second group, we are particularly faced with scale considerations. For the third group, the precision, reliability, and validity of measurements are of utmost importance, in order to avoid misconceptions.

5.3.3 Soil water retention characteristic

Soils differ in their capacity to retain water against gravity. The water binding properties of soils are represented by the relationship called soil water retention characteristics, which is coded as θ-h relationship. This is the relationship between amount of water in the soil and the potential energy with which it is bound by the soil (Jury et al., 1991). The θ-h relationship is a unique function for each soil, because of variation in soil particle size distribution and structure. Both of these factors influence the θ-h relationship by affecting the pore size distribution and the number of a given size pore in each size class (Dexter., 2004). The θ-h relationship is an important soil property that is needed for the study of plant available water, infiltration, drainage, hydraulic conductivity, irrigation scheduling, water stress on plants, and solute movement (Kern., 1995). In non swelling soils it reflects the geometry of the pores and this geometry, in turn, determines to a large extent the hydraulic conductivity. Since the pressure difference across an air-water interface is inversely proportional to the equivalent radius of the interface, the θ-h relationships can be converted into an equivalent pore size distribution (derivative curve), and the water content at any given suction is equal to the porosity contributed by the pores that are smaller than the equivalent diameter corresponding to that suction (Jury et al., 1991). The spatial patterns of water retention characteristics are important factors for studying the response of vegetation and hydrological systems in climate change (Dolph et al., 1992). Soil particle size distribution strongly affects the θ-h relationship at suction heads >100 kPa and to a lesser extent, at lower suctions where soil structure is also important (Hillel., 1998).

5.3.4 The Challenge of Determining Soil Hydraulic Properties

Determining soil hydraulic properties is demanding for a variety of reasons. Soils are porous media with a three-dimensional arrangement of interconnected voids that form a highly complex pore system. The topology of this system shows, in general, a hierarchical arrangement, with spatial and temporal variability on a multitude of scales. The microscopic properties of the pore system determine the macroscopic hydraulic behavior. A complete understanding of water flow in soils requires a thorough understanding of processes on scales much smaller than the usual measurement scale and the ability to express effective hydraulic properties at scales much larger than the measurement scale (Durner and Fluhler., 2005; Hopmans and Schoups., 2004). A specific problem in the determination of soil hydraulic properties lays in the fact that quality control and validation of measurement results is extremely difficult. Contrary to soil chemical analysis, there is virtually no possibility for reliable interlaboratory comparisons (Dirksen., 1999b). The reasons for this are: (i) as opposed to consolidated porous media, the soil pore system is not a stable structure. Just those parts of the pore system, which control the water transmission near saturation, are most fragile, and there is always a danger that the measurement process itself changes the system (Ghezzehei and Or., 2003). Therefore, repetitive measurements on the same soil sample by different laboratories are impractical. The sampling process itself often causes the most severe disturbance, when an “undisturbed” soil sample is isolated from the natural embedding. (ii) Soils exhibit considerable temporal variability (Mapa et al., 1986; Ahuja et al., 1998; Leij et al., 2002). Thus, measurements at the same site may yield different results if applied at different times (Van Es et al., 1999).

(iii) Soil is a living organism and the pore system is affected by a variety of interacting biological, chemical, and physical processes. Matrix surface properties are variegated and may change depending on physical, chemical, and biological factors, thereby changing the macroscopic hydraulic behavior. (iv) Spatial variability of hydraulic properties, finally, is probably the biggest problem (Nielsen et al., 1973, 1986). Different measurement methods use different sample volumes and sample numbers, dictated by standard procedures and the apparatus available for the various methods. This implies that, in a comparison of measurement methods, considerable uncertainty about the result of the comparison will always be induced by natural variability (Stolte et al., 1994; Munoz-Carpena et al., 2002). For example, the determination of field-saturated conductivity, K_{fs}, may vary two or more orders of magnitude among different field and laboratory methods. Testing measurement methods on synthetic soil-like porous media is not a solution to this dilemma. The pore system properties of repacked soil samples are often very different from the properties of an undisturbed soil (Torquato., 2001). It is notable that especially uniform fine sand, being the favorite material used for research purposes in soil physics, has properties that are quite untypical for a structured natural soil. Since the early observations of Kozeny., (1927) on particle segregation during packing, the problem of constructing a synthetic porous medium in a fully reproducible manner, with pore system properties comparable to a natural soil, has remained unresolved (Lebron and Robinson., 2003).

An overview on various field and laboratory methods for determining unsaturated hydraulic properties shows that many techniques have been proposed, but most of them are limited to relatively narrow ranges of water potential (h) or water content (θ). The existing experimental procedures all have their own unique advantages and limitations (Gee and Ward., 1999), and selecting the most appropriate measurement for a specific task is usually not trivial.

5.3.5 Methods of characterizing soil water retention characteristic

In literature, there are several methods available used to obtain measurements of θ-h relationship. It is impossible to cover all the soil water retention measurements methods that are presently in use. A complete discussion of measuring methods of θ-h relationships is given by Dirksen., (1999).

In the laboratory, the θ-h relationship may be measured on replicated samples over range of water contents. Virtually the entire range from water saturated soil to very dry soil may be covered by using a tensiometric box and pressure plate apparatus (Klute., 1986; Dirksen., 1999; Bohne., 2005). According to Jury et al., (1991), equilibrium water contents are usually obtained by exposing saturated, undisturbed soil sample to a tensiometric box at suctions < 10 kPa. The use of the tensiometric box is confined to this range because of the limitation in the length of hanging water column and due to possible cavitations (Jury et al., 1991). However, the pressure plate apparatus is normally used for the suction range of 30-1500 kPa (Jury et al., 1991). According to Reeve and Carter., (1991) the precision of pressure plate apparatus is very good, with a coefficient of variation of 1-2% attainable. However, clogging of the ceramic plates by soil particles or alga growth can occur after repeated use, reducing the efficiency of the plate (Townsend et al., 2001) and other problem is time taken to reach equilibrium if at all is reached because conductivities are so low at the dry end. The θ-h relationship in low suction range of 0-100 kPa is strongly influenced by soil structure and its natural pore size distribution (Hillel., 1998). Hence, undisturbed soil samples are recommended to be used (Dirksen., 1999). It is acceptable to use disturbed samples at suctions greater than 100 kPa, provided that the disturbance consists only in breaking off small pieces of soil and not in compressing or remolding the soil.

Soil properties affecting water retention and transport of water and chemicals in soils are manifold. The properties used most often in PTFs estimations, because of their availability or because they proved to be the most promising ones, are the following:

Particles size distribution is used in almost any pedotransfer function, different national and international classification systems use often quite different particle size classes. As a consequence, textural classes used in PTFs vary considerably. However using sand, silt and clay contents is a common approach (Maclean and Yager., 1972; Williams et al., 1992; Shein et al., 1995; Wosten et al., 1999). To characterize particle size distributions, the median diameter was found useful in soils with wide texture ranges (Bloemen., 1980; Campbell., 1985). Minasny et al., (1999) and Scheinost et al., (1997) used the median diameter along with the geometric standard deviation to predict soil water retention. Mishra et al., (1989) did the same to predict K_{sat}. To use the particle size distributions, it is desirable to have functions suitable to approximate the whole distribution or to approximate the particle size distribution within a large diameter range. This is needed when the textural particle size distribution is characterized by a limited number of fractions (Zeiliguer et al., 2000), or when data come from different sources with different fraction diameter ranges (Nemes et al., 1999).

Texture alone was reported to be a good predictor of saturated hydraulic conductivity in sandy soils (Jaynes and Tyler., 1984; El-Kadi., 1985b). Clay content was leading texture parameter to be correlated with K_{sat} in databases comprising of soils other than sandy soils (Puckett et al., 1985). It is good to remember that particle size distribution or texture itself is probably a poor predictor of for instance K_{sat}.

Porosity or bulk density was an important variable in PTFs developed by Rawls et al. (1982, 1983), Aina and Periaswamy., (1985), Rajkai and Varallyay., (1992), Bruand et al. (1996) and Wosten et al., (1999).

Limited water retention data at, for instance, two points on the water retention considerably improved predictions of water retention in the work of Ahuja et al., (1985), De Jong (1983), Rawls et al., (1982) and Paydar and Cresswell., (1996).

Mineralogical properties such as the proportion of montmorillonite or illite clay were by Ali and Biswas., (1968) to have little effect on water retention (about 9%) at -1500 kPa but amounts to 240% at -10 kPa pressure head. Baumer and Brasher., (1982) suggested the mineralogical composition as a primary grouping criteria to predict soil water retention.

Organic matter/carbon content was successfully used by Rawls et al., (1982, 1983) and Wosten et al., (1999) as PTF input. Bloemen., (1980) demonstrated a correlation between bulk density and organic matter content in his data sets and indicated that bulk density effectively substituted organic matter content.

Chemical properties such as content of iron oxides were dominating properties to affect soil water retention. Rajkai and Varallyay., (1992) found the $CaCO_3$ content to be the second most important PTF input to predict water retention at -1500kPa.

Landscape position was suggested to be used by Bork., (1988) as a topographic variable in pedotransfer functions along with basic soil properties. Pachepsky et al., (2001a) showed a good relationship of water retention with slope and curvature of soil surface computed over a 30×30m grid.

Soil structure and morphology descriptors are generally beneficial to pedotransfer function development. Williams et al., (1992) included the field attribute pedality in water retention PTFs. A detailed count of lengths and widths of voids allowed Anderson and Bouma., (1973) to compute hydraulic conductivity of an argillic horizon of silt loam soil using a Kozenzy-Carman equation for flow in slits.

Soil management in the form of no-till resulted in an observed soil water retention to be 0.03-0.12 m^3m^{-3} larger than in conventionally tilled soil in the range of capillary pressure from -30 to -400 kPa (Azooz et al., 1996). Comparison of pre- and post tillage shapes of water retention curves appears to be indicative for changes in hydraulic characteristics (Klute., 1982). If tillage operations produce an increase in bulk density of a soil with an unimodal particles size distribution, then K_{sat} will decrease 2-5 times. If on the other hand, tillage operations create a bimodal particle size distribution in a soil with essentially unimodal distribution, it is expected that both K_{sat} and water retention close to saturation will increase.

5.3.6 Mathematical description

Measured θ-h pairs are often fragmentary, and usually constitute relatively few measurements over the θ range of interest. According to Bohne., (2005) mathematical functions provide a valuable tool to smooth measured data and simplify interpolation between measured data points and fitted parameters used to predict water retention curve. Or and Wraith., (2002) state that mathematical expression describing the θ-h relationship should: (i) contain as few parameters as necessary to simplify its estimation and (ii) describe the θ-h relationship at the limits (i.e. both wet and dry ends) while closely fitting the nonlinear shape of θ-h data. But the choice of function depends on soil type, application, and personal preference (Kosugi et al., 2002).The use of parametric models in soil water retention studies has several advantages. For example, they allow for a more efficient representation and comparison of the θ-h relationships of different soils and horizons (Marion et al., 1994). They are also more easily used in scaling procedures for characterizing the spatial variability of soil hydraulic properties across the landscape (Kosugi et al., 2002). And, if shown to be physically realistic over a wide range of water contents, analytical expressions provide a method for interpolating or extrapolating to parts of the θ-h relationship for which there is missing data (Bohne., 2005) and appropriateness to application in unsaturated flow models (van Genuchten et al., 1991).

Several mathematical functions have been proposed to empirically describe the complete θ-h relationship (Leiji et al., 1999). Notable among those are the equations proposed by Brooks and Corey., (1964) and by Van Genuchten., (1980). Several researchers for example Van Genuchten and Nielsen., (1985) and Fare et al., (2000), have shown that the Van Genuchten., (1980) equation give good description of the observed retention data of large number of soils. The Van Genuchten., (1980) equations (VG) are given below:

$$S_e = \frac{(\theta - \theta_r)}{(\theta_s - \theta_r)} = \left[\frac{1}{1 + (\alpha h)^n}\right]^m \qquad (5.1)$$

where θ_r and θ_s are the residual and saturated water contents respectively, S_e is the dimensionless value water content, and α, n, and m are parameters directly dependent on the shape of the θ-h curve.

A considerable simplification is gained by assuming that m= 1-1/n (Van Genuchten., 1980). Thus, the parameters required for estimation are θ_r, θ_s, α and n. θs is usually known and is easy to obtain experimentally with good accuracy, in many cases. Note that θ_r may be taken as water content at a suction of 1500 kPa or air dry or a similar value (Van Genuchten., 1980). No physical meaning is attached to the parameters α, n and m.

Estimation of parameters from the observed retention data requires: (i) sufficient data points, at least five to eight θ-h pairs (ISO., 2009), and (ii) a program for performing nonlinear regression (Or and Wraith., 2002). Recent versions of computer spread sheets provide a relatively simple and effective mechanism to perform non linear regression. A more complete discussion of the computational steps required for fitting a model to the observed data using a commercially available spreadsheet is given in Van Genuchten et al., (1991), Kosugi et al., (2002), and Seki., (2007).

In this study, RETC computer program was adopted. Marion et al., (1994) and Fare et al., (2000) found that the RETC computer program coupled with the VG model produced promising fits for the measured retention data in their respective studies. The VG model has been used by several researchers to describe θ-h relationship with different soil types (Lorentz et al., 2001; Fare et al., 2000; Zhang et al., 2007).

5.4 Materials and methods

As we mentioned at the beginning of the chapter, the main objective of this part is to characterize and compare field, laboratory and estimated determined soil hydraulic properties of an experimental field in north of Italy and then to use those data to run the two hydrological models SWAP and IDRAGRA (chapter 6)

5.4.1 Laboratory retention curve measurements

Soil sampling and storage

By the end of the season 2010, two undisturbed core samples with a volume of 235.5 cm^3 (10 cm inner diameter and 3 cm height) were collected from each selected layer (7cm, 27cm, 47cm and 67cm) from both sites (PMI-1 and PMI-5). A core sampler was mounted vertically on the soil surface and forced to ensure sampling with minimum disturbance. Immediately after taking the core samples, both ends were trimmed carefully and sealed with plastic cups to prevent any soil disturbance during transportation. The undisturbed samples were used for determination of bulk density and the θ-h relationship at low suctions (< 300 kPa) using the tensiometric "sand box" technique (Stackman et al., 1969). Disturbed soil samples (14 cm^3) were used for the determination of the θ-h relationship at higher suctions (> 300 kPa) using a pressure plate apparatus (Richards., 1947), and for soil analyses. For both sites (PMI-1 and PMI-5) (see chapter 4), samples were collected at the midpoint of each of the forth selected layers (0-7, 7-27, 27-47, and 47-67 cm). The samples were transported carefully to avoid disturbance. The samples were stored in the laboratory at room temperature until time for measurement.

Because of limited budget for this experiment, only two replicates for each sampling point were taken.

Desorption measurements

The θ-h relationships were measured using a combination of desorption techniques in order to provide a detailed description of the whole water retention characteristics. The tensiometric "sand box" method was used at lower suctions 0 -5 kPa, and starting as close to saturation as possible to try to accurately identify the air entry suction. The pressure plate apparatus (Jury et al.,1991) was used to define the water retention characteristics at higher suctions; using undisturbed core samples at suctions between 10 and 300 kPa and disturbed samples for suctions between 300 and 1500 kPa.

Pressure plates apparatus method

Pressure plate apparatus are closed, metal chamber where soil samples are placed onto a ceramic porous plate (Figure 5.1). Samples are wet on the ceramic plates to achieve good contact between the soil and plate and sometimes they are covered with a polythene or cloth sheet to reduce evaporation. Usually the plates are soaked in distilled water overnight before being loaded with soil samples. The pressure chambers are then closed and a specified pressure is applied by an air compressor. The sample starts losing water that moves through the porous plate and is collected outside the pressure chamber. After the water ceases to drain, the samples are collected since the sample is considered in equilibrium at the specified pressure (the water potential). To reach equilibrium, three to four days were required at the lower tension steps and fifteen to twenty days at high pressure. The change in equilibration time was caused by two factors. First, the hydraulic conductivity of the cores decreased dramatically as the water content was lowered at the higher tensions. Second, the ceramic plates used over different pressure ranges had varying air-entry values and hydraulic conductivities.

The soil sample is then removed from the plates, weighted and placed into an oven, for gravimetric determination of soil water content. Repeated measurements at increasing pressures were performed to obtain several measurements of water content as function of the applied pressure (water potential).

The following is a brief description of the Richard pressure plate process.

Operating the Richard pressure plate involves the following steps:

1. Place a layer of water on the Richards pressure plate cell and let it stand overnight to ensure the cell is fully saturated.
2. Prepare the soil by sieving with a 2 mm round-hole sieve. The pressure plate cell used in this experiment can fit up to 12 samples (or retaining rings).
3. Use a spatula to place the samples into the retaining rings to avoid particle size segregation. Pouring out the sample creates a non-representative sample.
4. Level the soil in the retaining rings and raise the depth of water to completely saturate the soil samples from the bottom and let stand overnight.
5. The next day, when samples are fully saturated, remove excess water from the plate using a syringe and plug all unused outlet ports. Then carefully fasten the ring.
6. Seal the chamber by fastening the bolts. Be sure the bolt heads are properly set in the groves.

7. Place the outlet tube into a water holding container (e.g., a graduated cylinder).
8. Gradually increase pressure to the required setting and take precautions not to exceed the maximum pressure of the pressure plate cell inside the chamber.
9. When equilibrium is attained (i.e., no water flows from the outlet tube) turn off the pressure supply to the system, and never open the chamber until all pressure has been released. Immediately record sample weights.
10. Transfer the samples to an oven and dry the samples at 105 C for 24 hours. Record the weight after oven drying.

Figure 5.1 Plate of Richards and the determination of retention curves in the laboratory

Results

Figure 5.2 and Figure 5.3 report soil retention curves for PMI-1 and PMI-5 obtained interpolating occurred experimental values with the Van Genuchten retention curve using RETC software (Retention Curve Program For Unsaturated soils, Van Genuchten et al., 1991). For calibration, it was adopted the technique of General Least Squares (GLS), considering for each data the relative value of uncertainty, standard deviation. Data used were the average of soil water content of the two replications. Standard deviation was calculated using the equation

$$S = (u_1 - u_2)/\sqrt{2} \qquad (5.2)$$

Where u_1 and u_2 are the soil water content of the two replications.

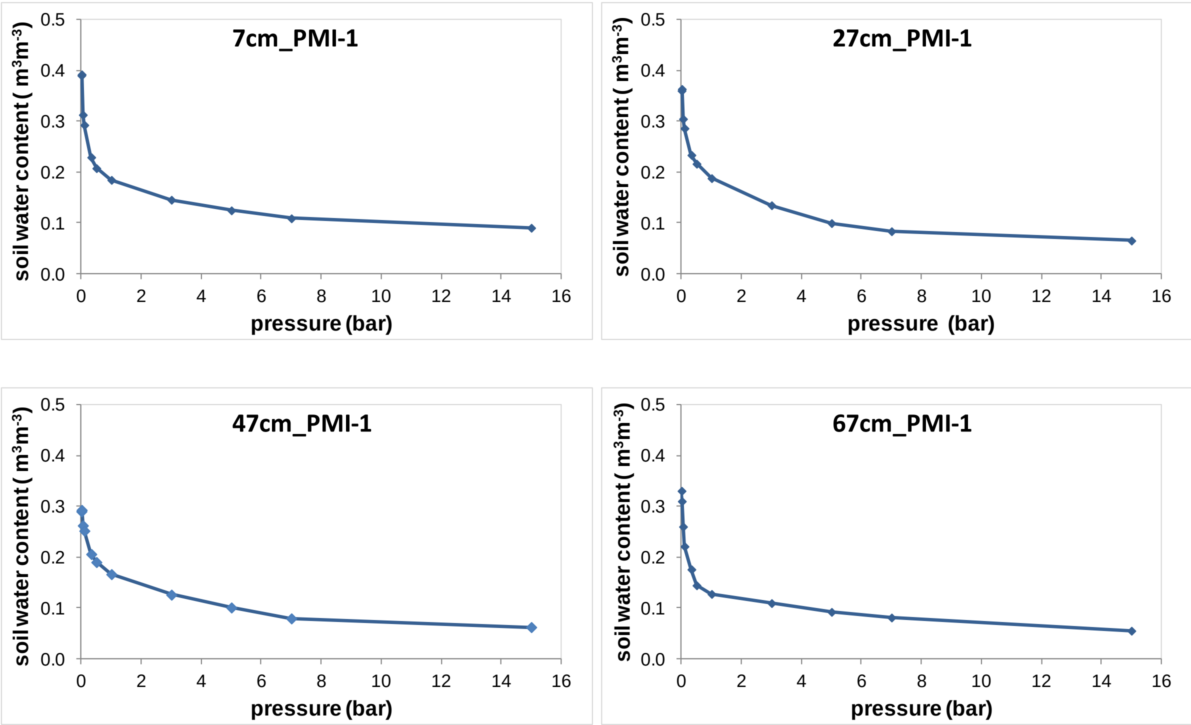

Figure 5.2 PMI-1: laboratory retention curve measured with the tensiometric box and Richard plate at the four depth

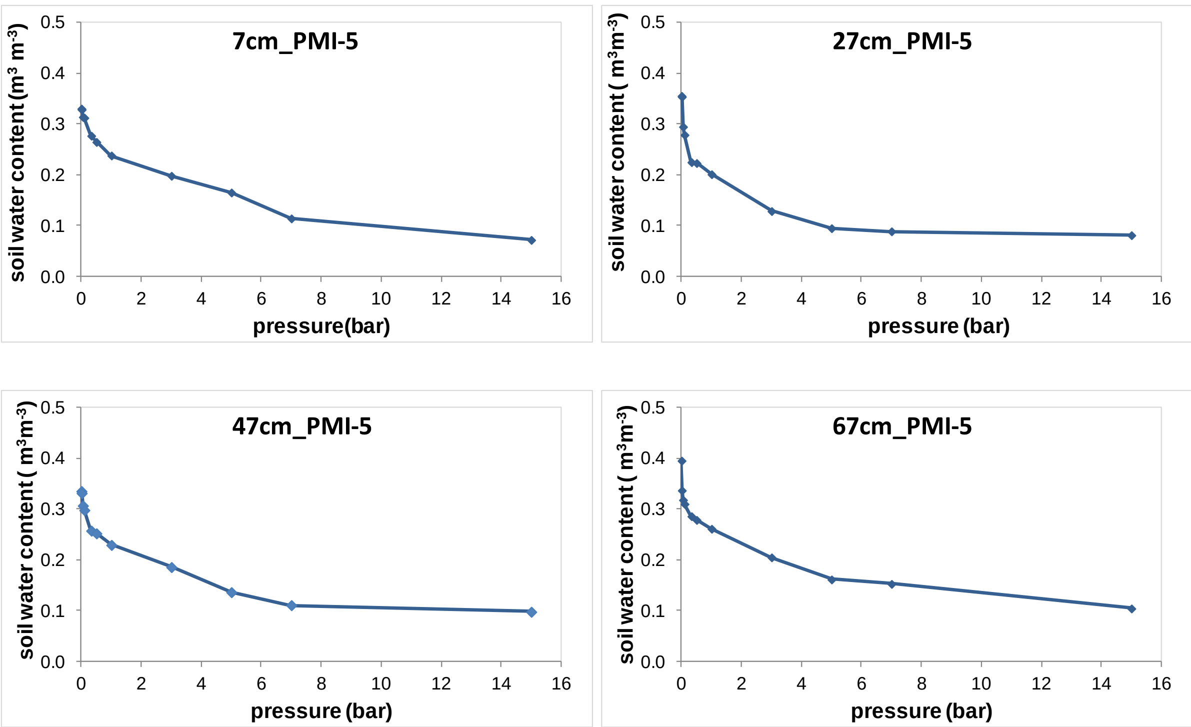

Figure 5.3 PMI-5: laboratory retention curve measured with the tensiometric box and Richard plate at the four depth

5.4.2 Field retention curve

The field retention curves were performed on two sites (PMI-1 and PMI-5) in two successive years (2010- 201, Figure 5.4 and Figure 5.5). The values of the field measured soil water content θ and soil water potential h at different depths were interpolated to the retention curves by analytical relation proposed by Van Genucthen., (1980). The adopted procedures were:

1- Selection of data set for θ-h excluding incorrect and outliers
2- Selection of saturated soil humidity values θ_s
3- Defining the humidity value for the "attractive pole" used for the calibration of residual humidity θ_r
4- Automatic calibration by MATLAB algorithm using least square method for non-linear model (*lsqcurvefit.m* of the MATLAB *Optimization Toolbox* - Coleman e Li., 1996) for the parameters of Van Genucthen curve a, n, and θ_r

The adopted procedure consists of the former points was pursued through the following observations

- ✓ the initial automatic calibration of θ_s together with all the other parameters of the retention curve has led to the selection of an intermediate value in the points of θ in correspondence to the values of water potential close to zero. The cloud of point is formed because of the non-consistency of the measured values by the humidity probe and the corresponding potentials at the same depth. The θ_s value for each depth was selected looking for a compromise value between the highest values measured by the probes;
- ✓ the value of θ_r, the lower limit of the water content in the soil, occurs in correspondence to particularly negative potential values that cannot occur in the field because of the limitation of tensiometers (tensiometers are emptied for potentials lower than -800/-1000 cm). Calibration of θ_r with the described data set cannot be carried out, therefore an attractive pole was added to the calibration data set: 100 identical data set of the couple θ-*h* with h = -15000 cm and θ= 0.1. The attractive pole allow the calibration algorithm to choose the parameters α, n, and θ_r so as to approach to the attraction point, thus regulating the tail of the curve, and prevent obtaining erroneous values of θ_r from the calibration. In some cases, the humidity of 0.1 was found to deform the fitting curve away from the observed values. In these cases it is then modified by assuming values slightly lower or higher, in the range of 0.05 to 0.25.

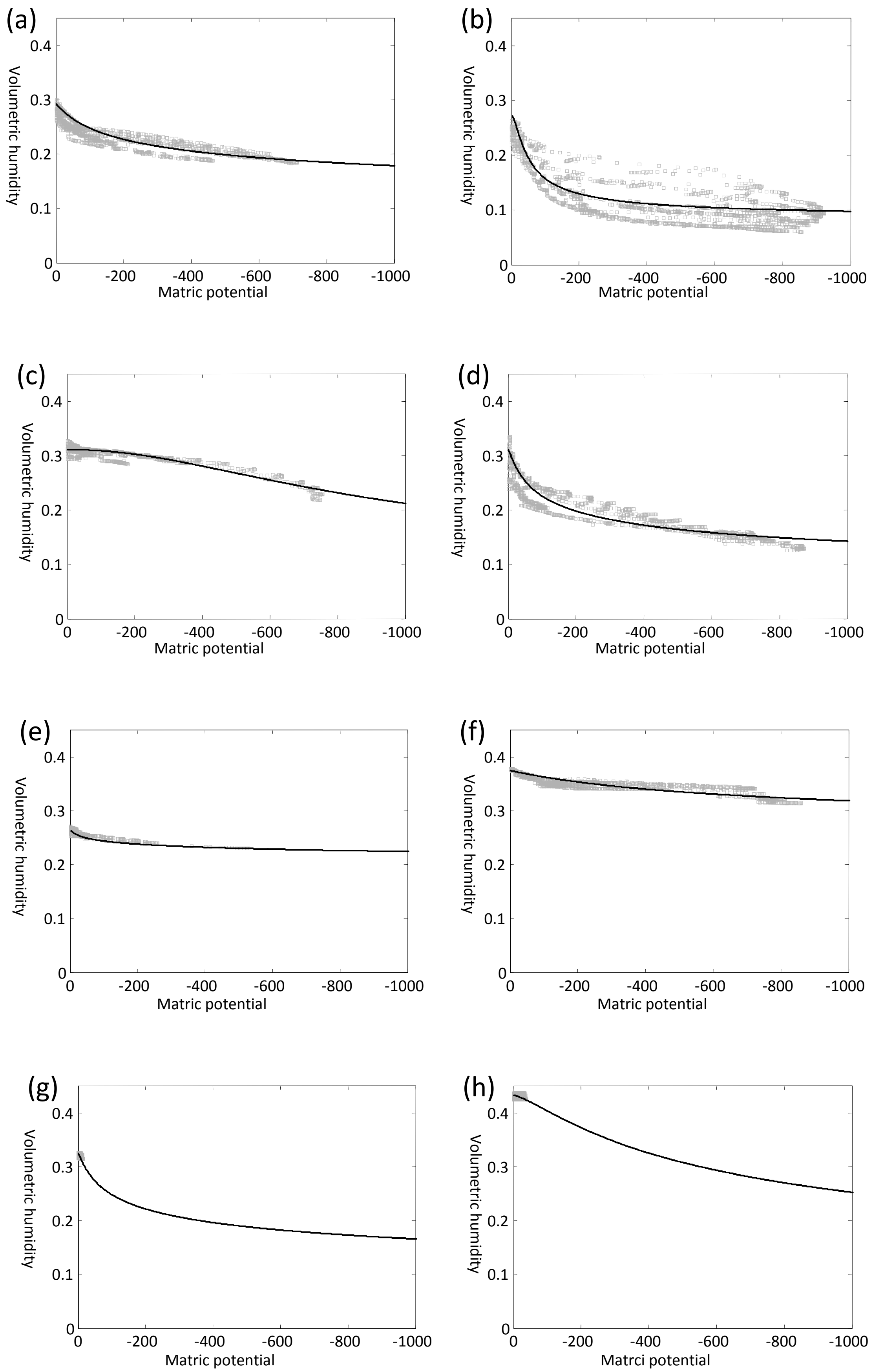

Figure 5.4 VG curves (solid lines) and experimental data (gray dots) in PMI-1 for four different depths and during the two experimental years: a) 7cm 2010, b) 7cm 2011, c) 27cm 2010, d) 27cm 2011, e) 47cm2010, f) 47cm 2011, g) 67cm 2010, h) 67cm 2011

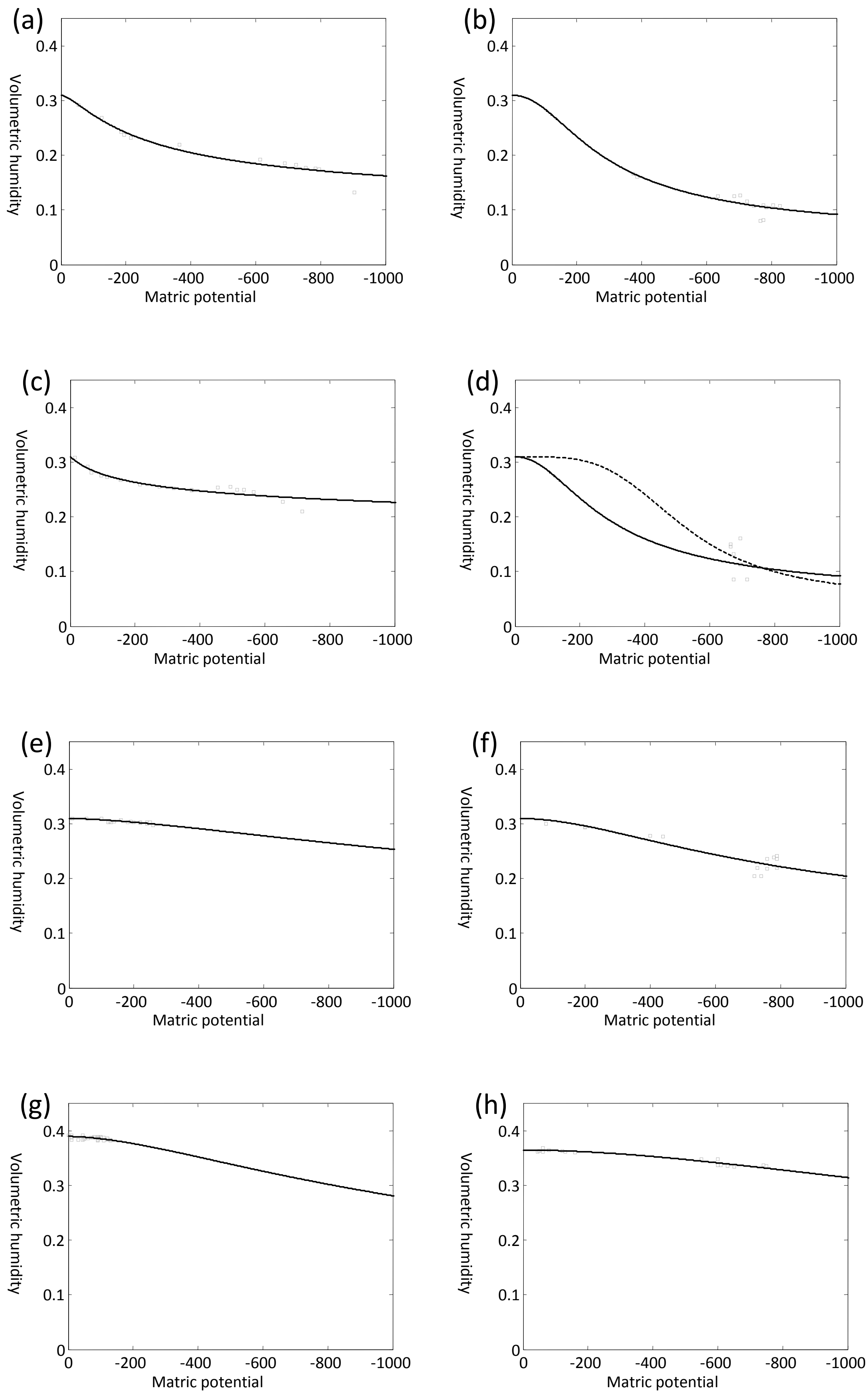

Figure 5.5 VG curves (solid lines) and experimental data (gray dots) in PMI-5 for four different depths and during the two experimental years: a) 7cm 2010, b) 7cm 2011, c) 27cm2010, d) 27cm 2011, e) 47cm2010, f) 47cm 2011, g) 67cm2010, h) 67cm 2011.

5.4.3 Estimated soil retention curve : Pedotransfert Functions (PTFs)

Description of the pedotransfert functions

A PTF is a function that uses basic data describing the soil as inputs (e.g., particle size distribution, bulk density and organic carbon content) and output results as an estimation of the water retention function and/or the unsaturated hydraulic conductivity function, including saturated hydraulic conductivity (Tietje and Tapkenhinrichs., 1993). The soil water retention function may be determined by estimating discrete water content values, θ_i, at specific pressure heads, h_i, or by estimating the parameters of selected close-form analytical functions θ(h) (Romano and Santini., 1997). The former method is referred to as the point regression method and the latter one as the functional parameter regression method (Tietje and Tapkenhinrichs., 1993). The Point Regression Method may result in non-monotonic retention functions mainly when water contents are calculated from different regressor variables at different pressure head values or when prediction is carried out for soils differing from those included in the calibration database.

The PTFs that estimate the retention function parameters are easy to use for modeling purposes (Tietje and Tapkenhinrichs., 1993).

In this study, two PTFs were applied which are based on the same input data: percentage of sand, loam and clay; organic matter and bulk density. Selection of PTFs was conducted according to their reliability as well as previous studies (Baroni et al., 2010.; Calzolari et al., 2001). In particular, the followings were selected:

- ✓ The PTF from Rawls and Brakensiek (1989, PTF-RB). The PTF-RB estimates the parameters (residual water content, $\theta_{r,}$ saturated water content, θ_s of the Van Genuchten retention function:

$$\theta = \theta_r + \left[(\theta_s - \theta_r)(\frac{1}{(1+(\alpha h)^n)^m})\right] \qquad (5.3)$$

The regression equations, were based on the same database from Rawls et al., (1982) and are valid for $5 \leq Sa \leq 70\%$ and $5 \leq Cl \leq 60\%$. Where Sa and Cl are percentage of sand and clay respectively.

- ✓ The PTF Rosetta (Schaap et al., 2001, PTF-R). It is based on artificial neural networks (Pachepsky et al., 1996, Minasny et al., 1999) and it works in a hierarchical approach which employs five different PTF to predict water retention curves (Schaap and Leij 1998, Schaap et al., 2001). An advantage of neural networks, as compared to traditional PTFs, is that neural networks require no a priori model concept. The relationships between input data and output data are obtained and implemented in an iterative calibration procedure, which extracts the maximum amount of information from the data (Schaap et al. 2001). Rosetta is a computer program that implements some of the PTFs published by Schaap et al., (1998), Schaap and Leij., (1998) and Schaap and Leij., (2000).

Soil properties used as input parameters in pedotransfer functions

The necessary data for these PTFs (Table 5.1) were determined in soil samples taken from different soil horizons in the same profile in which are installed the humidity probes and tensiometers. For each sample, the analysis of soil texture was performed (chapter 4).

The dry bulk density was measured by oven drying soil samples at 105°C for 24 h. The organic matter content was estimated from the organic carbon content determined by the Walkey–Black method.

Table 5.1 soil properties used as input parameter in PTFs

	Organic Carbon (%)	Mineral bulk density (g/cm^3)	Sand (%)	Clay(%)	Loam(%)
1C_7cm	1.23	1.50	63.02	29.34	7.64
1C_27cm	1.23	1.47	62.413	30.52	7.06
1C_47cm	1.10	1.46	60.284	27.07	12.65
1C_67cm	0.17	1.60	76.913	14.39	8.70
5C_7cm	1.10	1.46	59.002	32.99	8.00
5C_27cm	1.10	1.45	56.967	33.77	9.26
5C_47cm	1.10	1.40	49.281	39.26	11.46
5C_67cm	0.17	1.36	31.605	47.58	20.82

5.4.4 Van Genuchten model : RETC code

The unknown parameters (θr, θs, α, n and m) from field and laboratory measurements were obtained using the nonlinear least-squares optimization program RETC (Van Genuchten et al., 1991) from measured soil water retention data (field and laboratory). This model is expressed as:

$$S_e = [1 + (\alpha h)^n]^{1-\frac{1}{n}} \qquad (5.4)$$

Where h is the soil water pressure head, α and n are curve shape parameters. S_e is the relative saturation that is expressed in actual, residual and saturated volumetric water content (θ, θ_r, θ_s) as:

$$S_e = \frac{\theta - \theta_r}{\theta_s - \theta_r} \qquad (5.5)$$

5.4.5 Statistical Analysis

The performances of laboratory and PTFs in predicting the measured data were evaluated using four error measures. To test the match between predicted and fitted parameters we computed the coefficient of determination (R^2). The root mean square error *RMSE* between field measured and estimated water content with different methods was computed as:

$$RMSE = \sqrt{\frac{\sum_1^N \left(y_i - \hat{y}_i\right)^2}{N}} \qquad (5.6)$$

In addition we computed the mean error or bias (ME) and the mean absolute error (MAE) to quantify systematic errors :

$$ME\ (bias) = \frac{\sum_1^N (y_i - \hat{y}_i)}{N} \qquad (5.7)$$

$$\mathrm{MAE} = \frac{\sum_1^N \left|\mathrm{y_i} - \hat{y}_\mathrm{i}\right|}{\mathrm{N}} \qquad (5.8)$$

where: y_i denotes the measured value, $\hat{y}_i$ refers to the predicted value, and N is the total number of observations.

5.5 Results

Soil water characteristic curves (θ, h) obtained by different methods in the two experimental sites PMI 1 and PMI-5 and during the two agricultural seasons (2010 and 2011) are presented in the following figures (Figure 5.6, Figure 5.7, Figure 5.8, Figure 5.9).

For the years 2010 and 2011, the obtained curves for the same sites can be very different from each other. This may depend on the fact that probes of humidity have been uninstalled before field cultural practices at the beginning of the agricultural season 2011 and reinstalled immediately later. Therefore, the monitoring was not performed continuously for two years at the same site. This phenomenon can however influence more the top soil. The retention curves for the deepest layers may appear different in the two years, but these curves are usually the result of the wider range of values obtained from the extrapolation.

Most of the water-retention curves show a fairly consistent slope, which indicates that the release of water was generally very gradual as tension was increased. A sudden steepening of the slope indicates a distinct air-entry tension value, common for coarse or highly aggregated soils. However, no distinct air-entry value could be determined for most of the cores tested in this study, indicating that the samples had a wide range of pore sizes. However, no distinct air-entry value could be determined for most of the retention curves.

All the curves showed that a very high level of water was still held by the soil at 10480 cm tension. This water, which was held in the smallest pore spaces, was considered immobile or residual water. The values of residual water content ranged from 0.053 to 0.174 m^3/m^3.

Comparing to the field saturated water content, all the methods overestimate θs. The PTF-RB is always giving the highest saturated soil water content ranging from 0.401 to 0.503 m^3/m^3 . That can be justified because a complete saturation cannot be occurred in the field.

Different retention curves parameters are presented in Table 5.2 and Table 5.3

PMI-1_2010

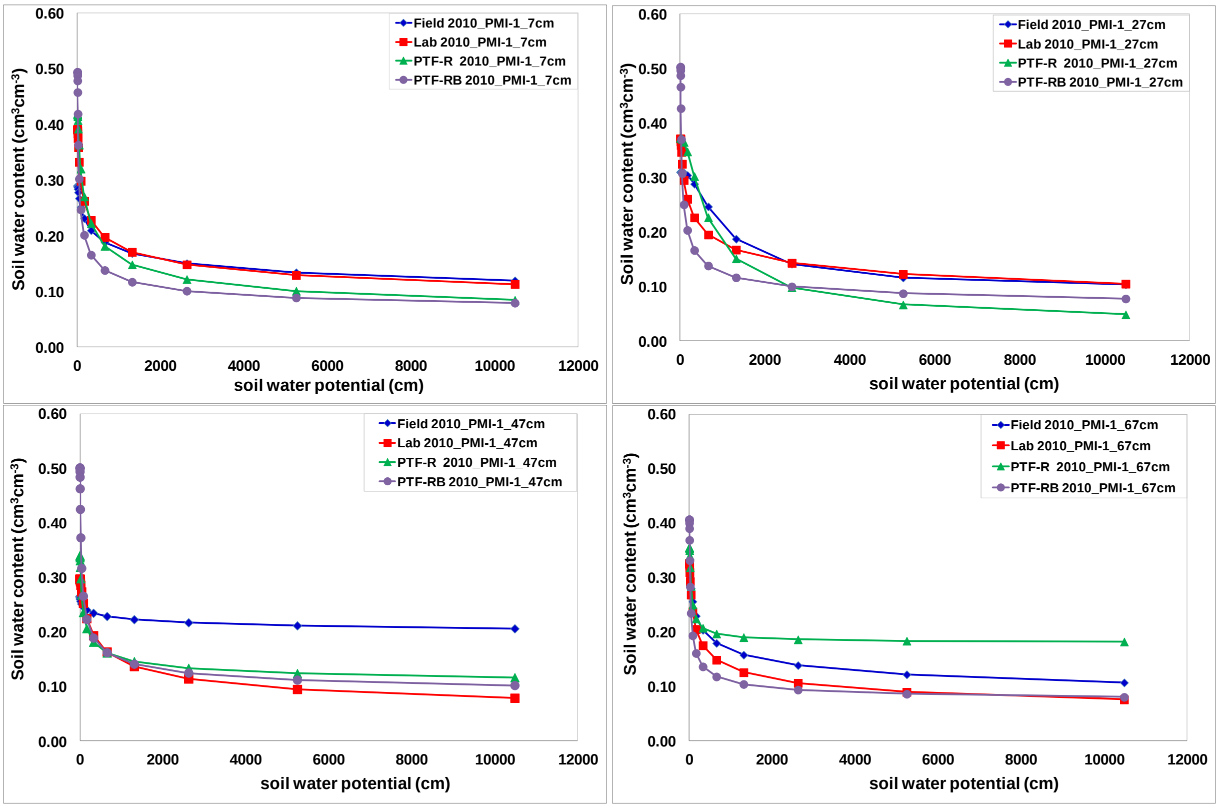

Figure 5.6 Soil retention curve measured at different depth with different methods at PMI-1_2010

PMI-5_2010

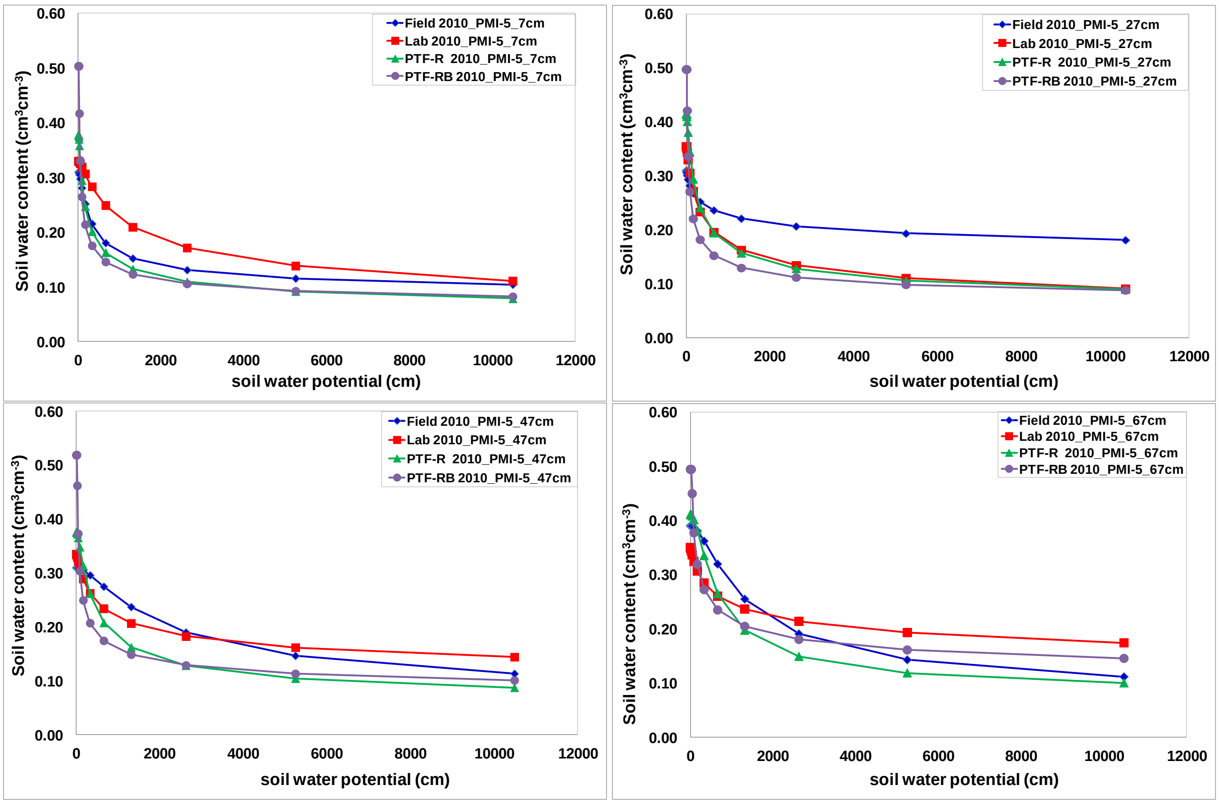

Figure 5.7 Soil retention curve measured at different depth with different methods at PMI-5_2010

PMI-1_2011

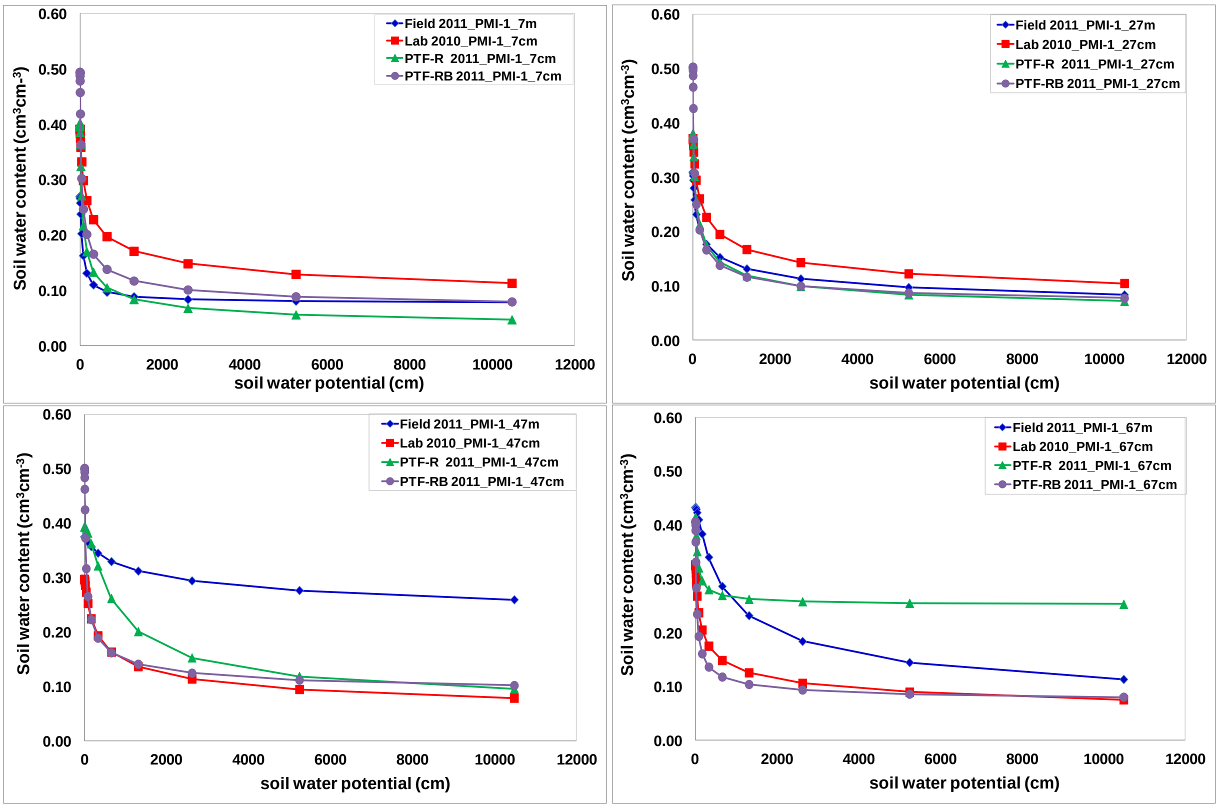

Figure 5.8 Soil retention curve measured at different depth with different methods at PMI-1_2011

PMI-5_2011

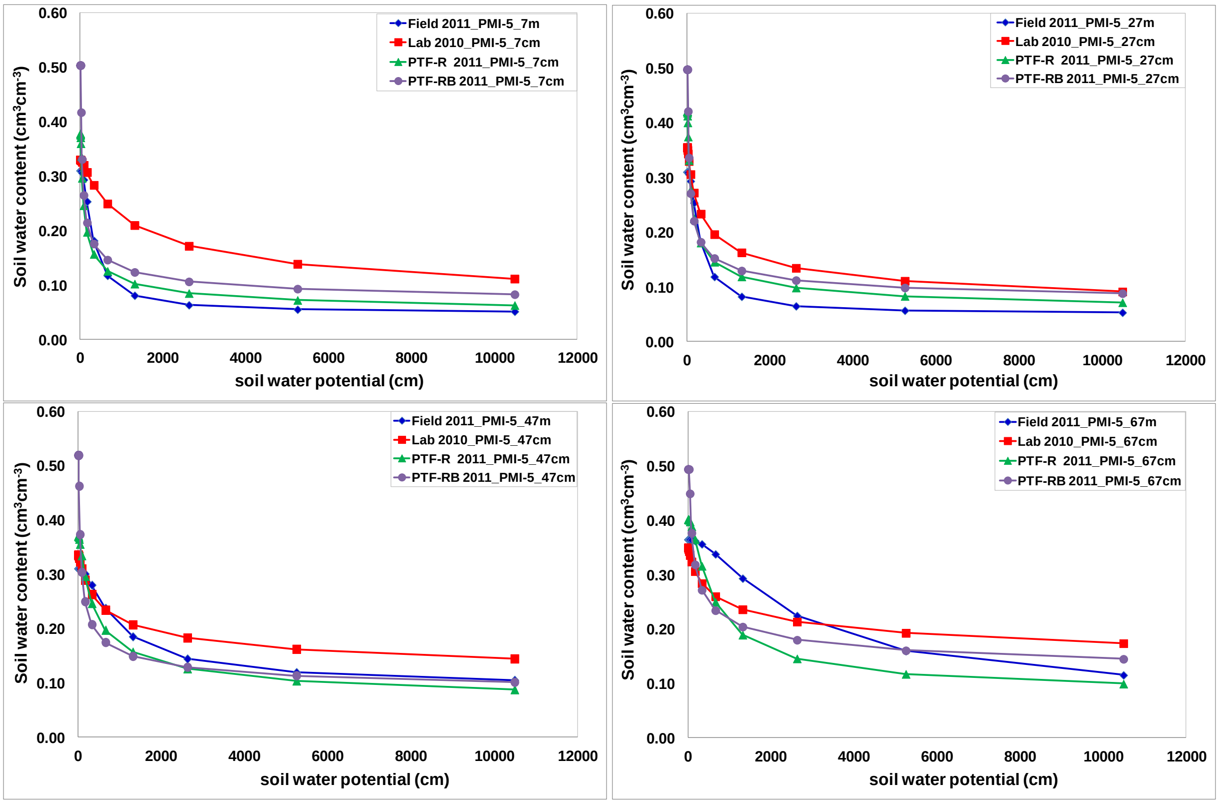

Figure 5.9 Soil retention curve measured at different depth with different methods at PMI-5_2011.

Table 5.2 Retention curve parameters obtained with different methods for PMI-1 and PMI-5 for seasons 2010

method	Depth (cm)	Site	θ_r (m3/m3)	θs (m3/m3)	α (cm^{-1})	n_{vG} (-)	m (-)
Field 2010	7	PMI-1	0.0000	0.290	0.019446	1.16659	0.14280
		PMI-5	0.0762	0.310	0.007673	1.48133	0.32493
	27	PMI-1	0.0919	0.310	0.001483	2.06889	0.51665
		PMI-5	0.0428	0.310	0.019917	1.12338	0.10983
	47	PMI-1	0.0000	0.265	0.078759	1.03776	0.03639
		PMI-5	0.0388	0.310	0.000944	1.55958	0.35880
	67	PMI-1	0.0001	0.325	0.035133	1.18811	0.15833
		PMI-5	0.0605	0.390	0.001327	1.70808	0.41455
Laboratory 2010	7	PMI-1	0.0260	0.391	0.03300	1.24600	0.19800
		PMI-5	0.0000	0.330	0.00273	1.32368	0.24453
	27	PMI-1	0.0000	0.372	0.02600	1.22600	0.18400
		PMI-5	0.0000	0.355	0.01194	1.28127	0.219524
	47	PMI-1	0.0000	0.297	0.01400	1.26800	0.21200
		PMI-5	0.0500	0.335	0.00800	1.2500	0.20000
	67	PMI-1	0.0000	0.326	0.03700	1.24400	0.19600
		PMI-5	0.0000	0.350	0.01000	1.15000	0.130435
PTF-R 2010	7	PMI-1	0.0252	0.41910	0.02060	1.35190	0.26030
		PMI-5	0.0379	0.37830	0.01740	1.40770	0.28962
	27	PMI-1	0.0252	0.37280	0.00240	1.83970	0.45640
		PMI-5	0.03970	0.415600	0.012700	1.412500	0.292035
	47	PMI-1	0.0894	0.33980	0.04970	1.35750	0.26335
		PMI-5	0.04920	0.376100	0.005500	1.529300	0.346106
	67	PMI-1	0.1797	0.35530	0.04180	1.70400	0.41310
		PMI-5	0.07340	0.411100	0.002700	1.757700	0.431075
PTF-RB 2010	7	PMI-1	0.049667	0.494208	0.092567	1.393034	0.282142
		PMI-5	0.049655	0.494208	0.084479	1.393052	0.282152
	27	PMI-1	0.046782	0.503081	0.091143	1.393228	0.282242
		PMI-5	0.046773	0.503081	0.080371	1.393237	0.282247
	47	PMI-1	0.066520	0.500588	0.102735	1.35989	0.264646
		PMI-5	0.066498	0.500588	0.070385	1.359934	0.26467
	67	PMI-1	0.063741	0.406758	0.116858	1.425329	0.298408
		PMI-5	0.058368	0.494206	0.035105	1.393655	0.282462

Table 5.3 Retention curve parameters obtained with different methods for PMI-1 and PMI-5 for seasons 2011.

method	Depth (cm)	Site	θ_r (m^3/m^3)	θs (m^3/m^3)	α (cm^{-1})	n_{vG} (-)	m (-)
Field 2011	7	PMI-1	0.0761	0.270	0.034088	1.71828	0.41802
		PMI-5	0.0479	0.310	0.004741	2.13624	0.53189
	27	PMI-1	0.0000	0.310	0.038613	1.21783	0.17886
		PMI-5	0.0479	0.310	0.004741	2.13624	0.53189
	47	PMI-1	0.0000	0.375	0.004859	1.09359	0.08558
		PMI-5	0.0872	0.310	0.001787	1.86888	0.46492
	67	PMI-1	0.0000	0.433	0.004114	1.35523	0.26212
		PMI-5	0.0528	0.365	0.000667	1.81749	0.44979
PTF-R 2011	7	PMI-1	0.0212	0.4026	0.0545	1.4237	0.297605
		PMI-5	0.0366	0.3779	0.0312	1.4457	0.3082
	27	PMI-1	0.0295	0.3809	0.0348	1.3582	0.263731
		PMI-5	0.0366	0.4211	0.0323	1.4119	0.291735
	47	PMI-1	0.0503	0.3932	0.0028	1.5995	0.374805
		PMI-5	0.0467	0.3703	0.0070	1.4823	0.325373
	67	PMI-1	0.02498	0.4142	0.0424	1.6378	0.389425
		PMI-5	0.0701	0.4021	0.0032	1.6883	0.407688

From Table 5.4 we can deduce that for PMI-1 and PMI-5, estimations using the PTF-RB provide RMSE values that are greater than the RMSE using the PTF-R and laboratory measurements. With PTF-RB, RMSE values range from 0.063 to almost 0.171 m^3/m^3 for PMI-1 and from 0.086 to 0.160 m^3/m^3 for PMI-5 that is 0.045 to 0.51 m^3/m^3 and 0.088 to 0.40 greater than RMSE values of laboratory measurements. There are however large improvements in some cases when going deeply in the soil profile. This is especially visible at 67 cm depth and at very low soil water potential (h lower than -600cm) on the agricultural season 2010 for both sites. This is presumably due to the fact that many soils in the PTF data set come from areas where conditions that govern soil development may be far from northern Italy conditions.

Laboratory measurements show the lowest RMSE for both sites during 2010 agricultural season followed by PTF-R. However, the RMSE for PTF-R becomes lower than that of laboratory measurements for PMI-1, but remains higher for PMI-5.

For PMI-5, laboratory measurements shows in most of the cases the lowest bias. The range values of bias is between -0.033 and 0.045 for both agricultural seasons. PTF-R showed bias from -0.019 to 0.077 for PMI-1 with slightly more accurate estimations for PMI-5.

It is interesting to see that bias remained positive most of the cases for both sites and during the two agricultural seasons, reflecting an overestimation of water content by all methods.

The mean absolute error (MAE) of laboratory data was the lowest for both sites during the agricultural season 2010 ranging between 0.012 to 0.065 m^3/m^3 for PMI-1 and between 0.023 to 0.046 m^3/m^3 for PMI-5.

The PTF-R provided lower mean absolute error than PTF-RB for both sites and during the two seasons.

For the 2011 season, MAE of PTF-R decreases in comparison to laboratory measurements for the PMI-1 and ranges between 0.044 and 0.084 m^3/m^3. However, it was greater for the PMI-5.

The MAE of PTF-RB was always very high with values between 0.060 and 0.151 m^3/m^3 for PMI-1 and 0.097 and 0.141 m^3/m^3 for PMI-5.

When considering the comparison between the two sites, different indices of performance show better results in PMI-5 than PMI-1 for the three methods.

Table 5.4 statistics for retention curve parameters values obtained from different method

			RMSE			Bias			MAE		
			Lab Vs field	PTF-R vs field	PTF-RB vs field	Lab Vs field	PTF-R Vs field	PTF-RB Vs field	Lab vs field	PTF-R Vs field	PTF-RB Vs field
Season 2010	PMI-1	7cm	0.077	0.101	0.144	0.064	0.077	0.092	0.065	0.089	0.122
		27cm	0.049	0.056	0.141	0.025	0.034	0.071	0.043	0.054	0.124
		47cm	0.056	0.068	0.171	-0.007	0.017	0.103	0.046	0.065	0.151
		67cm	0.018	0.034	0.064	-0.011	0.028	0.014	0.012	0.029	0.060
	PMI-5	7cm	0.035	0.052	0.144	0.027	0.031	0.094	0.031	0.046	0.120
		27cm	0.049	0.091	0.147	0.011	0.051	0.078	0.046	0.086	0.134
		47cm	0.024	0.059	0.161	0.011	0.028	0.099	0.023	0.057	0.141
		67cm	0.048	0.027	0.087	-0.033	0.003	0.050	0.046	0.024	0.080
Season 2011	PMI-1	7cm	0.112	0.098	0.162	0.109	0.077	0.137	0.109	0.084	0.137
		27cm	0.056	0.054	0.135	0.054	0.040	0.100	0.054	0.046	0.107
		47cm	0.119	0.067	0.127	-0.111	-0.019	-0.002	0.111	0.044	0.120
		67cm	0.120	0.058	0.114	-0.115	-0.012	-0.090	0.115	0.045	0.090
	PMI-5	7cm	0.060	0.051	0.144	0.045	0.033	0.113	0.045	0.046	0.120
		27cm	0.048	0.081	0.140	0.045	0.065	0.112	0.045	0.070	0.117
		47cm	0.025	0.049	0.157	0.020	0.030	0.108	0.023	0.045	0.132
		67cm	0.036	0.047	0.106	-0.021	0.006	0.063	0.030	0.042	0.097

From previous interpretation we can notice that the difference between the three methods and the field measurements is obvious when the soil water potential is lower or greater than -100cm . So, we plan to statistically analyze the data into two separate sets accounting soil water potential data. The first set includes values of h higher than -100cm ("wet" part). While the second set contains values lower than this limit (we can consider it as a "dry" part).Table 5.5 represents the whole set of the data showing the difference between the "wet" and the "dry " part of the SWRC during the two agricultural years and for both sites.

Changes in the simulated moisture content in the dry part of the SWRC are apparent for laboratory and PTF-R. These changes gradually weaken with increase of depth and soil water potential (h). While for PTF-RB differences between estimated and measured soil water content are obvious when h is higher than -100cm (wet part).

For instance, in PMI-1 and during the 2010 agricultural year, the RMSE of the laboratory measurements ranges between 0.006 and 0.093 m^3/m^3 going from 7 to 67 cm and for h going from 0 to -100cm and from 0.014 and 0.088 m^3/m^3 for h lower than -100cm (dry part). The PTF-R, the RMSE presents values between 0.028 and 0.122 m^3/m^3 for h varying from 0 to -100cm and between 0.027 and 0.073 m^3/m^3 for h lower than -100cm.

In addition, the PTF-RB shows a RMSE between 0.069 and 0.202 m^3/m^3 for the first range and from 0.045 and 0.080 for lowers values of h.

The results of the division of the SWRC into two parts highlights again what we previously said about larger differences in the top layers. This is showed by higher values of RMSE.

Table 5.5 RMSE for the "wet" and "dry" part of the retention curve obtained from different method at different depths during the two agricultural seasons and for both sites (a and c for PMI-1 and b and d for PMI-5).

a)

PMI-1 2010	Lab vs field		PTF-R vs field		PTF-RB vs field	
	RMSE 0-100cm	RMSE 100-10485cm	RMSE 0-100cm	RMSE 100-10485cm	RMSE 0-100cm	RMSE 100-10485cm
7cm	0.093	0.014	0.122	0.027	0.174	0.045
27cm	0.054	0.035	0.062	0.040	0.163	0.080
47cm	0.030	0.088	0.066	0.073	0.202	0.078
67cm	0.006	0.030	0.028	0.043	0.069	0.053

b)

PMI-5 2010	Lab vs field		PTF-R vs field		PTF-RB vs field	
	RMSE 0-100cm	RMSE 100-10485 cm	RMSE 0-100cm	RMSE 100-10485 cm	RMSE 0-100cm	RMSE 100-10485 cm
7cm	0.023	0.050	0.062	0.019	0.175	0.031
27cm	0.043	0.060	0.101	0.064	0.170	0.084
47cm	0.023	0.027	0.063	0.050	0.190	0.069
67cm	0.044	0.056	0.020	0.037	0.098	0.057

c)

PMI-1 2011	Lab vs field		PTF-R vs field		PTF-RB vs field	
	RMSE 0-100cm	RMSE 100-10485 cm	RMSE 0-100cm	RMSE 100-10485 cm	RMSE 0-100cm	RMSE 100-10485 cm
7cm	0.122	0.089	0.118	0.024	0.196	0.039
27cm	0.063	0.039	0.066	0.011	0.165	0.041
47cm	0.084	0.168	0.018	0.113	0.106	0.161
67cm	0.121	0.120	0.038	0.084	0.045	0.084

d)

PMI-5 2011	Lab vs field		PTF-R vs field		PTF-RB vs field	
	RMSE 0-100cm	RMSE 100-10485 cm	RMSE 0-100cm	RMSE 100-10485 cm	RMSE 0-100cm	RMSE 100-10485 cm
7cm	0.020	0.100	0.060	0.027	0.174	0.035
27cm	0.041	0.059	0.098	0.027	0.169	0.037
47cm	0.023	0.029	0.057	0.025	0.190	0.044
67cm	0.020	0.056	0.036	0.064	0.122	0.066

When applying a correlation (which is considered to be a good indices of performance used by many authors, Majou et al., 2007; Matula et al., 2007; Merdun., 2006) between measured and simulated water content for both sites (PMI-1 and PMI-5) and at each depth during the two agricultural seasons (see Figure 5.10, Figure 5.11, Figure 5.12, Figure 5.13 and Table 5.6).

the correspondence between measured and predicted retention curve is still the highest for laboratory and PTF-R. The R^2 values of laboratory range from 0.44 to 0.99 for PMI-1 and from 0.41 to 0.92 for PMI-5. For PTF-R, R^2 values ranges between 0.37 and 0.96 for PMI-1 and 0.68 to 0.94 for PMI-5.

For the PMI-1 we can see that for 2010, laboratory measurements show largest R^2 (0.44- 0.99) but for 2011 PTF-R become better and show highest value of R^2 (0.37-0.96). However for PMI-5, PTF-R provides the largest R^2.

PTF-RB is always showing the lowest coefficient of determination R^2, with values ranging from 0.32 to 0.95 for PMI-1 and between 0.53 and 0.94 for PMI-5.

Depending on angular coefficient (M) obtained with linear regressions imposing a zero intercept, i.e. the average proportion coefficient, most of the considered methods show a tendency to overestimate soil water content (see figure 5.10 to figure 5.13 and table 5.6). During 2010 season, The laboratory measurements show a coefficient between 0.97 and 1.28 for PMI-1 and between 0.87 and 1.21 for PMI-5. While for PTF-R values ranges between 1.088 and 1.35 for PMI-1 and between 1.021 and 1.21 for PMI-5. Whereas PTF-RB shows the highest overestimation of soil water content (1.1-1.35 for PMI-1 and 1.15-1.43 for PMI-5). Furthermore, during 2011 season and for PMI-1, angular coefficient is between 0.69 and 1.49 for laboratory measurements, between 0.93

and 1.43 for PTF-R and 0.77 to 1.73 for PTF-RB. For PMI-5, laboratory measurements presents a coefficient between 0.92 and 1.1 and PTF-R between 0.92 and 1.14. The angular coefficient in the case of PTF-RB ranges between 1.034 and 1.27.

PMI-1_2010

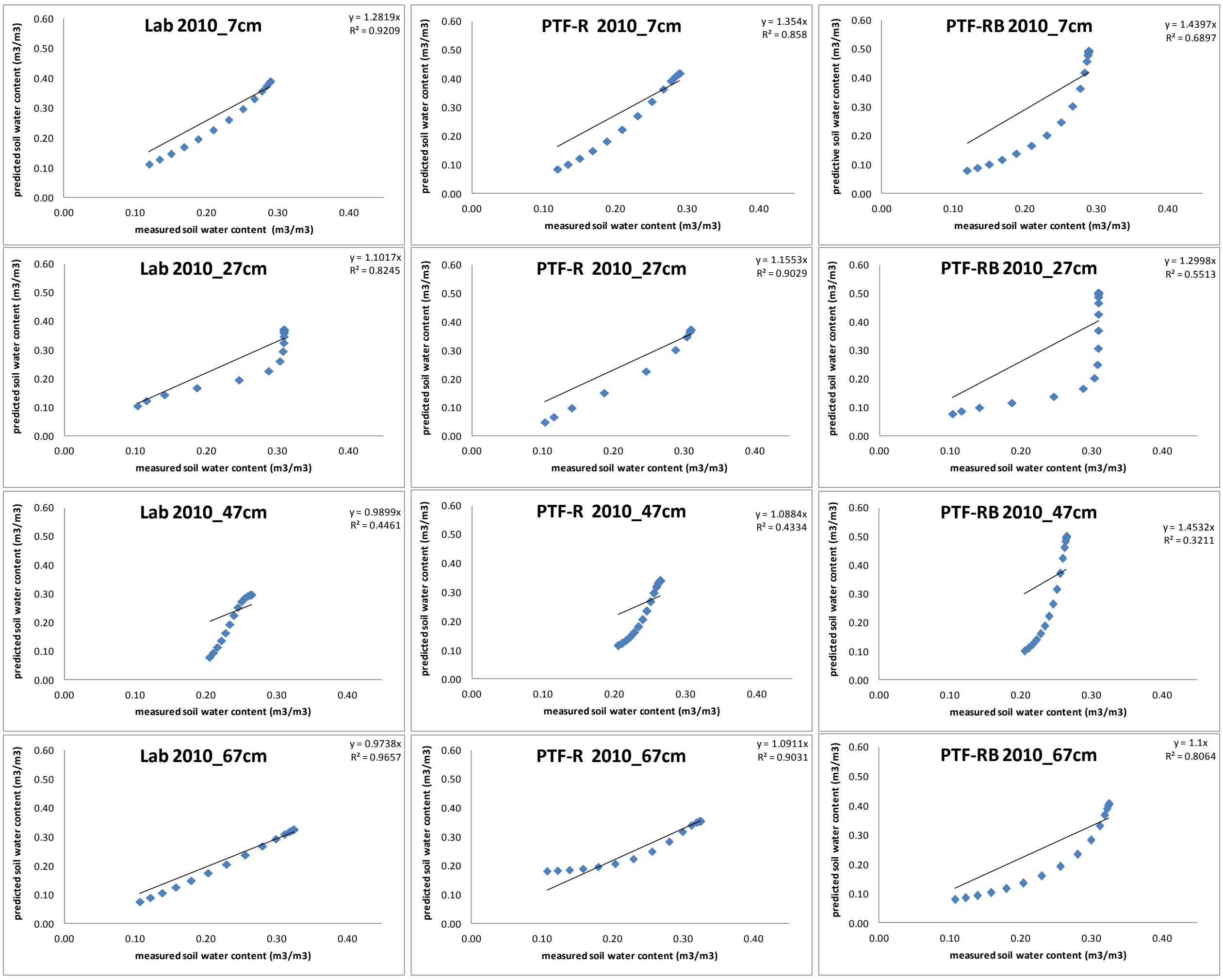

Figure 5.10 Correlation between measured (field) and simulated water content with different methods in PMI-1 during the agricultural season 2010

PMI-5_2010

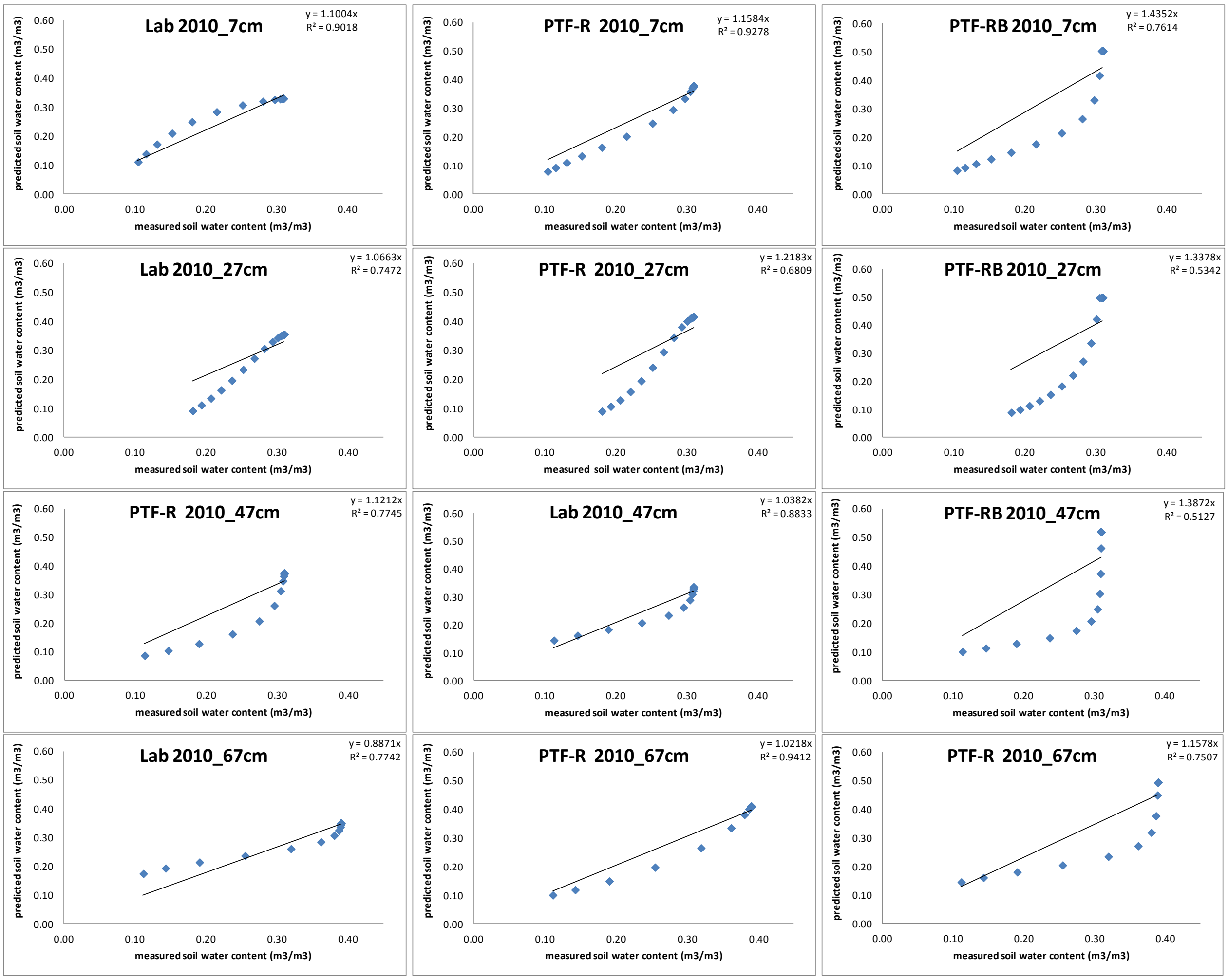

Figure 5.11 correlation between measured (field) and simulated water content with different methods in PMI-5 during the agricultural season 2010

PMI-1_2011

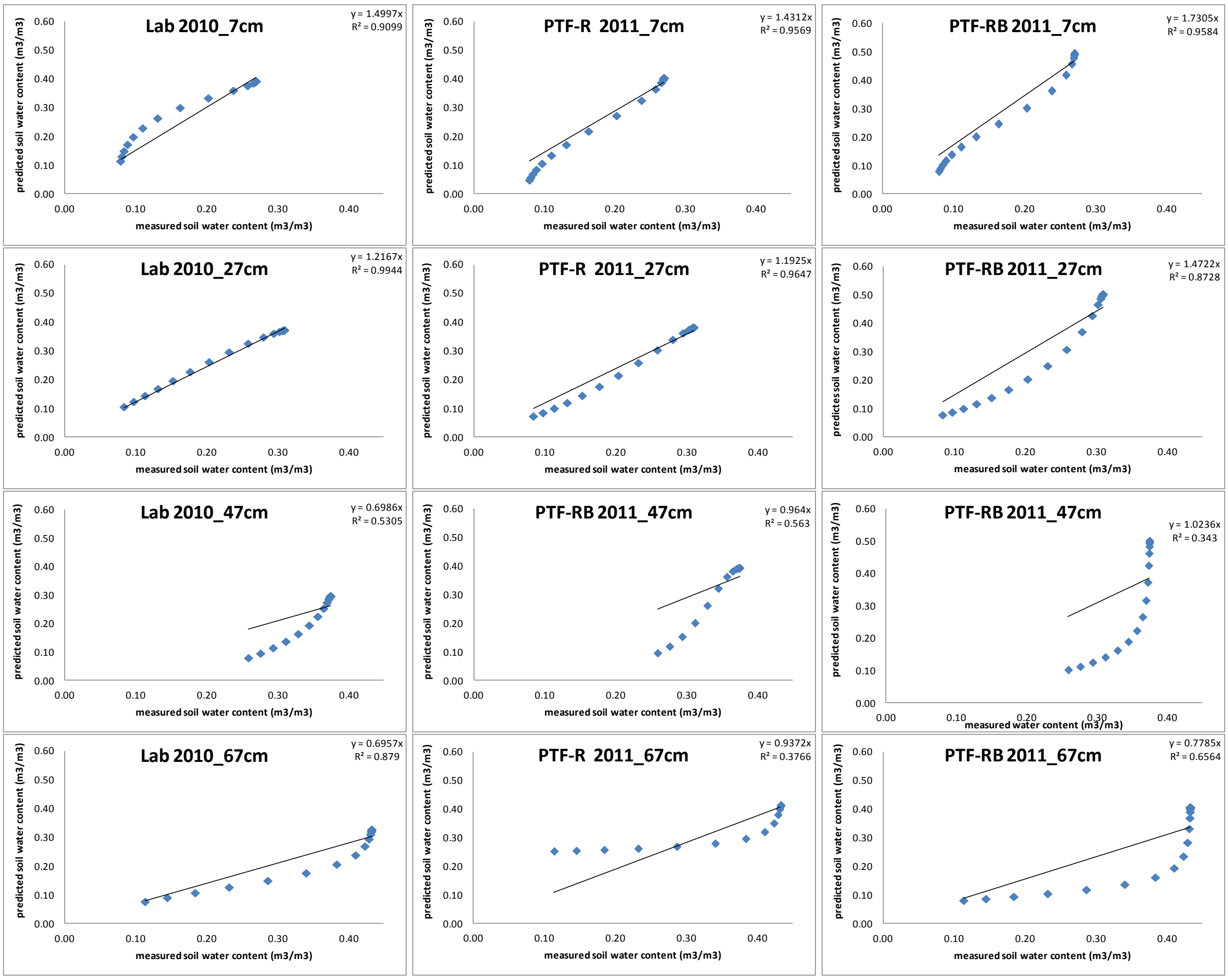

Figure 5.12 Correlation between measured (field) and simulated water content with different methods in PMI-1 during the agricultural season 2011

PMI-5_2011

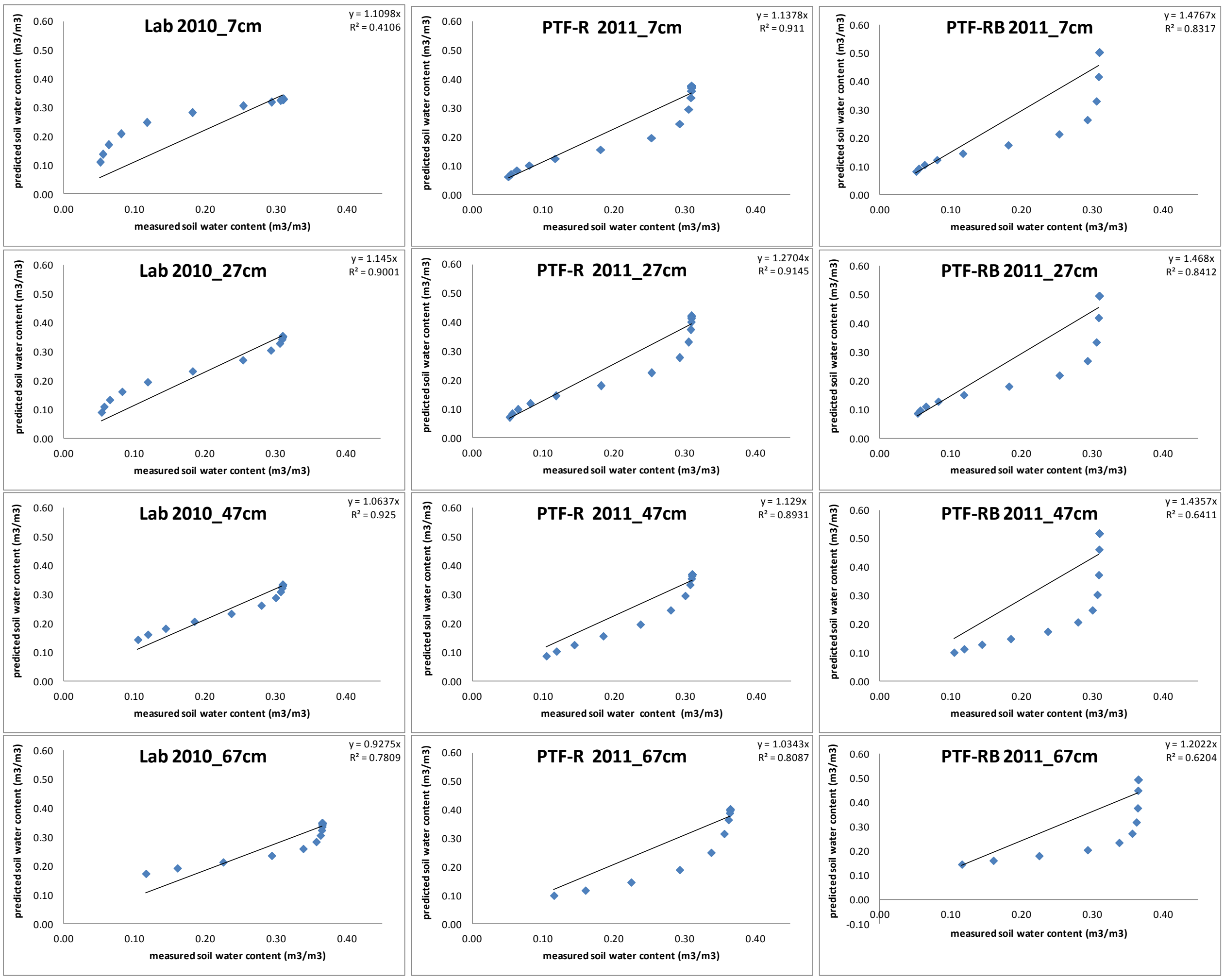

Figure 5.13 Correlation between measured (field) and simulated water content with different methods in PMI-5 during the agricultural season 2011

Table 5.6 parameters of the correlation between measured (field) and simulated soil water content obtained from different method at different depths during the two agricultural seasons and for both sites

			M			R^2		
			Lab Vs field	PTF-R vs field	PTF-RB vs field	Lab Vs field	PTF-R Vs field	PTF-RB Vs field
2010	PMI-1	7cm	1.282	1.354	1.439	0.920	0.858	0.689
		27cm	1.101	1.155	1.299	0.82	0.90	0.55
		47cm	0.989	1.088	1.453	0.446	0.433	0.321
		67cm	0.974	1.091	1.100	0.960	0.903	0.806
	PMI-5	7cm	1.1	1.158	1.435	0.90	0.92	0.761
		27cm	1.066	1.218	1.338	0.747	0.680	0.534
		47cm	1.211	1.038	1.287	0.774	0.883	0.512
		67cm	0.877	1.021	1.158	0.774	0.941	0.750
2011	PMI-1	7cm	1.499	1.431	1.73	0.909	0.957	0.958
		27cm	1.216	1.192	1.472	0.994	0.964	0.872
		47cm	0.698	0.964	1.023	0.530	0.563	0.343
		67cm	0.695	0.937	0.778	0.879	0.376	0.656
	PMI-5	7cm	1.109	1.137	1.476	0.410	0.911	0.831
		27cm	1.145	1.270	1.460	0.900	0.914	0.841
		47cm	1.063	1.129	1.435	0.925	0.893	0.641
		67cm	0.927	1.034	1.202	0.780	0.808	0.620

5.6 Discussion

Discrepancies between results of soil water retention obtained with the four methods in this study (field, laboratory, PTF-R and PTF-RB) confirm some reported results in the literature (Parkes and Waters, 1980; Field et al., 1985; Shein et al., 1993; Wosten et al, 2001; Nemes et al., 2003; Merdun., 2006; Maju et al., 2007; Matula et al., 2007; Baroni et al., 2010) .

According to the literature, differences between data from different sources were attributed to the poor depth-resolution of the humidity probes (Parkes and Waters., 1980), to the inadequate representation of large pores in the laboratory (Field et al., 1985), to the simple disturbance and spatial variability (Field et al., 1985; Shuh et al., 1988), to the hysteresis and/or over burden pressure (Shuh et al., 1988; Bouma and Dekker., 1984) to the overestimation of the soil water matric potential in tensiometer readings (Shein et al., 1993), and to the scale effects related to the sample size (Shuh et al., 1988).

Accounting possible errors in the field data, we must underline that, during the two agricultural seasons, we faced some problems with tensiometers particularly during the summer period when absence of precipitations within high temperatures emptied tensiometers and influenced readings.

The differences in location and scale of water content and pressure potential measurements in the field can result in differences in water retention data obtained in the field and in the laboratory.

Laboratory methods have the advantage of being conducted in a controlled environment, but are, however, subject to the limitation that some disturbance is introduced in manipulating the sample, even if “undisturbed” soil cores are used. In addition, the measurements may be affected by hydraulic effects not present in the field (Munoz-Carpena et al., 2002). Similarly to the finding of Chahal and Yong., (1965), trapped air or nucleation of air bubbles seen during the de-pressurization stage might lead to discrepancies between the actual and assumed potentials in the samples.

Another explanation might be that the drainage of the samples in the pressure plate apparatus is very slow or stops completely because of interruption in the water phase within the samples or between samples and plate.

Regardless of the methodology used to develop it, any PTF is likely to give less accurate or possibly even very poor predictions if used outside the range of soils from whose data they were derived. In this study, the lowest prediction accuracy is observed for the Rawls and Brakensiek (1985) PTF. These results are in contradiction with the finding of Calzolari et al., (2001) and Baroni., (2010). They concluded that the PTF-RB is well presenting the hydraulic characteristics of Lombardy plain.

This weakness is not specifically due to the lower performance of the Brooks and Corey., (1964) previously proved (Merdun., 2006) because in this study PTF-RB was implemented using the Van

Genuchten equation. If this had been the case, prediction errors would only be large in the near-saturation range of the measured and predicted moisture contents but are also quite considerable in the drier range of the retention curve.
In this study, it was found that for PTF-RB, soil water retention at the “wet” end (<100cm) strongly influences different indices by showing a big digression between measured and simulated data in the wet part of the curve. Similar results were reported by Cornelis et al., (2001); Calzolari et al., (2001) and Antinoro et al., (2008), where they got an overestimation of soil water content especially near the saturation using the same PTF.
The weak estimations of PTF-RB were proved previously by Antinoro et al (2008) and Romano and Santini., (1997) .While the well performance of PTF-R in Landriano field confirms the results found by Baroni., (2010).
A difference with field data in particular for laboratory measurements and PTF-R estimations was shown especially for low pressure (dry part) which confirms results of Bouma and Dekker., (1984). They compared the soil water characteristics curve obtained with the pressure plate method and tensiometer and neutron measurements in the field and found small discrepancies above -100cm potential but very big discrepancies between -100cm and -800 cm. As we previously described, the field soil retention curve was estimated for soil water potential lower than -800 cm, because actual tensiometer measurements can never approach such potential. Therefore, the error could be attributed to the inaccurate field retention curve in the dry part. In such case, laboratory estimated would be considered as more precious.
PMI-5 has higher clay content than PMI-1, and for both sites at the top layers, soil has a higher clay content than the deepest layers (Figure 4.21). According to Reichardt., (1990), one of the main factors affecting soil water retention is soil texture, as it determines the contact area between the solid particles and the water. Buckman and Brady., (1979) mentioned that sand has reduced water retention capacity due to its large space between granulometric particles and the quick water percolation flow which may explain the highest performance of the 3 methods in PMI-5.
The PTF of Rawls and Brakensiek., (1985) is valid for soils with a clay content of 5–60% and a sand content of 5–70%. In our study, the PMI-1 presents a percentage of sand (77%) at 67cm depth exceeding this range which can explain the bad simulation of this method especially at that depth.

Donatelli et al., (2004) suggested that the RMSE normally takes precedence over the other statistics in the evaluation procedure of different methods. According to this criterion, laboratory measurements yield the most reliable results among the tested methods during the agricultural season 2010 and for both sites. For 2011 season, PTF-R replaces laboratory measurements as better estimator for PMI-1, while for PMI-5 laboratory measurements remains as better method. Soil samples for the laboratory measurements that were carried out on 2010 were limited to the field conditions at that time, and this could explain the decrease in the rank of laboratory measurements.

5.7 Concluding remarks

Our knowledge of basic vadose zone flow and transport processes has advanced considerably over the last several decades. Unfortunately, the ability to determine process parameters has not kept pace with the ability to put the processes into numeric models. Although various field and laboratory methods for determining unsaturated hydraulic properties have been proposed, there remains a glaring lack of standardized procedures. Despite enormous investments of time and money made by soil scientists, hydrologists, and others, improvements over several decades in direct methods to measure hydraulic properties of field soils have been rather marginally achieved. Specialized equipment to measure the unsaturated hydraulic properties is generally expensive because of a relatively small market (Antinoro et al., 2008). Therefore, a disproportionate amount of time and money is still being used to conduct routine experimental work.

An understanding of hydrological processes is essential for assessing water resources as well as the changes to the resource caused by changes in the land use or climate. There is a relative abundance of literature dealing with the theory and application of soil hydraulic properties, but there are few studies that give detailed description of soil hydraulic properties on Northern Italy soils. This information is needed for improving understanding of the effects of soil management or land use on soil profile hydrology.

This study was intended to help fill this gap by measuring soil hydraulic properties of a part of these soils (Landriano field) and utilize the results from different approaches and compare the results to validate their applicability.

The soil water retention characteristics were determined using the tensiometric box and pressure plate apparatus, using field data and pedotransfert functions (Rawls and Brakensiek and Rosetta PTFs). The water retention characteristics in the laboratory for both sites were generally well defined with little variability between replicates. The main variations were due to texture differences between the sites. The clay rich site (PMI-5) were characterized by high water retention resulting in flat shapes in figures of water content vs. soil water suction.

The evaluation and comparison of the four techniques that were considered in this study enabled us to draw the following conclusions:

Laboratory measurements were the most accurate. They had the highest ranking for the five validation indices that were computed in this study.

The second best technique was the PTF Rosetta (Schaap et al., 2001). They perform only slightly poorer than the laboratory measurements. Their ranking was quite consistent for the five validation indices, and was between one and two when also considering the range-dependent evaluation.

The results obtained from Rawls and Brakensiek., (1989) PTF were also acceptable. Although the RMSE, Bias and MAE were relatively high, its determination coefficient was rather poor.

The uncertainty in the very wet range between saturation and -100cm is very large for the PTF-RB. Therefore this function should not be used in near saturation conditions. While for laboratory and PFT-R, the uncertainty was higher below -100cm.

Finally it can be concluded from this study that due to time and cost investments of laboratory measurements, Rosetta PTF developed by Schaap et al., (2001) could be the best alternative to predict the soil moisture retention curve from easily available soil properties.

5.8 Recommendations

For future studies on comparison of field, estimated and laboratory measured hydraulic properties of selected soil horizons, the following aspects can be recommended:

- Field and laboratory studies should continually be carried out, particularly on Northern Italy soils in order to quantitatively assess the field description of soil structure and improve on a better understanding.
- The pressure plate apparatus method is attractive when applied to relatively homogeneous soil profile where one-dimensional vertical flow can be expected after saturation. However it is not applicable to stratified soil profiles with slowly permeable layer and there is a need to devise a procedure for soil profile with slowly permeable layers.
- To improve the performance of PTFs, more information on soil properties may be required to reconstruct PTFs. So more analysis with more samples are required to solve the spatial variability problems.
- Field methods have the advantage of dealing with soil in natural conditions. However, small-scale heterogeneity in soil conditions may introduce large variation in measured values (Munoz-Carpena et al., 2002). Since most field measurements are confined to produce a single measurement at a single field location, adequate evaluation of field hydraulic properties requires a large number of measurements.

6 Comparison of SWAP and IDRAGRA models in simulating water fluxes in an agro-ecosystem of maize

6.1 Introduction

The water balance components in agro-ecological systems are indispensable for most physical and physiological processes within the soil–crop–climate system (Liu et al., 2006). It is important therefore to calculate the water budget parameters as accurately as possible to reduce uncertainties in the simulated outputs of crop and ecosystem models (Aggarwal., 1995; Addiscot et al., 1995).

Modeling water dynamics in the Soil-Plant-Atmosphere (SPA) continuum is an important aspects of crop water management and is difficult to be precise because this continuum is a very complicated system. Some simulation models of water dynamics in the soil-plant-atmosphere system and or/ soil crop system have already been developed (e.g. Feddes et al., 1979; Dierckx et al., 1988; Saxton et al., 1986; Gardner, 1991; Mc Gechan et al., 1997). In particular, deterministic models have been proposed to simulate all the components of the water balance, including actual crop evapotranspiration and water and solute transport (Van Dam et al., 1997; Ragab., 2002).

Soil water models range from very simple to detailed physical descriptions of soil water movement in the soil, depending on the application and available input data.

In spite of the large number of existing hydrological models, there are only two main approaches used for the mathematical representation of water flow in the unsaturated zone: numerical solutions of the Richards' equation and reservoir cascade schemes. Reservoir models are included in many hydrological models across scales (Gandolfi et al., 2006). Some examples like ALHyMUS (Facchi et al., 2003); SWAT (Neitsch et al., 1999); AGNPS (Young et al., 1987)

On the other hand physically based approaches, using numerical solutions of Richards' equations, first adopted in the local scale, have been incorporated into basin scale hydrological models: e.g SWAP(Van Dam et al., 1997); HYDRUS (Simunek et al., 1992) etc.

Unfortunately, the physically based agro-hydrological models, although very reliable, cannot often be used because of the high number of required variables and the complex, computational analysis. Therefore, the use of simplified agro-hydrological models may represent a useful and simple tool to simulate water fluxes in the soil-plant-atmosphere system.

The reliable simulation of evapotranspiration, water balance and soil water content is without doubt one of the crucial points in the application of any SPA model (Liu et al., 2006).

Two crop models SWAP (Van Dam et al., 1997) and IDRAGRA (Gandolfi et al., 2011) already introduced in chapter 2 were selected to evaluate their performance in simulating soil water balance parameters such as soil water content (SWC), actual evapotranspiration (ETact), capillary rise (CR) and deep percolation (DP) fluxes. The models were selected on the basis of several criteria chosen by the authors (see objectives of the thesis).

For detailed analysis and understanding of the different components on field scale, data on various agronomic aspects required for IDRAGRA and SWAP simple crop growth model and water balance components were collected for two growing seasons and in two representative sites of the field (PMI-1 and PMI-5). The agricultural seasons were conducted from 8 May to11 September 2010 and from 17 February to 1 September 2011. Field data collection was described in detail in a previous chapter (chapter 4).

First the two models were run with the PTF-Rosetta soil hydraulic parameters (see paragraph 6.2.5) intending comparing the two models with cost-effect, affordable work, and less sophisticated methodology to identify the soil characteristics. The two models were compared for actual evapotranspiration and soil water content in the evaporative and the transpirative layers. Then IDRAGRA and SWAP were run introducing field retention curves which are considered to be the most representative of actual field conditions. The two models were calibrated on the basis of saturated hydraulic conductivity (k_{sat}) that reliable field measured data were not available.

6.2 Input data for SWAP model

6.2.1 Meteorological data

Daily meteorological data used in SWAP were provided in a daily scale by ARPA (Agenzia Regionale per la protezione dell'ambiante della Lombardia) located in the same farm where was conducted our experiment; incoming solar radiation (KJ/m^2) , maximum and minimum temperature (°C), air humidity (kPa), rainfall (mm) and wind speed (m/s). The latter parameter was missed for the period between 31 March and 8 June 2011. In order to refill missing data (data imputation), we considered the best linear model based on the daily average values for wind speed from other two stations; the Eddy station located in the experimental field (see paragraph 4.4) and the weather station located in "Sant Angelo lodigiano" which is around 13 km from the experimental field. Data from Sant'Angelo Lodigiano station were measured at the standard height of 2m above the surface while data from ARPA and Eddy station were measured at 5.5m and 4.35m above the surface respectively. It was necessary in this case to adjust wind speed data acquired from the latter two stations. A logarithmic wind speed profile was used (FAO 56). The best linear models relating the data of the Landriano ARPA station and the additional data were chose based on the highest corrected regression coefficient R^2, taking the minimum between calibration and validation sets, both are half of the available datasets. The data out coming by the selected models in the time positions corresponding to the missing data was then used for the imputation. The resulting dataset is complete and sufficiently reliable for our application.

6.2.2 Crop data collection

Crop growth in SWAP is computed using the Leaf Area Index (LAI), crop height and rooting depth. The crop height needs to be specified for the calculation of the crops aerodynamic resistance. LAI is necessary for the computation of potential transpiration from crop reference evapotranspiration. The root depth determines from which depth water is withdrawn from the soil into the plant. These trends have been identified by linearly interpolating values measured in the field during the two agricultural season on the two representative sites (Figure 6.1).

The matric potential values that define drought stress and excess water stress are those proposed by Hupet et al., (2004) for maize in particularly

- -8000 cm is the threshold below which plant is not able to extract water;
- -325and -600 cm potentials below which starts transpiration stress;
- -10cm the threshold above which excess water stress starts,
- 0cm the threshold at which the plant does not extract more water because the soil is saturated.

The minimum canopy resistance was set equal to 70 sm^{-1}, while the crop reflection coefficient "Albedo" was equal to 0.23.

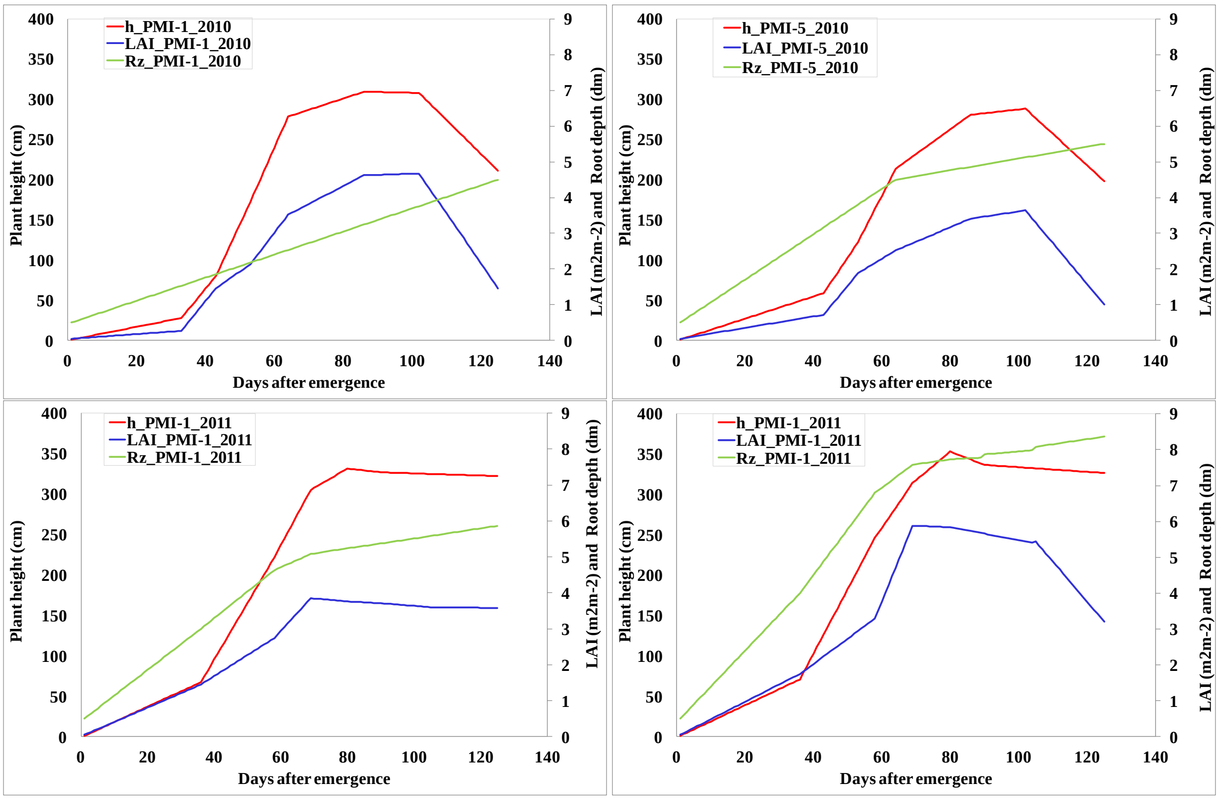

Figure 6.1 Linear interpolation between measured values of Leaf Area Index (LAI, m^2m^{-2}, in blue), crop height (h, cm, in red) and rooting depth (R_z, dm, in green) for PMI-1 and PMI-5 in 2010 and 2011.

6.2.3 Bottom boundary condition (groundwater level)

The experimental field was characterized by a shallow water table for that reason the daily measured groundwater table depth was used to describe the bottom boundary of the soil profile. In this case, groundwater level field-measurements are given on a daily basis for each site.

For the 2010 season, the piezometer and the pressure transducer were installed first in the PMI-5 between sowing and emergence date (3 May 2010). While in the PMI-1, installation was 12 days after emergence date. For the SWAP input, it was a period of missing data of 12 days in total and in order to refill this gap we adopted a simple linear relationship between groundwater level in PMI-5 and PMI-1 calibrating on the remaining part of the data. For the two sites, a missing period of 8 days was at the end of the season (during August) and it was adopted a linear interpolation to construct this gap taking into account rainfall and irrigation data. (Figure 6.2)

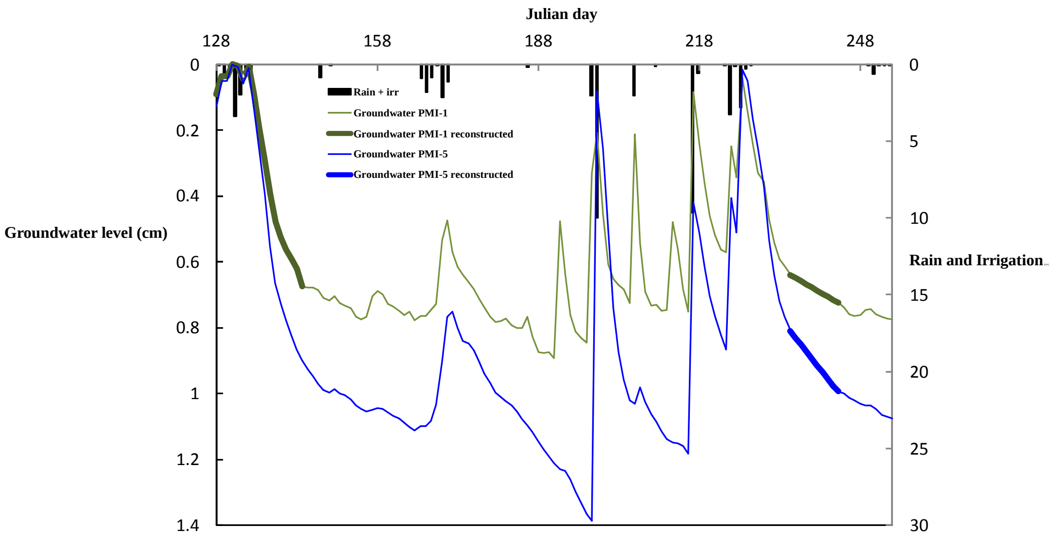

Figure 6.2 Measured (thin lines) and reconstructed (thick lines) of the groundwater level for the PMI-1 (in green) and the PMI-5 (in blue). Histograms represent the rain and irrigation (cm)

For the season 2011, the situation was more complicated; the period of missing data was long and started from 7 March 2011 until 1 May 2011. To solve this problem, models ARX were used (Auto Regressive model with eXogenous input). These models have been calibrated for each site in the basis of hourly data of groundwater level, adopting as exogenous input to the system hourly rainfall data (Figure 6.3).

The description of the ARX model is presented in the appendix (see Appendix 1)

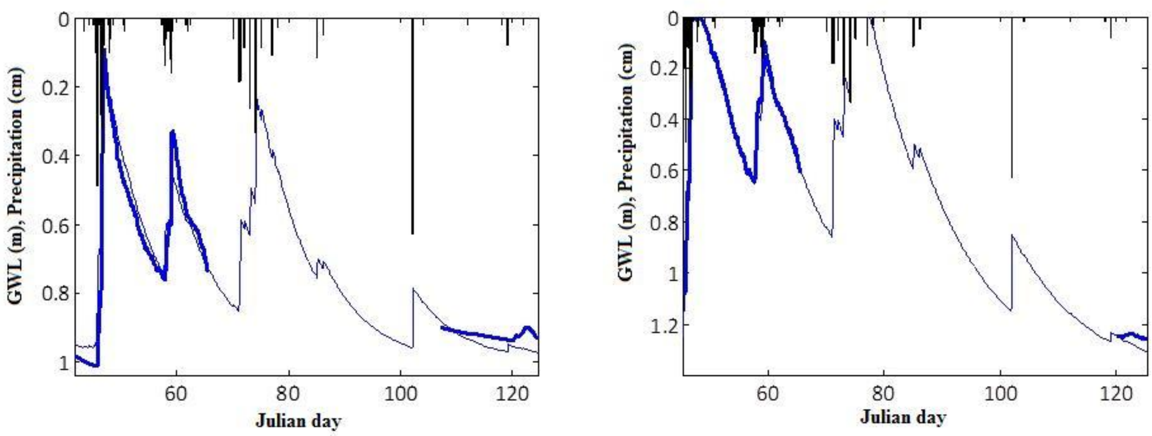

Figure 6.3 Measured (thick line) and simulated (thin line) of the groundwater depth for the PMI-1 2011 (left) and the PMI-5 2011 (right). Black values are for hourly precipitation.

The models used have shown a good performance to simulate the observed values.

6.2.4 Simulation period and initial condition

The data used as input in the model were collected during the two agricultural seasons from 10 May 2010 to 11 September 2010 and from 17 February to first of September 2011 respectively.

The initial condition was set to be the day before starting simulation in saturated soil for both seasons.

6.2.5 Soil retention curves

The field retention curves for the two sites PMI-1 and PMI-5 during the two agricultural seasons were obtained, as previously described in detail in chapter 5, interpolating occurred soil water content and soil water potential values with the analytical relation proposed by Van Genuchten., (1980). Retention curves were also estimated with the pedo-transfert function of Rosetta (Schaap et al., 2001) for the same two sites at different depths (7, 27, 47 and 67 cm). The deviations of estimated parameters from the field determined parameters were substantial.

Table 6.1 and Table 6.2 present a summary of the soil hydraulic parameters estimated from Rosetta PTF and from measured field data as introduced in SWAP

Table 6.1 Estimated Retention Curve Parameters with PTF-Rosetta

PMI	Year	Depth	$\theta_r(cm^3/cm^3)$	$\theta_s(cm^3/cm^3)$	$Alpha(cm^{-1})$	$n(-)$	$K_{sat}(cm/d)$
1	2010	7	0.0252	0.419	0.0206	1.3519	87.81
		27	0.0252	0.373	0.0024	1.8397	22.67
		47	0.0894	0.340	0.0497	1.3575	10.40
		67	0.1797	0.355	0.0418	1.7040	8.51
	2011	7	0.0212	0.4026	0.0545	1.4237	114.18
		27	0.0295	0.3809	0.0348	1.3582	59.22
		47	0.0503	0.3932	0.0028	1.5995	7.44
		67	0.0250	0.4142	0.0424	1.6378	4.24
5	2010	7	0.0379	0.378	0.0174	1.4077	44.82
		27	0.0397	0.415	0.0127	1.4125	83.99
		47	0.0492	0.376	0.0055	1.5293	12.52
		67	0.0734	0.411	0.0027	1.7577	6.78
	2011	7	0.0366	0.378	0.0312	1.446	66.2
		27	0.0366	0.421	0.0323	1.412	118.31
		47	0.0476	0.370	0.0070	1.482	13.74
		67	0.0701	0.402	0.0032	1.688	6.18

Table 6.2 Field Retention Curve Parameters

PMI	Year	Depth	$\theta_r(cm^3/cm^3)$	$\theta_s(cm^3/cm^3)$	$Alpha(cm^{-1})$	$n(-)$
1	2010	7	0.0000	0.290	0.019446	1.16659
		27	0.0919	0.310	0.001483	2.06889
		47	0.0000	0.265	0.078759	1.03776
		67	0.0001	0.325	0.035133	1.18811
	2011	7	0.0761	0.270	0.034088	1.71828
		27	0.0000	0.310	0.038613	1.21783
		47	0.0000	0.375	0.004859	1.09359
		67	0.0000	0.433	0.004114	1.35523
5	2010	7	0.0762	0.310	0.007673	1.48133
		27	0.0428	0.310	0.019917	1.12338
		47	0.0388	0.310	0.000944	1.55958
		67	0.0605	0.390	0.001327	1.70808
	2011	7	0.0479	0.310	0.004741	2.13624
		27	0.0479	0.310	0.004741	2.13624
		47	0.0872	0.310	0.001787	1.86888
		67	0.0528	0.365	0.000667	1.81749

We can notice that for the two years 2010 and 2011, the retention curves are different. The difference can be related to the de-installation of instruments done before the 2011 season and which could lead to a displacement of some meters due to the GPS position error. Moreover, culture practices done in the experimental field can also influence the soil characteristics especially in the topsoil (Baroni., 2007).

6.2.6 Irrigation

A surface irrigation was conducted during the first agricultural season 2010 on July and was done as following:

- ✓ 18 July: the irrigation was applied in the first part of the field which contain our two sites (PMI-1 and PMI-5)
- ✓ One week later (25 July) the second part of the field was irrigated. The embankments in this part were broken and water reached PMI-1 site.

PMI-1 received a total amount of water equal to 20mm (17July) 94.18 mm (18July) and 20mm (25July). While PMI-5 received a total amount of 20mm on 17 of July and 86.71mm the day after.

6.3 SWAP Calibration

6.3.1 Approach

One of the biggest constraint in using any model is the paucity of reliable field data. Integrity of data even when they are available is yet another challenge. Ability of the model to generate reliable output depends on proper input data no matter how sophisticated the model may be (Dorji., 2003). The SWAP model, used in this research is no exception.

The first simulations on SWAP were done keeping the obtained field hydraulic parameters and the saturated hydraulic conductivity (Ksat) which was estimated in a first step from the average between the values obtained using the ROSETTA PTF (Schaap et al., 2001). The related results demonstrated that the model was not able to describe well the measured soil water content and evapotranspiration. Therefore, the calibration of the model was crucial.

During the two seasons, it was difficult to directly measure saturated hydraulic conductivity at the four depths (7, 27, 47 and 67cm) except some points which can just be used as a verification later. Accordingly K_{sat} will have big bearing on the outputs of the model and will need better calibration. Other parameters can be fixed at their initial values.

6.3.2 The Optimization methodology: Algorithm SCEM-UA

Hydrologic models often contain parameters that cannot be measured directly but which can only be inferred by a calibration process that adjusts the parameter values to closely match the input-output behavior of the model to the real system it represents. Traditional calibration procedures, which involve ‘‘manual’’ adjustment of the parameter values, are labor-intensive, and their success is strongly dependent on the experience of the modeler (Douglas et al., 2000). Automatic methods for model calibration, which seek to take advantage of the speed and power of computers while being objective and relatively easy to implement, have therefore become more popular (Boyle et al., 2000). Duan et al., (1992) developed a powerful robust and efficient global optimization procedure, entitled the shuffled complex evolution (SCEM-UA) global optimization algorithm. Numerous case studies have demonstrated that the SCEM-UA algorithm is consistent, effective, and efficient in locating the optimal model parameters of a hydrological model (Duan et al., 1992, 1993; Sorooshian et al., 1993; Luce and Cundy., 1994; Gan and Biftu., 1996; Tanakamaru., 1995; Kuczera., 1997; Hogue et al., 2000; Boyle et al., 2000).

In this technique, simulations were carried out with a number of different initial values and the results are compared with the observed values. The procedure involves an intensified exploration of the parameter space close to the parameter sets that perform better. This leads to a number of runs of the model until the best set of parameters is found, i.e. the set of parameters minimizing the objective function (which is a weighted mean of the error between the observed and simulated values).

6.3.3 Results of the calibration

The following Table 6.3 presents SWAP calibration results on K_{sat} :

Table 6.3 optimal values of K_{sat} estimated from the calibration of SWAP model in PMI-1 and PMI-5 during 2010 and 2011 seasons

year	Site	K_s 7 (cm day^{-1})	K_s 27 (cm day^{-1})	K_s 47 (cm day^{-1})	K_s 67 (cm day^{-1})
2010 season	PMI-1	15.16	880.82	776.10	678.60
	PMI-5	10.99	18.15	59.60	18.69
2011 season	PMI-1	271.01	294.82	2.12	582.28
	PMI-5	3.35	80.67	0.03	24.34

6.4 Input data for IDRAGRA model

To have a fair and clearly comparison with SWAP , input data in IDRAGRA are almost the same as in SWAP. Their difference is restricted mainly to the subsoil part in which SWAP simulates the soil water flow in the root zone based on Richards equation combined with a sink term while IDRAGRA employs a simple water balance equation. Another difference exist also between the two models when calculating evapotranspiration.

6.4.1 Crop and soil parameters

Crop parameters for the implementation of the FAO method (Allen et al., 1998)

The crop parameters needed in IDRAGRA model to implement the FAO method are the following:

- ✓ Basal crop coefficient (K_{cb}) (Table 6.4): this parameter is calculated by subtracting the evaporative coefficient K_e from the total crop coefficient K_c. K_c is calculated as the ratio of the crop evapotranspiration to the reference evapotranspiration (ETc/ETo) utilizing field data. First, the reference evapotranspiration is calculated using the meteorological data acquired from ARPA. Then actual evapotranspiration is structured from the Eddy covariance data. The values of K_{cb} for different phenological stages (K_{cb-in}, K_{cb-mid} and $K_{cb-end)}$ were obtained from the corresponding values of K_c using the procedure proposed by FAO 56. In particular:

K_{cb-ini} : is 0.15 for all annual crops such as maize; K_{cb-mid} is calculated from the subtraction K_{c-mid}-0.05 for all crops with soil cover greater than 80% (such as maize). The corresponding K_{cb-mid} is equal to 0.93 (obtained from the calculation: 0.98- 0.05); $K_{cb\text{-}end}$ is calculated as $K_{c\text{-}end}$ - 0.05 for all crops that are not frequently irrigated or wetted by rain in the final stage (such as maize). The value of $K_{cb\text{-}end}$ is calculated for the maize at various times after the start of maturation and is equal to 0.84 for silage maize, 0.47 for pasture maize and 0.34 for the maize used for production of biogas.

Table 6.4 Kcb values inserted in IDRAGRA model (From Facchi et al., 2012)

	$K_{cb\text{-}ini}$	$K_{cb\text{-}mid}$	$K_{cb\text{-}end}$
Landriano 2010/2011	0.15	0.93	0.47

Crop height (hc)

This parameter is required by SWAP model, so the same input-values were introduced in IDRAGRA.

Root zone depth (Sr)

Similar to crop height, root depth are the same values in SWAP.

***Fraction of the total volume available in the soil (p)*:**

This fraction is used to calculate the readily available water for the plant. For 2010 season, roots did not exceed 55 cm for both sites so we decrease the value of p to 0.4. While for 2011, we keep the value proposed by Allen et al (1998) for maize and which is equal to 0.5.

Leaf area index (LAI)

Used for estimation of interception by the method of Braden (1985).

In IDRAGRA model, crop parameters are function of gradual degree days (GDD), while for SWAP crop parameters are function of time.

Land use classes

It is useful for the implementation of the CN method (USDA-SCS, 1972; 1986, see Appendix 2).

The trends of the parameters in each year of simulation (2010 and 2011) were determined taking into account the duration of different phenological stages.

Soil hydraulic parameters

The soil is divided into two layers: evaporative (surface) and transpirative layer. Evaporative layer is where processes of surface runoff, infiltration and evaporation take place, while transpiration layer is where processes of transpiration and deep percolation acquired. The two layers have thicknesses, respectively: Z_e with a value of 0.15 m, as indicated by Allen et al. (1998) and Z_t, which depends on the root depth (S_r, m) and is equal to (S_r - 0.15).

For each layer IDRAGRA asks for the following parameters:

- Saturated soil water content, θ_{sat};

- Soil water content at field capacity, θ_{fc};
- Soil water content at wilting point, θ_{wp};
- Residual soil water content, θ_r;
- Initial soil water content, θ_0;
- Saturated hydraulic conductivity, K_{sat}
- The factor n of the Brooks and Corey (1964) equation

The soil hydraulic parameters are first indirectly estimated with Pedo-Transfer Function methods (PTF) (Table 6.5) which allow to derive the value from physical-chemical properties (mainly organic carbon content and percentage of sand, silt and clay) obtained from the analysis in the laboratory (see paragraph (4.6.1)

The PTF adopted were implemented in Rosetta Package (Schaap et al., 2001, www.naldc.nal.usda.gov). Then we adopt the same field retention curve were fed in SWAP model (Table 6.6).

The soil hydraulic parameters are estimated for the same depth adopted in SWAP model (7cm, 27cm, 47cm and 67cm). Then to have them to the appropriate depth (Z_e and Z_r), the weighted arithmetic average is calculated, except for the saturated hydraulic conductivity which is calculated using the weighted harmonic mean.

Table 6.5 Soil hydraulic parameters inserted in IDRAGRA model and estimated with PTF-Rosetta for 2010 and 2011 seasons in PMI-1 and PMI-5.

			θ_{SAT}	θ_{fc}	θ_{wp}	θ_r	θ_0	K_{sat}	n
2010 agricultural season	Evaporative layer	PMI-1	0.419	0.30	0.074	0.0252	0.33	3.66	1.35
		PMI-5	0.378	0.30	0.074	0.0380	0.33	1.86	1.41
	transpirative layer	PMI-1	0.367	0.33	0.088	0.0420	0.30	1.01	1.68
		PMI-5	0.396	0.33	0.088	0.0438	0.30	0.481	1.46
2011 agricultural season	Evaporative layer	PMI-1	0.402	0.27	0.075	0.0212	0.33	4.75	1.42
		PMI-5	0.378	0.27	0.075	0.0366	0.33	2.76	1.44
	Transpirative layer	PMI-1	0.403	0.28	0.084	0.0157	0.30	0.686	1.49
		PMI-5	0.397	0.28	0.084	0.0506	0.30	0.513	1.52

Table 6.6 Field soil hydraulic parameters inserted in IDRAGRA model measured from field data during 2010 and 2011 seasons in PMI-1 and PMI-4.

			θ_{SAT}	θ_{fc}	θ_{wp}	θ_r	θ_0	n
2010 agricultural season	Evaporative layer	PMI-1	0.290	0.250	0.100	0.0000	0.33	1.17
		PMI-5	0.290	0.270	0.080	0.0000	0.33	1.48
	transpirative layer	PMI-1	0.296	0.270	0.090	0.0612	0.30	1.73
		PMI-5	0.310	0.290	0.080	0.0426	0.30	1.34
2011 agricultural season	Evaporative layer	PMI-1	0.270	0.235	0.074	0.0761	0.33	1.72
		PMI-5	0.310	0.235	0.075	0.0479	0.28	2.14
	Transpirative layer	PMI-1	0.345	0.31	0.0856	0.0038	0.30	1.19
		PMI-5	0.327	0.31	0.0845	0.0621	0.28	1.95

6.4.2 Meteorological data

Similar to SWAP model, daily values of meteorological variables were provided by ARPA and are: total rainfall (mm/day), maximum and minimum temperature (°C), wind speed (m/s), maximum and minimum relative humidity (%), solar radiation (MJ/m^{2}day).

6.5 IDRAGRA calibration

6.5.1 Adopted Approach

To accurately simulate what is actually present in the field requires knowledge of the physical meaning of all of the numerical parameters. Without this understanding a simulation that does not accurately reflect reality will be created and the simulation will be worthless in a predictive capacity (Douglas et al., 2009).

The K_{sat} estimated by PTF-Rosetta is a very good starting value for IDRAGRA simulation but need some modification before it is applicable with field soil retention parameters. And since the soil is divided into two layers in IDRAGRA model, so it was easy to manually calibrate the model.

Manual calibration is the process of changing simulation parameters to adjust the simulation output to match the observed values. Manual calibration takes a lot of experience and a lot of patience, but a good fit between the simulation and the observed data is possible.

The first step to calibrating our model was setting up and successfully running a reasonable simulation. All known parameters, such as crop data, meteorological data, soil retention hydraulic parameters are defined; all unknown parameters in particularly saturated hydraulic conductivity for the first (evaporative) and second (transpirative) layers were set to physically realistic values. Occasionally estimations from PTF-Rosetta for such parameters (hydraulic conductivity) were available. Such data are very valuable but it still may be necessary to calibrate on that specific parameter because a simulation parameter represents a uniform parameter over an area while Rosetta PTF results generate the parameter for a specific set of retention curve parameters.

Once the calibration variables have been decided upon and the valid range for each has been identified, the next step is to set an initial value for each variable. The usual process is to begin with the middle values. Later on, these values are modified little by little, either up or down. Beginning with the middle value of the range gives a good reference point for later simulations where what happens with a higher or lower value can be judged against the middle value to determine simulation trends.

For each set of parameters we compare simulated soil water content in the evaporative and transpirative layers to the measured data. Then we calculate the RMSE for each layer and we deduce the total RMSE for the root zone with the following formula:

$$RMSE_{root\ zone} = \sqrt{\frac{\left(RMSE_{evap}\right)^2 + \left(RMSE_{trasp}\right)^2}{2}} \qquad eq(6.1)$$

This comparison is the key step to calibrating our simulations. Using these statistical index judge how well the simulation output fits the measured soil water content.

6.5.2 Results of the calibration

The manually calibrated model parameter values (K_{sat}) for 2010 and 2011 agricultural season in PMI-1 and PMI-5 are identified in Figure 6.4 (a and b) and the optimal solutions are presented in the Table 6.7. The objective of the calibration was to minimize the RMSE between the observed and simulated water content while maximizing the model efficiency.

In Figure 6.4, the chromatic scale is related to the RMSE: the yellow color presents the highest values while the gradual change from light green to dark green shows a decrease in the RMSE values.

a)

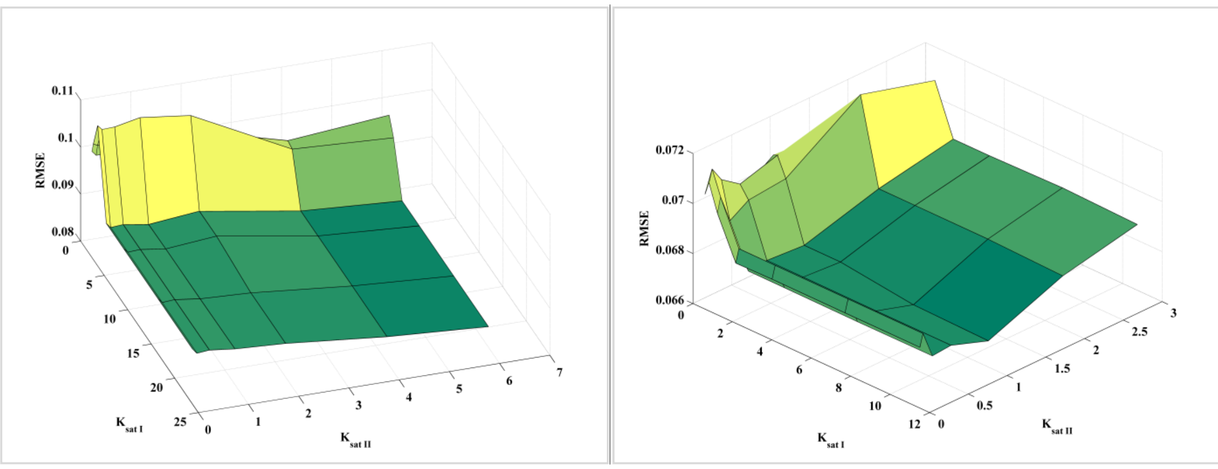

b)

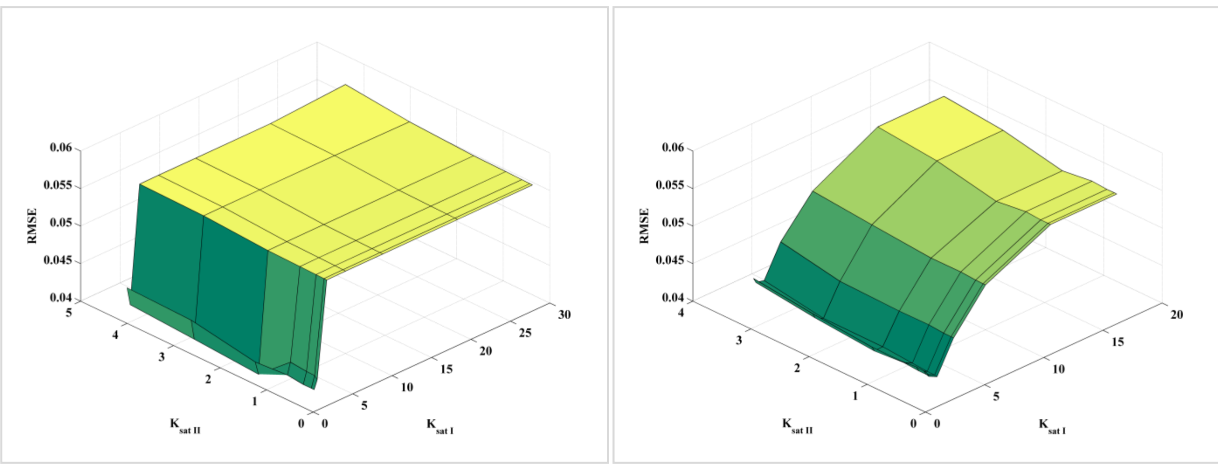

Figure 6.4 Results of the manual calibration of IDRAGRA for 2010 (a) and 2011 (b) agricultural seasons in PMI-1(left) and PMI-5 (right) the yellow color presents the highest values while the gradual change from light green to dark green shows a decrease in the RMSE values.

Table 6.7 The "optimal" value of Ksat in 2010 and 2011 seasons in PMI-1 and PMI-5

K_{sat} (cm h^{-1})	Evaporative layer		Transpirative layer	
	PMI-1	PMI-5	PMI-1	PMI-5
Agricultural season 2010	14.6	11.2	6.06	0.962
Agricultural season 2010	1.2	1.4	1.38	0.085

6.6 Evaluation of model outputs

The performance of SWAP and IDRAGRA is compared using field data collected (chapter 4).
The common outputs of the two models include daily values for soil water content and evapotranspiration. As the main objective of this study was to assess the reliability of the simulated outputs, several statistical methods were used to compare the simulated and observed results. These included a comparison of the root mean square error (RMSE), bias and the mean average error (MAE). The latter statistical indices are already discussed in detail in chapter 5 (see paragraph 5.4.4).

6.7 Results and Discussions

The simulations were applied in spring-summer maize during 2010-2011 and two models were executed at daily time step: SWAP (Soil Water Atmosphere Plant) and IDRAGRA.

6.7.1 Agricultural season 2010

Comparison of the two models With estimated soil hydraulic parameters from PTF-R

The two models were run with soil hydraulic parameters estimated from PTF-Rosetta:

ETact

Figure 6.5 shows the simulated evapotranspiration by SWAP and IDRAGRA and those measured in the field by Eddy covariance technique.

What emerges from the values shown in the Table 6.8 is that during 2010 agricultural season in PMI-1 estimated actual transpiration by both models SWAP and IDRAGRA is higher than that in the PMI-5, on the contrary is the case for the actual evaporation. This fact is certainly justified by the value of LAI, higher in the first than in the second site for the agricultural season 2010, particularly for SWAP which consider this parameter when calculating the evaporation and transpiration rates (see paragraph 2.3.5, Figure 4.18).

The total actual transpiration estimated by SWAP is lower than that estimated by IDRAGRA. This low value can be attributed to the zero values of transpiration during the rainy days (Kroes et al., 2008). This is because when calculating potential evaporation, SWAP is taking into consideration the evaporation rate of the water intercepted by the vegetation and is assuming that during this phenomena, the transpiration rate is negligible or equal to zero as it was shown in our case. While, SWAP compensates the total amount of the potential evaporation rate, and consequently, the actual evaporation rate, which can explain the higher values of actual and potential evaporation in comparison to IDRAGRA. This shows that in SWAP, loss of water due to interception from maize contributes significantly to the total loss of water due to evaporation.

On the other side, the potential evapotranspiration (sum of potential transpiration and potential evaporation) assumes a similar value for PMI-1 and PMI-5 (approximately 460 mm for SWAP and 530 mm for IDRAGRA), since the two terms are compensated. The actual evapotranspiration in the two sites is approximately equal to the potential value. In particular for the PMI-1, ETact is equal to 93% and 97% of the ETpot for SWAP and IDRAGRA respectively. While for the PMI-5, this value increases to 97% in comparison to PM-1 for SWAP and decreases to 94% for IDRAGRA. Both sites have therefore slightly suffered a water stress.

The comparison between the simulated and the measured ET (Figure 6.5) shows a reasonably good agreement between IDRAGRA simulations and Eddy measurements in the early stage and between SWAP simulations and Eddy measurements in the middle of the season.

Statistical analysis presented in the Table 6.9 shows a minor difference between the two models in simulating evapotranspiration. Generally, both models over-estimate the ET which is proved with a negative bias (-0.11, -0.14) and with a high angular coefficient ”M” (1.30-1.47), (Table 6.9). For PMI-1, SWAP slightly performs better than IDRAGRA with smaller values of RMSE (0.15), bias (-0.11) and MAE (0.12). On the other hand, IDRAGRA shows better results in PMI-5 with a RMSE value of 0.15 and a bias equal to -0.13 and a MAE of 0.13. According to Gandolfi et al., (2012) ,.eddy covariance measurements are characterized by a certain margin of error , appeared with an underestimation during energy balance closure (36%). That error can be attributed in a big part to an underestimation of the ET by eddy covariance measurement which is previously proved in literature by Meiresonne et al.,(2003), Ceulemans et al.,(2002) and Baldocchi and Vogel.,(1996) who found an underestimation of 25%, 30% and 25% respectively.

The underestimation of eddy technique within the absence of measured evapotranspiration during the last phases of the considered period does not allow the verification of which model performs better.

Table 6.8 Total water balance components (mm) for the agricultural season 2010 (cumulated in 125 days)

Non calibrated models		Precipitation	Irrigation	Tpot	Tact	Epot	Eact	Capillary rise	Deep percolation
PMI-1	IDRAGRA	335	134,2	380.6	366.4	144.2	141.7	203.4	147.1
	SWAP	335	134,2	207.2	188.1	261.1	247.6	162.5	233.1
PMI-5	IDRAGRA	335	86,7	382.1	357.3	159.6	154.5	198.5	161.8
	SWAP	335	86,7	170.8	159.4	291.5	291.5	255.6	269.1

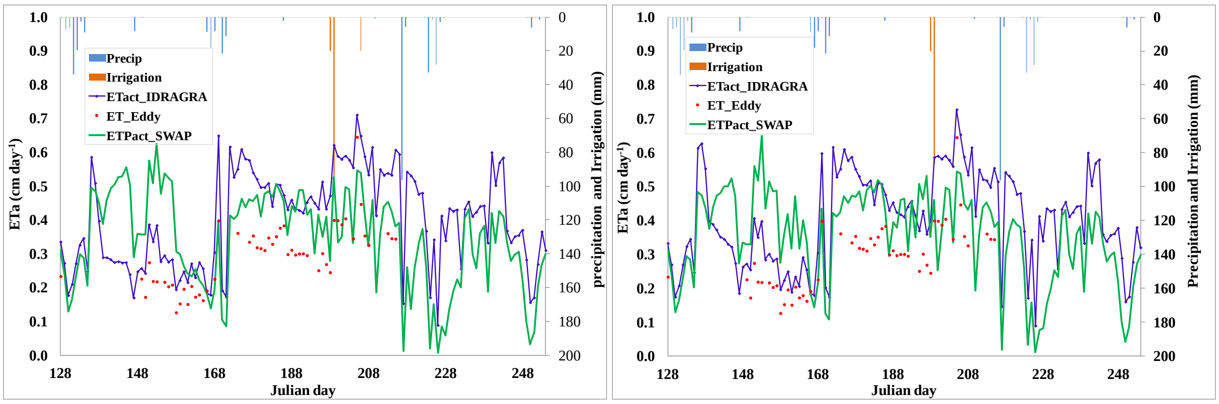

Figure 6.5 Actual evapotranspiration measured (red points) and estimated with SWAP (green) and IDRAGRA (blue) models during the 2010 season for the PMI-1 (left) and PMI-5 (right)

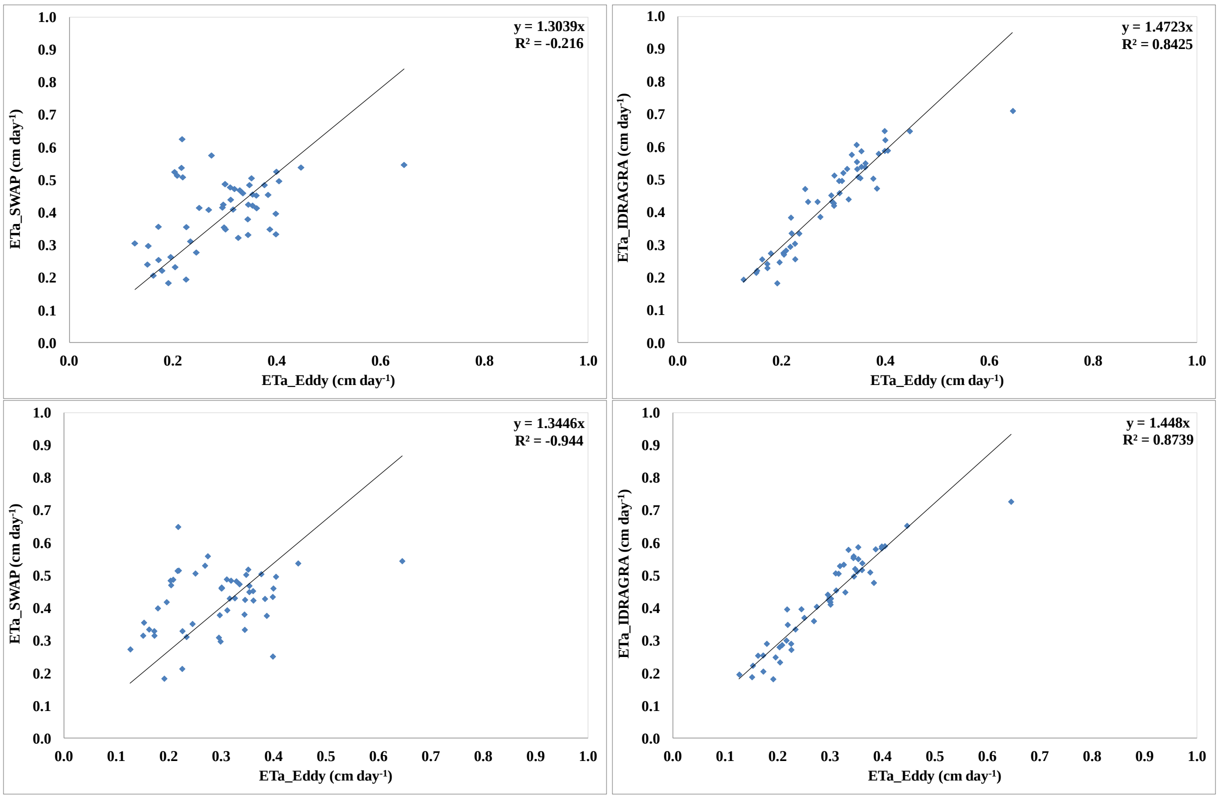

Figure 6.6 correlation between measured and estimated evapotranspiration with SWAP (left) and IDRAGRA (right) models for PMI-1 (up) and PMI-5 (down) during 2010 season.

Table 6.9. statistical analysis of the estimated evapotranspiration with the non-calibrated models SWAP and IDRAGRA compared to measured data during 2010 season.

Non calibrated models	ETa	M	R^2	RMSE	Bias	MAE
PMI-1	IDRAGRA	1.47	0.84	0.17	-0.14	0.14
	SWAP	1.30	-0.21	0.15	-0.11	0.12
PMI-5	IDRAGRA	1.45	0.87	0.15	-0.13	0.13
	SWAP	1.34	-0.94	0.17	-0.13	0.14

Soil water content

Observed and simulated soil water contents of the evaporative and transpirative layers are presented both in the form of charts (Figure 6.7) and tables (Table 6.10 and Table 6.11).

As shown in Figure 6.7, non calibrated SWAP model poorly predict the average soil water content during the whole season, for both sites and both layers. IDRAGRA shows better estimations at the last period of the season and particularly for the site PMI-5.

Differences between the two models are primarily observed at the beginning of the season, when simulated values of soil water content obtained with IDRAGRA are lower than those evaluated with the SWAP model, because of the higher simulated evapotranspiration fluxes, as shown in Figure 6.5.

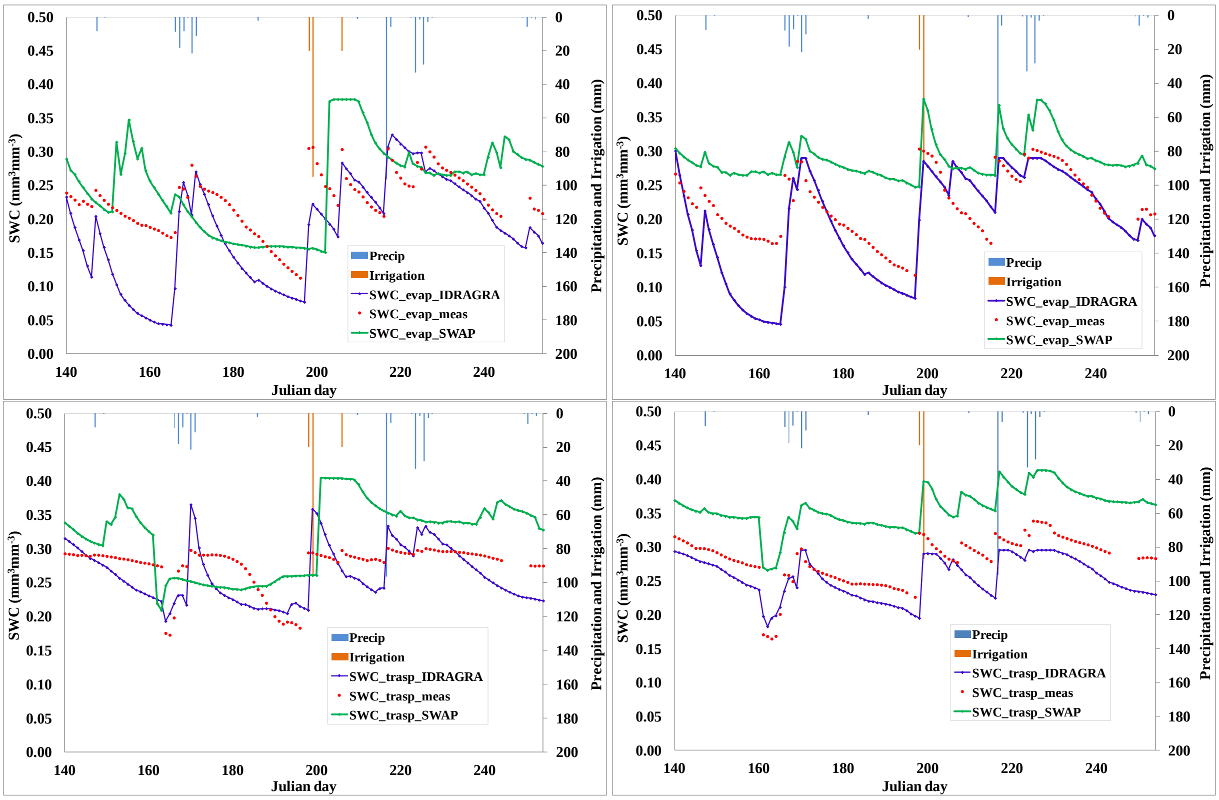

Figure 6.7 Soil water content in the evaporative l (up) and the transpirative (down) layers for PMI-1 (left) and PMI-5 (right) measured (red points) and estimated with SWAP (green) and IDRAGRA (blue) models during the 2010 season.

The soil water content in the transpirative layer decreases during the early part of the season (20 day after emergence) for both models. This was the result of roots distribution mainly in the top 15cm layer in the early stage and also the transpiration rate was small due to the small leaf area development.

We can notice also that for IDRAGRA model, soil water content in the evaporative layer decreases strongly between the days 147 and 165, then increases, and shortly decreases again between the days 171 and 197. This is also justified by a low evaporation in the same period. We can observe also that when we have external water supply (irrigation or precipitation), the results of the simulation show a good agreement with the measured data Similar behavior was seen also for the soil water content in the transpirative layer. We can observe also that IDRAGRA performs better in PMI-5 than in PMI-1 for both layers.

Looking to the groundwater level (Figure 4.10) during the same period (days 147-165 and 171-197), we can observe that the groundwater table is deeper than before and after that period. In addition, the absence of precipitation during the same period can explain the low values of water content in the root zone.

Table 6.10 and Table 6.11 confirm again that non-calibrated IDRAGRA performs slightly better than non-calibrated SWAP. The RMSE for IDRAGRA ranges between 0.032 and 0.065. That for SWAP varies between 0.062 and 0.077. IDRAGRA underestimates soil water content in both layers with a positive bias ranging between 0.013 and 0.042. On contrary, SWAP overestimates the soil water content with a negative bias varying between -0.076 and -0.022. The MAE is between 0.027 and 0.051 for SWAP and between 0.055 and 0.076 for IDRAGRA. So according to the last indices IDRAGRA performs better than SWAP in estimation soil water content in both evaporative and transpirative layers.

Table 6.10. Statistical analysis of the estimated soil water content in the evaporative layer with the non-calibrated SWAP and IDRAGRA models in comparison with the measured data for both sites during 2010 season

Non calibrated models	SWC_evap	RMSE	Bias	MAE
PMI-1	IDRAGRA	0.065	0.042	0.051
	SWAP	0.070	-0.022	0.055
PMI-5	IDRAGRA	0.035	0.013	0.030
	SWAP	0.062	-0.039	0.056

Table 6.11 Statistical analysis of the estimated soil water content in the transpirative layer with the non-calibrated SWAP and IDRAGRA models in comparison with the measured data for both sites during 2010 season.

Non calibrated models	SWC_trasp	RMSE	Bias	MAE
PMI-1	IDRAGRA	0.056	0.026	0.042
	SWAP	0.075	-0.068	0.069
PMI-5	IDRAGRA	0.032	0.024	0.027
	SWAP	0.077	-0.076	0.076

Calibrated models+ field retention curve

IDRAGRA and SWAP were run introducing field retention curves and were calibrated on the basis of saturated hydraulic conductivity (k_{sat}) that reliable field measured data were not available.

ETact

After calibrating the two models, we notice from Table 6.12 that the simulated ETact from IDRAGRA does not change so much but that from SWAP decreases and more stress can seen. The ETact presents 78% and 83% of the potential ET in PMI-1 and PMI-5 respectively. ETact for PMI-

1 is always higher than that on PMI-5 (Figure 6.8). As explained previously this is because of the highest LAI in the first site. The difference between the two models can be related to the difference in the methodology of calculating ET explained in detail in the second chapter of the thesis (see paragraph 2.3.5 and paragraphs 2.4.3; 2.4.4; 2.4.5).

RMSE, Bias and MAE values presented in the Table 6.13 give us a more detail picture of the two models performance. The general range for the two models in both sites in terms of RMSE is from 0.06 and 0.09 and between 0.14 and 0.15 for SWAP and IDRAGRA respectively. The bias varies between -0.02 and 0 for SWAP and -0.14 and -0.13 for IDREAGRA. The MAE ranges between 0.05 and 0.07. The results of the angular coefficient presented in the Table 6.14 show a high overestimation of the ET by IDRAGRA(42-47%) while the overestimation is slight with SWAP(15%). The coefficient of determination is higher for IDRAGRA showing that the regression line of IDRAGRA fits measured data better than in the case of SWAP.
According to that analysis, we can conclude that SWAP performs better than IDRAGRA in terms of ET. But when taking into account that measured data from eddy are underestimated by 36% as previously mentioned, that can alter our assumption and make IDRAGRA more efficient.

Table 6.12 Total water balance components (mm) for the agricultural season 2010 (cumulated in 125 days)

calibrated models		Precipitation	Irrigation	Tpot	Tact	Epot	Eact	Capillary rise	Deep percolation
PMI-1	IDRAGRA	335	134.2	380.6	361.6	160.5	156	219.3	111.8
	SWAP	335	134.2	207.2	181.4	261.1	183.6	213.7	331.2
PMI-5	IDRAGRA	335	86.7	382.6	351.6	163.4	156.5	144.5	94.9
	SWAP	335	86.7	170.8	153.6	291.5	230.9	201.0	263.1

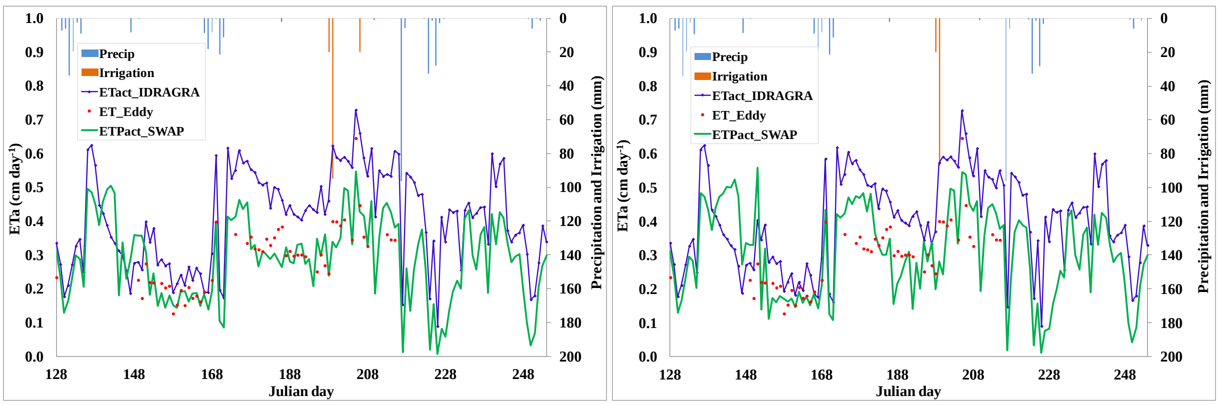

Figure 6.8 Actual evapotranspiration measured (red points) and estimated with SWAP (green) and IDRAGRA (blue) calibrated models during the 2010 agricultural season for the PMI-1 (left) and PMI-5 (right)

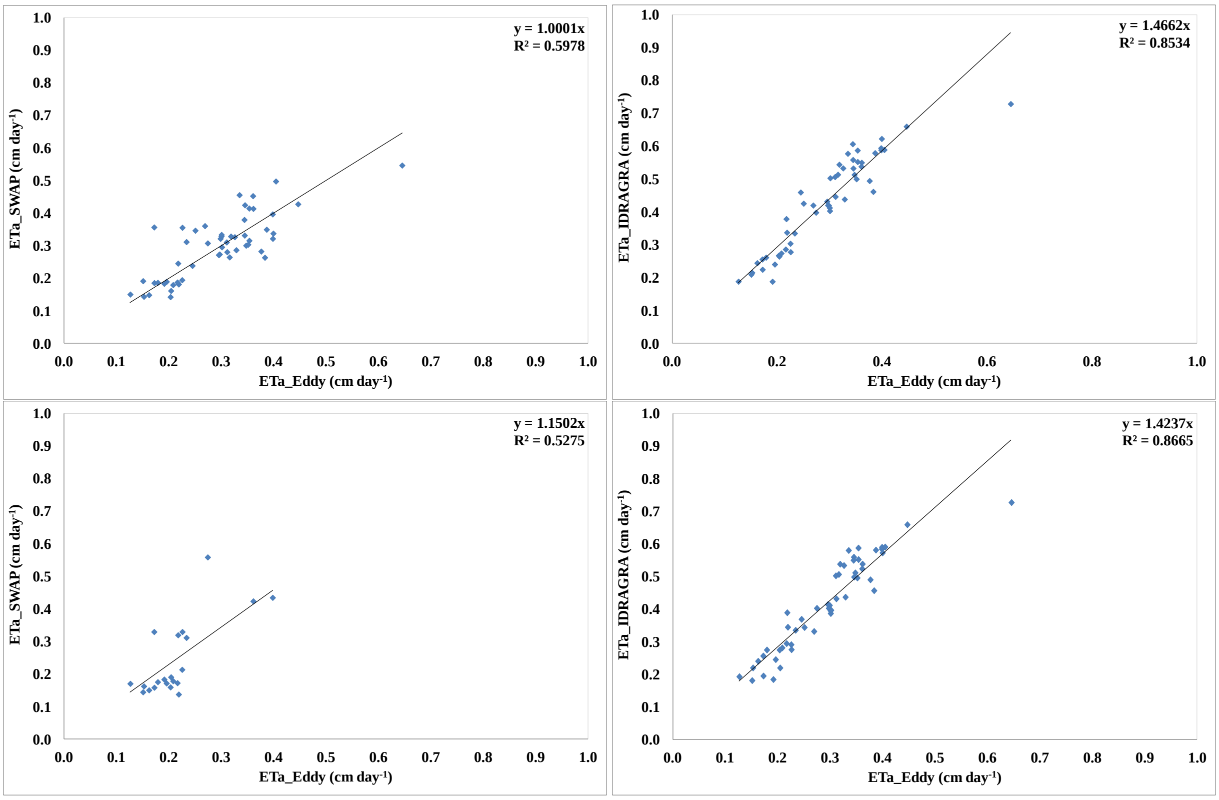

Figure 6.9 Correlation between measured and estimated evapotranspiration with SWAP (left) and IDRAGRA (right) calibrated models for PMI-1 (up) and PMI-5 (down) during 2010 season.

Table 6.13. Statistical analysis of the estimated evapotranspiration with SWAP and IDRAGRA models compared to measured data during 2010 season.

Calibrated models	ETa	M	R^2	RMSE	Bias	MAE
1C	IDRAGRA	1.47	0.85	0.15	-0.14	0.14
	SWAP	1.00	0.60	0.06	0.00	0.05
5C	IDRAGRA	1.42	0.87	0.14	-0.13	0.13
	SWAP	1.15	0.53	0.09	-0.02	0.07

Soil water content

As shown in Figure 6.10 (a and b) soil water content in the evaporative soil layer changes more drastically than the deeper soil layers throughout the simulation period. This is because the upper soil layers are much more greatly affected by the combined effects of the rainfall, ET and irrigation compared to the transpirative layer. In addition, greater fluctuation can be found during the summer growing period than that at the beginning of the growing period. This is due to the rainfall distribution which is not being uniform with more than 70% of the rainfall occurring in the summer maize season particularly during the month of August on 2010. Figure 6.10 show that the simulated soil water contents from SWAP in different layers agree accurately with the measured values. The average RMSE, bias and MAE values are only about 0.023cm^3cm^{-3}, -0.003 cm^3cm^{-3} and 0.015 cm^3cm^{-3} respectively for the evaporative layer (Table 6.14). For the transpirative layer (Table 6.15), the average values are 0.02 cm^3cm^{-3} (RMSE), -0.009 cm^3cm^{-3} (bias) and 0.012 cm^3cm^{-3} (MAE).

The comparison between soil water content estimated by IDRAGRA and that measured shows a good fitting end of the growing period particularly in the evaporative layer. The model is performing poorly at the beginning of the season which clearly influence values of RMSE, bias and MAE and increases them in comparison with values of SWAP.

In the Figure 6.10 (up-right) and for PMI-5, IDRAGRA shows a pick on the day 210 in the evaporative layer that is not present in actual data and those estimated by SWAP. It seems an external contribution that does not affect soil water content in the evaporative layer.

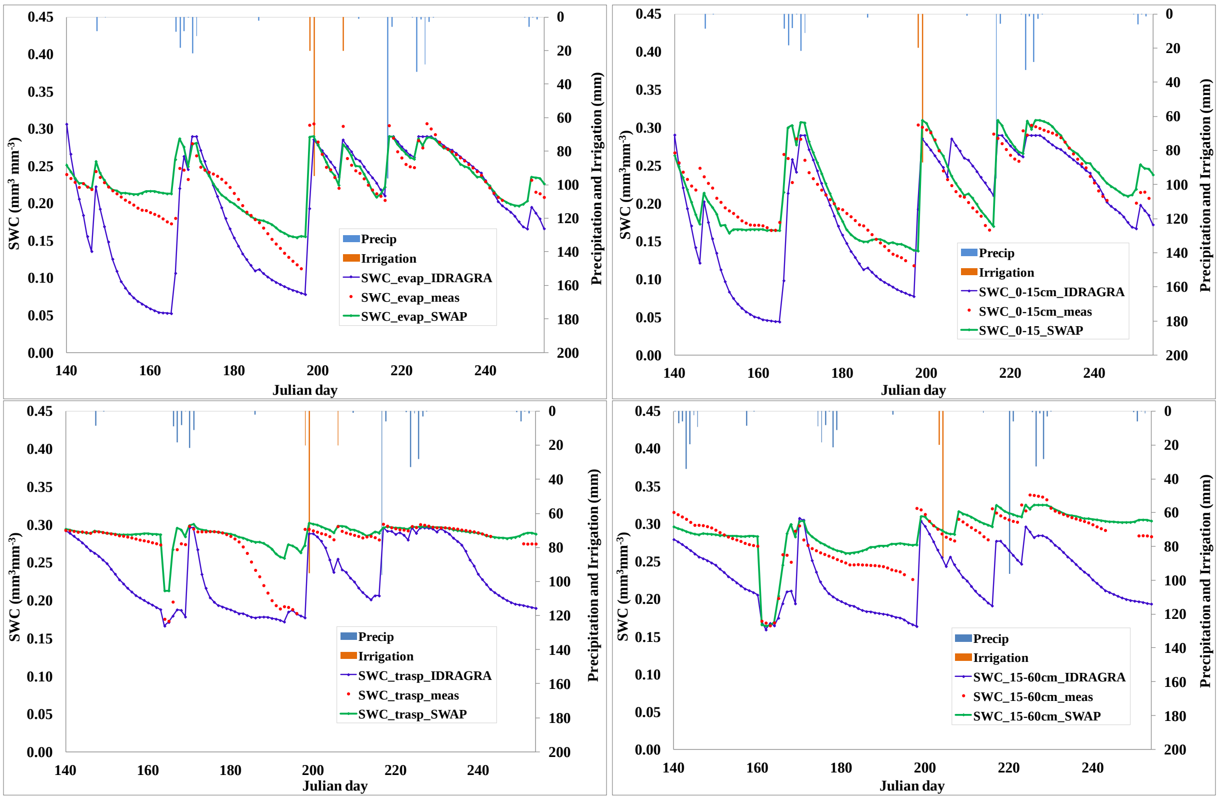

Figure 6.10 Soil water content in the evaporative (up) and the transpirative (down) layers for PMI-1 (left) and PMI-5 (right) measured (red points) and estimated with SWAP (green) and IDRAGRA (blue) after the calibration of the models during the 2010 season.

Table 6.14. Statistical analysis of the estimated soil water content in the evaporative layer with the calibrated SWAP and IDRAGRA models in comparison with the measured data for both sites during 2010 season

Calibrated models	SWC_evap	RMSE	Bias	MAE
1C	IDRAGRA	0.056	0.030	0.040
	SWAP	0.017	-0.007	0.012
5C	IDRAGRA	0.059	0.029	0.044
	SWAP	0.029	0.000	0.018

Table 6.15 Statistical analysis of the estimated soil water content in the transpirative layer with the calibrated SWAP and IDRAGRA models in comparison with the measured data for both sites during 2010 season

Calibrated models	SWC_trasp	RMSE	Bias	MAE
1C	IDRAGRA	0.055	0.043	0.043
	SWAP	0.024	-0.011	0.012
5C	IDRAGRA	0.057	0.051	0.052
	SWAP	0.016	-0.007	0.013

6.7.2 Agricultural season 2011

Comparison of the two models With estimated soil hydraulic parameters from PTF-R

ETact

In 2011 agricultural season, the emergence of maize occurred on 20th of April (Julian day 110), while the harvest was made on 1st of September (Julian day 244). Figure 6.11 shows the trends of the daily actual evapotranspiration for the two sites measured (Eddy) and simulated by SWAP and IDRAGRA. In Table 6.16 are reported the components of the water balance (in mm) accumulated over the entire agricultural season 2011 (135 days) in PMI-1 and 5.

Table 6.16. Total water balance components (mm) for the agricultural season 2011(accumulated in 135 days)

Non-Calibrated models		Precipitation	Irrigation	Tpot	Tact	Epot	Eact	Capillary rise	Deep percolation
1C	IDRAGRA	138,0	0,0	328.8	228.9	157.1	117.7	293.6	31.2
	SWAP	138,0	0,0	351.7	347	212.8	129.5	266.9	42.9
5C	IDRAGRA	138,0	0,0	404.8	377.9	102	96.4	199.4	11.7
	SWAP	138,0	0,0	400.5	398.8	182	144.4	415	25.8

By looking to the components of the water balance for 2011 (Table 6.16), we notice that the potential evaporation is higher in PMI-1 than in PMI-5, the opposite happens for potential transpiration. This is due to the fact that in 2011 the maize in the PMI-1, after an initial phase of normal development, has suffered stunted growth (see paragraph 4.5.1). The potential evapotranspiration for both sites totaled around 496 mm (IDRAGRA) and 573mm (SWAP), then a higher value for SWAP compared to 2010 but lower value for IDRAGRA. The actual evapotranspiration reaches 71% and 84% of the potential ET in PMI-1 for IDRAGRA and SWAP respectively. While up to 93% in the PMI-5 for both models. Although physiological measures listed in chapter 4 (LAI, plant height, canopy cover etc) highlighted the results of simulations made with the two models: in 2011, the PMI-5 did not show any sign of water stress, however the stress was evident in the PMI-1 despite the groundwater level was higher in this site. This can be attributed to the soil texture which is more clay in PMI-5 so that more water retention in this site which is verified by higher soil water content (see the following paragraph).

Table 6.17 illustrates statistical analysis between measured (Eddy) and estimated ETact (SWAP and IDRAGRA).

We can notice that in PMI-1, IDRAGRA slightly under-estimates ETact (13%) and this is also highlighted by a positive bias (0.05). the same value of bias is found in PMI-5 but with a negative sign showing a slight over-estimation of the ETact (16%). Showing negative bias (-0.11 and -0.09), SWAP overestimates ET in both sites (21-24%). The RMSE values range between 0.09 and 0.12 for IDRAGRA and is equal 0.12 for SWAP. The MAE is between 0.07 and 0.10 for IDRAGRA and between 0.10 and 0.12 for SWAP. The determination coefficient is higher for IDRAGRA (0.54-0.82) than for SWAP (0.13-0.43).

According to that analysis we can conclude that, for 2011 agricultural season, IDRAGRA is performing better than SWAP in simulating ET. Similar results were found by Baroni. (2007) who compared SWAP and ALHyMus (uses the the FAO dual crop coefficient methodology to estimate ETact) models and got better results for the second model with PTF-Rosetta parameters.

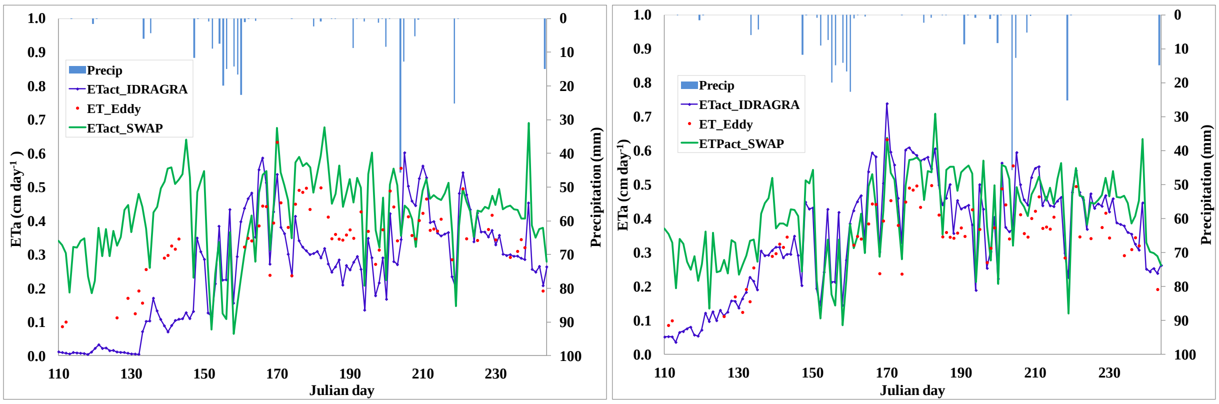

Figure 6.11 Actual evapotranspiration measured (red points) and estimated with SWAP (green) and IDRAGRA (blue) non calibrated models during the 2011 season for the PMI-1 (left) and PMI-5 (right)

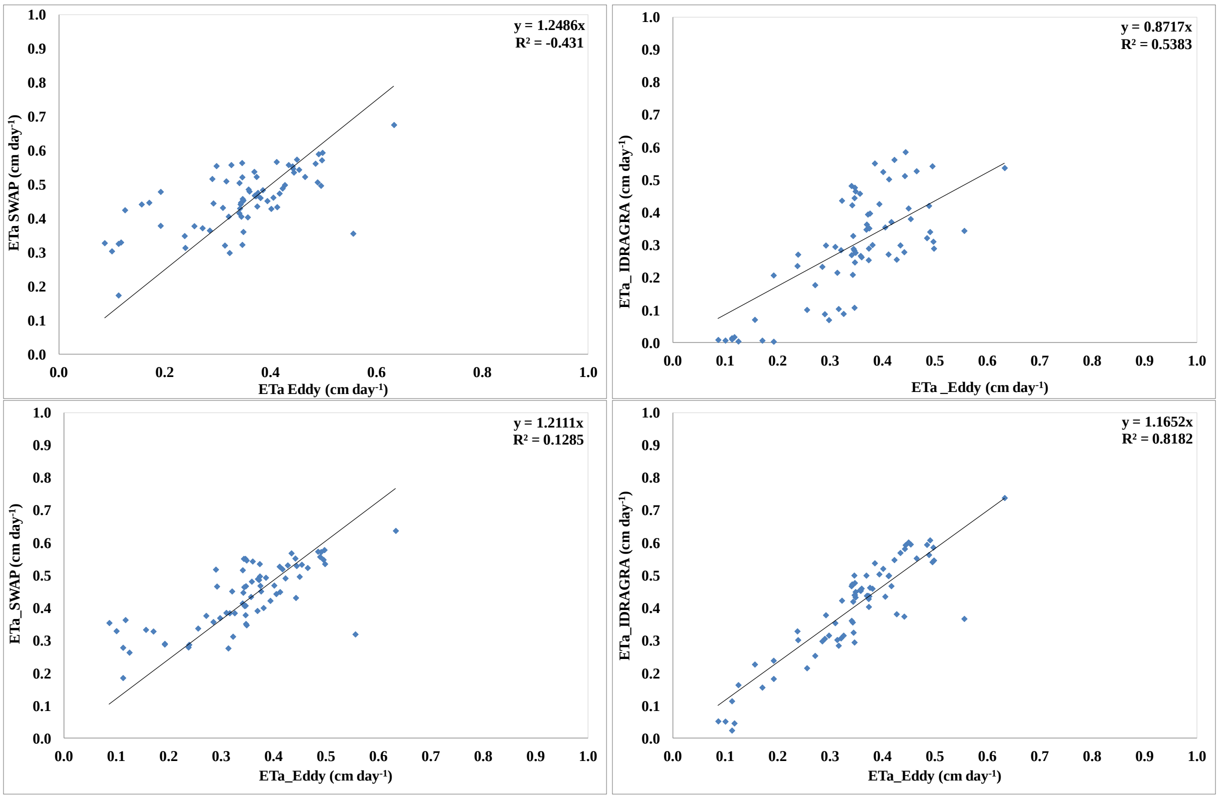

Figure 6.12 Correlation between measured and estimated evapotranspiration with SWAP (left) and IDRAGRA (right) models for PMI-1 (up) and PMI-5 (down) during 2011 season.

Table 6.17. Statistical analysis of the estimated evapotranspiration with the non-calibrated models SWAP and IDRAGRA compared to measured data during 2011 season.

Calibrated models	ETa	M	R^2	RMSE	Bias	MAE
1C	IDRAGRA	0.87	0.54	0.12	0.05	0.10
	SWAP	1.24	0.43	0.14	-0.11	0.12
5C	IDRAGRA	1.16	0.82	0.09	-0.05	0.07
	SWAP	1.21	0.13	0.12	-0.09	0.10

The calculation of the potential evapotranspiration using the Penman-Monteith equation available in SWAP depends on atmospheric conditions and aerodynamics terms which include the aerodynamic and minimum canopy resistance (Kroes et al., 2008). However, specific minimum canopy resistance for the vegetation type under consideration (maize) are not available. Hence, the average canopy resistances obtained from different literature were used for the current study. Thus, the slightly lower performance of the SWAP model when calculating evapotranspiration could be attributed to the uncertainties in the canopy resistances and other parameters required for the application of Penman-Monteith equation.

Soil water content

Results on water content in the two layers (Figure 6.13) can be related to those on evapotranspiration. As a main cause of the over-estimation of ET by SWAP, soil water content in the both layers is overestimated. Nevertheless, the RMSE, bias and MAE are lower on soil water content than on ET (Table 6.18 and Table 6.19). In both layers, water content is better represented by IDRAGRA model. The RMSE is less than 0.07cm^{3}cm^{-3} for each layer. The bias is between -0.01 and -0.04 cm^{3}cm^{-3} and the MAE is ranging between 0.04 and 0.05 cm^{3}cm^{-3}. Statistical indices RMSE (0.06-0.07 cm^{3}cm^{-3}), bias (-0.07- -0.06 cm^{3}cm^{-3}) and MAE (0.06-0.08 cm^{3}cm^{-3}) for SWAP are greater than those of IDRAGRA.

So we can conclude that non-calibrated IDRAGRA performs better than SWAP in simulating soil water content during the 2011 agricultural season.

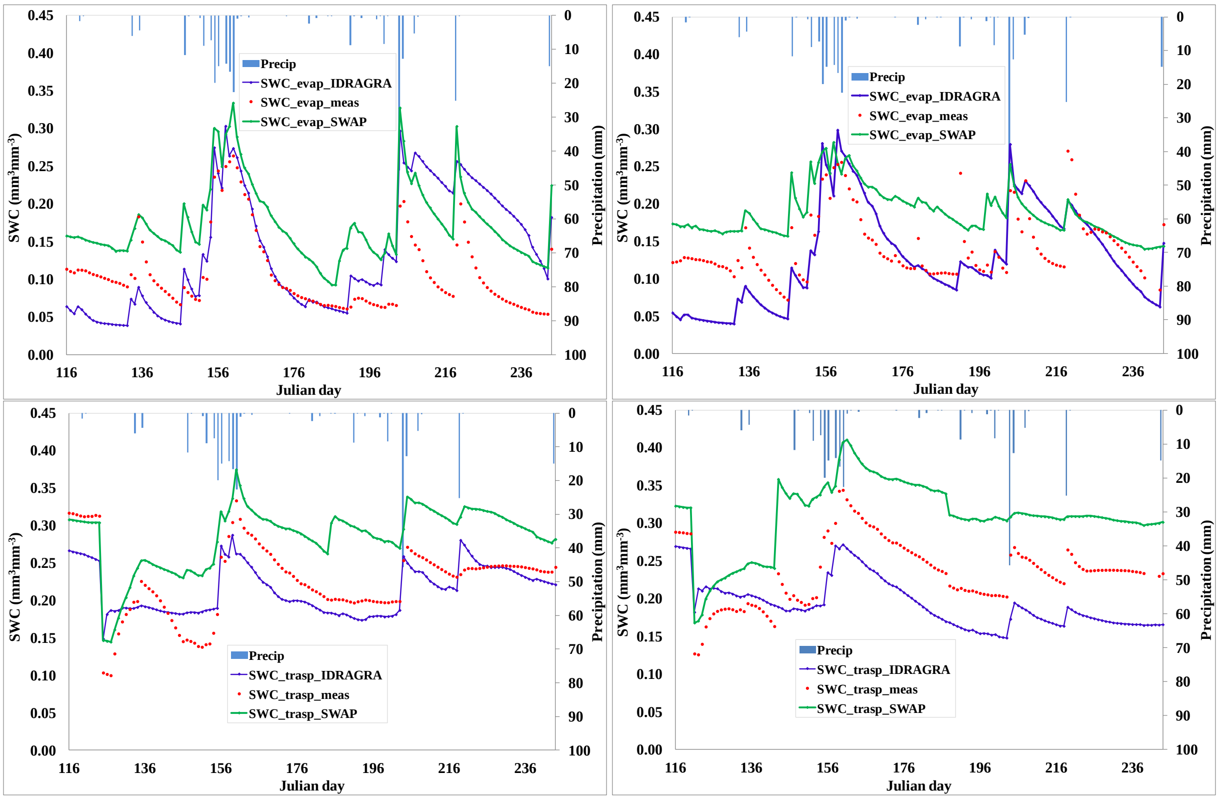

Figure 6.13 Soil water content in the evaporative (up) and the transpirative (down) layers for PMI-1 (left) and PMI-5 (right) measured (red points) and estimated with SWAP (green) and IDRAGRA (blue) models during the 2011 season.

Table 6.18 Statistical analysis of the estimated soil water content in the evaporative layer with the non-calibrated SWAP and IDRAGRA models in comparison with the measured data for both sites during 2011 season.

Calibrated models	SWC_evap	RMSE	Bias	MAE
1C	IDRAGRA	0.07	-0.03	0.05
	SWAP	0.07	-0.06	0.06
5C	IDRAGRA	0.04	0.01	0.04
	SWAP	0.06	-0.04	0.05

Table 6.19 Statistical analysis of the estimated soil water content in the transpirative layer with the non-calibrated SWAP and IDRAGRA models in comparison with the measured data for both sites during 2011 season.

Calibrated models	SWC_trasp	RMSE	Bias	MAE
1C	IDRAGRA	0.03	0.01	0.03
	SWAP	0.06	-0.06	0.06
5C	IDRAGRA	0.05	0.04	0.05
	SWAP	0.08	-0.08	0.08

Calibrated models+field retention curve

<u>ETact</u>

Figure 6.14 illustrates measured (Eddy) and simulated (IDRAGRA and SWAP) actual evapotranspiration in PMI-1 and PMI-5.

Both SWAP and IDRAGRA show similar patterns of under and over estimations of actual ET by a mean value of 20% and 16% respectively. The IDRAGRA slightly underestimated ET early in the season and overestimated late in the season. The largest ET difference between SWAP and measured data was during the beginning of the season. When there is a rain event, ETact estimated by both models increases quickly which resulted in overestimation on measured ET.

According to IDRAGRA simulations, PMI-1 did not suffer any water stress (99% of the ETpot) and a slight water stress was observed in PMI-5 (94% of the ETpot). Despite with SWAP simulation, both sites suffer a water stress and ETact presents 74% and 88% of the ETpot in PMI-1 and PMI-5 respectively (

Table 6.20).

Statistical analysis results are presented in Table 6.21 and according to those results SWAP model slightly perform better in PMI-1 and similarly to IDRAGRA in PMI-5.

Table 6.20 Water balance components (mm) for the agricultural season 2011

Calibrated models		Precipitation	Irrigation	Tpot	Tact	Epot	Eact	Capillary rise	Deep percolation
1C	IDRAGRA	138,0	0,0	397.5	393.7	98.3	97.8	273.3	37.6
	SWAP	138,0	0,0	351.7	321	212.8	98.4	221.8	50.1
5C	IDRAGRA	138,0	0,0	413.6	390.4	99.9	94.9	199.4	22.7
	SWAP	138,0	0,0	400.5	393.3	182	123.6	356.7	0

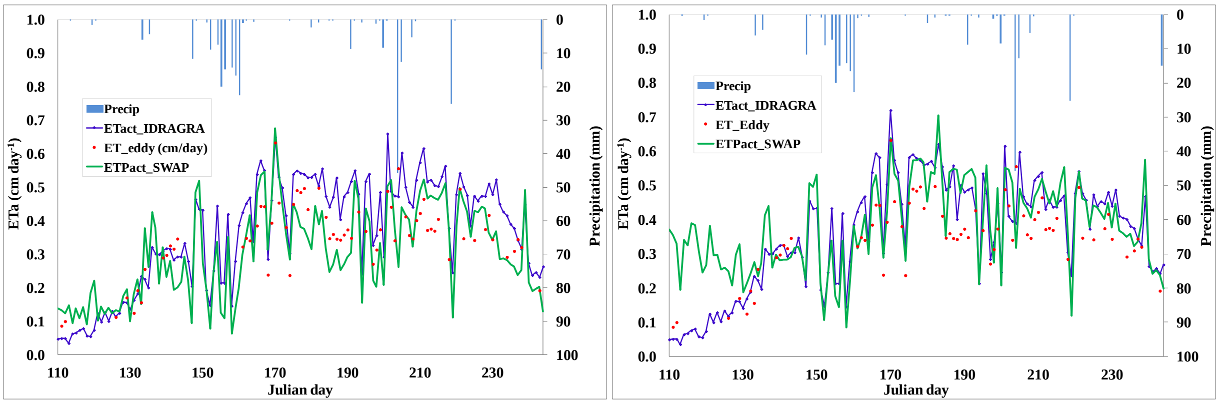

Figure 6.14 Actual evapotranspiration measured (red points) and estimated with SWAP (green) and IDRAGRA (blue) calibrated models during the 2011 season for the PMI-1 (left) and PMI-5 (right)

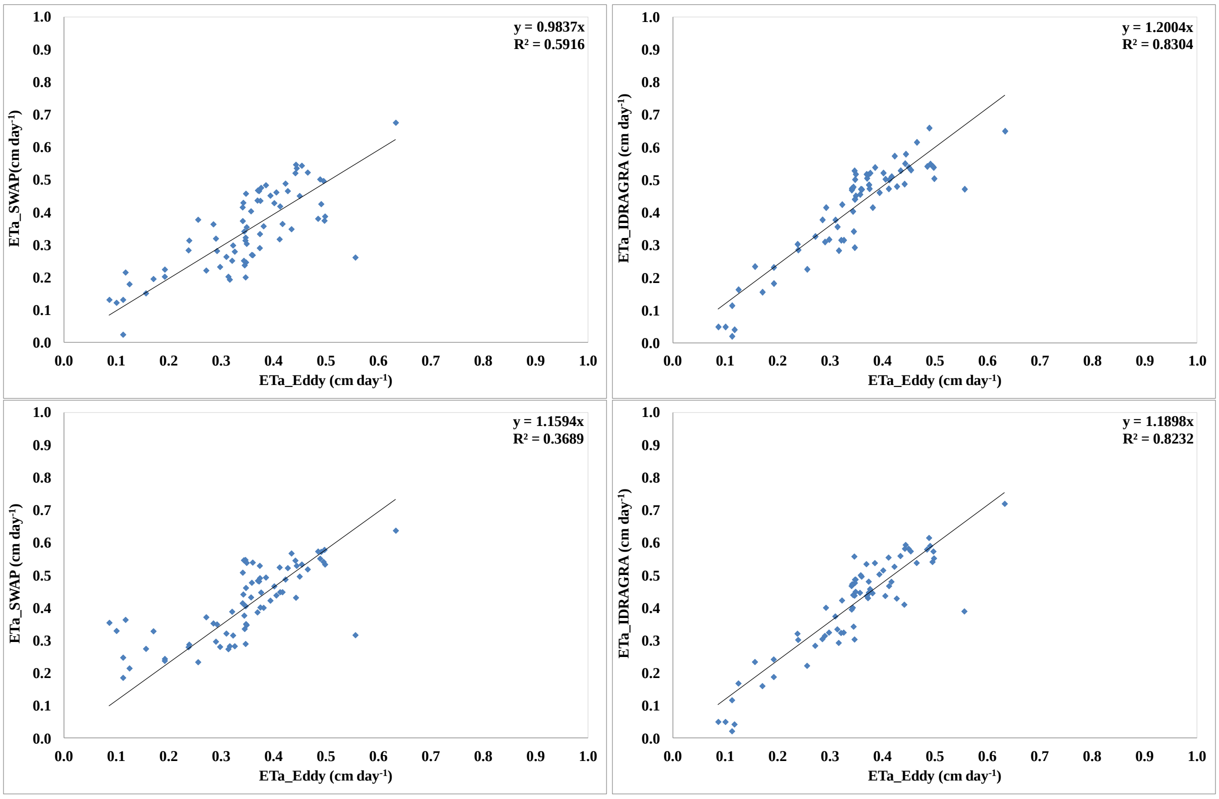

Figure 6.15 Correlation between measured and estimated evapotranspiration with SWAP (left) and IDRAGRA (right) calibrated models for PMI-1 (up) and PMI-5 (down) during 2011 season.

Table 6.21. Statistical analysis of the estimated evapotranspiration with the calibrated models SWAP and IDRAGRA compared to measured data during 2011 season.

Calibrated models	ETa	M	R^2	RMSE	Bias	MAE
1C	IDRAGRA	1.20	0.83	0.09	-0.07	0.080
	SWAP	0.98	0.59	0.08	0.00	0.070
5C	IDRAGRA	1.19	0.82	0.09	-0.06	0.079
	SWAP	1.16	0.37	0.10	-0.07	0.082

Soil water content

Figure 6.16 shows measured and simulated soil water contents at two different depths for PMI-1 and PMI-5. The graph shows that the soil water content trend simulated by IDRAGRA model is in good agreement with the measured data for both sites. The RMSE (Table 6.22 and Table 6.23) for the soil water content of both depths for PMI-1 is ranging between 0.030 and 0.005 cm^3cm^{-3} and for PMI-5, it is 0.05 cm^3cm^{-3}. These RMSE values show a very good matching between measured and simulated values by IDRAGRA. The model predictions closely matched observations particularly in the transpirative layer indicating model's ability in simulating soil water content.
The RMSE for SWAP model is 0.03 and 0.04 cm^3cm^{-3} for the evaporative layer in PMI-1 and PMI-5 respectively and 0.03 cm^3cm^{-3} for the transpirative layer in both sites. Results illustrated in tables 11 and 12 also show that the model prediction of subsurface soil moisture (transpirative layer) was better than surface soil moisture (0-15 cm). The top soil layers have slightly lower water contents than lower layers. In the case of SWAP application, measured soil moisture was about 5–10% higher than predicted soil moisture for the top two layers.
In general, the top soil layer had greater fluctuations as compared to the layers below for the entire growing season. It is because the top layer forms the bio-sphere, which receives moisture in pulses of rainfall (Irmak and Kamble., 2009). The same water is eliminated through evaporation and transpiration by plants. As the depth increases, the soil layer tends to hold more water with less fluctuations throughout the season. Higher water content with depth can be due to capillary rise from the ground water table.
According to the latter results, IDRAGRA performs similarly to SWAP in simulating soil water content in the root zone.

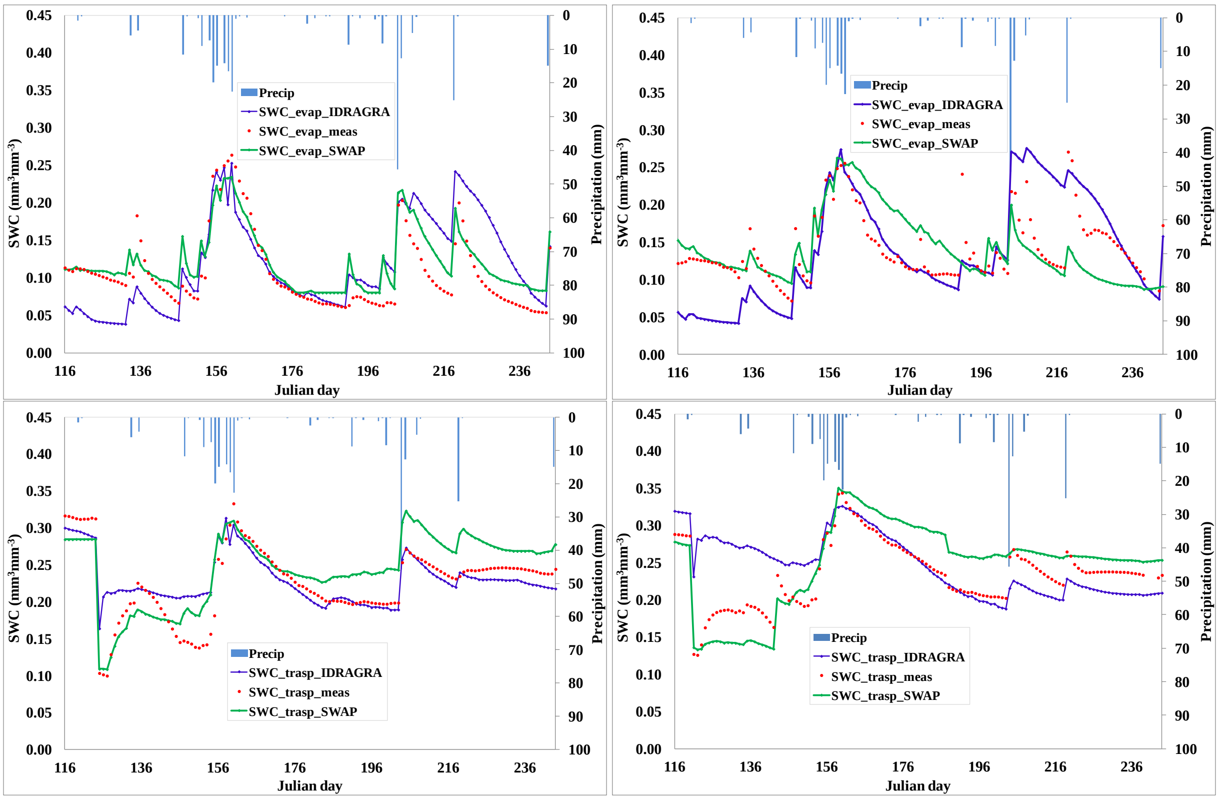

Figure 6.16 Soil water content in the evaporative l (up) and the transpirative (down) layers for PMI-1 (left) and PMI-5 (right) measured (red points) and estimated with SWAP (green) and IDRAGRA (blue) calibrated models during the 2011 season

Table 6.22 Statistical analysis of the estimated soil water content in the evaporative layer with the calibrated SWAP and IDRAGRA models in comparison with the measured data for both sites during 2010 season

Calibrated models	SWC_evap	RMSE	Bias	MAE
1C	IDRAGRA	0.05	-0.01	0.04
	SWAP	0.03	-0.01	0.02
5C	IDRAGRA	0.05	0.00	0.04
	SWAP	0.04	0.00	0.03

Table 6.23. Statistical analysis of the estimated soil water content in the transpirative layer with the calibrated SWAP and IDRAGRA models in comparison with the measured data for both sites during 2011 season

Calibrated models	SWC_trasp	RMSE	Bias	MAE
1C	IDRAGRA	0.03	0.00	0.02
	SWAP	0.03	-0.02	0.03
5C	IDRAGRA	0.05	-0.01	0.03
	SWAP	0.03	-0.01	0.03

6.8 Models (SWAP and IDRAGRA) application to assess capillary rise contribution to satisfy crop water requirement and groundwater recharge

6.8.1 Capillary Rise contribution

Calibrated SWAP and IDRAGRA models were used in this study to generate the capillary rise fluxes through the bottom boundary of the root zone for different groundwater table depths. The groundwater table depths were fixed virtually at 0.8m, 1m, 1.5m, 2m and 3m. The aim of considering the groundwater table depths was to understand at which depth the groundwater table contribute majorly to satisfy the crop water requirement.

Agricultural season 2010

Capillary rise from a daily variation of a shallow water table

Figure 6.17 shows upward (capillary rise) movement of water from the root zone in PMI-1 (left) and PMI-5 (right).

The graphs show that there are fluctuations in the bottom flux after an irrigation or rainfall event. Capillary rise is quite similar for both models in the PMI-1 and is contributing by 41% (IDRAGRA) and 46% (SWAP) of the total maize water requirement. In PMI-5 the contribution of the groundwater estimated by SWAP is slightly similar to that in PMI-1 and is about 43%. IDRAGRA estimates lower contribution in this site which is just 27% of the total maize water requirement.

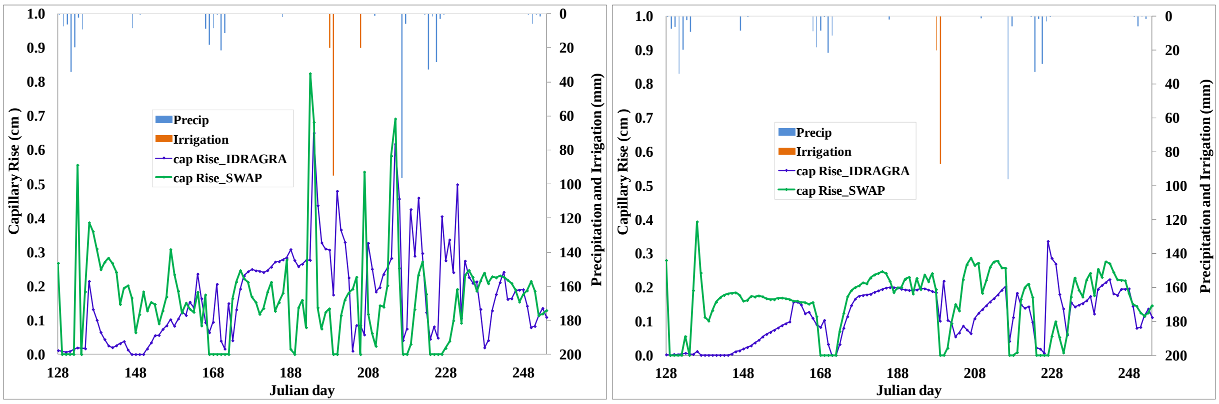

Figure 6.17 Capillary rise fluxes estimated with SWAP (green) and IDRAGRA (blue) calibrated models during 2010 season in PMI-1 (left) and PMI-5(right).

Capillary rise from fixed shallow water table depth

The daily capillary rise is higher under shallower water table (Figure 6.18 Figure 6.20). In PMI-1, the daily capillary rise under 0.8m of water table depth ranges from 0 to 0.35 cm day^{-1} for

IDRAGRA and from 0 to 0.2cm day^{-1} for SWAP. Whereas under a water table depth of 1m the capillary rise decreases to be between 0 and 0.27cm day^{-1} for IDRAGRA and between 0 and 0.12cm day^{-1} for SWAP. Daily capillary rise are much lower for 1.5-3 m of groundwater table depth.

In PMI-5, the daily capillary rise under 0.8m of groundwater depth is between 0 and 0.4 cm day^{-1} for both models. Similarly to PMI-1, the capillary rise decreases increasing groundwater depth.

The total capillary rise from groundwater at water table depths 0.8 m and 1 m, are equal to 18.1 and 14.7 cm, respectively, from IDRAGRA model in PMI-1, as well as 16.2 and 10 cm from SWAP.

In PMI-5, results from both IDRAGRA and SWAP models displayed 17.6 and 14.6cm, 27.3 and 21.8cm, respectively. These results were recorded when the groundwater was at depths of 0.8m and 1 m respectively.

In the other side, the total capillary rise from groundwater at water table depths of 1.5m decreases to 8.5cm for IDRAGRA in both sites and for SWAP to 4 and 14 cm in PMI-1 and PMI-5 respectively. While when the water table depth is higher than 1.5m (2-3 m), the total capillary rise is lower than 5cm and 10 cm from IDRAGRA and SWAP estimations respectively .

We can also notice that for both models that the capillary rise from groundwater at 1-3 m depths shows slight variations at the beginning of the season, but dramatic changes afterwards. This might be due to the seasonal variations of soil evaporation and transpiration by maize. At the beginning of the agricultural season (May), maize is at earlier growing stage, and soil temperature is not as high as in July and August. Hence soil evaporation and plant transpiration are relatively low. From June to September maize grows fast and roots and leaf area index increases rapidly. The dramatic increase in plant transpiration and plant root depth might cause the significant increase in capillary rise.

We can also observe that IDRAGRA displays a quite similar results in both sites, while in SWAP the capillary rise in PMI-5 is much higher than that in PMI-1 and this can be related to differences in soil texture between the two sites and a difference in saturated hydraulic conductivity.

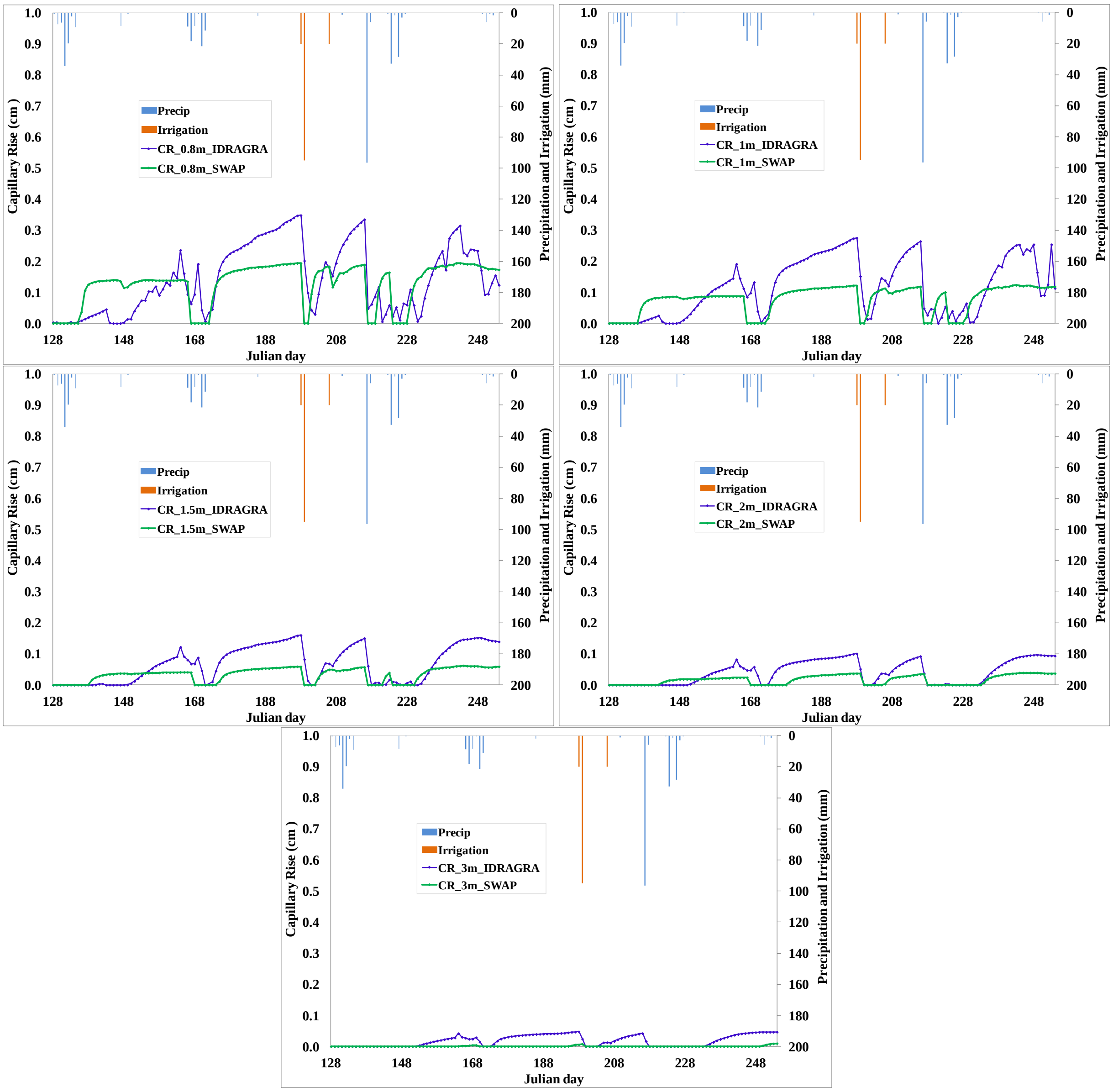

Figure 6.18 Estimated Capillary Rise by IDRAGRA (blue) and SWAP (green) in PMI-1 during 2010 season at different groundwater level (0.8m, 1m, 1.5m, 2m, 3m)

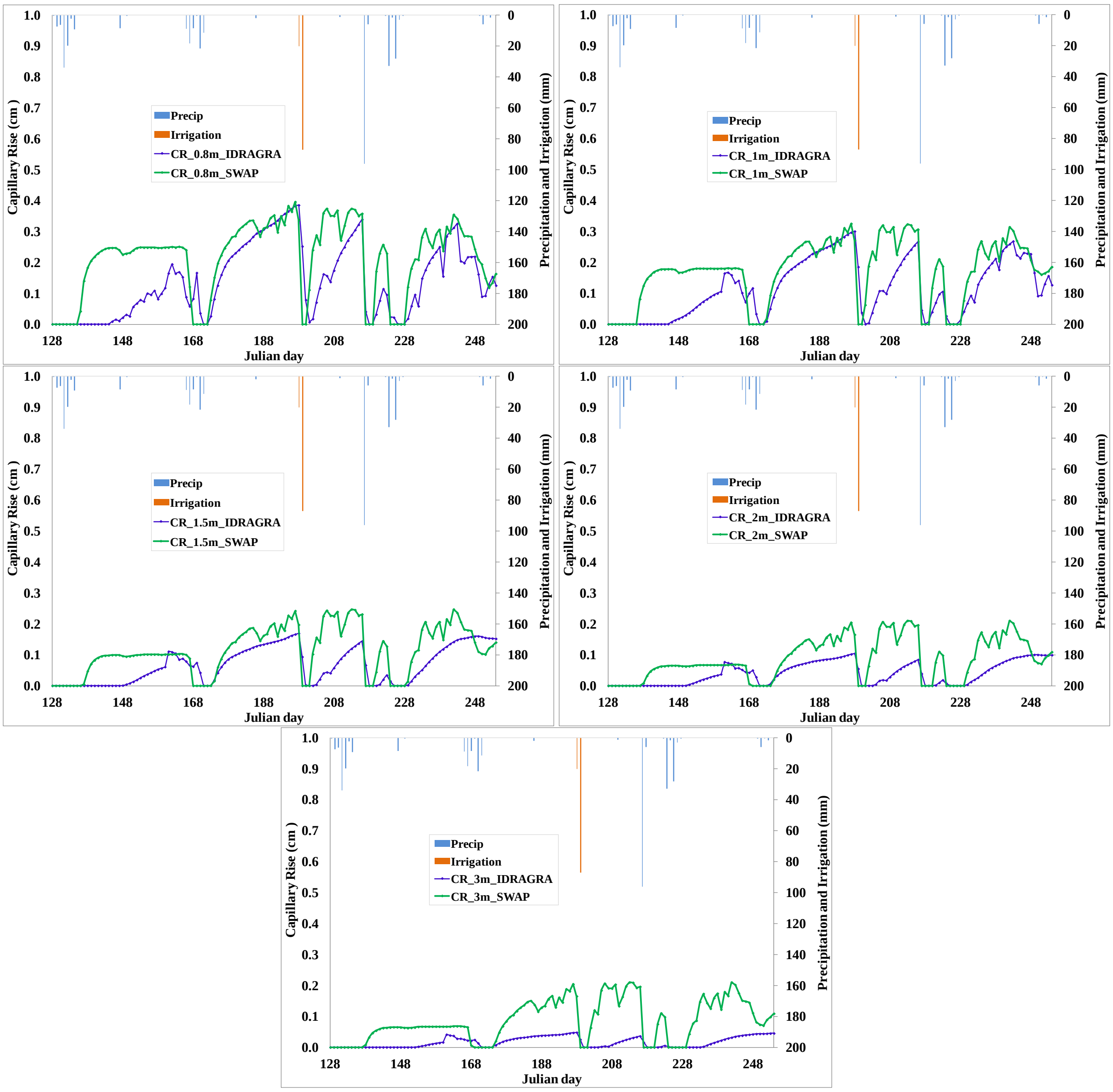

Figure 6.19 Estimated Capillary Rise by IDRAGRA (blue) and SWAP (green) in PMI-5 during 2010 season at different groundwater level (0.8m, 1m, 1.5m, 2m, 3m)

Relation between capillary rise and groundwater level

It was found that the capillary rise from groundwater decreases with the increase of the groundwater table depth (Figure 6.20). When the water table depth reached 3m the capillary was extremely low. A power function exists between capillary rise and groundwater table depth, and this function has a high correlation coefficient for both models; e.g. this coefficient ranges between 0.95 and 0.98 for IDRAGRA in PMI-1 and PMI-5 respectively and for SWAP it ranges between 0.87 and 0.94 in the two sites respectively. This is consistent with the steady state analyses of Gardner (1958) and Warrick (1988), who showed that the maximum soil limited capillary rise from groundwater was directly proportional to the water table depth. That is also consistent with the results of Yang et al

(2011), who showed the power function relationship between capillary rise and groundwater table depths.

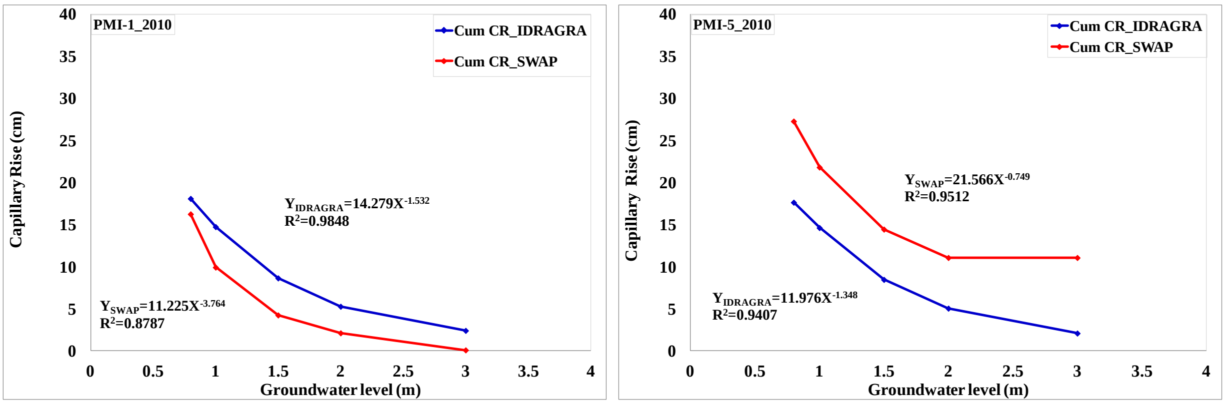

Figure 6.20 Correlation between capillary rise and water table depths in 2010 agricultural season

Capillary rise contribution was the highest under shallowest water table conditions for both models, that gradually reduced with increasing water table depth (Table 6.24) which was also previously proved by many authors (Babajimopoulos et al., 2007; Kahlown et al., 2005; Ayars., 2003; Raes et Deproost., 2003). Maize was able to take up more than 40% of its water from the groundwater according to SWAP simulations and more than 30% of its water from the groundwater when the water table depth was 0.8m according to IDRAGRA simulations. Estimations of both models are in accordance with findings of Kahlown et al., (2005). He found that maize was able to obtain about 40% of its water needs when the water table was very shallow.

For a water table between 0.8 m and 1.5 m, SWAP and IDRAGRA present similar results in PMI-1. while in PMI-5, the contribution from SWAP appears to be the double of that from IDRAGRA.

Under a groundwater table depth higher than 3m, the capillary rise contribution decreases dramatically and is not able to meet more than 4% of maize water requirement in PMI-1 from both models. While for PMI-5 and according SWAP estimations, the water table is able to contribute up to 27% of total maize water requirement.

Table 6.24 Capillary rise contribution in PMI1 and PMI-5 at different groundwater table depth during 2010 season

		0.8m	1m	1.5m	2m	3m
1C	IDRAGRA	38%	28%	16%	10%	4.5%
	SWAP	41%	26%	11%	5%	0%
5C	IDRAGRA	32%	27%	16%	9%	4%
	SWAP	68%	54%	36%	27%	27%

Agricultural season 2011

Capillary rise from a daily variation of shallow water table

The capillary flux (Figure 6.28) estimated by IDRAGRA is equal to 273.3mm and 199.4mm in PMI-1 and PMI-5 respectively. While for SWAP model it is equal to 221.8mm and 356.4mm in both sites. So that the contribution of the capillary rise to satisfy maize water requirement is about 55% (IDRAGRA) and 39% (SWAP) on PMI-1 and 39% (IDRAGRA) and 69% (SWAP) in PMI-5. Estimated capillary rise by SWAP on PMI-5 is higher than that on PMI-1 and this can be due to highest crop parameters particularly LAI and root depth despite the deepest groundwater table is in the same site. This clearly influences IDRAGRA simulation resulting on lower contribution on PMI-5.

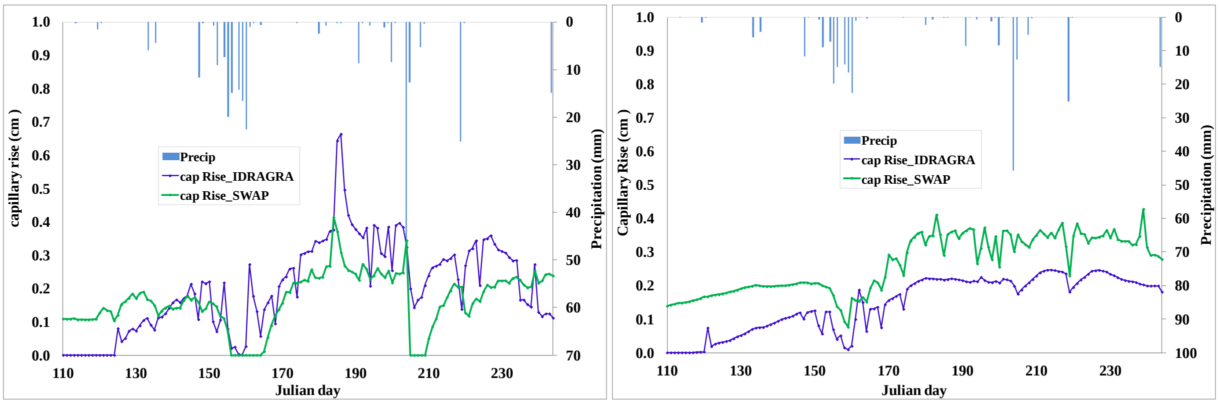

Figure 6.21 Capillary rise fluxes estimated with SWAP (green) and IDRAGRA (blue) calibrated models during 2011 season.

Capillary rise from fixed shallow water table depth

Figure 6.22 and Figure 6.23 present the daily capillary rise under different groundwater depth in 2011 agricultural season.

These figures show that capillary rise is highly dependent upon the groundwater depth. Similarly, capillary rise is increasing when the water table is shallower, which resemble the trend of capillary rise in 2010. While, in 2011 the capillary rise generally shows higher values compared to 2010 season. This observation could be attributed to plant roots depth which was higher in 2011.

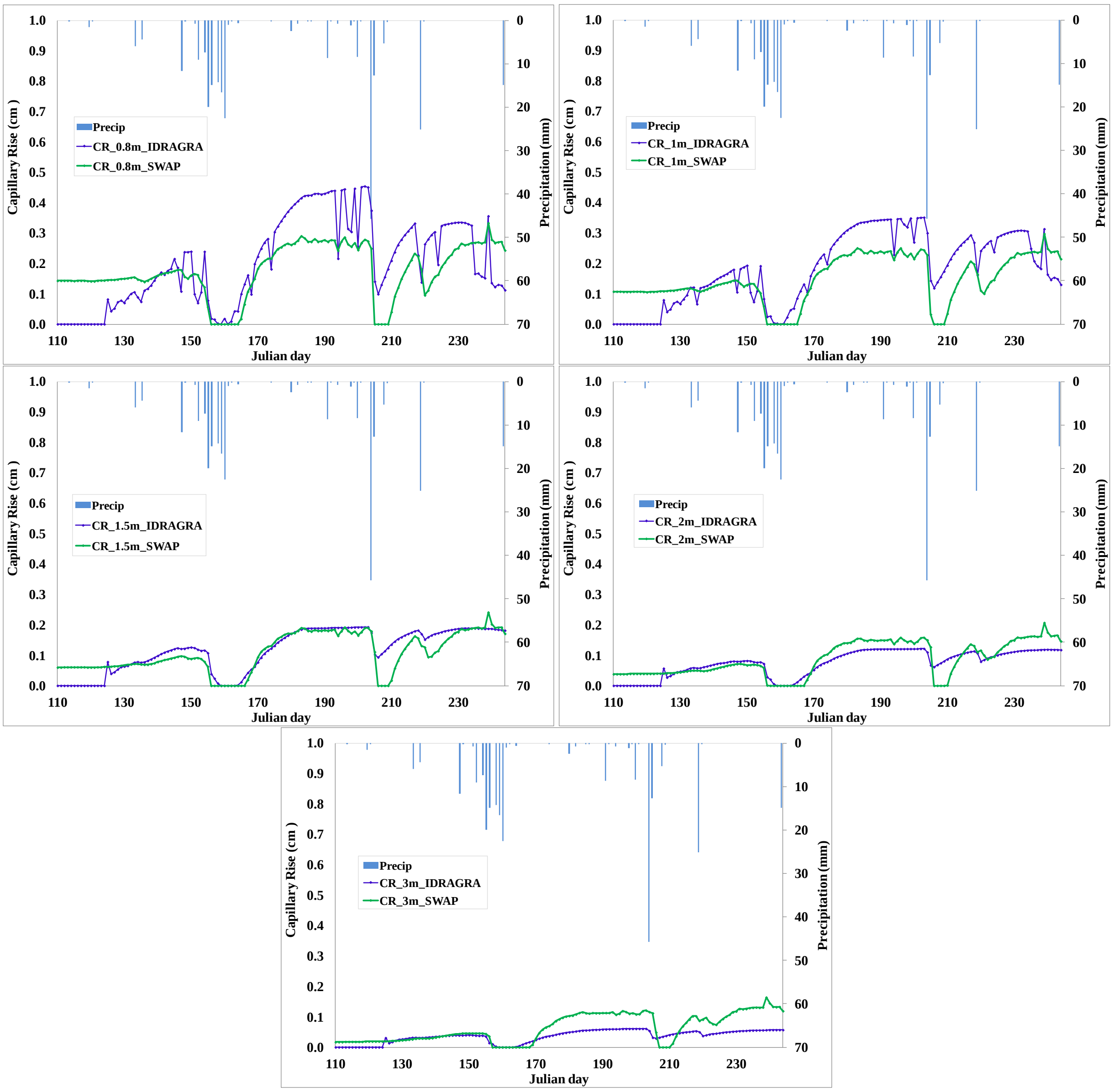

Figure 6.22 Estimated Capillary Rise by IDRAGRA (blue) and SWAP (green) in PMI-1 during 2011 season at different groundwater level (0.8m, 1m, 1.5m, 2m, 3m)

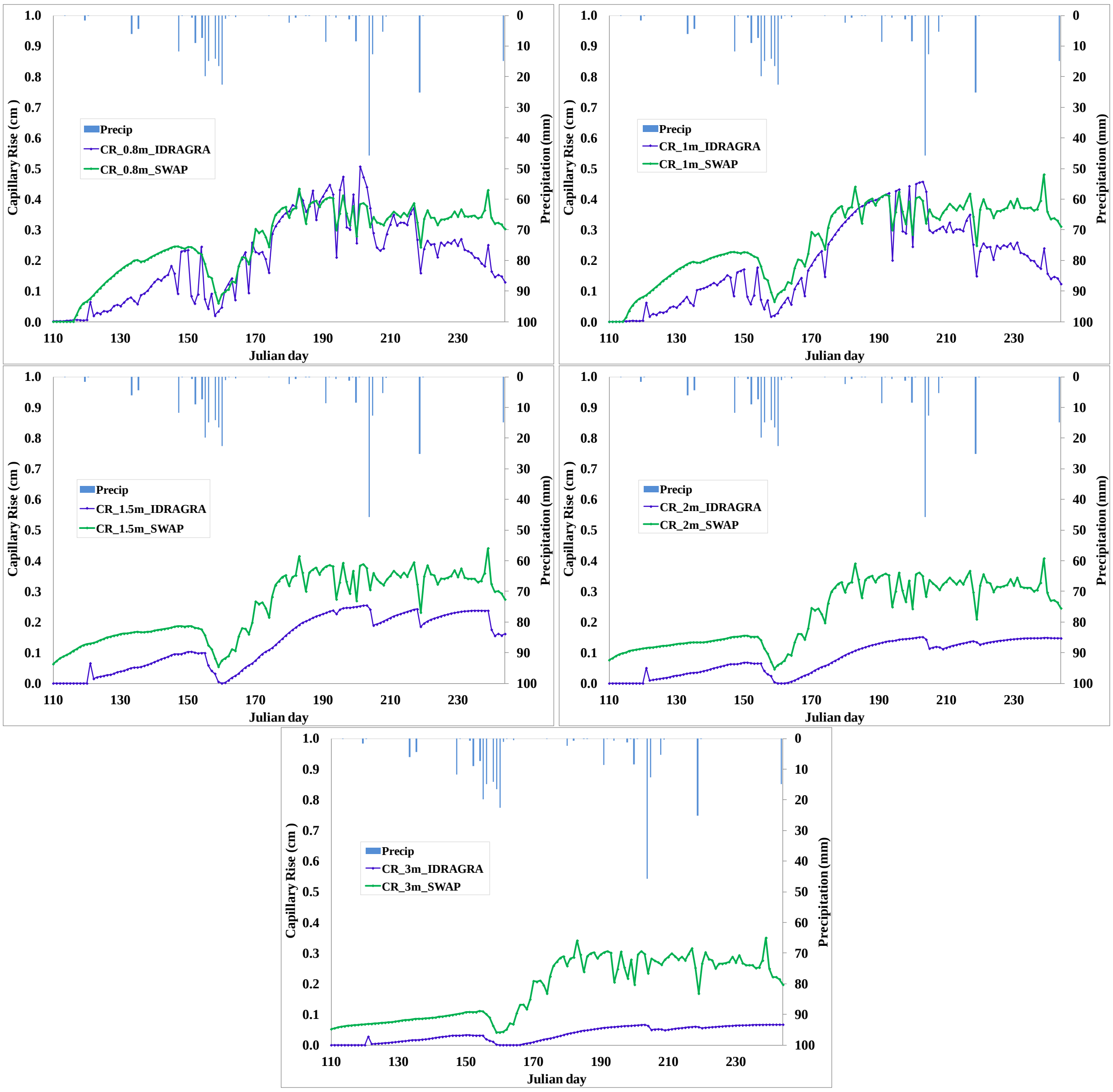

Figure 6.23 Estimated Capillary Rise by IDRAGRA (blue) and SWAP (green) in PMI-5 during 2011 season at different groundwater level (0.8m, 1m, 1.5m, 2m, 3m)

Relation between capillary rise and Groundwater level

In 2011 season, the capillary rise follow a power function relation with groundwater table depth in PMI-1,that is in concordance with 2010 findings (Figure 6.24). While for PMI-5, the capillary rise follows different trend. The capillary rise from a groundwater table at 0.8m is lower than expected and lower than capillary rise from deeper groundwater table (see Figure 6.24). An explanation for this trend could be that a part of the roots (5cm) was submerged in the groundwater table; e.g. the fixed groundwater table was at 0.8m while plant roots depth was 0.85m. Whereas, the capillary rise decreases when the groundwater table depth is higher than 1m.

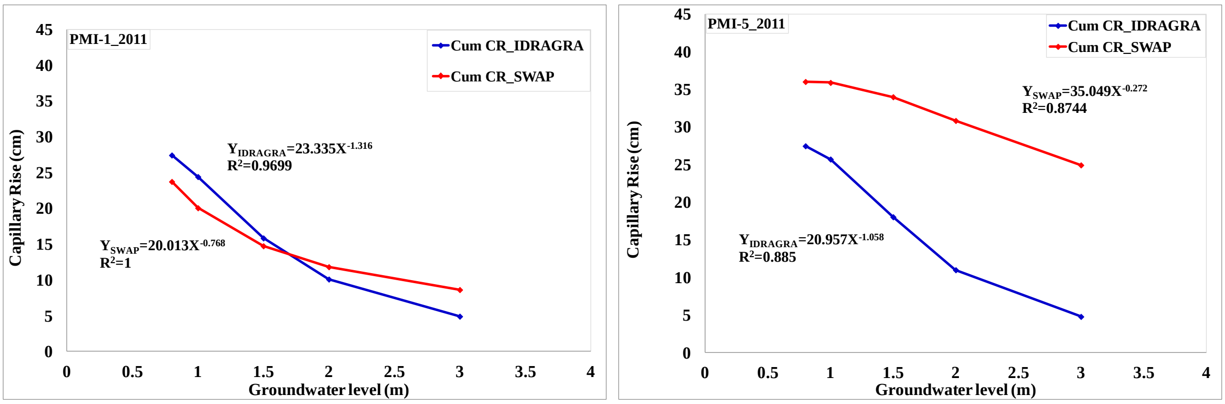

Figure 6.24 Correlation between capillary rise and Groundwater table depth in 2011 agricultural season

Similarly to 2010 season and for both models, large groundwater capillary rise contributed to crop water use during the crop growing period (Table 6.25). In PMI-1 and except when the groundwater table is higher than 1.5m , both models show similar results and groundwater contribution is able to meet 56 to 32% of maize water requirement. In PMI-5, IDRAGRA estimates slightly higher groundwater contribution in comparison to PMI-1 and that can be explained by a higher root depth in this site.

In PMI-5 and for a groundwater table higher than 1m depth, estimated contribution by SWAP decreases in comparison to the contribution of a groundwater table lower than 1m because a big part of the roots was submerged in water. When water table is very shallow, soil water logging limits the root growth due to the reduced oxygen concentration of the soil. Similar results are reported by Brisson et al., (2002).

At 0.8m, IDRAGRA estimates that groundwater contribution to satisfy maize water requirement is about 55%. That result is in accordance with Gupa and Yadov., (1993)

Water table as deep as 2m are still likely to have a positive impact on maize water balance and are able to contribute up to 10% for IDRAGRA and up to 40% for SWAP. That was previously proved by Hurst et al., (2004) who found that groundwater is able to met a considerable part of maize water requirement.

Table 6.25 Capillary rise contribution in PMI1 and PMI-5 at different groundwater table depth during 2011 season

		0.8m	1m	1.5m	2m	3m
1C	IDRAGRA	55%	49%	32%	20%	10%
	SWAP	56%	48%	35%	28%	20%
5C	IDRAGRA	56%	53%	37%	23%	10%
	SWAP	67%	69%	65%	60%	48%

6.8.2 Groundwater Recharge

Agricultural season 2010

Groundwater recharge from a daily variation of a shallow water table

Figure 6.25 shows the daily variation of estimated deep percolation with SWAP (green) and IDRAGRA (blue) in PMI-1 (left) and PMI-5 (right) during 2010 season.

We can observe from figures that the deep percolation flux shows a high temporal variability and follows a pattern similar to precipitations and irrigation rates. The recharge rate was high at the beginning of the season 2010 due to the big amount of precipitation. Then the recharge decreases to zero with absence of precipitations and irrigation to increase again the day 167 after rainfall. The recharge is the highest after irrigation events (day 198) and during August because of more rainfall and lower evapotranspiration associated with a decline on leaf area index attributed to maize maturation. The recharge peaks are related to the maxima in precipitation and irrigation.
The deep percolation estimated by SWAP is much higher than that estimated by IDRAGRA in both sites. It represents 24% (IDRAGRA) and 71% (SWAP) of the total water coming from precipitation and irrigation in PMI-1. While in PMI-5, the recharge rate is lower than that in PMI-1 and is about 22% from IDRAGRA and 62% from SWAP. That can be due to the higher holding capacity of clayey soil that characterizes PMI-5.
Differences between the two models can be related to actual transpiration which was lower in SWAP than IDRAGRA during the rainy days because of the effect of saturation and rain on this rate. So that when transpiration is equal to zero we have more available water in the soil. This water is leaving the root zone via deep percolation.
When we try to neglect days in which we have actual transpiration equal to zero, deep percolation decreases dramatically and becomes close to the deep percolation estimated by IDRAGRA. That confirms what we previously hypothesized about effect of rainy days.

Unfortunately, the absence of measured upward and downward fluxes prevented us from judging which model is performing better.

A clear distinction should be made between relative amount of water available for recharge from the soil zone which is equal to the deep percolation and the actual or the net recharge reaching the water table and which is obtained from the difference between deep percolation and capillary rise. According the net recharge estimated from SWAP is about 60 to 117 mm in PMI-5 and PMI-1 respectively. While the net recharge is negligible from IDRAGRA simulations due to deep percolation which is always lower than capillary rise.

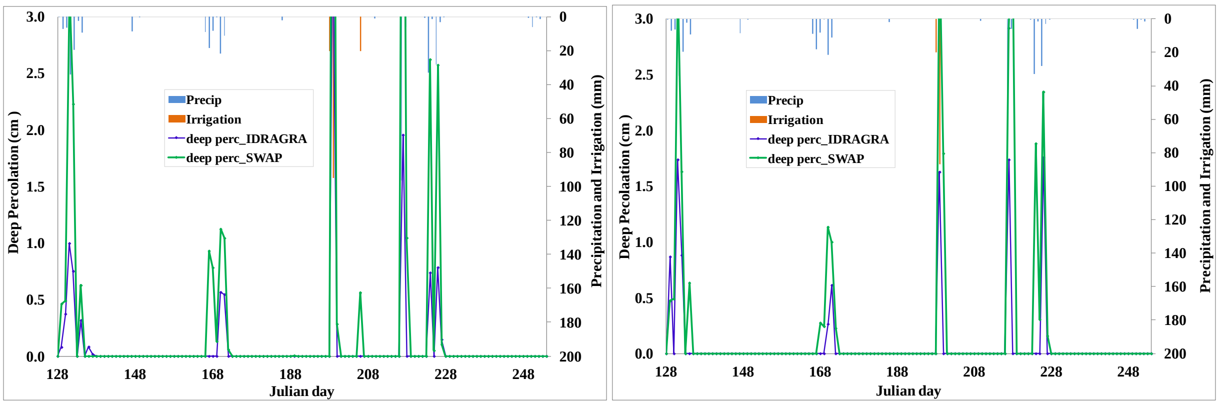

Figure 6.25 Deep percolation fluxes estimated with SWAP (green) and IDRAGRA (blue) calibrated models in PMI-1 (left) and PMI-5 (right) during 2010 season.

<u>Groundwater recharge from a fixed water table depth</u>

Figure 6.26 and Figure 6.27 present the daily variation of deep percolation estimated by SWAP (green) and IDRAGRA (blue) in PMI-1 and PMI-5 respectively at different groundwater table depths (0.8m; 1m; 1.5m; 2m; 3m) during 2010 season.

What we can observe from our figures is that the total deep percolation for 2010 season varies considerably at different groundwater depth. The highest seasonal deep percolation occurred with a 0.8 m water table depth for both sites and both models. The lowest deep percolation at the seasonal scale was about 66 mm from IDRAGRA estimation and higher than 200mm for SWAP at a groundwater table deeper than 2 m. The groundwater recharge is always higher from simulations of SWAP than for IDRAGRA and that is due to the lowest transpiration rate estimated by SWAP as previously explained.

When considering the net recharge (Table 6.26), we find that net recharge tends to increase as the groundwater table depth increases. For both models the net recharge is lower than the total downward flow to the groundwater table. Negative values displayed particularly from IDRAGRA simulation indicate that capillary rise flux is higher than the deep percolation flux. So accordingly added water was lost mainly by transpiration. While for SWAP the net recharge always exist due to the high estimated deep percolation in comparison to IDRAGRA.

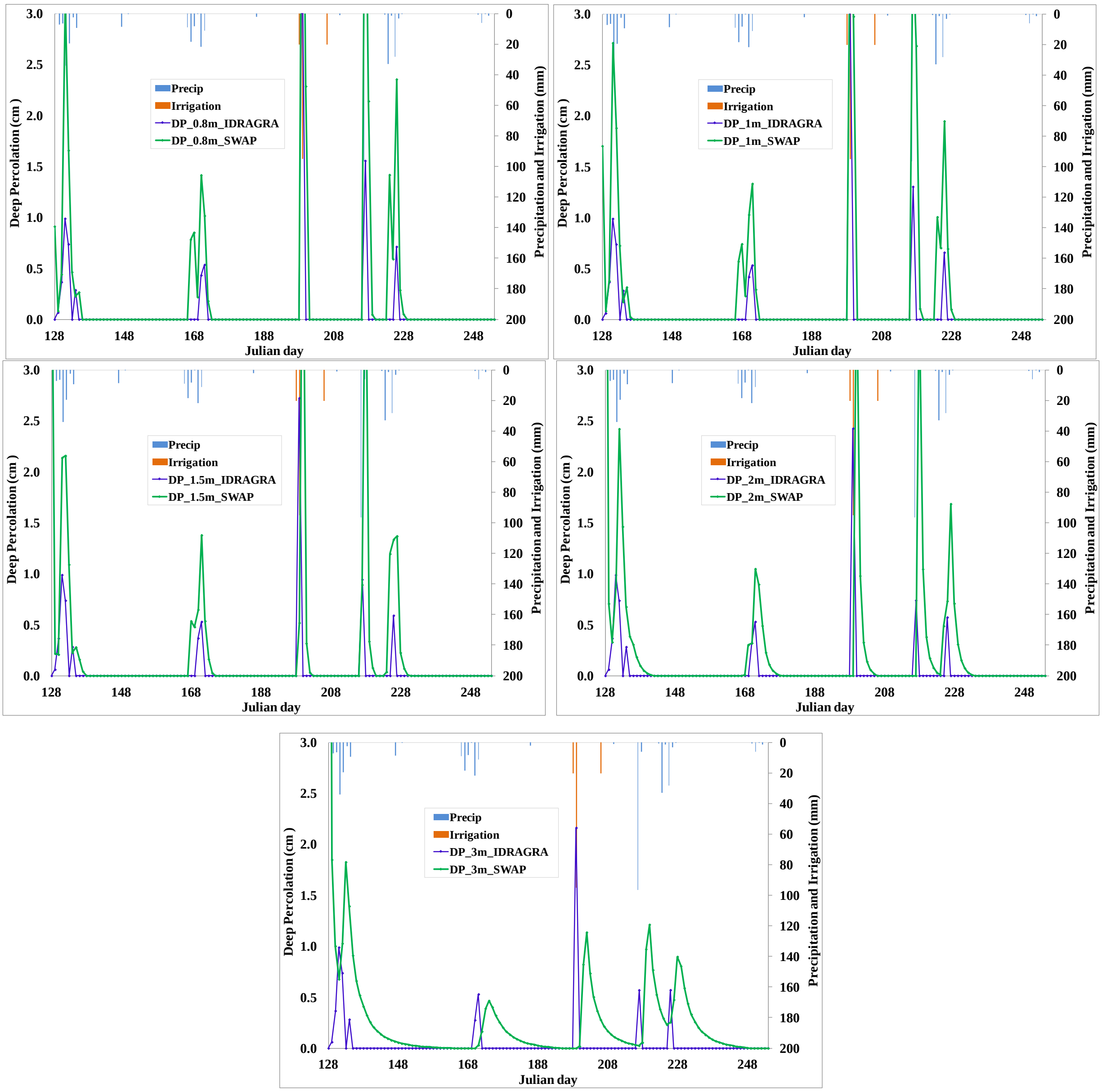

Figure 6.26 Estimated deep percolation by IDRAGRA (blue) and SWAP (green) in PMI-1 during 2010 season at different groundwater level (0.8m, 1m, 1.5m, 2m, 3m)

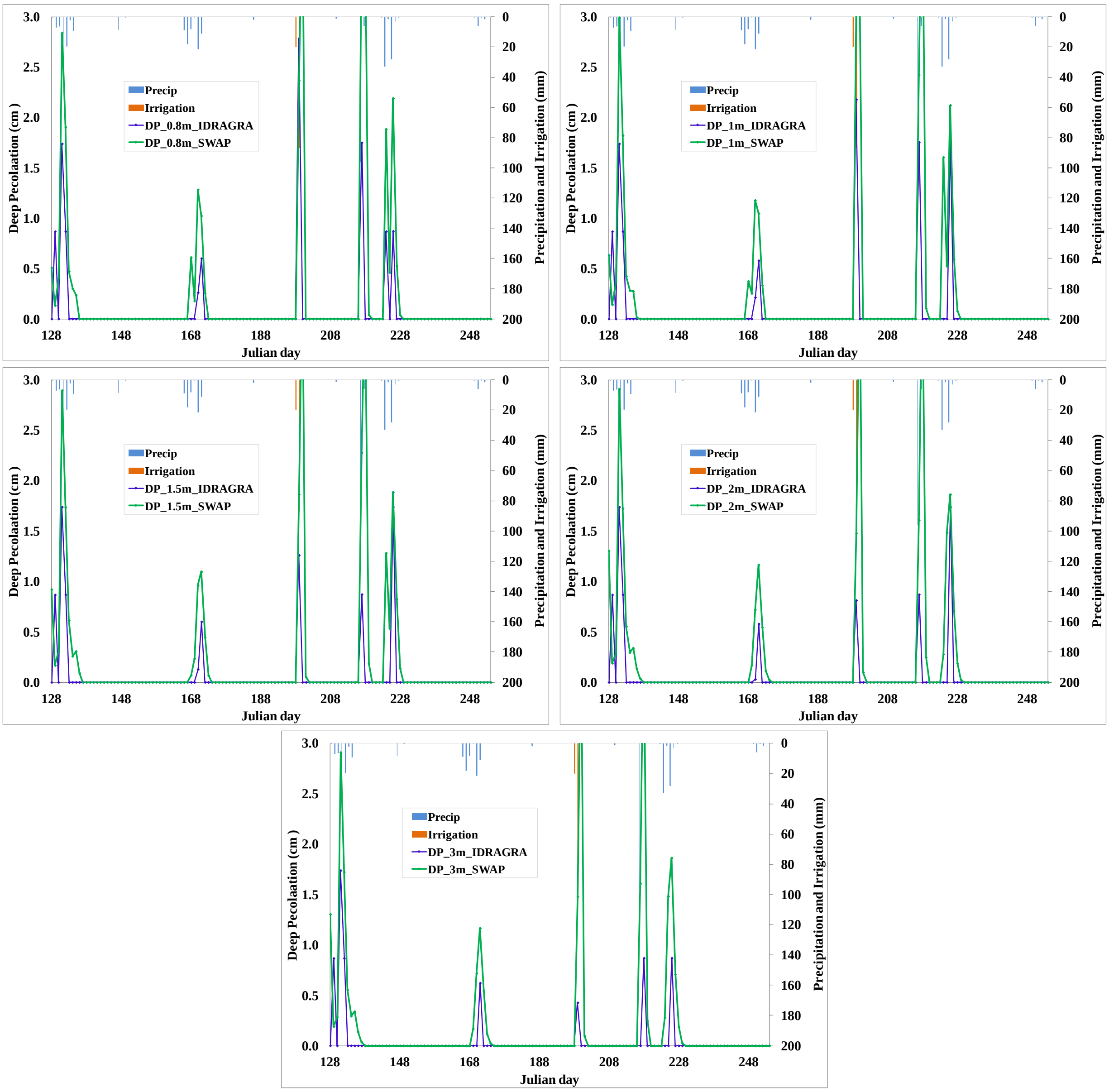

Figure 6.27 Estimated deep percolation by IDRAGRA (blue) and SWAP (green) in PMI-5 during 2010 season at different groundwater level (0.8m, 1m, 1.5m, 2m, 3m)

Table 6.26 Net recharge estimated with SWAP and IDRAGRA at different groundwater table depths during 2010 season

Net Groundwater recharge (mm)		0.8m	1m	1.5m	2m	3m
1C	IDRAGRA	-87	-61	-10	18	42
	SWAP	156	203	265	316	420
5C	IDRAGRA	-70	-47	-4	25	42
	SWAP	24	67	129	158	197

Agricultural season 2011

Groundwater recharge from daily variation of a shallow water table

The deep percolation (Figure 6.28) in both sites is negligible in comparison to the capillary flux and in comparison to the 2010 season and this can be justified by the low amount of rain occurred and the absence of irrigation for this year. In PMI-1, the recharge is presenting from 30 to 36% of the total amount of precipitation. While in PMI-5, the deep percolation is absent according to SWAP model and this can be related to the saturated hydraulic conductivity which is very low for the deepest layer considered in SWAP model. On the other hand we can find that deep percolation steel exist according to IDRAGRA model which is slightly influenced by saturated hydraulic conductivity (see paragraph 6.5 IDRAGRA calibration). The estimated recharge is presenting just 16% of the total amount of precipitation. On the other hand the net recharge is negligible for both models.

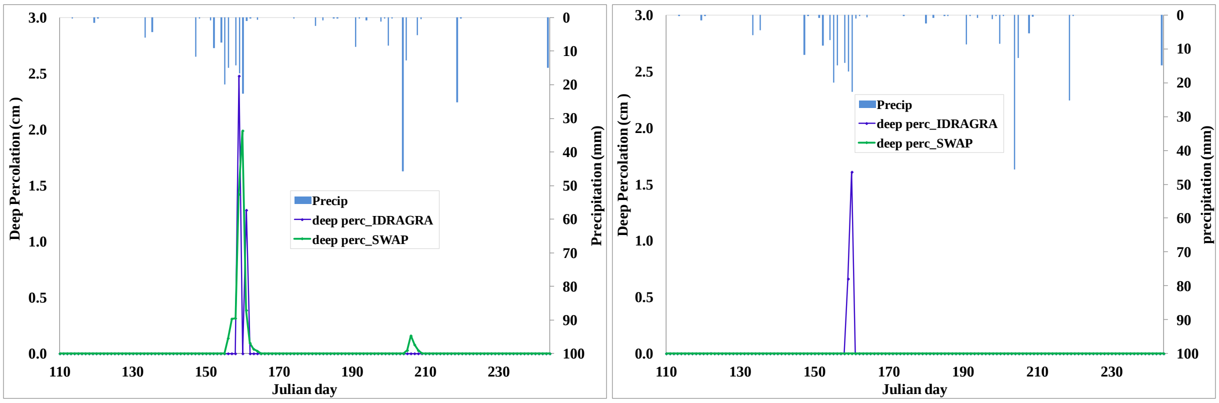

Figure 6.28 Deep percolation fluxes estimated with SWAP (green) and IDRAGRA (blue) calibrated models during 2011 season.

Groundwater recharge from fixed water table depth

Figure 6.26 and Figure 6.27 present the daily variation of deep percolation estimated by SWAP (green) and IDRAGRA (blue) in PMI-1 and PMI-5 respectively at different groundwater table depths (0.8m; 1m; 1.5m; 2m; 3m) during 2011 season.

For 2011 agricultural season the net recharge (Table 6.27) is lower in comparison to 2010 season and this is probably due to the lower amount of precipitation. In PMI-5, we can notice that for both models the net recharge is always negative which indicates the absence of recharge to the water table in that site due to the absence of the deep percolation previously explained.

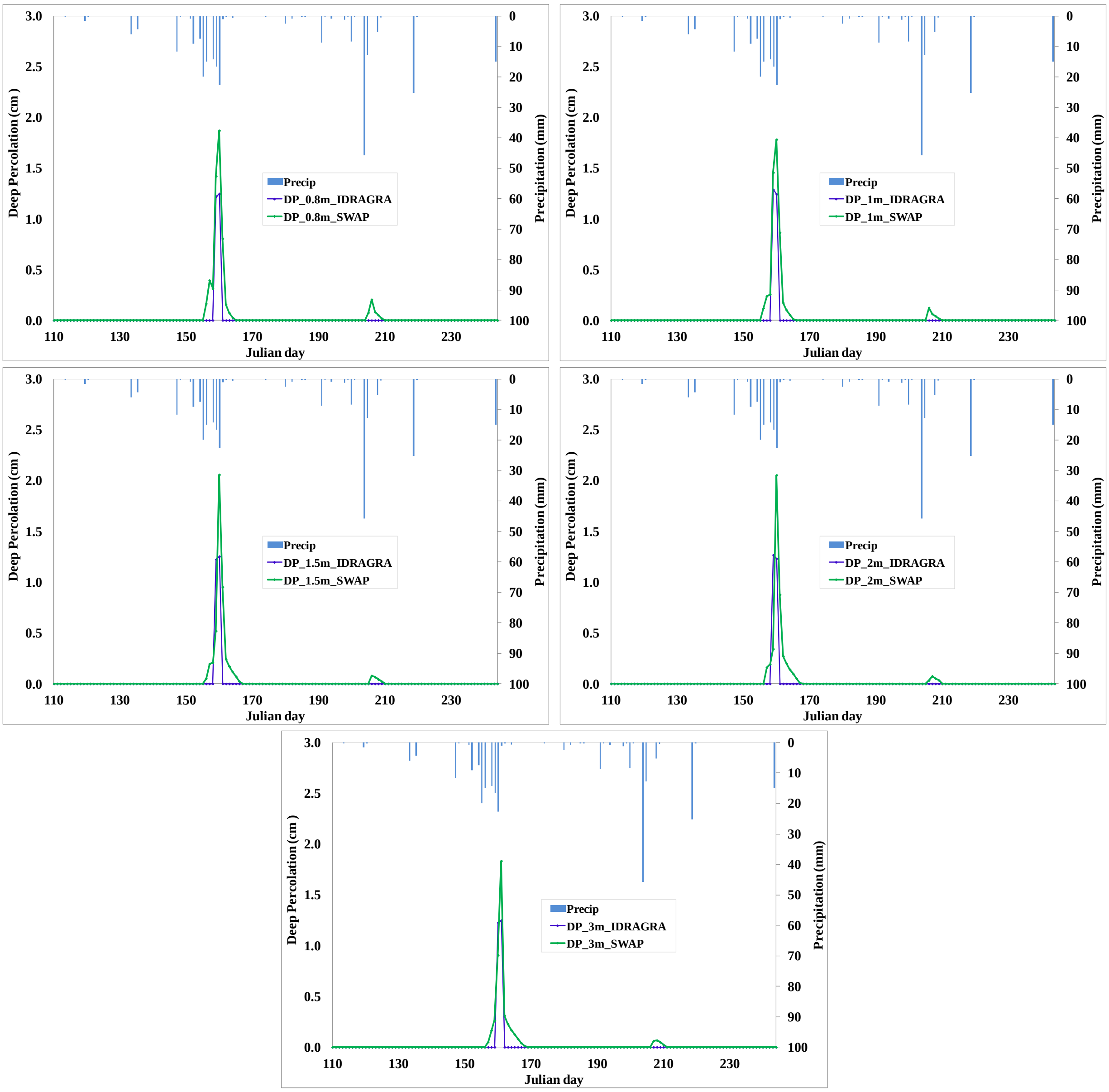

Figure 6.29 Estimated deep percolation by IDRAGRA (blue) and SWAP (green) in PMI-1 during 2011 season at different groundwater level (0.8m, 1m, 1.5m, 2m, 3m)

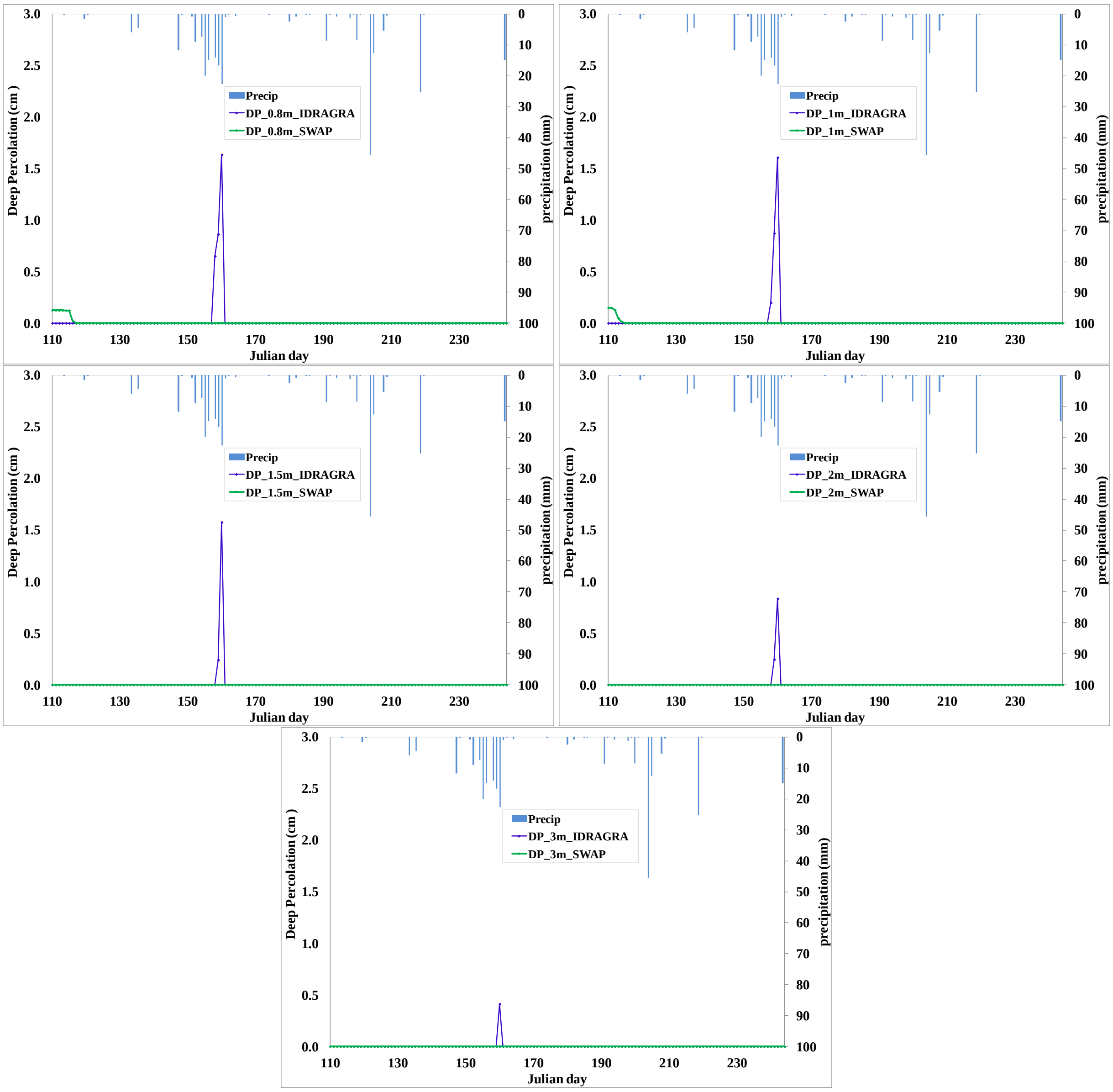

Figure 6.30 Estimated deep percolation by IDRAGRA (blue) and SWAP (green) in PMI-5 during 2011 season at different groundwater level (0.8m, 1m, 1.5m, 2m, 3m).

Table 6.27 Net recharge estimated with SWAP and IDRAGRA at different groundwater table depths during 2011 season

Net Groundwater recharge (mm)		0.8m	1m	1.5m	2m	3m
1C	IDRAGRA	-250	-219	-133	-75	-24
	SWAP	-181	-147	-99	-71	-42
5C	IDRAGRA	-243	-230	-162	-99	-40
	SWAP	-341	-354	-340	-310	-249

6.9 Conclusion

The chapter presents the results of the simulations carried out with SWAP and IDRAGRA models, implemented for the two agricultural years, 2010 and 2011, using observed data for the two PMI sites (1 and in the field, “Campo dei Sassi” (Landriano).

Firstly, the two models were run with the estimated soil hydraulic parameters from PTF-Rosetta and are compared in terms of actual evapotranspiration and soil water content in the evaporative and transpirative layers. The output of the two models are compared to the measured data collected during the monitoring activities.

Results of actual evapotranspiration on 2010 showed a reasonably good agreement between IDRAGRA simulations and Eddy measurements in the early stage and between SWAP and Eddy in the middle of the season. Actual ET measured with eddy covariance technique seems to be underestimated during 2010 season and that makes it difficult to clearly understand which model is performing better. Altought in general, both models over-estimate the actual ET.

IDRAGRA simulated with a satisfactory approximation the measured values of average soil water content in the evaporative and transpirative layers. While SWAP showed a poor prediction and overestimated the soil water content in both layers.
On 2011, IDRAGRA performed better than SWAP in simulating actual ET and soil water content.

Subsequently, the models were run using field retention parameters and calibrated on the basis of saturated hydraulic conductivity, which lack reliable measurements. The two models were compared to verify their performance. The following conclusions are found:
On 2010 season, both models showed an improvement in simulating actual evapotranspiration and soil water content in the root zone in comparison to previous simulations.
SWAP performed better than IDRAGRA in terms of actual ET.
The comparison between soil water content estimated by IDRAGRA and measured soil water content showed a good fitting at the end of the growing period particularly in the evaporative layer. While the model performed poorly at the beginning of the season.
Soil water contents from SWAP in different layers agree accurately with the measured values.
During the 2011 season and after calibration, both models performed similarly on terms of ET with clear improvement in comparison to previous simulations.

IDRAGRA model simulates reliable values of average soil water content, even if, compared with the measured data, a certain underestimation beginning of the season and overestimation end of the season are observed. While SWAP poorly estimated soil water content. So that it was concluded that IDRAGRA slightly performs better than SWAP in simulating soil water content in the root zone.

With both models, soil water content in the evaporative soil layer changes more considerably than the deeper soil layers throughout the simulation period. This is because the upper soil layers are much more greatly affected by the combined effects of the rainfall, ET and irrigation compared to the transpirative layer.
However, we must underline that soil water content was overestimated using the two sets of retention curves in both sites and during the two agricultural years with SWAP. While IDRAGRA tends to underestimate the soil water content.

Finally the two tested models (SWAP and IDRAGRA) were applied to assess capillary rise contribution to satisfy maize water requirement and groundwater recharge from a shallow water table.

At the beginning the two models were run using the daily variation of groundwater table and it was found that during 2010 season, capillary rise was similar for both models in PMI-1 and is contributing by 41% (IDRAGRA) and 46% (SWAP) of the total maize water requirement. In PMI-5 the contribution of the groundwater estimated by SWAP is slightly similar to that in PMI-1 and is about 43%. IDRAGRA estimates lower contribution in this site which is just 27% of the total maize water requirement. The deep percolation estimated by SWAP is much higher than the one estimated by IDRAGRA in both sites due to lower estimation of actual transpiration.

During 2011 season, the estimated capillary flux with SWAP model was higher than that with IDRAGRA particularly on PMI-5. The capillary rise was able to contribute more than 50% of the total maize requirement for both models. On the other side, both models showed a negligible deep percolation in comparison to the capillary flux and in comparison to the 2010 season.

Later, groundwater table depths were fixed virtually at 0.8m, 1m, 1.5m, 2m, 3m. The aim of considering fixed groundwater table depths was to unveil at which depth the groundwater table contribute majorly to satisfy the crop water requirement and how much we can have groundwater recharge.

One major finding was that the capillary rise from groundwater decreases with the increase of the groundwater table depth. A higher contribution is observed when the water table is higher or equal to 1m. When the water table depth reached 2m the capillary was steel contributing to maize water requirement for both models and during the two agricultural seasons. A power function was found between capillary rise and groundwater table depth, and this function has a high correlation coefficient for both models.

As far as the groundwater recharge is concerned, we found that net recharge tended to increase as the groundwater table depth increased. For both models the net recharge was lower than the total downward flow to the groundwater table. According to IDRAGRA simulation and for both seasons, there was not a real recharge to the water table for a groundwater table depth lower than 2m. While for SWAP model, the net recharge exist even under shallower water table and that can be attributed to the higher deep percolation estimated with the same model.

During 2011 season, the recharge was negligible due to the lowest amount of rain that occurred during the same period.

7 General Conclusions

Understanding the interaction between soil, vegetation, atmosphere processes and groundwater dynamics is of paramount importance in water resources planning and management in many practical applications. Hydrological models of complex water resource systems need to include a number of components and should therefore seek a balance between capturing all relevant processes and maintaining data requirement and computing time at an affordable level. Water transfer through the unsaturated zone is a key hydrological process connecting atmosphere, surface water and groundwater (Gandolfi et al., 2006).

In the last two decades, physically based agro-hydrological models have been developed to simulate mass and energy exchange processes in the Soil-Plant-Atmosphere (SPA) system (Feddes et al., 1978; Bastiaanssen et al., 2007). In particular, deterministic models have been proposed to simulate all the components of the water balance, including actual crop evapotranspiration, water and solute transport (van Dam et al., 1997; Ragab., 2002). Unfortunately, the physically based agro-hydrological models, although very reliable, cannot often be used because of the high number of required variables and the complex computational analysis. Therefore, the use of simplified agro-hydrological models may represent a useful and simple tool.

For this thesis, a physically based approach model using numerical solutions of Richards' equations (Soil Water Atmosphere Plant; SWAP) that was developed at the University of Waginengen (Kroes and Van Dam, 2003 and a conceptual model, based on reservoir cascade schemes, IDRAGRA (Idraulica Agraria), developed in the engineering department of the University of Milan (Gandolfi et al., 2011) have been selected.

During the agricultural season 2010 and 2011, intensive monitoring work was carried out in a maize field located in the experimental farm "A. Menozzi" (Landriano-Pavia) of the Agricultural Faculty of the University of Milan. Monitoring activities were involved in a wider project AC-CA (Aqua-Carbonio) founded by Lombardy region. Field activities were carried out in collaboration with the Department of Environmental, Hydraulic, Infrastructures and Surveying Engineering of the Polytechnic of Milan and within Plant Production and Agricultural chemistry Department of the University of Milan. The monitoring activities were divided into: (a) continuous measurements of water and energy fluxes between the ground and the lower atmosphere that were made through a modern micrometeorological station, Eddy covariance (EC, located in the center of the field), completed with TDR probes and tensiometers placed at various depths in the soil. (b) periodic and distributed measurements across the field and during the entire cultural development, of soil moisture, groundwater level, soil matric potential, biometric data etc.

Field activities were indispensable for the monitoring of water balance components in a field scale (soil humidity, evapotranspiration, soil water potential, groundwater table depth etc.). During the experimental course, some technical difficulties were encountered concerning maintenance of equipment, particularly, concerning eddy covariance station. The used instruments were generally solid and reliable with some exception also reported by other authors like some problems concerning tensiometers which emptied quickly during the summer period and had to be checked frequently to avoid unreliable reading.

Application of simulation models to predict transport of water in unsaturated soils is often limited by the lack of representative data for soil hydraulic properties. There is a relative abundance of literature dealing with the theory and application of soil hydraulic properties, but there are very few studies that give detailed description of soil hydraulic properties on Northern Italy (Calzolari et al., 2001; Baroni et al., 2010).

In the present thesis, the soil water retention characteristics were determined using the tensiometric box and pressure plate apparatus, using field data and pedotransfer functions (Rawls and Brakensiek or Rosetta PTFs).

In comparison to field data, laboratory measurements were the most accurate. They had the highest ranking for most of performance indices that were computed in this study.
The second best technique was the PTF Rosetta (Schaap et al. 2001). They perform only slightly poorer than the laboratory measurements. PTF-RB, showed the weakest estimation of soil water content which is in contradiction to the previous founding by Baroni et al. (2010) and Calzolari et al.(2001).

We conclude that the Rosetta PTF developed by Schaap et al (2001) appears to be well suited to predict the soil moisture retention curve from easily available soil properties in the Lombardy area and further field investigations would be useful to reinforce this finding.

For detailed analysis and understanding of the different components on field scale, two models were first run with the estimated soil hydraulic parameters from PTF-Rosetta for the two agricultural seasons 2010 and 2011 in two sites (PMI-1 and PMI-5). The comparison focused on 2 output variables, i.e. actual evapotranspiration and soil water content in the evaporative and the transpirative layers.

A first observation is that both models overestimated actual evapotranspiration on 2010. The agreement was improved on 2011 season.

The reservoir model (IDRAGRA) simulated with a satisfactory approximation the measured values of average soil water content in the evaporative and transpirative layers on 2011 season. While on 2010 the model presented a considerable decrease of soil water content in the evaporative layer in comparison to SWAP estimation and field measured data. SWAP showed a poor prediction and overestimated the soil water content in both layers during two years
It was concluded that IDRAGRA performs better than SWAP with estimated soil retention parameters estimated from PTF-R.

In order to improve our results, IDRAGRA and SWAP were run introducing presented field retention curves and were calibrated to the saturated hydraulic conductivity which data were not available. As expected, the improvement was seen for both models.

SWAP showed better performance in estimating all the parameters in the two sites and during the two agricultural years. Similarly, IDRAGRA showed good fitting for all parameters. Although, IDRAGRA performed slightly better on 2011 season.

SWAP model, implementing the Richards equation, considers the unsaturated and saturated zone of the profile as a continuous unique-system where the water moves under the effect of potential gradient. However, we must underline that soil water content was overestimated using the two sets of retention curves. Further investigations in this direction seems necessary.

Tested SWAP and IDRAGRA models were used to generate the capillary rise and deep percolation fluxes through the bottom boundary of the root zone which are considered to be a very important from the viewpoint of water conservation, but very difficult and uncertain components to estimate in groundwater budget.

When considering the daily variation of the groundwater table, groundwater contribution was able to meet from 47 to 61% for IDRAGRA and from 40 to 65% for SWAP of total maize water requirement.

The deep percolation estimated by SWAP was much higher than the one estimated by IDRAGRA. Accordingly the net recharge to the water table was considerable with SWAP simulations and was between 60 and 170mm during 2010 season. While for IDRAGRA model the deep percolation was always lower than the capillary rise which lead to a negligible net recharge .

During 2011 season, both models showed a negligible deep percolation in both sites in comparison to the capillary flux and in comparison to the 2010 season.

Subsequently the two models were run with the purpose of virtually fixing the groundwater table depth for the sake of understand at which depth capillary rise can mainly contribute to satisfy maize water requirement and at which depth we start to have major net recharge to the water table.

For both models, it was observed a higher contribution under a water table depth lower than 1m. Water table as deep as 2m are still likely to have a positive impact on maize water balance and are able to contribute up to 20% of the maize water requirement**.**

During 2010 season, the net recharge to the water table was considerable from SWAP simulation. While it was negligible from those of IDRAGRA due to lower deep percolation in comparison to capillary rise fluxes.

During 2011 season, the total amount of precipitation received was lower than that occurred during 2010. Accordingly the net recharge was negligible from both models.

Taking all these results together we conclude that a simpler model like IDRAGRA can provide comparable performances to a more complex model, like SWAP, and could therefore be a good tool for estimating water balance components for practical applications, especially for irrigation management.

Bibliographic references

Ahmad, A., Bastiaanssen, W.G.M., Feddes, R.A., 2002. Sustainable use of groundwater for irrigation: a numerical analysis of the subsoil water fluxes. Irrig. Drain. 51 (3), 227–241.

Aina, P.O., Periaswamy, S.P., 1985. Estimating available water-holding capacity of western Nigerian soils from soil texture and bulk density, usng core and sieved samples. Soil. Sci.140, 55-58.

Ali, M.H., Biswas, T.D., 1968. Soil water retention and release as related to mineralogy of soil clays. Proc. 55th Indian Sci. Congr. 3,633. In Rawls, W.J., Pachepsky, Y., Shen, M.H., 2001. Testing soil water retention estimation with MUUF pedotransfer model using data from the southern united states. Journal of hydrology 251, 177-185.

Antinoro, C., Bagarello, V., Castellini, M., Giangrosso, A., Lovino, M., Sgroi, A., 2008. Predicting the soil water retention characteristic of Sicilian soils by pedotransfert functions. Options Mediterranéenne , A n° 84, Irrigation in Mediterranean Agriculture: Chalenges and innovation for the next decades.

Anuraga, T.S., Ruiz, L., Mohan Kumar, M.S., Sekhar, M., Leijnse, A., 2006. Estimating groundwater recharge using land use and soil data: a case study in South India. Agric. Water Manage. 84, 65–76 .

Ayar,s J.E., Schoneman, R.A., 1986. Use of saline water from a shallow water table by cotton. Trans ASAE 29:1674–1678 .

Ayars , J. E., Christen, E. W., Soppe, R., W., Meyer, W. S., 2006. The resource potential of in situ shallow ground water use in irrigated agriculture: a review.Irrigation scince ,24,147-160.

Ayars JE (1999) Integrated management of irrigation and drainage systems. In: Goosen MFA, Shayya WH (eds) Water management, purification and conservation in arid climates. Technomic, Lancaster. 1, 139–164.

Ayars, JE., Hutmacher, RB., Schoneman, RA., Vail, SS., Pflaum, T., 1993. Long term use of saline water for irrigation. Irrigation Sci 14, 27–34.

Ayars, J.E., 1996. Managing irrigation and drainage systems in arid areas in the presence of shallow groundwater:case studies. Irrigation Drainage Syst. 10, 227–244.

Ayars, J.E., 2003. Pre-plant irrigation. Encyclopedia of water science. In: Stewart BA, Howell TA (eds) Marcel Dekker, Inc.70 Madison Avenue, New York. On-line publication,. 498–501.

Ayars, J.E., Christen, E.W., Soppe, R.W., Mayers, W.S., 2006. The resource potential of in situ shallow ground water use in irrigated agriculture: a review. Irrig. Sci. 24 (3), 147–160.

Ayars, J.E., Shouse, P., Lesch, S.M., 2009. In situ use of groundwater by alfalfa. Agric. Water Manage. 96, 1579–1586.

Azooz, R.H., Arshad, M.A., Franzluebbers, A.J., 1996. Pore size distribution and hydraulic conductivity affected by tillage in northwestern Canada. Soil Sci. Soc. Am. J. 60, 1197- 1201.

Babajimopoulos, C., Panoras, A., Georgoussis, H., Arampatzis, G., Hatzigiannakis, E., Papamichail., D., 2007. Contribution to irrigation from shallow water table under field conditions. agricultural water management.92, 205-210.

Baldocchi, D.D., Vogel, C.A., 1996. Energy and CO2 flux densities above and below a temperate broad-leaved forest and a boreal pine forest. Tree Physiology 16, 5–16.

Bandyopadhyay, P.K., Mallick, S., 2003. Actual evapotranspiration and crop coefficients of wheat (Triticum aestivum) under varying moisture levels of humid tropical canal command area. Agr Water Manage. 59, 33-47.

Baroni, G., Facchi, A., Gandolfi, C., Ortuani, B., Horeschi, D., Van Dam, J.C., 2010. Uncertainty in the determination of soil hydraulic parameters and its influence on the performance of two hydrological models of different complexity. Hydrol Earth Syst Sci 14:251–270.

Bastiaanssen, W.G.M., Singh, R., Kumar, S., Schakel, J.K. & Jhorar, R.K. 1996. Analysis and Recommendations for Integrated On-Farm Water Management in Haryana, India: a Model Approach. Wageningen (The Netherlands), DLO Winand Staring Centre, Report. 118, 152.

Baumer, O.W., Brasher, B.R., 1982. Prediction of water content at selected suctions. Am. Soc. Agr. Eng. Paper 82-2590. In: Gijsman, A.J., Jagtap, S.S., Jones, J.W.,2003. Wading through aswamp of complete confusion: how to choose a method for estimating soil water retention parameters for crop models. Europ. J. Agronomy 18 ,77-106.

Beekman, H.E., Gieske, A., Selaolo, E.T., 1996. GRES: groundwater recharge studies in Botswana 1987–1996. Botsw J Earth Sci . 3, 1–17.

Beekman, H.E., Gieske, A., Selaolo, E.T., 1996. GRES: groundwater recharge studies in Botswana 1987–1996. Botsw J Earth Sci. III, :1–17.

Bekesi, G.,. McConchie, J., 1999. Groundwater recharge modelling using the Monte Carlo technique, Manawatu region, New Zealand. Journal of Hydrology, 224 , 137–148

Belmans, C., Wesseling, J.C., Feddes, R.A., 1983. Simulation of the water balance of a cropped soil: SWATRE. J. Hydrol. 63, 271–286.

Beltrao, J., Da Silva, A. A., Ben Asher, J., 1996. Modeling the effect of capillary water rise in corn yield in Portugal. Irrigation and Drainage Systems. 10, 179-189.

Bennie, A.T.P., Hoffman, J.E., Coetzee, M.J., Vrey, H.S., 1994. Storage and utilization of rain water in soils for stabilizing crop production in semi-arid areas [Afr]. Report No 227/1/94, Water Research Commission, Pretoria, pp. 31–110.

Benz, L.C., Doering, E.J., Reichman, G.A., 1981. Watertable management saves water and energy. Trans ASAE. 24, 995–1001.

Benz, L.C., Reichman, G.A., Doering, E.J., Follett, R.F., 1978. Watertable depth and irrigation effects on applied-water-use efficiencies of three crops. Trans ASAE. 21, 723–728.

Berendrecht, W., 2004. State space modeling of groundwater fluctuation. PhD Thesis, Delft university, 149.

Bethune, M. G., Selle, B., Wang Bethune, Q. J., 2008. Understanding and predicting deep percolation under surface irrigation. Water resources research, 44.

Bethune, M.G., Batey, T.J., 2002. Impact on soil hydraulic properties resulting from irrigating saline-sodic soils with low salinity water. Aust. J. Exp. Ag. 42, 273–279.

Bittelli, M., 2010. Measuring Soil Water Potential for Water Management in Agriculture: A Review. Sustainability, 2, 1226-1251.

Bloemen, G.W., 1980. Calculation of hydraulic conductivities from texture and organic matter content. Zeitschrift fur Pflanzenerna¨hrung und Bodenkunde 143, 581– 605.In: McBratney, A. B.

Minasny, B., Stephen, R.., Cattle, R.., Vervoort, W., 2002. From pedotransfer functions to soil inference systems.

Boesten, J.J.T.I., Van Der Linden, A.M.A., 1991. Modeling the influence of sorption and transformation on pesticide leaching and persistence. J. Environ. Qual. 20, 425-435.

Bohne, K., Roth, C., Leij, F.J., Van Genuchten, M.Th., 1993 Rapid method for estimating the unsaturated hydraulic conductivity from infiltration measurements. Soil Science. 155, 237–244.

Bork, H.R., Diekrugger, B., 1990. Scale and regionalization problems in soil science. Trans. 14 Int. Congr. Soil. Sci. 1:178–181.

Bouma J., Belmans, C., Dekker, L.W., Jeurissen, W.J.M., 1983. Assessing the suitability of soils with macro-pores for subsurface liquid waste disposal. Journal of Environmental Quality. 12, 305–311.

Bouma, J., 1989. Using soil survey data for quantitative land evaluation. Advances Soil Sci. 9, 177-213.

Bouma, J., Dekkerl, W., 1984. Soil physical investigations for land evaluation. In Progress in Land Evaluation (eds J. C . F. M. Haans er al.), pp.209-224. A. A. Balkema, Rotterdam.

Brisson, N., Rebisre, B., Zimmer, D., Renault, P., 2002. Response of the root system of a winter wheat crop to waterlogging. Plant Soil. 243, 43-55.

Brooks, R.H., Corey, A.T., 1964. Hydraulic Properties of Porous Media. Hydrology Paper Vol. 3, Colorado State University: Fort Collins, pp. 1–27.

Bruand, A., Duval, O., Gaillard, H., Darthout, R., Jamagne, M., 1996. Variabilité des propriétés de rétention en eau des sols: importance de la densité apparente. Etude et Gestion des Sols, 3, 1, 27-40.

Buckman, H. O., Brady, N. C., 1979. Natureza e propriedade dos solos. Rio de Janeiro: Biblioteca Universitária Freitas Bastos,. 5. Ed, 647 p.

Calzolari, C., Ungaro, F., Busono, E., Salvador Sanchiz P.S., 2001. Metodi indiretti per la stima delle proprietà fisico idrologiche dei suoli. Validazione di pedo-funzioni da letteratura. Progetto SINA- Carta pedologico in aree a rischio ambientale. Convezione:” Studio del comportamento fisico-idrologico degli strati superficiali del suolo”. Rapporto n.9.1.

Campbell, G.S., 1985.Soil Physics with Basic, 1st ed., Elsevier: Amsterdam, The Netherlands.

Campbell, G.S., Norman, J.H., 1998. An Introduction to Environmental Biophysics, 2nd ed., Springer-Verlag: New York, NY, USA.

Ceulemans, R., Kowalski, A.S., Berbigier, P., Dolman, H., Elbers, J., Grelle, A., Janssens, I.A., Lindroth, A., Moors, E., Rannik, U., Vesala, T., 2002. Carbon and water fluxes of pine (Pinus) forests: their balances, ecological and ecophysiological Determinants, In: Valentini, R., (Ed.), Ecological Studies: Fluxes of Carbon, Water and Energy of European Forests, Springer, Berlin.

Chahal, R.S., Yong, R.N., 1965. Validity of the soil water characteristics determined with the pressurized apparatus. Soil Sci. 99:98–103. In: Tuller. M., Or, D., 2003. Retention of water in soil and the soil water characteristic curve.

Chimungu, J.G., 2009. Comparison of field and laboratory measured hydraulic properties of selected diagnostic soil horizons. Department of Soil, Crop and Climate SciencesFaculty of Natural and Agricultural Sciences,University of the Free State,Bloemfontein, South Africa.

Clarke, CJ., George, RG., Bell, RW., Hatton, TJ., 2002. Dryland salinity in southwestern Australia: its origins, remedies, and future research directions .Australian Journal Soil Res,1, 40.

Cornelis, W.M., Ronsyn, J., Van Meirvenne, M., Hartmann, R., 2001. Evaluation of pedotransfer functions for predicting the soil moisture retention curve. Soil Science Society of America Journal 65, 638– 648.

Cresswel, H.P., Paydar, Z., 1996. Water retention in Australian soils. I. Description and prediction using parametric functions. Australian Journal of Soil Research, 34(2) 195-212.

D'Urso, G., 2001. Simulation and management of on-demand irrigation systems: a combined agrohydrological and remote sensing approach. PhD dissertation, Wageningen University.

Dardanelli, J., Collino, D.J., 2002. Water table contribution to alfalfa water use in different environments of the Argentine Pampas. Agriscientia . XIX, 11-18

De Jong. R., 1983. Soil water desorption curves estimated from limited data. Soil Sci. 63:697-703.

De Laat, P.J.M., 1995. Design and operation of a subsurface irrigation scheme with MUST. In: Pereira, L.S., van den Broek, B.J., Kabat, P., Allen, R.G. (Eds.), Crop-Water- Simulation Models in Practice. Wageningen Pers, Wageningen, pp. 123–140. Jorenush and Sepaskhah., 2003

Delleur, J.W., 1998. The groundwater engineering (2nd ed.). CRC Press.

Dirksen C., 1999b. Direct conductivity measurements for evaluating approximate and indirect determinations. In Proceedings of the International Workshop on Characterization and Measurement of the Hydraulic Properties of Unsaturated Porous Media, van Genuchten M.Th., et al. (Eds.), University of California, Riverside, 271–278.

Doering E.J., Benz, L.C., Reichman, G.A., 1982. Shallow-water-table concept for drainage design in semiarid and subhumid regions. In: American Society of Agricultural Engineers (eds) Advances in drainage, proceedings of the fourth national drainage symposium. American Society of Agricultural Engineers, 12–82, 34–41 .

Dolph, J., Marks, D., King, G.A., 1992. Sensitivity of the regional water balance in the Columbia River Basin to climate variability. application of a spatially distributed water balance model. In: Naiman, R. J. (ed.) Watershed management: balancing sustainability and environmental change. Springer-Verlag, New York, 233-265

Donatelli, M., Wosten, J.H.M., Belocchi, M., 2004. Methods to evaluate pedotransfer functions. In: Antinoro, C., Bagarello, V., Castellini, M., Giangrosso, A., Lovino, M., Sgroi, A., 2008. Predicting the soil water retention characteristic of Sicilian soils by pedotransfert functions. Options Mediterranéenne , A n° 84, Irrigation in Mediterranean Agriculture: Chalenges and innovation for the next decades.

Droogers, P., Torabi, M., Akbari, M., Pazira, E., 2001. Field-scale modeling to explore salinity problems in irrigated agriculture. Irrigation and Drainage. 50, 77–90.

Durner, W., Fluhler, H., 2005. Soil hydraulic properties, Encyclopaedia of Hydrological Sciences, this issue, John Wiley & Sons.

El Kadi, A.I., 1985b. On estimating the hydraulic properties of soil, 2. A new empirical equation for estimating hydraulic conductivity for sands. Adv. Water resources. 8, 148-153.

Elsenbeer, H., 2001. Hydrologic flowpaths in tropical rainforest soilscapes—a review. Hydrological Processes15(10), 1751-1759.

Fare, A., Alva, A., Nkedi-Kizza, P., Elrashidi, M., 2000. Estimation of soil hydraulic properties of a sandy soil using capacitance probes and guelph permeameter. Soil Sci. 165, 768-777.

Feddes, R. A., Kowalik, P. J., Zaradny, H., 1978. Simulation of Field Water Use and Crop Yield, 189 pp., PUDOC, Wageningen, Netherlands.

Feddes, R.A., Kaba,t P., Van Bakel, P.J.T., Bronswijk, J.J.B., Halbertsma, J., 1988. Modelling soil and water dynamics in the unsaturated zone–state of the art. Journal of Hydrology. 100, 69–111.

Field, J.A., J.C. Parker, and N.L. Powell. 1985. Comparison of field- and laboratory measured and predicted hydraulic properties of soil with macropores. Soil Sci. 138:385–396.

Follett, R.F., Doering, E.J., Reichman, G.A., Benz, L.C., 1974. Effect of irriation and water table depth on crop yield. Agron Journal. 66, 304– 308.

Gee, G.W., Ward, A., 1999. Innovations in two-phase measurements of hydraulic properties. In Proceedings of the International Workshop on Characterization and Measurement of the Hydraulic Properties of Unsaturated Porous Media, van Genuchten M.Th., et al. (Eds.), University of California, Riverside. 241–270.

Gehrels, JC., 1999. Groundwater level fluctuations. Separation of natural from anthropogenic influences and determination of groundwater recharge in the Veluwe area, The Netherlands. PhD Thesis, Vrije Universiteit, Amsterdam, 269 .

Ghezzehei, T.A., Or, D., 2003. Stress-induced volume reduction of isolated pores in wet soil. Water Resources Research, 39(3), 1067, doi:10.1029/2001WR001137.

Gowing, J.W., Rose, D.A., Ghamarnia, H., 2009. The effect of salinity on water productivity of wheat under deficit irrigation above shallow groundwater. Agr Water Manage. 96, 517-524.

Grismer, M.E., Gates, T.K., 1988. Estimating saline water table contributions to crop water use. Calif Agric. 42(2), 23–24 .

Gupta, R., Yadav, R.L., 1993. Ground water contribution to evapo-transpiration of sugarcane during summer. Cooperative Sugar. 25, 113–115.

Gutowski, W. J., Vorosmarty, Jr.C. J., Person, M., Otles, Z., Fekete, B., York, J., 2002. A coupled land–atmosphere simulation program (CLASP): Calibration and validation. J. Geophys. Res., 107, 4283, doi:10.1029/2001JD000392.

Hendrickx, J.M.H., Nieber, J.L., Siccama, P.D., 1994. Effect of tensiometer cup size on field soil water tension variability, Soil Sci. Soc. Am. J., *58*, 309–315.

Hendrickx, JMH., Walker, GR., 1997. Recharge from precipitation. In: Simmers I (ed) Recharge of phreatic aquifers in (semi-)arid areas. IAH Int Contrib Hydrogeol 19. AA Balkema, Rotterdam, 19–111.

Hillel, D., 1998. Environmental Soil Physics. Academic Press, San Diego, CA.

Homaee, M., 1999. Root water uptake under non-uniform transient salinity and water stress. PhD thesis, Wageningen University, The Netherlands, 173 p.

Homaee, M., Feddes, R.A., Dirksen, C., 2002. Simulation of root water uptake II. Non-uniform transient water stress usingdifferent reduction functions. Agricultural water management. 57, 111-126.

Hopmans, J.W., Schoups, G.H., 2004 Soil water flow at different scales, Encyclopedia of Hydrological Sciences, This issue, John Wiley & Sons.

Hunsigi, G., Srivastava, S.C., 1977. Modulation of ET (evapotranspiration) values of sugar cane because of high water table. In: Proceedings of the 16th ISSCT Congress. 1557–1564.

Hurst, C.A., Thornburn, P.J., Lockington, D., Bristow, K.L., 2004. Sugarcane water use from shallow water tables: implications for improving irrigation water use efficiency. Agric. Water Manage. 65, 1–19.

Hutmacher, R.B., Ayars, J.E., Vail, S.S., Bravo, A.D., Dettinger, D., Schoneman, R.A., 1996. Uptake of shallow groundwater by cotton: growth stage, groundwater salinity effects in column lysimeters. Agric.Water Manage. 31, 205–223.

International Organization for standardization (ISO), 2009. Determination of the soil water retention characteristics. Version 1.3, FUTMON-soil moisture workshop, International Organization for Standardization, Geneva, 1-12. http:// www.iso.ch (accessed 23/07/2009).

Jaber, F.H., Shukla, S., Srivastava, S., 2006. Recharge, upflux and water table response for shallow water table conditions in southwest Florida. Hydrological Processes ,20, 1895–1907.

Jaynes, D.B., Tyler, E.J., 1984. Using soil physical properties to estimate hydraulic conductivity. Soil Sci. 138, 298-305.

Ji, X.B., Kang, E.S., Chen, R.S., Zhao, W.Z., Zhang, Z.H., Jin, B.W., 2007. A mathematical model for simulating water balances in cropped sandy soil with conventional flood irrigation applied. Agric. Water Manage. 87, 337–346.

Jiménez-Martínez, J., Skaggs, T.H., Van Genuchten, M.Th., Candela, L., 2009. A root zone modelling approach to estimating groundwater recharge from irrigated areas. J Hydrol 367, 138–149 .

Jury, W.A., Gardner, W.R., Gardner. W.H., 1991. Soil physics. 5th ed. John Wiley & Sons, New York.

Jyrkama, M.I., Sykes, J.F ., 2007. The climate change on spatialy groundwater recharge in the grand river watershed (Ontrrio). J Hydrol 3-4,338, 237-250 .

Kabat, P., Van Den Broek, B.J., Feddes, R.A., 1992. SWACROP: a water management and crop production simulation model. ICID Bull. 41 (2), 61–84.

Kahlown, M.A., Ashraf, M., Zia–ul–Haq, 2005. Effect of shallow groundwater table on crop water requirements and crop yields. Agric. Water Manage. 76 (1), 24–35.

Keese, K.E., Scanlon, B.R., Reedy, R.C., 2005. Assessing controls on diffuse groundwater recharge using unsaturated flow modeling. Water resources research.41.

Kern, J.S. 1995. Evaluation of soil water retention models based on basic soil physical properties. Soil Sci. Soc. Am. J. 59:1134–1141.

Klute, A., Dirksen, C., 1986. "Hydraulic Conductivity and Diffusivity: Laboratory Methods." In: Klute, A., (ed), Methods of Soil Analysis, Part 1, Physical and Mineralogical Methods (2nd ed.), American Society of Agronomy, Chapter 28, pp. 687-700.

Kool, J., Parker, J., 1987. Development and evaluation of closedform expressions for hysteretic soil hydraulic properties. Water Resour. Res. 23, 105–114.

Kosugi, K., 1999. Lognormal distribution model for soil hydraulic properties, In Proceedings of the International Workshop on Characterization and Measurement of the Hydraulic Properties of Unsaturated Porous Media, van Genuchten M.Th., Leij F. and 19–30.

Kozeny, J., 1927. U¨ber kapillare Leitung des Wassers im Boden (Aufstieg, Versickerung und Anwendung auf die Bew¨asserung). Sitzungsbericht der Akademie der Wissenschaften zu Wien, 136, 271–306.

Kroes, J.G., Van Dam, J.C., 2003. Reference manual SWAP version 3.03, Alterra Green World Research, Alterra Report 773, Wageningen University and Research Centre, Wageningen, The Netherlands. ISSN: 1566-7197.

Kruse, E.G., Champion , D.F., Cuevas, D.L., Yoder, R.L., Young, D., 1993. Crop water use from shallow, saline water tables. Trans ASAE. 36, 696–707.

Kruse, E.G., Young, D.A., Champion, D.F., 1985. Effects of saline water table on corn irrigation. In: Keyes CG, Ward TJ (eds) Development and management aspects of irrigation and drainage systems [Proceedings of Specialty Conference ed.]. ASCE, New York. 444–453.

Kutílek, M., 2004. Soil hydraulic properties as related to soil structure. Soil and Tillage Research In Soil Physical Quality, Vol. 79, No. 2. pp. 175-184.

Fiedler, L.R., Dunn, G.H., Benjamin, J.G., Garrison, A., 1998. Changes in soil water retention curves due to tillage and natural reconsolidation. Soil Science Society of America Journal. 62, 1228–1233.

Larsen, F., Owen, R., Dahlin, T., Mangeya, P., 2002. A preliminary analysis of the groundwater recharge to the Karoo formations, mid-Zambezi basin, Zimbabwe. Phys Chem Earth. 27, 765–772 .

Lebron, I., Robinson, D.A., 2003. Particle size segregation during hand packing of coarse granular materials and impacts on local pore-scale structure. Vadose Zone Journal, 2, 330–337.

Leij, F.J., Ghezzehei, T.A., Or, D., 2002. Analytical models for soil pore-size distribution after tillage. Soil Science Society of America Journal. 66, 1104–1114.

Lerner, D.N., Issar, A., Simmers, I., 1990. Groundwater recharge—A guide to understanding and estimating natural recharge: International Contributions to Hydrogeology, 8, 147.

Liu, T., Luo, Y., 2011. Effects of shallow water tables on the water use and yield of winter wheat (*Triticum aestivum* L.) under rain-fed condition. Australian journal of Crop Science. 5(13), 1692-1697.

Lorentz, S., Goba, P., Preterious, J., 2001. Hydrological process research: Experiments and measurements of soil hydraulic characteristics. Water Research Commission (WRC) Report No 744/1/01, Pretoria.

Lu, X., Jin, M., Van Genuchten, M.Th., Wang, B., 2009. Groundwater Recharge at Five Representative Sites in the Hebei Plain, China. Ground Water (2), 49, 286-294.

Maas, E.V., Hoffman, G.J., 1977. Crop salt tolerance current assessment. J. Irrig. Drain. Div. 103, 115–134.

Maclean, A.H., Yager, T.U., 1972. Available water capacities of Zambian soils in relation to pressure plate measurements and particle size analysis. Soil SCi.113, 23-29.

Mapa R.B., Green R.E. and Santo L. (1986) Temporal variability of soil hydraulic properties with wetting and drying subsequent to tillage. Soil Science Society of America Journal, 50, 1133–1138.

Marion, G. M. 1996. Temperature enhancement experiments. Pages 14–19 *in* U. Molau and P. Mølgaard, editors. The ITEX Manual. Danish Polar Center, Copenhagen, Denmark.

Marion, G. M., Henry, G.H. R., Mølgaard, P., Oechel, W.C., Jones, M.H., Vourlitis, G.L., 1993. Open-top devices for manipulating field temperatures in tundra ecosystems. Pages 205–210 *in* Lunardini, V.J., Bowen, S.L.,(editors). Proceedings of the Fourth International Symposium on Thermal Engineering and Science for Cold Regions. CRREL Special Report 93-22, U.S. Army Cold Regions Research and Engineering Laboratory, Hanover, New Hampshire, USA.

Marion, J., OR, Rolston, D., Kavvas, D., Biggar, J.M., 1994. Evaluation of methods for determining soil-water retentivity and unsaturated hydraulic conductivity. Soil Sci. 158, 1-13.

Meiresonne, L., Sampson, D.A., Kowalski, A.SJanssens, I.A., Nadezhdina, N., Cerma, J., Van Slycken, J., Ceulemans, R., 2003. Water flux estimates from a Belgian Scots pine stand: a comparison of different approaches. Journal of hydrology.270, 230-252.

Merdun, H., 2006. Pedotransfer functions for point and parametric estimations of soil water retention curve. Plant soil envi., 52,(7): 321‑327.

Mileham, L., Taylor, R., Thompson, J., Todd, M., Tindimugaya, C., 2007. Impact of rainfall distribution on the parameterisation of a soil-moisture balance model of groundwater recharge in equatorial Africa. Journal of Hydrology . 359, 46– 58.

Minasny, B., McBratney, A.B., Bristow, K.L., 1999. Comparison of different approaches to the development of pedotransfer functions for water-retention curves. Geoderma 99, 225–253.

Moon, S.K., Woo, N.C., Lee, K.S., 2004. Statistical analysis of hydrographs and water-table fluctuation to estimate groundwater recharge. Journal of Hydrology ,292 ,198–209.

Mualem, Y., 1976. A new model for predicting the hydraulic conductivity of unsaturated porous media. Water Resour. Res., 12, 513-522.

Munoz-Carpena, R., Regalado, C.M., Alvarez-Benedi, J., Bartoli, F., 2002. Field evaluation of the new philip-dunne permeameter for measuring saturated hydraulic conductivity. Soil Science. 167(1), 9–24.

Nemes, A., Schaap, M.G., Wosten, J.H.M., 2003. Functional Evaluation of Pedotransfer Functions Derived from Different Scales of Data Collection. Soil Science Society of America Journal. 67: 1093‑1102.

Nemes, A., Schaap, M.G., Wosten, J.H.M., 2003. Functional Evaluation of Pedotransfer Functions Derived from Different Scales of Data Collection. Soil Science Society of America Journal, 67: 1093‑1102.

Nielsen, D.R., Biggar, J.W., Erh, K.T., 1973. Spatial variability of field-measured soil-water properties. Hilgardia, 42, 215–259.

Nielsen, D.R., Van Genuchten, M.T., Biggar, J.W., 1986. Water flow and solute transport processes in the unsaturated zone. Water Resources Research, 22, 89–108.

Nosetto, M.D., Jobbagy, E.G., Jackson, R.B., Sznaider, G.A., 2009. Reciprocal influence of crops and shallow ground water in sandy landscapes of the inland pampas. Field Crop Res. 113, 138-148.

Obakeng, O.T., 2007. Soil moisture dynamics and evapotranspiration at the fringe of the Botswana Kalahari, with emphasis on deep rooting vegetation. PhD Thesis, Free University, the Netherlands.

Ochoa, C.G., Fernald, A.G., Guldan, S.J., Shukla, M.K., 2007. Deep percolation and its effects on shallow groundwater level rise following flood . American Society of Agricultural and Biological Engineers.50, 73-81.

Ochoa, C.G., 2011. Surface water and groundwater interactions in an agricultural valley of northern New Mexico Ph.D. dissertation. New Mexico State University, 196.

Or, D., Wraith, JM., 1999. Temperature effects on soil bulk dielectric permittivity measured by time domain reflectometry: a physical model. Water Resources Research 35(2): 371–383.

Pachepsky, Y.,*. Rawls, W.J., Gimenez, D., 2000a. Comparison of soil water retention at field and laboratory scales. Soil Sci. Soc. Am. J. 65, 460–462

Packepsky, Ra.A., Rawls, W.J., Gimenez, D., Watt, J.P.C., 1998. Use of soil penetration resistance and group methods of data handling to improve soil water estimates. Soil Tillage Res. 49, 117-126.

Parkes, M.E., and P.A. Waters. 1980. Comparison of measured and fested estimated unsaturated hydraulic conductivity. Water Resour. Res. 16:749–754.

Portela, S.I., Andriulo, A..E., Jobba´gy, E.G., Sasal, M.C., 2009. Water and nitrate exchange between cultivated ecosystems and groundwater in the Rolling Pampas. Agriculture, Ecosystems and Environment 134, 277–286

Prasad, R., 1988. A linear root water uptake model. J. Hydrol. 99, 297–306.

Prathapar, S.A., Meyer, W.S., 1992. Measurement and estimation of capillary upflow from water tables under maize on irrigated soils. Aust. J. Soil Res. 31, 119–130.

Pratharpar, S.A., Qureshi, A.S., 1998. Modelling the effects of deficit irrigation on soil salinity, depth to water table and transpiration in semi-arid zones with monsoonal rains. Int J Water Resour. 15, 141-159.

Puckett, W.E., Dane, J.H., Hajek, B.F., 1985. Physical and mineralogical data to determine soil hydraulic properties. Soil Sci. Soc .Am J. 49, 831-836.

Raes, D., Deproost, P., 2003. Model to assess water movement from a shallow water table to the root zone. Agricultural Water Management. 62, 79–91.

Rajkai, R., Varallyay, G., 1992. Estimating soi retention from simpler properties by regression techniques. In: Van Genuchten, M.Th., Leij, F.J., Lund, L.J. (Eds). Methods for estimating the hydraulic properties of unsaturated soils. Proceeding of the international workshop on Indirect Methods for Estimating The Hydrulic Properties of Unsaturated Soils. Riverside , Californa, 11-13 October 1989, pp. 417-426.

Rathore, T.R., Warsi, M.Z.K., Lothrop, J.E., Singh, N.N., 1996. Production of maize under excess soil moisture (water logging) conditions. 1st Asian Regional maize Workshop, 10-12 Feb 1996, P.A.U., Ludhiana, pp. 56-53.

Rawls, W.J., Brakensiek, D.L., 1985. Prediction of soil water properties for hydrologic modeling. In: Jones E., Ward T.J. (eds): Watershed Management in the Eighties. Proc. Symposium of Irrigation and Drainage Division ASCE, April 30‑May 1, 1985, Denver, ASCE, New York.

Rawls, W.J., Brakensiek, D.L., 1982. Estimation of soil water retention from soil properties. ASCE Journal of Irrigation and Drainage. 108(IR2), 166-171.

Rawls, W.J., Brakensiek, D.L., 1989. Estimation os soil water retention and hydraulic properties. In unsaturated flow in hydrologic modeling theory and Practices ed. H.J. Morel-Seytoux 275-300. Dordrecht : Kluwer Academic Publishers.

Rawls, W.J., Brakensiek, D.L., Saxton, K.E., 1982. Estimation of soil water properties. Transactions of the ASAE 25, 1316– 1320, 1328.

Rawls, W.J., Gish, T.J., Brakensiek, D.L., 1991. Estimating soil water retention from soil physical properties and characteristics. Advances in Soil Science 16, 213– 234.

Reichardt, K. A 1990. Aguaem sistemas agrícolas. São Paulo, Editora Manoele Ltda, 188.

Rhoades, J.D., Bingham, F.T., Letey, J., Hoffman, G.J., Dedrick, A.R., Pinter, P.J., Replogle, J.A., 1989. Use of saline drainage water for irrigation: imperial valley study. Agricl Water Manag 16:25–36.

Rogers, M.E., 2001. The effect of saline irrigation on lucerne production: shoot and root growth, ion relations and flowering incidence in six cultivars grown in northern Victoria. Austr. Irrig. Sci. 20, 55–64.

Romano, N., Santini, A., 2002. Field. In: J. Dane, & G. Topp, (eds.). Methods of soil analysis, Part 4, Physical methods, Book Series No 5, SSSA., Madison, Wisconsin. 721-738.

Romano, N., Santini, A., 1999. Determining soil hydraulic functions from evaporation experiments by a parameter estimation approach: Experimental verifications and numerical studies. Water M Resour. Res. 35, 3343–3359.

Romano, N., Santini, A., 1997. Effectiveness of using pedo-transfer functions to quantify the spatial variability of soil retention characteristics. J.Hydrol. 265, 56-75.

Russo, D., 1988. Determining soil hydraulic properties by parameter estimation: on the selection of a model for the hydraulic properties. Water Resources Research, 24, 453–459.

Sarwar, A., Bastiaanssen., W.G.M., Van Dam, J.C., Boers, M.Th., 2000. Evaluating drainage design parameters for the fourth drainage project, Pakistan by using SWAP model: Part I—calibration. Irrigational Drainage Systems. 14, 257–280.

Scanlon, B.R., Healy, R., Cook, P.G., 2002. Choosing appropriate techniques for quantifying groundwater recharge.. Hydrogeology Journal. 10, 18–39.

Scanlon, B.R., Keese, K.E., Flint, A.L., Flint, L.E., Gaye, C.B., Edmunds, W.M., Simmers, I., 2006. Global synthesis of groundwater recharge in semiarid and arid regions. Hydrol. Process. 20, 3335–3370.

Schaap, M. G., Leij, F. J., Van Genuchten, M. T., 2001. ROSETTA: A computer program for estimating soil hydraulic parameters with hierarchical pedotransfer functions, J. Hydrol. 251, 163–176.

Schaap, M.G., Leij. F.J., Van Genuchten, M.Th., 1998. Neural properties. Soil Sci. Soc. Am. J. 62:847–855.

Schaap, M.G.,2005. Models for Indirect Estimation of Soil Hydraulic Properties. Hydrological Sciences,2.

Scheinost, A.C., Sinowski, W., Auerswald, K., 1997. Regionalization of soil water retention curves in a highly variable soilscape: I. Developing a new pedotransfer function. Geoderma 78, 129–143.

Seki, K., 2007. SWRC fit- a nonlinear fitting program with a water retention curve for soils having unimodal and bimodal pore structure. Hydrol Earth Syst. Sci. 4, 407-437.

Sepaskhah, A.R., Kanooni, A., Ghasemi, M.M., 2003. Estimating water table contributions to corn and sorghum water use. Agric Water Manag. 58, 67–79.

Shah, T., Molden, D., Sakthivadivel, R., Seckler, D., 2000. The global groundwater situation: Overview of opportunities and challenges.Colombo, Sri Lanka: International Water Management Institute.

Shein, E.V., Gudima, I.I., Mokeichev, A.V., 1993. Methods of determination of main hydro-physical functions to be used In modeling. Moscow Univ. Soil Sci. Bull. 48:14–19.

Shuh, W.M., Cline, R.D., Sweeney, M.D., 1988. Comparison of a laboratory procedure and a textural model for predicting in situ soil water retention. Soil Sci. Soc. Am. J. 52:1218–1227.

Sibanda, T., Nonner, J.C., Uhlenbrook, S., 2009. Comparison of groundwater recharge estimation methods for the semi-arid Nyamandhlovu area, Zimbabwe. Hydrogeology Journal. 17, 1427–1441.

Siebert, S., Döll, P., 2007. Irrigation water use – A global perspective. In: Lozán, J.L., Graßl, H., Hupfer, P., Menzel, L., Schönwiese, C-D., (eds.): Global Change: Enough Water for all? Universität Hamburg / GEO, 104-107.

Simunek, J., 2005. Models of Water Flow and Solute Transport in the Unsaturated Zone, Hydrological Sciences,2.

Simunek, J., Hopmans, J.W., 2009. Modeling compensated root water and nutrient uptake. Ecol. Model. 220, 505–521.

Sisson, J.B., Gee, G.W., Hubbell, J.M., Bratton, W.L., Ritter J.C., Ward, A.L., Caldwell ,T.G., 2002. Advances in tensiometry for longterm—monitoring of soil water pressures. Vadose Zone J., 1, 310–315.

Slavich, P.G., Petterson, G.H., Griffin, D., 2002. Effects of irrigation water salinity and sodicity on infiltration and Lucerne growth over a shallow watertable. Aust. J. Exp. Agric. 42, 281–290.

Smets, S.M.P., Kuper, M., Van Dam, J.C., Feddes, R.A., 1997. Salinization and crop transpiration of irrigated fields in Pakistan's Punjab. Agric. Water Mgmt. 35, 43-60.

Sophocleous, M., 2004. Groundwater recharge and sustainability in the High Plains aquifer in Kansas, USA. Hydrogeology Journal,13, 351–365.

Soppe, R.W.O., Ayars, J.E., 2003. Characterizing groundwater use by safflower using lysimeters. Agric. Water Manage. 60, 59–71.

Stephens, D. B., 1996: Vadose Zone Hydrology. Lewis Publishers, 339 pp.

Stolte, J., Freijer, J.I., Bouten, W., Dirksen, C., Halbertsma, J.M., Van Dam, J.C., Van den Berg J.A., Veerman, G.J. W¨osten, J.H.M., 1994. Comparison of six methods to determine unsaturated soil hydraulic conductivity. Soil Science Society of America Journal, 58, 1596–1603.

Sun, H., Cornish, P.S., 2005. Estimating shallow groundwater recharge in the headwaters of the Liverpool Plains using SWAT.Hydrological processes. 19, 795-807.

Tamari, S., Gaudu, J.C., Simmoneau, T., 1993. Tensiometric measurement with metastable state of water under tensions. Soil Sci. 156, 149–155.

Taylor, R.G., Howard, K.W.F., 1996. Groundwater recharge in the Victoria Nile basin of east Africa: support for the soil moisture balance approach using stable isotope tracers and flow modelling. Journal of Hydrology 180, 31–53.

Tietje, O., and M. Tapkenhinrichs. 1993. Evaluation of pedo-transfer functions. Soil Sci. Soc. Am. J. 57:1088–1095.

Torquato, S., 2001. Random heterogeneous materials: microstructure and macroscopic properties. Interdisciplinary Applied Mathematics, Vol. 16, Springer: New York.

Torres, J.S., Hanks, R.J., 1989. Modeling water table contribution to crop evapotranspiration. Irrigation Sci. 10, 265–279.

T5-X. User Manual, Available online: http://www.ums-muc.de/en/products/tensiometer/ t5.html (accessed on 10 November 2009).

United Nations Educational Scientific and cultural Organisation., 2004. Meeting Basic Needs. UNESCO World Water Assessment Programme.

Van Dam, J.C., Feddes, R.A., 1996. Numerical simulation of infiltration evaporation and shallow groundwater levels with the Richards equation. Journal of Hydrology.

Van Dam, J.C., Feddes, R.A., 2000. Numerical simulation, evaporation and shallow groundwater levels with Richards equation. Journal of Hydrology. 233, 72–85.

Van Dam, J.C., Groenendijk, P., Hendriks, R.F.A., Kroes, J.G., 2008. Advances of modeling water flow in variably saturated soils with SWAP. Vadose Zone J. 7, 640–653.

Van Dam, J.C., Huygen, J., Wesseling, J.G., Feddes, R.A., Kabat, P., Van Waslum, P.E.V., Groenendjik, P., Van Diepen, C.A., 1997. Theory of SWAP version 2.0: simulation of water flow and plant growth in the soil–water–atmosphere–plant environment. Tech Doc 45. Wageningen Agric Univ and DLO Winand Staring Centre, Wageningen, The Netherlands, p 167

Van Es, H.M., Ogden, C.B., Hill, R.L., Schindelbeck, R.R., Tsegaye, T., 1999. Integrated assessment of space, time, and management-related variability of soil hydraulic properties. Soil Science Society of America Journal, 63, 1599–1607.

Van Genuchten, M.Th., 1980. A closed–form equation for predicting the hydraulic conductivity of unsaturated soils. Soil Science Society of America Journal, **44**, 892–898.

Van Genuchten, M.Th., Leij, F.J., Wu, L., 1999a. Proceedings of the International Workshop on Characterization and Measurement of the Hydraulic Properties of Unsaturated Porous Media, University of California: Riverside.

Van Genuchten, M.Th., Leij, F.J., Wu, L., 1999b. Characterization and measurement of the hydraulic properties of unsaturated porous media, In Proceedings of the International Workshop on Characterization and Measurement of the Hydraulic Properties of Unsaturated Porous Media, van Genuchten M.Th., *et al.* (Eds.), University of California: Riverside, pp. 1–12.

Van Genuchten, M.Th., Leij, F.J., Yates, S.R., 1991. The RETC Code for Quantifying the Hydraulic Functions of Unsaturated Soils. US Environmental Protection Agency. Available at http://www.scisoftware.com/products/ retc_overview/retc_overview.html. (accessed on 23 Aug. 2007).

Van Genuchten, M.Th., 1987. A numerical model for water and solute movement in and below the root zone. Res. Report, US Salinity Laboratory, Riverside, CA.

Van Rensburg, LD., 1988. Die voorspelling van grondgemduseerde plant waterstremming vir geselekteerde grond-plant-atmosfeer-sisteme. Unpublished MSc Agric thesis, University Orange Free State, Bloemfontein, RSA.

Vanclooster, M., Viaene, P., Diels, J., Christiansen, K., 1994. WAVE, a deterministic model for simulating water and agrochemicals in the soil and vadose environment. Inst. Land and Water Management, K.U. Leuven.

Vereecken, H., J. Maes, J. Feyen, and P. Darius. 1989. Estimating the soil moisture retention characteristic from texture, bulk density and carbon content. Soil Sci. 148:389–403.

Vrugt, J.A., Gupta, H.V, Bastidas, L., Bouten, W., Sorooshian, S., 2003b. Effective and efficient algorithm for multi-objective optimization of hydrologic models. Water Resour. Res. 39, 1214.

Vrugt, J.A., Gupta, H.V., Bouten, W., Sorooshian, S., 2003a. A Shuffled Complex Evolution Metropolis algorithm for optimization and uncertainty assessment of hydrologic model parameters. Water Resour. Res. 39, 1201.

Wallender, W.W., Grimes, D.W., Henderson, D.W., Stromberg, L.K., 1979. Estimating the contribution of a perched water table to the seasonal evapotranspiration of cotton Agron. J. 71,1056-1060.

Wang, P., Song, X., Han, D., Zhang, Y., Zhang, B., 2012. Determination of evaporation, transpiration and deep percolation of summer corn and winter wheat after irrigation. Agricultural Water Management. 105, 32– 37.

Wesseling, J.G., Elbers, J.A., Kabat, P., Van den Broek, B.J., 1991. SWATRE: instructions for input. Internal note, Winand Staring Center, Wageningen, The Netherlands. International Waterlogging and Salinity Research Institute, Lahore, Pakistan, 29 pp.

Williams, R.D., Ahuja, L.R., Naney, J.W., 1992. Comparison of methods to estimate soil water characteristics from soil texture, bulk density and limited data. Soil Sci. 153, 172-184.

Willis, T. M., Black, A. S., Meyer W. S., 1997. Estimates of deep percolation beneath cotton in the Macquarie Valley. Irrig. Sci, 17(4), 141-150.

Wosten, J.H.M., Lilly, A., Nemes, A., le Bas, C., 1999. Development and use of a database of hydraulic properties of European soils. Geoderma, 90: 169‑185.

Wosten, J.H.M., Pachepsky, Y.A., Rawls W.J., 2001. Pedotransfer functions: Bridging the gap between available basic soil data and missing soil hydraulic characteristics. Journal of Hydrology, 251: 123‑150.

Wosten, J.H.M., Van Genuchten, M.Th., 1988. Using texture and other soil properties to predict the unsaturated soil hydraulic conductivity. Soil Sci. Soc. Am. J., 52: 1762-1770.

Wösten, J.H.M., Lilly, A., Nemes, A., Le Bas, C., 1998. Using existing soil data to derive hydraulic parameters for simulation models in environmental studies and in land use planning. Report 156, Alterra Green World Research, Wageningen, 106 pp.

Xu, X., Huang, G., Zhan, H., Qu, Z., Huang, Q., 2012. Integration of SWAP and MODFLOW-2000 for modeling groundwater dynamics in shallow water table areas. Journal of Hydrology. 412–413 , 170–181

Yang, F., Zhang, G., Yin, X., Liu, Z., Huang, Z., 2011. Study on capillary rise from shallow groundwater and critical water table depth of a saline-sodic soil in western Songnen plain of China. Environ Earth Sci. 64, 2119–2126.

Yang, J., Li, B., Shiping, L., 2000. A large weighing lysimeter for evapotranspiration and soil-water-groundwater exchange studies. Hydrological processes. 14(10) , 1887-1897.

York, J.P., Person, M., Gutowski, W.J., Winter, T.C., 2002. Putting aquifers into atmospheric simulation models: An example from the Mill Creek Watershed, northeastern Kansas. Adv. Water Resour. 25, 221–238.

Zeiliguer, A.M., Pachepsky, Y.A., Rawls, W.J., 2000. Estimating water retention of sandy soils using the additivity hypothesis. Soil Science 165, 373–383.

Zeineldin, , F.I., Aldakheel, Y.J., 2010. Evaluation Contribution of Ground shallow Water table to Irrigation of Date palm trees under Irrigation Reduction in Saudi Arabia. International Conference on Chemistry and Chemical Engineering, (ICCCE 2010).

Zhang, L., Dawes, W. R., Hatton, T. J., Reece, P. HBeale, ., G. T. H., Packer I., 1999. Estimation of soil moisture and groundwater recharge using the TOPOG_IRM model, Water Resour. Res., 35, 149– 161.

Zhang, S., Lovdahl, L., Grip, H., Tong, Y., 2007. Soil hydraulic properties of two loess soils in China measured by various field-scale and laboratory methods. Catena 69, 264-273.

Appendix

Appendix 1

Models ARX

The models ARX (Autoregressive model with exogenous innovation) of order p have the general formula:

$$Y_{(t)} = \sum_{i=1}^{p} \propto Y_{(t-i)} + \sum_{j=1}^{m} \beta_j X_{(t-j)} + \varepsilon_t \qquad eq(1)$$

where: Y state variable of the system; X is the exogenous variable (innovation); ε is the error with mean=0 ; t temporal index; α_i, β_j are respectively the parameters of the component auto-regressive and exogenous.

For the application to a our specific case, the model adopted is auto-regressive and exogenous of the first order where the exogenous entrance is a subject of a delay of n hours and then has the formula:

$$Y_{(t)} = \propto Y_{(t-1)} + \beta X_{(t-n)} + \varepsilon_t \qquad eq(2)$$

In the absence of inputs, the variable Y (t), tends to 0. In the present case there is no a limit value for which the variable tends, but by observing trends of groundwater we can notice that these trends are decreasing to a limit value which can be useful as a parameter of calibration. So that the groundwater is not represented by the value Y (t) but is obtained through the following linear transformation:

$$S_{(t)} = 2 - Y_{(t)} + c \qquad eq(3)$$

Where c is the fourth parameter of calibration. So the parameters to be calibrated are the following: α (the system memory), β (exogenous parameter), n (delay of the input), c (additive constant).

1.1.1. Calibration of models ARX

The models calibration was made on the basis of rainfall data (values of the variable X) and measured groundwater depth data (values of the variable S).

Figure 6.3 shows measured and simulated groundwater within the period of calibration of the two models, while Table 7.1 shows the periods containing valid data before (1) and after (2) the range of missing data within the calibration period, the values of the parameters of calibration and the value of efficiency (ME Nash-Sutcliffe, 1970) of the two models. The latter is an index of model validity. ME reaches the maximum value, when simulated and measured values are equal and is equal to zero when the error of the simulation is equal to the standard deviation of the observed data and takes negative values in cases where the model demonstrates poor performance.

Table 7.1 Periods with valid data considered before (1) and after (2) missing data, the model parameters (α, β, n and c) and the efficiency simulation value (ME)

PMI	period 1	period 2	α	β	n	c	ME
1	11-Feb16:00 07-Mar 16:00	18-Apr 00:00 05-May 15:00	0.995098	0.013884	2	-0.99566	0.95
5	15-Feb 10:00 07-Mar 10:00	02-May 02:00 06-May 10:00	0.997011	0.024034	0	-0.58783	0.94

Appendix 2: An example of Land use and hydrological and pedological parameters inputs in IDRAGRA model

Grid File Header:	
ncols	1
nrows	1
xllcorner	1552630
yllcorner	4911200
cellsize	250
NODATA_value	-9999

parameter	**format**	**type**	**value**	
birrigui	asc	int	1	
codice_metodo	asc	int	1	
dominio	asc	int	1	
dren	asc	int	2	classe CN
eff_metodo	asc	double	0.65	
eff_rete	asc	double	0.65	
gr_idr	asc	int	2	ABCD del CN
Ksat_I	asc	double	4.75	
Ksat_II	asc	double	0.686	
Meteo_1	asc	double	2.00	
N_I	asc	double	1.42	
N_II	asc	double	1.49	
ParRisCap_a1	asc	double	320.80	
ParRisCap_a2	asc	double	303.20	
ParRisCap_a3	asc	double	-0.15	
ParRisCap_a4	asc	double	7.55	
ParRisCap_b1	asc	double	-0.16	
ParRisCap_b2	asc	double	-0.54	
ParRisCap_b3	asc	double	2.10	
ParRisCap_b4	asc	double	-2.03	
pendenza	asc	double	0.0007	
REW_I	asc	double	12.484838	
REW_II	asc	double	12.300156	
soggiacenza	asc	double	0.80	
TetaII_0	asc	double	0.30	
TetaII_FC	asc	double	0.2775	
TetaII_r	asc	double	0.0157	
TetaII_sat	asc	double	0.4043	
TetaII_WP	asc	double	0.0845	
TetaI_0	asc	double	0.33	
TetaI_FC	asc	double	0.2707	
TetaI_r	asc	double	0.0212	
TetaI_sat	asc	double	0.4026	

TetaI_WP	asc	double	0.0755
usosuolo	asc	int	1